

Some pages of this thesis may have been removed for copyright restrictions.

If you have discovered material in Aston Research Explorer which is unlawful e.g. breaches copyright, (either yours or that of a third party) or any other law, including but not limited to those relating to patent, trademark, confidentiality, data protection, obscenity, defamation, libel, then please read our [Takedown policy](#) and contact the service immediately (openaccess@aston.ac.uk)

FORMATION OF A LIPOSOME – CARBON NANOTUBE COMPLEX THROUGH THE USE OF BATH SONICATION SYSTEMS

PETER JOHN STONE

Doctor of Philosophy

ASTON UNIVERSITY

September 2018

©Peter John Stone, 2018, asserts his moral right to be identified as the author of this thesis.

This copy of the thesis has been supplied on condition that anyone who consults it is understood to recognise that its copyright rests with its author and that no quotation from the thesis and no information derived from it may be published without proper acknowledgement.

Aston University

FORMATION OF A LIPOSOME – CARBON NANOTUBE COMPLEX THROUGH THE USE OF BATH SONICATION SYSTEMS

Peter John Stone

Doctor of Philosophy

September 2018

Thesis Summary

Liposomes were selected as a delivery system due to their amphiphilic nature and their use in a wide variety of medications already on the market. Carbon nanotubes were selected as there is still uncertainty as to their influence on biological systems and, due to their increasing prevalence, this needs to be addressed. This includes the uncertainty surrounding their influence on the immune system and whether this is a positive or a negative effect.

Liposomes quite often require size reduction after being formed through lipid film hydration. This size reduction can occur through several different methods including probe sonication, bath sonication and extrusion. The Bioruptor bath sonication systems were used in this study to reduce the size of liposomes from the micron range to below 100 nm. A number of different systems were studied, and all were shown to be effective. A number of different formulations were investigated, and this culminated in a study showing a number of different lipophilic drugs being loaded into the liposomes formed using this bath sonication system.

Carbon nanotubes were successfully dispersed in water using a number of different surfactants including MPC, which is a biologically safe phospholipid. These were all done using the Bioruptor bath sonication systems. Carbon nanotubes were also successfully defected using an acid mixture and it was shown that increasing the temperature too much caused total carbon nanotube destruction. Finally, the carbon nanotubes were added to the liposomal formulations.

It was shown that the bath sonication systems employed could be used to formulate small liposomes that could be used for vaccine and drug delivery. The same systems were used to disperse carbon nanotubes in water, which could then be used for a number of different biological uses.

Key words: bath sonication, drug delivery, covalent functionalisation, non – covalent functionalisation

Acknowledgments

I would like to thank Professor Yvonne Perrie and Dr Craig Russell for being my primary supervisors through this project. Their guidance and help through all the biological and liposome aspects of my PhD has been invaluable for the successful completion of this project. I would also like to thank Dr Alex Rozhin for his contribution and help towards the photonics and carbon nanotubes aspects of this project. I would also like to thank the team at Diagenode, specifically Jerome Kroonen, Irina Panteleeva, Wassim Lakhal and Didier Allaer, for their guidance and help with the Bioruptor bath sonicator systems. Dmytro Korytko and Sergei Alekseev must also be acknowledged coming over from Ukraine with their help with the heavy wet acid chemistry in modifying the carbon nanotubes.

The Biotechnology and Biological Sciences Research Council (BBSRC) and Diagenode must also be thanked for their financial contributions to this project.

Lastly, I would like to thank my wife, my family and my friends for their unwavering support and help with all aspects of life throughout the last four years which has allowed me to complete this work and be in the fortunate position that I am now in.

Contents

Table of Contents

FORMATION OF A LIPOSOME – CARBON NANOTUBE COMPLEX THROUGH THE USE OF BATH SONICATION SYSTEMS	1
Acknowledgments	3
Contents	4
List of Figures	12
List of Tables.....	31
Abbreviations	32
List of publications.....	35
1. Introduction.....	39
1.2 Liposomes as a spherical nanoscale drug and vaccine delivery system.....	41
1.2.1 Liposomes background	41
1.2.2 Current methods for the formation of liposomes	43
1.2.3 Analysis of liposomes after formation	47
1.2.4 Uses today.....	49
1.3 Carbon nanotubes dispersion, modification and uses.....	52
1.3.1 Carbon nanotubes background.....	52
1.3.2 Carbon nanotube analysis	57
1.3.3 Carbon nanotubes uses today	58
1.4 Current methods for the dispersion of carbon nanotubes in water for biological systems.....	60
1.4.1 Carbon nanotubes dispersed with surfactants	60
1.4.2 Carbon nanotube carboxylation	62
1.4.3 Carbon nanotube cutting.....	64
1.4.4 Carbon nanotube separation	66
1.5 Previous liposome – carbon nanotube work	68

1.5.1 Nano-trains.....	68
1.5.2 Porins	68
1.6 Bioruptor® applications	69
1.6.1 The need for a cheap and fast method of internally validating optimised sonication conditions	69
1.6.2 The need for a new version of the Diagenode (Bioruptor® Pico) Formalin-Fixed Paraffin-Embedded (FFPE) DNA kit to increase profitability.....	70
2 Formation and optimisation of the process of reducing liposome size through bath sonication using the Bioruptor® bath sonicator systems	74
2.1 Aims and objectives	75
2.2 Materials and Methods	76
2.2.1 Lipid Film Hydration Method for the production of MLV	76
2.2.2 Formulation of size reduced liposomes using probe sonication	76
2.2.3 Formulation of size reduced liposomes by the high shear mixing (HSM) homogenisation method studies	78
2.2.4 Formulation of size reduced liposomes using Bioruptor® XL studies.....	78
2.2.5 Formulation of size reduced liposomes using Bioruptor® Standard studies	79
2.2.6 Formulation of size reduced liposomes using Bioruptor® Plus studies.....	82
2.2.7 Formulation of size reduced liposomes using Bioruptor® Pico studies.....	83
2.2.8 Characterisation of liposomes	84
2.3 Results and discussion	84
2.3.1 A probe sonication study into liposome size reduction.....	84
2.3.1.1 Initial probe sonication study	87
2.3.1.2 Probe sonication study into how amplitude level and time affects liposome size reduction	88

2.3.1.3	Probe sonication study into how cholesterol concentration affects liposome size reduction	91
2.3.1.4	Probe sonication study into how concentration affects DMPC liposome size reduction	93
2.3.1.5	Probe sonication study using the optimised conditions.....	94
2.3.1.6	Discussion	95
2.3.2	Developing and optimising a protocol for the production of SUV using DMPC and DMPC: Cholesterol lipid formulations using high shear mixing	97
2.3.2.1	High shear mixing study into the effect of rpm parameters on vesicle size reduction	97
2.3.2.2	High shear mixing study into the effect of time on liposome size reduction.....	100
2.3.2.3	Discussion	102
2.3.3	Bioruptor® XL liposome size reduction studies	103
2.3.3.1	Bioruptor® XL study into how the number of cycles affects liposome size reduction	103
2.3.3.2	Bioruptor® XL study into how the power level affects liposome size reduction .	106
2.3.3.3	Bioruptor® XL study into how volume affects liposome size reduction	108
2.3.3.4	Bioruptor® XL study into how concentration affects liposome size reduction	110
2.3.3.5	Discussion	112
2.3.4	Bioruptor® Standard liposome size reduction studies.....	113
2.3.4.1	Bioruptor® Standard study into how power level affects liposome size reduction	113
2.3.4.2	Bioruptor® Standard study into how power level with continuous sonication affects liposome size reduction	115

2.3.4.3	Bioruptor® Standard study into how pulse settings affects liposome size reduction	117
2.3.4.4	Bioruptor® Standard study into how time affects liposome size reduction	119
2.3.4.5	Bioruptor® Standard study into how a longer period of time affects liposome size reduction	121
2.3.4.6	Bioruptor® Standard study into how volume affects liposome size reduction	123
2.3.4.7	Bioruptor® Standard study into how the use of larger tubes affects liposome size reduction	125
2.3.4.8	Bioruptor® Standard study into how position within the water bath affects liposome size reduction.....	127
2.3.4.9	Bioruptor® Standard study into how temperature affects liposome size reduction	129
2.3.4.10	Bioruptor® Standard study into how the use of PP tubes and power level affects liposome size reduction.....	131
2.3.4.11	Bioruptor® Standard study into how the use of PP tubes and time affects liposome size reduction.....	133
2.3.4.12	Bioruptor® Standard study into how the use of PP tubes and volume affects liposome size reduction.....	135
2.3.4.13	Bioruptor® Standard study into how the use of larger PP tubes affects liposome size reduction.....	137
2.3.4.14	Bioruptor® Standard study into how formulation affects liposome size reduction	139
2.3.4.15	Discussion	142
2.3.5	Bioruptor® Plus liposome size reduction studies	144

2.3.5.1	Bioruptor® Plus study into how the length of sonication and power level affects liposome size reduction.....	144
2.3.5.2	Bioruptor® Plus study into how concentration affects liposome size reduction .	148
2.3.5.3	Bioruptor® Plus study into how temperature affects liposome size reduction	150
2.3.5.4	Bioruptor® Plus study into how volume affects liposome size reduction	152
2.3.5.5	Bioruptor® Plus study into how different plastics using a 1.5 mL tube affects liposome size reduction.....	154
2.3.5.6	Bioruptor® Plus study into how different plastics using a 50 mL tube affects liposome size reduction.....	155
2.3.5.7	Bioruptor® Plus study into how different plastics using a 15 mL tube and power level affects liposome size reduction.....	158
2.3.5.8	Bioruptor® Plus study into how DMPC: Cholesterol ratio affects liposome size reduction	160
2.3.5.9	Bioruptor® Plus study into how lipid concentration affects liposome size reduction	163
2.3.5.10	Discussion	167
2.3.6	Bioruptor® Pico liposome size reduction studies	168
2.3.6.1	Bioruptor® Pico study into how number of cycles affects liposome size reduction	168
2.3.6.2	Bioruptor® Pico study into how volume affects liposome size reduction	169
2.3.6.3	Discussion	171
2.4	Conclusion.....	171
3	Bioruptor bath sonicator systems: applications in the spheres of liposomes, DNA extraction and sonicator efficiency	174
3.6	Aims and objectives	175

3.2.2 Investigating more cost effective methods of demonstrating bath sonicator efficiency	175
3.2.2.1 Conditions to test on the Bioruptor® Pico:	176
3.2.2.2. Conditions to test on the Bioruptor® Plus	177
3.2.3 Investigating more cost effective materials for DNA extraction using the Bioruptor® Pico	179
3.2.3.1 Assay 1	180
3.2.3.2 Assay 2:	180
3.2.3.3 Assay 3	181
3.2.3.4 Analysis of DNA ran with DNA fragment analyser	181
3.7 Results and discussion	182
3.3.1	182
3.3.2 Investigating more cost effective methods of demonstrating bath sonicator efficiency	182
3.3.2.1 Bioruptor® Pico	182
3.3.2.2 Bioruptor® Plus data	191
3.3.2.3 Discussion	205
3.3.3 Investigating more cost effective materials for DNA extraction using the Bioruptor® Pico	206
3.3.3.1 Assay 1	207
3.3.3.2 Assay 2	208
3.3.3.3 Assay 3	209
3.4 Conclusion	210
4. Water dispersion of carbon nanotubes	212
4.1 Aims and Objectives	213
4.2 Materials and methods	213
4.2.1 Dispersion of carbon nanotubes using the Bioruptor®® Plus	213
4.2.1.1 Temperature studies	214
4.2.1.2 Cycles study	214
4.2.1.3 DMPC study	215

4.2.1.4 Dilution study	215
4.2.1.5 Surfactant study	216
4.2.1.6 Carbon nanotubes stability study	216
4.2.2 Dispersion of carbon nanotubes using the probe sonicator	216
4.2.3 Analysis of carbon nanotubes	217
4.3 Results and discussion	218
4.3.1 Dispersion of carbon nanotubes with the Bioruptor® Plus	218
4.3.1.1 Water dispersion of carbon nanotubes using SDS as the surfactant compared to SDBS.....	218
4.3.1.2 Water dispersion of carbon nanotubes using SDBS as the dispersal surfactant	221
4.3.1.2.1 SDBS dispersed carbon nanotubes sonicated at different temperatures.....	221
4.3.1.2.2 Dispersion of carbon nanotubes at a number of different cycle settings using the Bioruptor Plus.....	227
4.3.1.2.3 Dilution study of dispersed carbon nanotubes in SDBS	229
4.3.2 Probe sonication of carbon nanotubes with SDBS	232
4.3.3 Water dispersion of carbon nanotubes using biologically safe surfactants.....	237
4.3.3.1 Dispersion of carbon nanotubes using MPC as a surfactant	237
4.3.3.2 Dispersion of carbon nanotubes using the phospholipid DMPC as the surfactant...	240
4.3.4 Combination of surfactants	242
4.3.4.1 Carbon nanotube dispersion surfactant study comparing like for like surfactants....	242
4.3.4.2 Stability study of water dispersed carbon nanotubes using SDS, SDBS and MPC	247
4.4. Conclusion.....	250
5. Carbon nanotube modification and addition to liposomal solution	252
5.1 Aim and objectives	253

5.2	Materials and methods	253
5.2.1	Carbon nanotube carboxylation	253
5.2.1.1	Chemical treatment procedure.....	253
5.2.1.2	Dispersion of carbon nanotubes post chemical treatment.....	254
5.2.2	Carbon nanotube cutting with probe	254
5.2.3	Carbon nanotube cutting with bath.....	255
5.2.4	Carbon nanotube addition to liposomes	255
5.2.5	Analysis of carbon nanotubes	256
5.2.5.1	UV – Vis spectroscopy	256
5.2.5.2	Photo luminescence mapping.....	256
5.2.5.3	Size analysis using DLS	257
5.2.5.4	TEM.....	257
5.3	Results and Discussion	258
5.3.1	Chemical cutting and carboxylation of carbon nanotubes	258
5.3.1.1	Basic HiPco carbon nanotube data.....	258
5.3.1.2	Carbon nanotubes carboxylated with oleum experiment.....	261
5.3.2	Cutting of carbon nanotubes using the probe and bath sonicators	269
5.3.2.1	Carbon nanotubes cut using probe sonicator.....	269
5.3.2.2	Carbon nanotube cutting using the bath	271
5.3.3	Addition of carbon nanotubes to liposomes	273
5.4	Conclusions.....	276
6.	Final discussion and conclusion	277
6.1	Final conclusions	278
6.1.1	Liposome formation and size reduction.....	278
6.1.2	Bioruptor® protocols	279
6.1.3	Non covalent functionalization of carbon nanotubes	281
6.1.4	Covalent functionalization of carbon nanotubes.....	282
6.2	Further work	283
7.	References	285

List of Figures

Figure 1.1: The shapes and structures formed by the lipids and surfactants used in this work as well as their structures and approximate CPP values.....42

Figure 1.2: Liposomes being produced using the top down method, whereby lipids form a bilayer, and then using the lipid hydration method are formed into MLV and then through a variety of methods such as sonication, both bath and probe, extrusion and high shear mixing, are reduced in size to the SUV level (Avanti, 2015, Rathod and Deshpande, 2010).....43

Figure 1.3: Bath (A) and probe (B) sonication diagrams showing how each method works to reduce the size of the sample. For bath sonication, the samples are placed into a temperature controlled water bath. This whole water bath is then sonicated using a device fitted to the bottom of the water bath, thereby giving non-contact sonication to the sample, reducing its size. For probe sonication, the sonic energy is transmitted directly down a probe that is placed directly into the sample.....44

Figure 1.4: Probe sonication liposome size reduction method. Sample is sonicated in a glass vial with the tip of the probe touching the sample. Sample changes from milky to clear. Sample is then centrifuged in a centrifuge tube to remove titanium particles and large MLV which settle to the bottom.....45

Figure 1.5: Method for producing MLV through lipid film hydration and then forming SUV through bath sonication. Lipid in Chloroform: Methanol is added to a round bottom flask and then the solvents are removed through the use of a rotary evaporator. Buffer is warmed and added to the lipid film that forms on the bottom of the flask and vortexed to form a milky solution of MLV. Sample is added to a warmed water bath in plastic tubes and sonicated.....46

Figure 1.6: A) A pristine carbon nanotube surface made up of carbon atoms with no defects or modification. This makes these tubes highly hydrophobic. B) A carbon nanotube surface post carboxylation, with the carboxyl groups increasing the hydrophilicity of the carbon nanotube, and also disrupting the carbon nanotubes surface, affecting its properties.....53

Figure 1.7: Sodium dodecyl sulfate (SDS) dispersed carbon nanotubes showing the SDS non – covalently bound to the carbon nanotube surface, allowing for dispersion in an aqueous solution, but no change to the carbon nanotube surface and therefore keeping its properties as before.....54

Figure 1.8: Structures of the three surfactants used in these studies to non – covalently disperse the carbon nanotubes. They are SDS, Sodium dodecylbenzenesulfonate (SDBS) and MPC.....54

Figure 1.9: Chirality of carbon nanotubes with either A) armchair B) chiral) or C) zig zag conformation.....55

Figure 1.10: Carbon nanotube conformation showing the A) armchair B) chiral and C) zigzag conformations.....55

Figure 1.11: A schematic of the various pharmaceutical applications carbon nanotubes are used for (He et al., 2013a). These include delivery of drugs, tissue regeneration and as biosensor vehicles for diagnostics.....60

Figure 1.12: A) Method for dispersion of carbon nanotubes using SDS non – covalently so no damage to the carbon nanotube surface. B) Method for the dispersion of carbon nanotubes using a surfactant and bath sonication. Carbon nanotubes are placed in water with surfactant and then sonicated in a warmed water bath. These are then centrifuged and analysed using UV – Vis – NIR and PL.....62

Figure 1.13: covalently functionalised carbon nanotube surface with carboxyl groups showing the disruption to the carbon nanotube structure and shortening that occurs with the addition of

acid that causes defects in the carbon nanotube surface that eventually form larger defects and cause the carbon nanotube to become cut.....64

Figure 1.14: Cutting and functionalisation of carbon nanotubes using both covalent and non-covalent functionalisation methods. These use either harsh acids or mechanical power to cause defects in the carbon nanotube surface in such a way that causes bigger and bigger defects to occur that eventually results in the cutting of the carbon nanotube into shorter pieces.....66

Figure 2.1: Number of publications for microfluidics, sonication and extrusion for liposome formation using the name of the method and the word liposome in their titles on all databases on web of science.....86

Figure 2.2: A and B) Size of probe sonicated DMPC liposomes sonicated over 10 minutes with samples taken every minute at either 8 (A) or 10 (B) amplitude. C and D) PDI of probe sonicated DMPC liposomes sonicated over 10 minutes with samples taken every minute at either 8 (A) or 10 (B) amplitude.....90

Figure 2.3: A – C) Size of 3 different formulations; DMPC (A), DMPC: Cholesterol 6:2 (B) and DMPC: Cholesterol 4:4 (C) sonicated over a 10 minute time period at 10 amplitude. D - F) PDI of 3 different formulations; DMPC (D), DMPC: Cholesterol 6:2 (E) and DMPC: Cholesterol 4:4 (F) sonicated over a 10 minute time period at 10 amplitude.....92

Figure 2.4: A) Size of sonicated DMPC liposomes at a range of concentrations from 2 to 30 mM sonicated at 10 amplitude for 6 minutes. B) PDI of sonicated DMPC liposomes at a range of concentrations from 2 to 30 mM sonicated at 10 amplitude for 6 minutes.....93

Figure 2.5: A) Size of final formulations of DMPC, DMPC: Cholesterol 6:2 and DMPC: Cholesterol 4:4 made using optimised sonication conditions of 10 amplitude for 6 minutes. B) PDI of final formulations of DMPC, DMPC: Cholesterol 6:2 and DMPC: Cholesterol 4:4 made using optimised sonication conditions of 10 amplitude for 6 minutes.....95

Figure 2.6: A – C) Size of 3 different formulations; DMPC (A), DMPC: Cholesterol 6:2 (B) and DMPC: Cholesterol 4:4 (C) high shear mixed over 5000 to 25000 rpm. D – F) PDI of 3 different formulations; DMPC (D), DMPC: Cholesterol 6:2 (E) and DMPC: Cholesterol 4:4 (F) high shear mixed over 5000 to 25000 rpm.....99

Figure 2.7: A – C) Size of 3 different formulations; DMPC (A), DMPC: Cholesterol 6:2 (B) and DMPC: Cholesterol 4:4 (C) high shear mixed over 5 to 30 minutes. D – F) PDI of 3 different formulations; DMPC (D), DMPC: Cholesterol 6:2 (E) and DMPC: Cholesterol 4:4 (F) high shear mixed over 5 to 30 minutes.....101

Figure 2.8: A – B) Size of sonicated liposomes over various time and cycle settings up to a maximum of 20 minutes for DMPC (A) and DMPC: Cholesterol 6:2 (B) sonicated at power level M2 at 45°C using 1000 µL in 1.5 mL tubes. C – D) PDI of sonicated liposomes over various time and cycle settings up to a maximum of 20 minutes for DMPC (A) and DMPC: Cholesterol 6:2 (B) sonicated at power level M2 at 45°C using 1000 µL in 1.5 mL tubes....105

Figure 2.9: A – B) Size of DMPC (A) and DMPC: Cholesterol 6:2 (B) liposomes sonicated using the 4 different power levels over 15 minutes of continuous sonication at 45°C using 1000 µL in 1.5 mL tubes. C – D) PDI of DMPC (A) and DMPC: Cholesterol 6:2 (B) liposomes sonicated using the 4 different power levels over 15 minutes of continuous sonication at 45°C using 1000 µL in 1.5 mL tubes.....107

Figure 2.10: A – B) Size of DMPC (A) and DMPC: Cholesterol 6:2 (B) liposomes sonicated using a range of volumes from 0.1 to 0.75 mL over 15 minutes of continuous sonication at 45°C using 1000 µL in 1.5 mL tubes at power level M2. C – D) PDI of DMPC (A) and DMPC: Cholesterol 6:2 (B) liposomes sonicated using a range of volumes from 0.1 to 0.75 mL over 15 minutes of continuous sonication at 45°C using 1000 µL in 1.5 mL tubes at power level M2.....109

Figure 2.11: Size (A) and PDI (B) of DMPC liposomes sonicated at power level M2 at 45°C using 300 µL in 1.5 mL tubes for 15 minutes of continuous sonication.....111

Figure 2.12: A – B) Size of DMPC (A) and DMPC: Cholesterol 4:4 (B) liposomes were produced using the Bioruptor® Standard at 45°C using 300 µL in 1.5 mL tubes. They were then sonicated for 15 minutes of 30, 30 at the 3 different power levels of L, M and H. C – D) PDI of DMPC (A) and DMPC: Cholesterol 4:4 (B) liposomes were produced using the Bioruptor® Standard at 45°C using 300 µL in 1.5 mL tubes. They were then sonicated for 15 minutes of 30, 30 at the 3 different power levels of L, M and H.....114

Figure 2.13: A – B) Size of DMPC (A) and DMPC: Cholesterol 4:4 (B) liposomes were produced using the Bioruptor® Standard at 45°C using 300 µL in 1.5 mL tubes. They were then sonicated for 15 minutes of 30, 0 at the 3 different power levels of L, M and H. C – D) PDI of DMPC (A) and DMPC: Cholesterol 4:4 (B) liposomes were produced using the Bioruptor® Standard at 45°C using 300 µL in 1.5 mL tubes. They were then sonicated for 15 minutes of 30, 0 at the 3 different power levels of L, M and H.....116

Figure 2.14: A – B) Size of DMPC (A) and DMPC: Cholesterol 4:4 (B) liposomes were produced using the Bioruptor® Standard at 45°C using 300 µL in 1.5 mL tubes. They were then sonicated for 15 minutes at power level L with time on kept constant at 30 seconds and time off ranging from 0 to 30 seconds. C – D) PDI of DMPC (A) and DMPC: Cholesterol 4:4 (B) liposomes produced using the Bioruptor® Standard at 45°C using 300 µL in 1.5 mL tube. They were then sonicated for 15 minutes at power level L with time on kept constant at 30 seconds and time off ranging from 0 to 30 seconds.....118

Figure 2.15: A – B) Size of DMPC (A) and DMPC: Cholesterol 4:4 (B) liposomes produced using the Bioruptor® Standard at 45°C using 300 µL in 1.5 mL tubes. They were then sonicated at power level L for 30 seconds on, 30 seconds off for between 5 and 15 minutes. C – D) PDI of DMPC (A) and DMPC: Cholesterol 4:4 (B) liposomes produced using the Bioruptor® Standard at 45°C using 300 µL in 1.5 mL tubes. They were then sonicated at power level L for 30 seconds on, 30 seconds off for between 5 and 15 minutes.....120

Figure 2.16: A – B) Size of DMPC (A) and DMPC: Cholesterol 4:4 (B) liposomes produced using the Bioruptor® Standard at 45°C using 300 µL in 1.5 mL tubes. They were then sonicated at power level L for 30 seconds on, 30 seconds off for between 15 and 30 minutes. C – D) PDI of DMPC (A) and DMPC: Cholesterol 4:4 (B) liposomes produced using the Bioruptor® Standard at 45°C using 300 µL in 1.5 mL tubes. They were then sonicated at power level L for 30 seconds on, 30 seconds off for between 15 and 30 minutes.....122

Figure 2.17: A – B) Size of DMPC (A) and DMPC: Cholesterol 4:4 (B) liposomes produced using the Bioruptor® Standard at 45°C using a range of volumes from 0.1 to 1 mL in a 1.5 mL tube. They were sonicated at power level M for 15 minutes of 30 seconds on, 0 seconds off cycle. C – D) PDI of DMPC (A) and DMPC: Cholesterol 4:4 (B) liposomes produced using the Bioruptor® Standard at 45°C using a range of volumes from 0.1 to 1 mL in a 1.5 mL tube. They were sonicated at power level M for 15 minutes of 30 seconds on, 0 seconds off cycle.....124

Figure 2.18 A – B) Size of DMPC (A) and DMPC: Cholesterol 4:4 (B) liposomes produced using the Bioruptor® Standard at 45°C using a range of volumes from 0.5 to 3 mL in a 15 mL tube. They were sonicated at power level M for 15 minutes of 30 seconds on, 0 seconds off cycle. C – D) PDI of DMPC (A) and DMPC: Cholesterol 4:4 (B) liposomes produced using the Bioruptor® Standard at 45°C using a range of volumes from 0.5 to 3 mL in a 15 mL tube. They were sonicated at power level M for 15 minutes of 30 seconds on, 0 seconds off cycle.....126

Figure 2.19: A – B) Size of DMPC (A) and DMPC: Cholesterol 4:4 (B) liposomes produced using the Bioruptor® Standard and then sonicated for 15 minutes of 30, 0 at the power level M using a 0.1 mL sample. Each position in the holder was assigned an arbitrary number between 1 and 6 and each ran 3 times to compare how much variability there was in the same position over multiple tests and between the 6 different positions available. C – D) PDI of DMPC (A) and DMPC: Cholesterol 4:4 (B) liposomes produced using the Bioruptor® Standard and then sonicated for 15 minutes of 30, 0 at the power level M using a 0.1 mL sample. Each position in the holder was assigned an arbitrary number between 1 and 6 and each ran 3 times

to compare how much variability there was in the same position over multiple tests and between the 6 different positions available.....128

Figure 2.20: Figure 6.7: A – B) Size of DMPC (A) and DMPC: Cholesterol 4:4 (B) liposomes produced using the Bioruptor® Standard at 45°C using a range of volumes from 0.5 to 3 mL in a 15 mL tube. They were sonicated at power level M for 15 minutes of 30 seconds on, 0 seconds off cycle. C – D) PDI of DMPC (A) and DMPC: Cholesterol 4:4 (B) liposomes produced using the Bioruptor® Standard at 45°C using a range of volumes from 0.5 to 3 mL in a 15 mL tube. They were sonicated at power level M for 15 minutes of 30 seconds on, 0 seconds off cycle.....130

Figure 2.21: A – B) Size of DMPC (A) and DMPC: Cholesterol 4:4 (B) liposomes were produced using the Bioruptor® Standard at 45°C using 300 µL in 1.5 mL PP tubes. They were then sonicated for 15 minutes of 30, 30 at the 3 different power levels of L, M and H. C – D) PDI of DMPC (A) and DMPC: Cholesterol 4:4 (B) liposomes were produced using the Bioruptor® Standard at 45°C using 300 µL in 1.5 mL PP tubes. They were then sonicated for 15 minutes of 30, 30 at the 3 different power levels of L, M and H.....132

Figure 2.22: A – B) Size of DMPC (A) and DMPC: Cholesterol 4:4 (B) liposomes were produced using the Bioruptor® Standard at 45°C using 300 µL in 1.5 mL PP tubes. They were then sonicated for 5 to 15 minutes of 30, 30 at power level M. C – D) PDI of DMPC (A) and DMPC: Cholesterol 4:4 (B) liposomes were produced using the Bioruptor® Standard at 45°C using 300 µL in 1.5 mL PP tubes. They were then sonicated for 5 to 15 minutes of 30, 30 at power level M.....134

Figure 2.23: A – B) Size of DMPC (A) and DMPC: Cholesterol 4:4 (B) liposomes were produced using the Bioruptor® Standard at 45°C using 100 to 1000 µL in 1.5 mL PP tubes. They were then sonicated for 15 minutes of 30, 0 at power level M. C – D) PDI of DMPC (A) and DMPC: Cholesterol 4:4 (B) liposomes were produced using the Bioruptor® Standard at

45°C using 100 - 1000 µL in 1.5 mL PP tubes. They were then sonicated for 15 minutes of 30, 0 at power level M.....136

Figure 2.24: A – B) Size of DMPC (A) and DMPC: Cholesterol 4:4 (B) liposomes were produced using the Bioruptor® Standard at 45°C using 0.5 to 2 mL in 15 mL PP tubes. They were then sonicated for 15 minutes of 30, 0 at power level M. C – D) PDI of DMPC (A) and DMPC: Cholesterol 4:4 (B) liposomes were produced using the Bioruptor® Standard at 45°C using 0.5 to 2 mL in 15 mL PP tubes. They were then sonicated for 15 minutes of 30, 0 at power level M.....138

Figure 2.25: Size (A), PDI (B) and zeta potential (C) for 6 formulations that were investigated. DMPC, DMPC: Cholesterol 4:4, PC: Cholesterol 4:4, DSPC: Cholesterol 4:4, DMPC: Cholesterol: DMPG 4:4:1 and DMPC: Cholesterol: DOTAP 4:4:1 liposomes were produced using the Bioruptor® Standard and then sonicated for 15 minutes of 30, 0 at the power level M with a 100 µL volume in a 1.5 mL TPX® tube.....141

Figure 2.26: A – B) Size of DMPC (A) and DMPC: Cholesterol 4:4 (B) liposomes produced using the Bioruptor® Plus at 40°C using 0.1 mL of sample in 1.5 mL tubes. They were then sonicated for 5 to 30 cycles at H power. C – D) PDI of DMPC (C) and DMPC: Cholesterol 4:4 (D) liposomes were produced using the Bioruptor® Plus at 40°C using 0.1 mL of sample in 1.5 mL tubes. They were then sonicated for 5 to 30 cycles at H power.....146

Figure 2.27: E - F) Size of DMPC (E) and DMPC: Cholesterol 4:4 (F) liposomes produced using the Bioruptor® Plus at 40°C using 0.1 mL of sample in 1.5 mL tubes. They were then sonicated for 5 to 30 cycles at L power. G - H) PDI of DMPC (G) and DMPC: Cholesterol 4:4 (H) liposomes were produced using the Bioruptor® Plus at 40°C using 0.1 mL of sample in 1.5 mL tubes. They were then sonicated for 5 to 30 cycles at L power.....147

Figure 2.28: A) Size of DMPC liposomes at 8, 16 and 24 mM produced using the Bioruptor® Plus at 40°C using 0.1 mL of sample in 1.5 mL tubes. They were then sonicated for 15 cycles at H power. B) PDI of DMPC liposomes at 8, 16 and 24 mM produced using the Bioruptor®

Plus at 40°C using 0.1 mL of sample in 1.5 mL tubes. They were then sonicated for 15 cycles at H power.....149

Figure 2.29: A) Size of DMPC and DMPC: Cholesterol 4:4 liposomes produced using the Bioruptor® Plus at 20, 30 and 40°C using 0.1 mL of sample in 1.5 mL tubes. They were then sonicated for 15 cycles at L and H power. B) PDI of DMPC and DMPC: Cholesterol 4:4 liposomes produced using the Bioruptor® Plus at 20, 30 and 40°C using 0.1 mL of sample in 1.5 mL tubes. They were then sonicated for 15 cycles at L and H power.....151

Figure 2.30: A) Size of DMPC and DMPC: Cholesterol 4:4 liposomes produced using the Bioruptor® Plus at 40°C using 0.1, 0.2 or 0.3 mL of sample in 1.5 mL tubes. They were then sonicated for 15 cycles at L and H power. B) PDI of DMPC and DMPC: Cholesterol 4:4 liposomes produced using the Bioruptor® Plus at 40°C using 0.1, 0.2 or 0.3 mL of sample in 1.5 mL tubes. They were then sonicated for 15 cycles at L and H power.....153

Figure 2.31: A) Size of DMPC liposomes produced using the Bioruptor® Plus at 40°C using 0.1 mL of sample in TPX® or PP 1.5 mL tubes. They were then sonicated for 15 cycles at H power. B) PDI of DMPC liposomes produced using the Bioruptor® Plus at 40°C using 0.1 mL of sample in TPX® or PP 1.5 mL tubes. They were then sonicated for 15 cycles at H power.....154

Figure 2.32: A - D) Size of DMPC liposomes produced using the Bioruptor® Plus at 40°C using 0.5, 1 or 2 mL of sample in a TPX® (A), PCT (B), PS (C) or PPCO (D) 50 mL tube. They were then sonicated for 15 cycles at H power.....156

Figure 2.33: A - D) PDI of DMPC liposomes produced using the Bioruptor® Plus at 40°C using 0.5, 1 or 2 mL of sample in a TPX® (A), PCT (B), PS (C) or PPCO (D) 50 mL tube. They were then sonicated for 15 cycles at H power.....157

Figure 2.34: A – B) Size of DMPC liposomes produced using the Bioruptor® Plus at 40°C using 0.1 mL (A) or 0.5 mL (B) of sample in 15 mL TPX® or PP tubes. They were then sonicated for 15 cycles at L and H power levels. C – D) PDI of DMPC liposomes produced

using the Bioruptor® Plus at 40°C using 0.1 mL (C) or 0.5 mL (D) of sample in 15 mL TPX® or PP tubes. They were then sonicated for 15 cycles at L and H power levels.....159

Figure 2.35: A – B) Size of DMPC: Cholesterol liposomes produced using a range of ratios using the Bioruptor® Plus at 40°C using 0.1 mL sample in a 1.5 mL TPX® tube. They were then sonicated for 15 cycles at L (A) and H (B) power levels. C – D) PDI of DMPC: Cholesterol liposomes produced using a range of ratios using the Bioruptor® Plus at 40°C using 0.1 mL sample in a 1.5 mL TPX® tube. They were then sonicated for 15 cycles at L (C) and H (D) power levels.....162

Figure 2.36: A – C) Size of DMPC: Cholesterol liposomes produced with the addition of 1, 2 or 4 mM of DOPE (A), DMPG (B) or DOTAP (C) lipid. The Bioruptor® Plus was used at 40°C using 0.1 mL sample in a 1.5 mL TPX® tube. They were then sonicated for 15 cycles at H power level. D - F) PDI of DMPC: Cholesterol liposomes produced with the addition of 1, 2 or 4 mM of DOPE (D), DMPG (E) or DOTAP (F) lipid. The Bioruptor® Plus was used at 40°C using 0.1 mL sample in a 1.5 mL TPX® tube. They were then sonicated for 15 cycles at H power level.....165

Figure 2.37: A - C) Zeta potential of DMPC: Cholesterol liposomes produced with the addition of 1, 2 or 4 mM of DOPE (A), DMPG (B) or DOTAP (C) lipid. The Bioruptor® Plus was used at 40°C using 0.1 mL sample in a 1.5 mL TPX® tube. They were then sonicated for 15 cycles at H power level.....166

Figure 2.38: A – B) Size (A) and PDI (B) of DMPC and DMPC: Cholesterol liposomes produced using the Bioruptor® Pico at 40°C using 0.1 mL sample in a 1.5 mL TPX® tube. They were then sonicated for up to 10 cycles. C – D) Size (C) and PDI (D) of DMPC and DMPC: Cholesterol liposomes produced using the Bioruptor® Pico at 40°C using 0.1 to 0.3 mL sample in a 1.5 mL TPX® tube. They were then sonicated for 10 cycles.....170

Figure 3.1: A) Average absorption for Experiment 1 settings, 0.65 ml tubes were sonicated with 0.1 ml samples in Pico, from 3 to 15 cycles with standard deviation. B) Relative standard deviation for Experiment 1 from 3 to 15 cycles.....	182
Figure 3.2: A) Average absorption for Experiment 2 settings, 0.65 ml tubes were sonicated with 0.2 ml samples in Pico, from 3 to 15 cycles with standard deviation. B) Relative standard deviation for Experiment 2 from 3 to 15 cycles.....	183
Figure 3.3: A) Average absorption for Experiment 3 settings, 0.5 ml tubes were sonicated with 0.1 ml samples in Pico, from 3 to 15 cycles with standard deviation. B) Relative standard deviation for Experiment 3 from 3 to 15 cycles.....	182
Figure 3.4: A) Average absorption for Experiment 4 settings, 1.5 ml tubes were sonicated with 0.3 ml samples in Pico, from 3 to 15 cycles with standard deviation. B) Relative standard deviation for Experiment 4 from 3 to 15 cycles.....	185
Figure 3.5: A) Average absorption for Experiment 5a settings, 1.5 ml TPX® tubes were sonicated with 0.1 ml samples in Pico, from 3 to 15 cycles with standard deviation. B) Relative standard deviation for Experiment 5a from 3 to 15 cycles.....	186
Figure 3.6: A) Average absorption for Experiment 5b settings, 1.5 ml TPX® tubes were sonicated with 0.2 ml samples in Pico, from 3 to 15 cycles with standard deviation. B) Relative standard deviation for Experiment 5b from 3 to 15 cycles.....	187
Figure 3.7: A) Average absorption for Experiment 5c settings, 1.5 ml TPX® tubes were sonicated with 0.3 ml samples in Pico, from 3 to 15 cycles with standard deviation. B) Relative standard deviation for Experiment 5c from 3 to 15 cycles.....	188
Figure 3.8: (A) Overall line plot showing absorption of the different Pico experiments absorption averages. Absorption peak heights for (B) 3, (C) 5, (D) 10 and (E) 15 cycles...	190

Figure 3.9: A) Average absorption for Experiment 6 settings, 1.5 ml TPX® tubes were sonicated with 0.3 ml samples at H power in Plus, from 3 to 15 cycles with standard deviation.	
B) Relative standard deviation for Experiment 6 from 3 to 15 cycles.....	191
Figure 3.10: A) Average absorption for Experiment 7 settings, 1.5 ml TPX® tubes were sonicated with 0.3 ml samples at L power in Plus, from 3 to 15 cycles with standard deviation.	
B) Relative standard deviation for Experiment 7 from 3 to 15 cycles.....	192
Figure 3.11: A) Average absorption for Experiment 8 settings, 1.5 ml BioSigma tubes were sonicated with 0.3 ml samples at H power in Plus, from 3 to 15 cycles with standard deviation.	
B) Relative standard deviation for Experiment 8 from 3 to 15 cycles.....	193
Figure 3.12: A) Average absorption for Experiment 9 settings, 1.5 ml BioSigma tubes were sonicated with 0.3 ml samples at L power in Plus, from 3 to 15 cycles with standard deviation.	
B) Relative standard deviation for Experiment 9 from 3 to 15 cycles.....	194
Figure 3.13: A) Average absorption for Experiment 10 settings, 1.5 ml TPX® tubes were sonicated with 0.1 ml samples at H power in Plus, from 3 to 15 cycles with standard deviation.	
B) Relative standard deviation for Experiment 10 from 3 to 15 cycles.....	195
Figure 3.14: A) Average absorption for Experiment 11 settings, 1.5 ml TPX® tubes were sonicated with 0.2 ml samples at H power in Plus, from 3 to 15 cycles with standard deviation.	
B) Relative standard deviation for Experiment 11 from 3 to 15 cycles.....	196
Figure 3.15: A) Average absorption for Experiment 12 settings, 1.5 ml BioSigma tubes were sonicated with 0.1 ml samples at H power in Plus, from 3 to 15 cycles with standard deviation.	
B) Relative standard deviation for Experiment 12 from 3 to 15 cycles.....	197
Figure 3.19: A) Average absorption for Experiment 13 settings, 1.5 ml BioSigma tubes were sonicated with 0.2 ml samples at H power in Plus, from 3 to 15 cycles with standard deviation.	
B) Relative standard deviation for Experiment 13 from 3 to 15 cycles.....	198

Figure 3.17: (A) Overall line plot showing absorption of the experiments 10 to 13 absorption averages. Absorption peak heights for (B) 3, (C) 5, (D) 10 and (E) 15 cycles.....	199
Figure 3.18: A) Average absorption for Experiment 14 settings, 1.5 ml BioSigma tubes were sonicated with 0.1 ml samples at H power at 10 °C in Plus, from 3 to 15 cycles with standard deviation. B) Relative standard deviation for Experiment 14 from 3 to 15 cycles.....	200
Figure 3.19: A) Average absorption for Experiment 15 settings, 1.5 ml BioSigma tubes were sonicated with 0.2 ml samples at H power at 10 °C in Plus, from 3 to 15 cycles with standard deviation. B) Relative standard deviation for Experiment 15 from 3 to 15 cycles.....	201
Figure 3.20: A) Average absorption for Experiment 16 settings, 1.5 ml BioSigma tubes were sonicated with 0.1 ml samples at H power at 20 °C in Plus, from 3 to 15 cycles with standard deviation. B) Relative standard deviation for Experiment 16 from 3 to 15 cycles.....	202
Figure 3.21: A) Average absorption for Experiment 17 settings, 1.5 ml BioSigma tubes were sonicated with 0.2 ml samples at H power at 20 °C in Plus, from 3 to 15 cycles with standard deviation. B) Relative standard deviation for Experiment 17 from 3 to 15 cycles.....	203
Figure 3.22: (A) Overall line plot showing absorption of the experiments 14 to 17 absorption averages. Absorption peak heights for (B) 3, (C) 5, (D) 10 and (E) 15 cycles.....	204
Figure 3.23: Assay 1 results showing the difference in DNA concentration achieved with or without a filter stage.....	207
Figure 3.24: Assay results showing DNA concentration results for each of the 3 chosen buffers.....	208
Figure 3.25: Assay results showing DNA concentration for three different conditions.....	209

Figure 4.1 All runs were with Bioruptor® Plus, 0.01 % carbon nanotube concentration, 0.1 % surfactant concentration, 5 or 13°C water bath temperature, 2 mL sample size, Nalgene™ Polycarbonate tubes, cycle set up of 60 cycles of 60 seconds on, 15 seconds off, L power level. Ultracentrifugation for 150 minutes at 40, 000 G at 17°C. A) SDS dispersed carbon nanotubes at 13 °C. B) SDS dispersed carbon nanotubes at 5 °C. C) SDBS dispersed carbon nanotubes at 13 °C. D) SDBS dispersed carbon nanotubes at 5 °C.....220

Figure 4.2 A: All runs were with Bioruptor® Plus, 0.01 % carbon nanotube concentration, 0.1 % SDBS concentration, 2 mL sample size, Nalgene™ Polycarbonate tubes, cycle set up of 60 cycles of 60 seconds on, 15 seconds off, L power level. Ultracentrifugation for 150 minutes at 40, 000 G at 17°C. Results represent n = 3. Sonication temperature of 5 °C (grey), 13 °C (orange), 20 °C (blue), 30 °C (yellow), 40 °C (green). B) Absorption peak averages for the three runs at 976 nm for the 5 temperatures investigated. C) Absorption peak averages for the three runs at 566 nm for the 5 temperatures investigated.....224

Figure 4.3 All runs were with Bioruptor® Plus, 0.01 % carbon nanotube concentration, 0.1 % surfactant concentration, 5 or 13°C water bath temperature, 2 mL sample size, Nalgene™ Polycarbonate tubes, cycle set up of 60 cycles of 60 seconds on, 15 seconds off, L power level. Ultracentrifugation for 150 minutes at 40, 000 G at 17°C. A) SDS dispersed carbon nanotubes at 5 °C B) SDBS dispersed carbon nanotubes at 13 °C C) SDBS dispersed carbon nanotubes at 20 °C D) SDBS dispersed carbon nanotubes at 30 °C. E) SDBS dispersed carbon nanotubes at 40 °C.....225

Figure 4.4 All runs were with Bioruptor® Plus, 0.01 % carbon nanotube concentration, 0.1 % surfactant concentration, 2 mL sample size, Nalgene™ Polycarbonate tubes, cycle set up of 60 cycles of 60 seconds on, 15 seconds off, L power level. Ultracentrifugation for 150 minutes at 40, 000 G at 17°C. A) PL plot of 5 °C sample. B) PL plot of 13 °C sample. C) PL plot of 20 °C sample. D) PL plot of 30 °C sample. E) PL plot of 40 °C sample.....226

Figure 4.5 A) Average UV –Vis spectra showing dispersion of carbon nanotubes using different cycle settings. B) Average peak height at each cycle setting at 566 nm. C) Average peak height at each cycle setting at 976 nm.....228

Figure 4.6 All runs were with Bioruptor® Plus, 0.01 % carbon nanotube concentration, 0.1 % surfactant concentration, 5 or 13°C water bath temperature, 2 mL sample size, Nalgene™ Polycarbonate tubes, cycle set up of 60 cycles of 60 seconds on, 15 seconds off, L power level. Ultracentrifugation for 150 minutes at 40, 000 G at 17°C. A) Carbon nanotubes sonicated at 5 °C with no dilution, diluted 1 in 2 and 1 in 10. B) Carbon nanotubes sonicated at 13 °C with no dilution, diluted 1 in 2 and 1 in 10. C) Carbon nanotubes sonicated at 20 °C with no dilution, diluted 1 in 2 and 1 in 10.....230

Figure 4.7 A) 566 and 976 nm peak heights for diluted samples compared to theoretical peak height for 50 % and 10 % of initial peak height. B) Difference from the theoretical value for the peak height for the 1/2 and 1/10 dilutions.....231

Figure 4.8 All runs were with probe sonicator, 0.01 % carbon nanotube concentration, 0.1 % surfactant concentration, in an ice bath, 2 mL sample size, 10 amp power level. Ultracentrifugation for 150 minutes at 40, 000 G at 17°C. A) Carbon nanotubes dispersed in SDBS over time using the probe sonicator. Absorption peak height at 976 nm. B) Carbon nanotubes dispersed in SDBS over time using the probe sonicator. Absorption peak height at 566 nm.....234

Figure 4.9 All runs were with probe sonicator, 0.01 % carbon nanotube concentration, 0.1 % surfactant concentration, in an ice bath, 2 mL sample size, 10 amp power level. Ultracentrifugation for 150 minutes at 40, 000 G at 17°C. A) Carbon nanotube size dispersed with SDBS at varying times using the probe sonicator. B) Carbon nanotube PDI dispersed with SDBS at varying times using the probe sonicator.....235

Figure 4.10: All runs were with probe sonicator, 0.01 % carbon nanotube concentration, 0.1 % surfactant concentration, in an ice bath, 2 mL sample size, 10 amp power level. Ultracentrifugation for 150 minutes at 40, 000 G at 17°C. A) PL plot of probe sonicated carbon nanotubes after 30 minutes. B) PL plot of probe sonicated carbon nanotubes after 60 minutes. C) PL plot of probe sonicated carbon nanotubes after 90 minutes. D) PL plot of probe sonicated carbon nanotubes after 120 minutes.....236

Figure 4.11: All runs were with Bioruptor® Plus, 0.01 % carbon nanotube concentration, 0.1 % surfactant concentration, 13°C water bath temperature, 2 mL sample size, Nalgene™ Polycarbonate tubes, cycle set up of 60 cycles of 60 seconds on, 15 seconds off, L power level. Ultracentrifugation for 150 minutes at 40, 000 G at 17°C. A) Average peak heights at 566 nm for each of the three surfactants tested. B) Average peak heights at 976 nm for each of the three surfactants tested. C) PL dispersion of MPC dispersed carbon nanotubes. D) PL of MPC without carbon nanotubes present.....239

Figure 4.12: All runs were with Bioruptor® Plus, 0.01 % carbon nanotubes concentration, 0.1 % surfactant concentration, 2 mL sample size, Nalgene™ Polycarbonate tubes, cycle set up of 60 cycles of 60 seconds on, 15 seconds off, L power level. Ultracentrifugation for 150 minutes at 40, 000 G at 17°C. Results represent n = 3. DMPC (grey), SDBS (orange) and SDS (blue).....241

Figure 4.13: All runs were with Bioruptor® Plus, 0.01 % carbon nanotube concentration, 0.1 to 1 % surfactant concentration, 13°C water bath temperature, 2 mL sample size, Nalgene™ Polycarbonate tubes, cycle set up of 60 cycles of 60 seconds on, 15 seconds off, L power level. Ultracentrifugation for 150 minutes at 40, 000 G at 17°C. A) Absorption peak height at 566 nm for each sample at each surfactant concentration. B) Absorption peak height at 976 nm for each sample at each surfactant concentration. C) Absorption peak height at 995 nm for each sample at each surfactant concentration.....244

Figure 4.14 All runs were with Bioruptor® Plus, 0.01 % carbon nanotube concentration, 0.1 to 1 % surfactant concentration, 13°C water bath temperature, 2 mL sample size, Nalgene™ Polycarbonate tubes, cycle set up of 60 cycles of 60 seconds on, 15 seconds off, L power level. Ultracentrifugation for 150 minutes at 40, 000 G at 17°C. A) PL plot of SDBS 5 mg sample. B) PL plot of SDBS 3 mg sample. C) PL plot of SDBS 1 mg sample. D) PL plot of SDS 5 mg sample. E) PL plot of SDS 3 mg sample. F) PL plot of SDS 1 mg sample.....245

Figure 4.15: All runs were with Bioruptor® Plus, 0.01 % carbon nanotube concentration, 0.1 to 1 % surfactant concentration, 13°C water bath temperature, 2 mL sample size, Nalgene™ Polycarbonate tubes, cycle set up of 60 cycles of 60 seconds on, 15 seconds off, L power level. Ultracentrifugation for 150 minutes at 40, 000 G at 17°C. A) PL plot of MPC 5 mg sample. B) PL plot of MPC 3mg sample. C) PL plot of MPC 1 mg sample.....246

Figure 4.16 All runs were with Bioruptor® Plus, 0.01 % carbon nanotube concentration, 0.1% surfactant concentration, 13 or 40 °C water bath temperature, 2 mL sample size, Nalgene™ Polycarbonate tubes, cycle set up of 60 cycles of 60 seconds on, 15 seconds off, L power level. Ultracentrifugation for 150 minutes at 40, 000 G at 17°C. A) Absorption peak height value at 566 nm for each stability study sample. B) Absorption peak height value at 976 nm for each stability study sample.....248

Figure 4.17: All runs were with Bioruptor® Plus, 0.01 % carbon nanotube concentration, 0.1% surfactant concentration, 13 or 40 °C water bath temperature, 2 mL sample size, Nalgene™ Polycarbonate tubes, cycle set up of 60 cycles of 60 seconds on, 15 seconds off, L power level. Ultracentrifugation for 150 minutes at 40, 000 G at 17°C. A) Percentage difference from week 0 for each stability study sample at 566 nm. B) Percentage difference from week 0 for each stability study sample at 976 nm.....249

Figure 5.1: All runs were with Bioruptor® Plus, 0.01 % carbon nanotube concentration, 0.1% surfactant concentration, 13 or 40 °C water bath temperature, 2 mL sample size, Nalgene™ Polycarbonate tubes, cycle set up of 60 cycles of 60 seconds on, 15 seconds off, L power level. Ultracentrifugation for 150 minutes at 40, 000 G at 17°C. A) PL plot of a typical HiPco carbon nanotube sample dispersed with SDBS. B) UV – Vis – NIR plot of HiPco carbon nanotubes in D₂O. C) UV – Vis – NIR plot of CoMoCat carbon nanotubes in D₂O.....259

Figure 5.2: A - C: The CoMoCat sample initial - All runs were with Bioruptor® Plus, 0.01 % carbon nanotube concentration, 0.1% surfactant concentration, 13 or 40 °C water bath temperature, 2 mL sample size, Nalgene™ Polycarbonate tubes, cycle set up of 60 cycles of 60 seconds on, 15 seconds off, L power level. Ultracentrifugation for 150 minutes at 40, 000 G at 17°C. CoMoCat nanotubes, dispersed in NMP 0.01 mg / ml (standard US, hard plastic Eppendorf), centrifuged at 13400 rpm, 30 min, deposited on a standard TEM grid.....260

Figure 5.3: 40 mg initial carbon nanotube weight oleum: nitric acid carboxylation modification method, s8 at 65 °C sand bath temperature, s11 at 20 °C sand bath temperature, UV – Vis – NIR data for each of the samples.....262

Figure 5.4: 40 mg initial CoMoCat carbon nanotube weight, oleum: nitric acid carboxylation modification method, s9 at 20 °C sand bath temperature. A) Pre centrifuge sample. B) Post centrifuge and surfactant addition sample.....263

Figure 5.5: A - C: Sample D13_17 - CoMoCat nanotubes after oxidative treatment at 20 ° C. The dry sample was dispersed in NMP 0.01 mg / ml (standard US, Eppendorf's from hard plastic), centrifuged 13400 rpm, 30 min, deposited on a standard TEM grid. The tubes are tangled, but less dense than for initial CoMoCat, there are metal particles in them, but clearly there are less of them than in CoMoCat. Individual tubes are the same curves and dirty. Length of tubes: bundles of several microns, as in CoMoCat. It is possible to find individual bundles with 200 – 500 nanometres in length.....264

Figure 5.6 A - D: Sample s8_17. A) PL map of CoMoCat nanotubes after oxidative treatment at 65 ° C. B – D) TEM of CoMoCat nanotubes after oxidative treatment at 65 ° C. The dry sample (1 mg / ml) is dispersed (standard US, hard Eppendorf) in aqueous NaOH (10⁻³ mol / L), centrifuged 13400 rpm, 30 minutes (quite a lot of sediment - obviously aging of the sample, diluted 10-fold, again sound + centrifugation. The deposition is on the standard TEM grid (in Aston). We observe an amorphous matter that clogs the pores of the grating. Perhaps some dark particles, about 20 nm in size which are quickly deteriorating under the beam (so we could not make a good picture in high resolution).....265

Figure 5.7: 40 mg initial HiPco carbon nanotube weight, oleum: nitric acid carboxylation modification method, s10 at 65 °C sand bath temperature, s11 at 20 °C sand bath temperature. A) Pre centrifuge sample. B) Post centrifuge sample. C) Post centrifuge with surfactant addition sample.....266

Figure 5.8: 40 mg initial carbon nanotube weight oleum: nitric acid carboxylation modification method, s8 and s10 at 65 °C sand bath temperature, s9 and s11 at 20 °C sand bath temperature. A) DLS data for all samples. B) PDI data for all samples.....268

Figure 5.9: A) Probe sonicated carbon nanotubes after 1 hour at 40 %. B) Probe sonicated carbon nanotubes after 1 hour at 100 %. C) Probe sonicated carbon nanotubes after 2 hours. D) Probe sonicated carbon nanotubes after 3 hours. E) Probe sonicated carbon nanotubes after 4 hours.....270

Figure 5.10: F. DLS of probe sonicated carbon nanotubes from 1 to 4 hours.....271

Figure 5.11: A) Bath sonicated carbon nanotubes after 1 cycle. B) Bath sonicated carbon nanotubes after 2 cycles. C) Bath sonicated carbon nanotubes after 3 cycles. D) UV – Vis peak heights at 566 nm. E) UV – Vis heights at 976 nm.....272

Figure 5.12: A) DLS size of liposomes in conjunction with carbon nanotubes either sonicated beforehand or not. B) PDI of liposomes in conjunction with carbon nanotubes either sonicated

beforehand or not. C) UV – Vis data showing both types of carbon nanotubes before or after sonication.....274

Figure 5.13: A) carbon nanotubes plus liposomes with no sonication – HiPco carbon nanotubes. B) Carbon nanotubes plus liposomes with no sonication – CoMoCat carbon nanotubes. C) Carbon nanotubes plus liposomes with sonication – HiPco carbon nanotubes. D) Carbon nanotubes plus liposomes with sonication – CoMoCat carbon nanotubes.....275

List of Tables

Table 1.1: Current approved liposome formulations on the market. Nearly all liposome formulations on the current market contain cholesterol to be a stabilising agent, nearly all are administered intravenous, many contain PEG and many contain multiple lipids to optimise the formulation for its role. Roles include to fight cancer, pain management and to combat fungal infections.....50

Table 1.2: Advantages and disadvantages of each Bioruptor machine used in the formation and optimisation of the liposome size reduction protocols.....73

Table 2.1: Initial experimental results for DMPC and DMPC Cholesterol 6:4 using the lipid hydration and sonication methods.....88

Table 4.1: Bioruptor® Plus bath sonicator system cycle settings used for this study keeping the total time as similar as possible.....215

Abbreviations

AFM – Atomic Force microscopy

AM – Ammonium Molybdate

ANOVA – Analysis Of Variance

CF – Carboxyfluorescein

CPP – Critical Packing Parameter

DCC - N, N'-dicyclohexylcarbodiimide

DDA - Dimethyldioctadecylammonium (Bromide Salt)

DilC - 1, 1'-Dioctadecyl-3, 3', 3'-Tetramethylindocarbocyanine Perchlorate

DLS – Dynamic light scattering

DMPC - 1, 2-ditetradecanoyl-sn-glycero-3-phosphocholine

DMPG - 1, 2-Dimyristoyl-Sn-glycero-3-phospho-rac-(1-glycerol) sodium salt

DNA - Deoxyribonucleic acid

DOPE - 1, 2-Dioleoyl-sn-glycero-3-phosphoethanolamine

DOTAP - N-[1-(2, 3-Dioleoyloxy) propyl]-N, N, N-trimethylammonium chloride

DPPC - 1, 2-Dipalmitoyl-sn-glycero-3-phosphocholine

DPPG - 1, 2-Dipalmitoyl-Sn-glycero-3-phospho-rac-(1-glycerol) ammonium salt

DSPE - 1, 2-Distearoyl-sn-glycero-3-phosphoethanolamine

DSPC - 1, 2-Distearoyl-sn-glycero-3-phosphocholine

DSPC – PEG₂₀₀₀ - 1, 2-Distearoyl-sn-glycero-3-phosphocholine

DSPG - 1, 2-Distearoyl-Sn-glycero-3-phospho-rac-(1-glycerol) sodium salt

DW – Double walled

EDC - N-(3 - dimethylaminopropyl) - N'-ethylcarbodiimide

EDTA - Ethylenediaminetetraacetic acid

EM - Emission

EPC - 1, 2-dioleoyl-sn-glycero-3-ethylphosphocholine (chloride salt)

EX - Excitation

FFPE - Formalin-Fixed Paraffin-Embedded

H - High

HPLC – High Performance Liquid Chromatography

HSM – High Shear Mixing
HSPC - L- α -phosphatidylcholine, hydrogenated (Soy)
ICH - International Conference on Harmonisation
KI – Potassium Iodide
L - Low
LH – Lipid Film Hydration
LOD – Limit of detection
LOQ – Limit of quantification
LUV – Large Unilamellar Vesicles
M - Medium
M1 – Medium Low
M2 – Medium High
MLV – Multilamellar Vesicles
MPC - 1-ditetradecanoyl-sn-glycero-3-phosphocholine
MW – Multi walled
NBD – F - N-(7-nitrobenz-2-oxa-1, 3-diazol-4-yl) dioleoyl phosphatidylethanolamine
NHS - N-hydroxysuccinimide
PBS – Phosphate Buffered Saline
PC - Phosphatidylcholine
PCT – Polycarbonate Tube
PCR - Polymerase chain reaction
PDI - Polydispersity
PL - Photoluminescence
PP - Polypropylene
PPCO – Polypropylene Co-polymer
PTFE - Polytetrafluoroethylene
RSD – Relative Standard Deviation
RT – Room temperature
SD – Standard Deviation
SDBS - Sodium dodecylbenzenesulfonate
SDOC - sodium cholate
SDS - Sodium dodecyl sulfate

SEC – Size exclusion chromatography

SUV – Small Unilamellar Vesicles

TDB - D-(+)-trehalose 6, 6'-dibehenate

TEM – Transmission Electron Microscopy

TFA - Trifluoroacetic acid

UV – Vis – NIR – Ultra Violet – Visible – Near Infra-Red

XPS - X-ray photoelectron spectroscopy

List of publications

1. Swapnil Khadke, Peter Stone, Aleksey Rozhin, Jerome Kroonen, Yvonne Perrie, Point of use production of liposomal solubilised products, International Journal of Pharmaceutics, Volume 537, Issues 1–2, 2018, Pages 1-8.
2. Roces, Carla B and Kastner, Elisabeth and Stone, Peter and Lowry, Deborah and Perrie, Yvonne (2016) Rapid quantification and validation of lipid concentrations within liposomes. Pharmaceutics, 8 (29). pp. 1-11.
3. That's about the size of it. Article for UKICRS 2015 newsletter, page 36. Winner of travel award for CRS. Author – Peter Stone.

Abstracts

1. A comparison between different surfactants for dispersion of carbon nanotubes Peter Stone, Dr Craig Russell, Prof Yvonne Perrie, Jerome Kroonen, Dr Alex Rozhin, 2018 UKICRS symposium, Belfast, UK. Abstract #50, Accepted 3rd May 2018.

2. Stone, P J, Russell, C, Rozhin, A, Kroonen, J, Perrie, Y. (2017) a study into how plastic composition affects liposome size reduction efficiency using the Bioruptor® plus bath sonicator. LHS research day Aston University, Birmingham, UK. Accepted 30th May 2017.
3. Stone, P J, Russell, C, Rozhin, A, Kroonen, J, Perrie, Y. (2017) Optimizing liposome size reduction using Bioruptor® Plus bath sonicator systems. APS 8th International PharmSci Conference 2017, Hatfield, UK. Abstract # 59. Accepted 28th April 2017.
4. Stone, P J, Russell, C, Rozhin, A, Kroonen, J, Perrie, Y. (2017) a study into how plastic composition affects liposome size reduction efficiency using the Bioruptor® plus bath sonicator. 2017 UKICRS symposium, Glasgow, UK. Abstract # 47. Accepted 26th April 2017.
5. Stone, P J, Russell, C, Rozhin, A, Kroonen, J, Perrie, Y. (2017) Optimizing liposome size reduction using Bioruptor® Plus bath sonicator systems. The 44th Annual Meeting and Exposition of the controlled release society, Boston, USA. Abstract # 3517. Accepted 30th March 2017.
6. Stone, P J, Rozhin, A, Kroonen, J, Perrie, Y. (2016) New developments in sonication to produce small, homogenous liposome populations. APS 7th International PharmSci Conference 2016, Glasgow, UK. Abstract # 135. Accepted: 13th June 2016.

7. Stone, P J, Perrie, Y, Kroonen, J, Rozhin, A (2016) Dispersion of CoMoCat® nanotubes using the Bioruptor Plus® bath sonicator for the preparation of single-walled carbon nanotubes. APS 7th International PharmSci Conference 2016, Glasgow, UK. Abstract # 129. Accepted: 13th June 2016.
8. Stone, P J, Rozhin, A, Kroonen, J, Perrie, Y. (2016) Preparation of bilayer loaded liposomes via sonication. The 43rd Annual Meeting and Exposition of the controlled release society, Seattle, USA. Abstract #613. Accepted: 18th May 2016.
9. Stone, P J, Perrie, Y, Kroonen, J, Rozhin, A (2016) Dispersion of CoMoCat® single-walled nanotubes using the Bioruptor Plus® bath sonicator. LHS research day Aston University, Birmingham, UK. Accepted: 6th May 2016.
10. Stone, P J, Rozhin, A, Kroonen, J, Perrie, Y. (2016) formulation of sonicated bilayer loaded liposomes. 2016 UKICRS symposium, Cardiff, UK. Accepted: 7th March 2016.
11. Stone, P J, Rozhin, A, Kroonen, J, Perrie, Y. (2015) Small scale rapid production of liposomes using The Bioruptor® bath sonication device. ILS 2015 meeting, liposomes in drug and vaccine delivery, London, UK. Accepted: 16th November 2015.
12. Stone, P J, Rozhin, A, Kroonen, J, Perrie, Y. (2015) New developments in sonication to produce small, homogenous liposome populations. APS 6th International PharmSci Conference 2015, Nottingham, UK. Abstract #18. Accepted: 8th June 2015.

13. Stone, P J, Rozhin, A, Allaer, D, Perrie, Y. (2015) Bath sonication: A better method for the production of size reduced liposomes than probe sonication? LHS research day Aston University, Birmingham, UK. Accepted: 21st April 2015.
14. Stone, P J, Rozhin, A, Allaer, D, Perrie, Y. (2015) High shear mixing: An alternative approach for the size reduction of liposomes. The 42nd Annual Meeting and Exposition of the controlled release society, Edinburgh, UK. Abstract #669. Accepted: 6th April 2015.
15. Stone, P J, Rozhin, A, Allaer, D, Perrie, Y. (2015) Size reduction of liposomes: A comparative study between high shear mixing and probe sonication. 2015 UKICRS symposium, Nottingham, UK. Accepted: 5th March 2015.

1. Introduction

1.1 The problem at hand

Vaccines are a vital part of the healthcare system throughout the world and are a major preventer of disease. Vaccines work by inducing an immune system response with what is known as an antigen. An antigen is any substance such as a virus, bacteria or fungi that stimulates a response from the immune system to create antibodies. These antibodies are then used when the actual disease does invade the body as the immune system is now prepared to recognise the foreign body and destroy it before the disease can take hold and cause damage (Schwendener, 2014). Liposomes are already in use as a vaccine delivery system as their amphiphilic structure allows for delivery of the antigen and other parts such as an adjuvant which is used to enhance the immune response, as well as possibly antibiotics, preservatives and stabilisers (Tandrup Schmidt et al., 2016). Carbon nanotubes could be used in conjunction with the liposomes to enhance the immune system response and this was the aim of this work. Carbon nanotubes have been shown in some forms to suppress the immune system and others shown to enhance the response. Some forms have been shown to be toxic and others have been shown to cause no toxicity (Fadel and Fahmy, 2014). Therefore, this work also wanted to focus on forming multiple different forms of carbon nanotubes, different in length, chirality and modification, to investigate their toxicity and other effects on cells.

1.2 Liposomes as a spherical nanoscale drug and vaccine delivery system

1.2.1 Liposomes background

Liposomes are spherical vesicles made up of mostly phospholipid bilayers that can be in either the nanometre or micrometre range in diameter. Liposomes can be formed with multiple bilayers encapsulating a hydrophilic centre such as multilamellar vesicles (MLV), or just have the one lipid bilayer such as small unilamellar vesicles or large unilamellar vesicles (SUV and LUV) (Szoka and Papahadjopoulos, 1978, Philippot and Schuber, 1994, Liu, 2011).

Depending on the critical packing parameter (CPP), lipids can also form a micelle, where a single layer of lipids comes together to form a spherical structure with the head groups on the outside and the tails within the ball as shown below in Figure 1.1 (Menger, 1979, Dominguez et al., 1997).




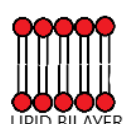
SHAPE	CPP VALUE	EXAMPLE COMPOUNDS STRUCTURES FORMED
 Cone	$CPP = < 1/3$	SDS <chem>CCCCCCCCCCCCCCCCOS(=O)(=O)[O-].[Na+]</chem> SDBS <chem>CCCCCCCCC1=CC=C(C=C1)S(=O)(=O)[O-].[Na+]</chem> 14:0 Lyso PC <chem>CCCCCCCCCCCCCCCC(=O)OCCOP(=O)([O-])OCC[N+](C)(C)C.[Na+]</chem>  SPHERICAL MICELLES
 Cylinder	$CPP = \sim 1$	DMPC <chem>CCCCCCCCCCCCCCCC(=O)OCCOP(=O)([O-])OCC[N+](C)(C)C.[Na+]</chem> <chem>CCCCCCCCCCCCCCCC(=O)OCCOP(=O)([O-])OCC[N+](C)(C)C.[Na+]</chem>  LIPID BILAYER

Figure 1.1: The shapes and structures formed by the lipids and surfactants used in this work as well as their structures and approximate CPP values.

The equation used to describe the critical packing parameter is defined as v/a_0l_c . V is defined as the volume of the lipophilic chain, a_0 is the area occupied by the hydrophilic head group, and l_c is the length of the lipophilic chain (Israelachvili, 2011). The CPP then can be used to predict the particular packing arrangement an individual lipid will take. A lipid with a CPP value of $1/3$ or smaller favours forming a spherical micelle, because of the large hydrophilic head group. Those between $1/3$ and $1/2$ favour the cylindrical micelle conformation. For a flexible vesicle, the CPP should be somewhere between $1/2$ and 1 and for a bilayer it should be approximately 1 . The final structure that can be formed is an inverted micelle where the lipophilic chains are larger than the head group.

A large range of lipids are used for liposome formulations, with many formulations having a mixture of lipids to combine the good factors of the different lipids used. They can be modified in many different ways depending on their purpose. This can include the addition of polyethylene glycol (PEG) to allow the liposomes to hide from the immune system and therefore reach their site of action without being removed. This is done by reducing the charge of the liposome surface closer to neutral and by occupying the space immediately next to the liposome surface; since PEG is a large molecule, this inhibits other macromolecules from

interacting with the liposome, such as macrophages. The addition of cholesterol helps stabilise the lipid bilayer membranes. They can also be thermally modified to allow release of the drug inside at a certain temperature, using an external device to heat the certain area once the liposomes have been injected. They can also be magnetised which means when the liposomes are injected and then a magnet applied to the area where the liposomes are required, they are held and release their drug over time. This reduces the side effects as the liposomes then do not release their drug in other areas of the body.

1.2.2 Current methods for the formation of liposomes

Lipids on their own do not have the energy to form these lipid bilayers below their lipid film transition temperature and therefore energy is required to be added into the system to form bilayers for many lipids (Gregoriadis and Perrie, 2010). The formation of liposomes can be done in a number of different ways (Torchilin and Weissig, 2003). Some methods, such as extrusion and probe sonication have been around nearly as long as liposomes have been known about since the 1960s (Bangham et al., 1965). These methods generally follow the top down approach (Figure 1.2).

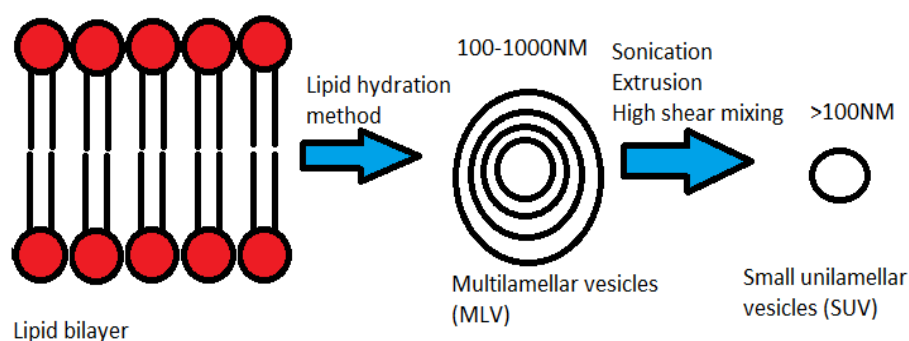


Figure 1.2: Liposomes being produced using the top down method, whereby lipids form a bilayer, and then using the lipid hydration method are formed into MLV and then through a variety of methods such as sonication, both bath and probe, extrusion and high shear mixing, are reduced in size to the SUV level (Avanti, 2015, Rathod and Deshpande, 2010).

One of the most common and well used top down methods of liposome production is sonication (Kreuter, 1994). Sonication works by using sonic energy that puts pressure on the MLV bilayer and breaks them up so that they form smaller liposomes within the Nano size range (Maulucci et al., 2005, Dua, 2012). Sonication is a common and often preferred method because it is quick and easy with only two relatively simple steps of sonication and centrifugation (Akbarzadeh et al., 2013). This method is split into two different forms, probe sonication and bath sonication (Figure 1.3). Probe sonication is the more common method used as it is a cheap, simple and quick method and has been far more extensively investigated compared to bath sonication (Lapinski et al., 2007, Duzgunes, 2005, Liu, 2008, Jain, 2008, Vo-Dinh, 2003). However, it can cause lipid degradation resulting from excessive heat and titanium contamination from the probe tip, necessitating subsequent centrifugation to remove these particles (Philippot and Schuber, 1994, Foged et al., 2014, Venkateswarlu I, 2011). A methodology for probe sonication liposome size reduction is shown below in Figure 1.4.



Figure 1.3: Bath (A) and probe (B) sonication diagrams showing how each method works to reduce the size of the sample. For bath sonication shown in Figure 1.3 A, the samples are placed into a temperature-controlled water bath. This whole water bath is then sonicated using a device fitted to the bottom of the water bath, thereby giving non-contact sonication to the sample, reducing its size. For probe sonication shown in Figure 1.3 B, the sonic energy is transmitted directly down a probe that is placed directly into the sample.

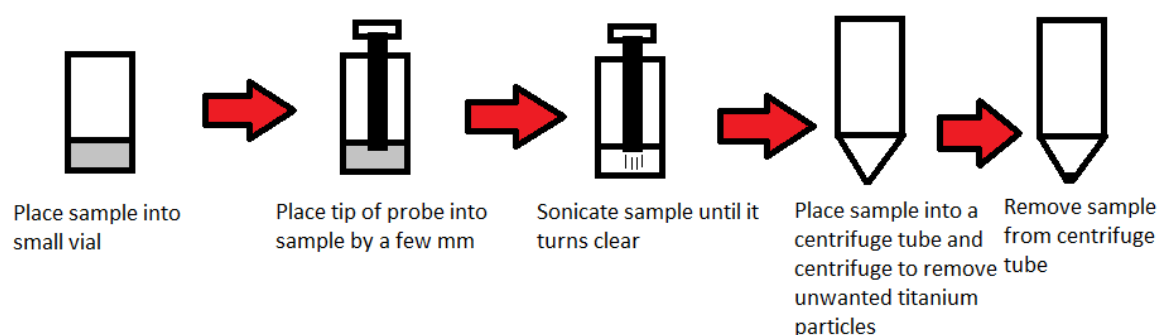


Figure 1.4: Probe sonication liposome size reduction method. Sample is sonicated in a glass vial with the tip of the probe touching the sample. Sample changes from milky to clear. Sample is then centrifuged in a centrifuge tube to remove titanium particles and large MLV which settle to the bottom.

However bath sonication does offer advantages, including better temperature control and the ability to run multiple samples under exactly the same conditions at the same time (Dua, 2012). Another major advantage of bath sonication, particularly with the Bioruptor® system, is that multiple samples can be prepared simultaneously. This reduces the risk of inter – sample variability. However, issues currently with bath sonication revolve around two main issues: that there is limited research done using a bath sonicator and liposomes, and those processes used tend to be slow compared to probe sonication and other methods (hielscher, 2015). A methodology for bath sonication liposome size reduction is shown below in Figure 1.5.

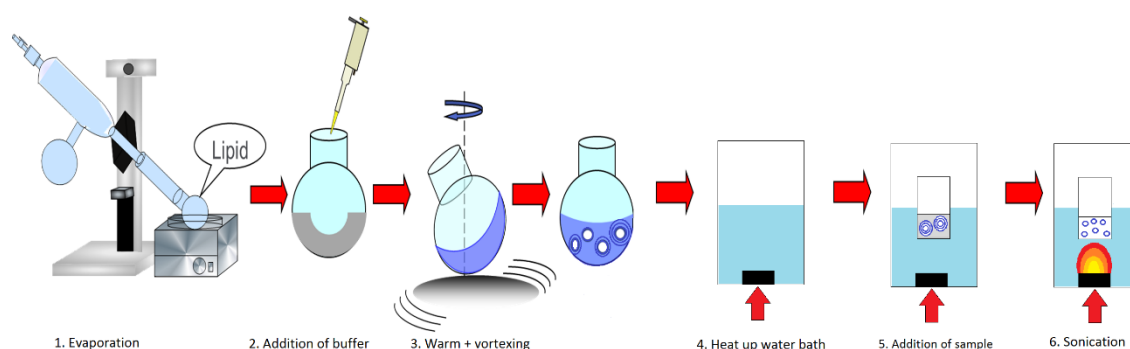


Figure 1.5: Method for producing MLV through lipid film hydration and then forming SUV through bath sonication. Lipid in Chloroform: Methanol is added to a round bottom flask and then the solvents are removed through the use of a rotary evaporator. Buffer is warmed and added to the lipid film that forms on the bottom of the flask and vortexed to form a milky solution of MLV. Sample is added to a warmed water bath in plastic tubes and sonicated.

As mentioned, other methods of size reduction, such as extrusion and high shear mixing, have also been investigated (Bhardwaj and Burgess, 2010, Cagdas et al., 2011, Lasic and Barenholz, 1996, Olson et al., 1979). Extrusion works by forcing the liposomes in solution through smaller and smaller membranes which have a set pore size (Berger et al., 2001, Nayar et al., 1989, Chapman et al., 1991, Turanek, 1994). This method can give very good size results with extremely good polydispersity (PDI) of below 0.1 but suffers from contamination issues and limited size range due to the use of membranes. Other methods such as microfluidics and high shear mixing have come around in more recent decades, with microfluidics becoming more prominent in the last 15 to 20 years (Yu et al., 2009, van Swaay and deMello, 2013, Kastner et al., 2014, Jahn et al., 2007). These newer methods look to build on what the original methods could do, with added bonuses or by reducing the unwanted side effects. High shear mixing has been used for other lipids, notably the formulation of cationic liposome adjuvants (Andreasan, 2013, Foged et al., 2014). Whereas sonication works by inducing massive stress, high shear mixing works by the milling effect. Microfluidics

is a different method for producing liposomes within the nanometre range. It is known as a bottom up instead of a top down method. This is because instead of producing large MLVs first and then reducing their size, the lipid is instead formed into SUV through just the one process. This done through the fluid streams of lipid and solvent forming a well-defined interface by laminar flow (Yu et al., 2009), Bath sonication was chosen as the alternative method to probe sonication because bath sonication allows for a much higher throughput of samples compared to high shear mixing, extrusion and microfluidics. Also, the temperature control which can be achieved through the use of the water bath is a distinct advantage of bath sonication compared to probe sonication in particular. This is because the water bath allows for the sample temperature to be controlled to within a degree or two, but the probe sonicator can only be cooled using an ice bath which allows for much less control.

1.2.3 Analysis of liposomes after formation

Dynamic light scattering (DLS) is the main form of analysis post liposome formation. DLS allows for size and PDI data to be gathered in a quick and efficient way. Samples of liposomes are simply diluted in water and placed in a cuvette and ran in a couple of minutes. DLS works simply by the sample being illuminated with a laser and then the changes in the scattered light are detected at a known scattering angle by the detector. Different sized particles change the scattered light distribution and various algorithms and equations are used to infer the particle size from the amount of scattering.

High performance liquid chromatography (HPLC) can be used to quantify how much lipid is left after the liposomes have been made, to avoid significant loss of lipid through the process (Graeve and Janssen, 2009, Rodríguez-Alcalá and Fontecha, 2010, Rocha et al., 2010). Lipid

quantification is needed to prove that all or almost all the lipid put in at the beginning of the process is recovered at the end of the process.

HPLC can also be used to quantify other substances such as propofol. Propofol is a lipophilic drug so can be used as an example drug to show the encapsulation efficiency of particular formulations formed using a specific method (Kastner et al., 2015, Ali et al., 2013).

One of the most common methods used to image and track liposomes is the use a fluorescent dye. These images can be used to investigate structural attributes, size and cellular and biodistribution (Parker et al., 1981, Verma et al., 2003). For this, two different dyes can be used separately, Carboxyfluorescein (CF) and 1, 1'-Diocadecyl-3, 3, 3', 3'-Tetramethylindocarbocyanine Perchlorate (DiIc).

CF is a hydrophilic green dye and as such gets trapped in the hydrophilic core of a liposome (Ralston et al., 1981, Stevenson et al., 1984, Chen and Knutson, 1988). For example, Barbeau et al used CF to investigate the stability of their drug delivery molecule, an archaeosome, and compare it to other drug carriers including PEGylated liposomes (Barbeau et al., 2011). The slower release of the CF from their study showed that their drug carrier was significantly more stable than the liposome. CF has also been used as a molecular beacon by Zhou et al in the detection of deoxyribonucleic acid (DNA) damage, with the different quenching efficiencies being an indicator as to whether DNA damage had or had not occurred (Zhou et al., 2012).

The red DiIc dye is added along with the lipid when it is in its organic solvent. This then gets trapped within the lipid bilayers of the liposomes, as DiIc is hydrophobic (Kamperdijk et al., 2012, N. A. Abdul Nasir, 2013 , Kaur et al., 2014, Joshi et al., 2014). DiIc has been used for example as an alternative cell marker for Mesenchymal stem cells and as a neuronal tracer (Weir et al., 2008, Supprian et al., 1993).

Both dyes can then be imaged using a confocal microscope (Kamperdijk et al., 2012, N. A. Abdul Nasir, 2013). The reasons for these images being required is to prove that the liposomes being produced using the probe sonication and bath sonication methods in particular, are small unilamellar vesicles, and no other structures such as micelles of multilamellar vesicles (Forssen et al., 1996). Confocal microscopy is particularly useful as liposomes, due to their amphiphilic nature, can be loaded with either a lipophilic fluorescent dye such as DiIC or a hydrophilic dye such as CF. In some cases, both dyes are loaded at the same time so both the liposome core and bilayer can be investigated. A major use for this technology with liposomes is to study liposomal uptake into mammalian and bacterial cells such as Ducat et al (Ducat et al., 2011). Ahmed et al took a slightly different approach and investigated uptake of liposomes into the biofilm of bacteria (Ahmed et al., 2002). These techniques could be useful for this project to look into liposomal uptake into various cells associated with the immune system response.

1.2.4 Uses today

A large range of lipids are used for liposome formulations, with many formulations having a mixture of lipids to combine the good factors of the different lipids used. Some of the formulations currently on the market are shown below in Table 1.1 (Fan and Zhang, 2013).

Table 1.1: Current approved liposome formulations on the market. Nearly all liposome formulations on the current market contain cholesterol to be a stabilising agent, nearly all are administered intravenous, many contain PEG, and many contain multiple lipids to optimise the formulation for its role. Roles include to fight cancer, pain management and to combat fungal infections.

Drug	Product name	Type	Lipid Composition	Route of administration	Approved treatment
Amphotericin B	Ambiosome	Liposome	L- α -phosphatidylcholine, hydrogenated (Soy) (HSPC), 1, 2-Distearoyl-Sn-glycero-3-phospho-rac-(1-glycerol) sodium salt (DSPG) and cholesterol	Intravenous	Severe fungal infection
Doxorubicin	Myocet	Liposome	1, 2-dioleoyl-sn-glycero-3-ethylphosphocholine (chloride salt) (EPC) and cholesterol	Intravenous	Metastatic breast cancer Kaposi's sarcoma, ovarian and breast cancer Kaposi's sarcoma, ovarian and breast cancer
	Doxil	PEGylated liposome	HSPC, cholesterol and 1, 2-Distearoyl-sn-glycero-3-phosphocholine - Polyethylene Glycol (DSPC – PEG ₂₀₀₀)	Intravenous	
	Lipo – dox	PEGylated liposome	1, 2-Distearoyl-sn-glycero-3-phosphocholine (DSPC), cholesterol and	Intravenous	

			DSPC – PEG ₂₀₀₀		
Daunorubicin	Daunoxome	Liposome	DSPC and cholesterol	Intravenous	Blood cancer
Verteporfin	Visudyne	Liposome	EPC and 1, 2-ditetradecanoyl-sn-glycero-3-phosphocholine (DMPC)	Intravenous	Age – related molecular degeneration
Cytarabine	Depocyt	Liposome	DOPC, 1, 2-Dipalmitoyl-sn-glycero-3-phosphocholine (DPPC), cholesterol and triolein	Spinal	Neoplastic meningitis and lymphomatous meningitis
Morphine sulfate	DepoDur	Liposome	DOPC, 1, 2-Dipalmitoyl-Sn-glycero-3-phospho-rac-(1-glycerol) ammonium salt (DPPG), cholesterol and triolein	Epidural	Pain
Vincristine sulfate	Marqibo	Liposome	Egg sphingomyelin and cholesterol	Intravenous	Acute lymphoblastic leukaemia

The most common type of lipid used is phospholipids because they are commonly found within the body cell membranes and their amphiphilic nature. The formulation that is chosen looks at taking advantage of the wide variety of transition temperatures, possible addition of cholesterol, zeta potential charge, cost and how saturated the fatty acid tails are which affects stability of the formulation of the different lipids (Lasic, 1996). Transition temperature is when the ordered gel phase to the disordered liquid crystalline phase. When the lipid bilayer is in its ordered gel state, its tails are more closely packed and hydrophobically bonded to each other which doesn't allow the bilayer to change or deform, so cannot be worked with. However, above the transition temperature the fatty acid tails are more mobile and bent, allowing the bilayer to be broken and reformed (Das, 1978). Highly cationic lipids have been

shown to have preferential cell uptake due to being able to electrostatically react with the negative cell surface, but may suffer problems with toxicology and have modified behaviour in the presence of serum (Alonso and Garcia-Fuentes, 2014). Highly anionic liposomes meanwhile are more readily taken up by macrophages due to scavenger receptors (Coates et al., 2011).

When cholesterol is added to the formulation, the rigid ring system of the cholesterol molecule allows less movement within the lipid bilayer, thereby elevating the transition temperature of the formulation. This lower membrane fluidity increases the stability of the bilayer in vitro and in vivo which is useful for many of the current liposome formulations on the market by preventing lipoprotein-induced vesicle destabilisation and release of the drug within at the wrong time in the wrong place (Duzgunes, 2005). However, with the right amount of cholesterol the drug release can be controlled, a vital part to any drug delivery system (Torchilin and Weissig, 2003).

1.3 Carbon nanotubes dispersion, modification and uses

1.3.1 Carbon nanotubes background

Since their discovery back in 1991 by Sumio Iijima (Iijima, 1991), carbon nanotubes have been the source of much interest for a wide variety of different areas of science and engineering (Zhang et al., 2013, De Volder et al., 2013, Thostenson et al., 2001). These uses are far ranging from chemical sensors (Kong et al., 2000), field emission materials (Tans et al., 1998), catalyst support (Planeix et al., 1994), electronic devices (Peng et al., 2014), high sensitivity nanobalance for nanoscopic particles (Lucci et al., 2007), nanotweezers (Kim and Lieber, 1999), reinforcements in high performance composites, and as nanoprobe in meteorology

and biomedical and chemical investigations, anode for lithium ion in batteries (Che et al., 1998), nanoelectronic devices (Zhbanov et al.), supercapacitors (Pan et al., 2010) to hydrogen storage (Dillon et al., 1997).

Carbon nanotubes are formed of individual carbon atoms put together into a tube made up of benzene rings and can be made up of just one layer or many layers. It is analogous to graphene, although rolled as opposed to a flat sheet. These tubes can be up to several microns in length but are just 1 – 2 nm in width in the case of single walled carbon nanotubes (Chen et al., 2014). For double – walled or multi – walled carbon nanotubes, their width can be in the tens of nanometres with a gap between each layer of less than 0.5 nm. These differences in the number of layers is known to effect for example the electrical and stability properties of the carbon nanotubes (Asgari and Lohrasbi, 2013). Figure 1.6 below shows the difference between a carbon nanotube surface that is pristine. This means that no modification or defects have occurred. It also shows the changes that occur when defects and modifications are introduced, and this is known as covalent functionalisation.

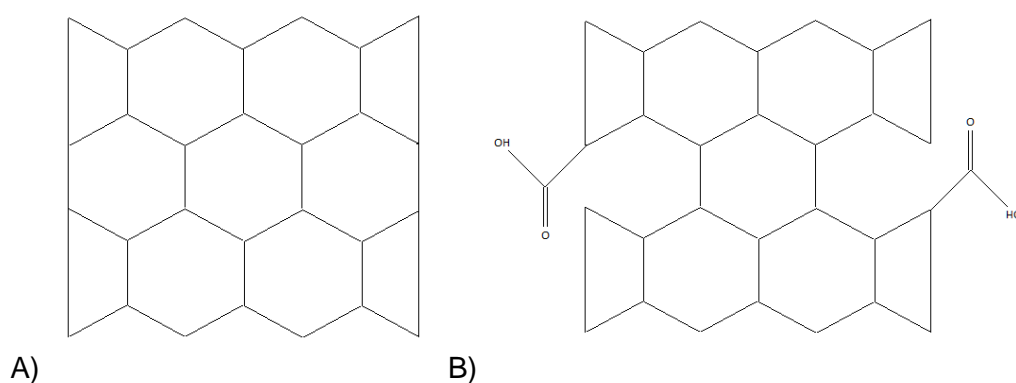


Figure 1.6: A) A pristine carbon nanotube surface made up of carbon atoms with no defects or modification. This makes these tubes highly hydrophobic. B) A carbon nanotube surface post carboxylation, with the carboxyl groups increasing the hydrophilicity of the carbon nanotube, and also disrupting the carbon nanotubes surface, affecting its properties.

Non – covalent functionalisation can also occur and is shown below in Figure 1.7. This is where the surface remains untouched but instead a surfactant is used which non – covalently binds to the surface of the carbon nanotube. Examples of such surfactants are shown below in Figure 1.8.

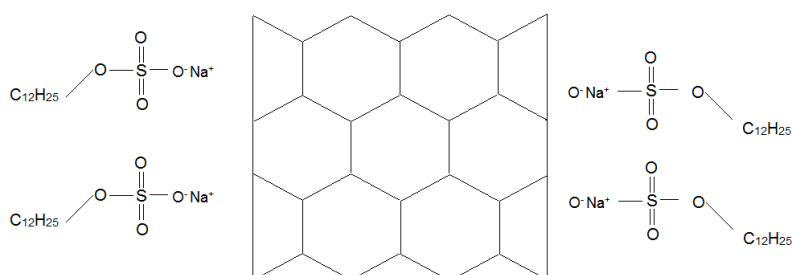


Figure 1.7 Sodium dodecyl sulfate (SDS) dispersed carbon nanotubes showing the SDS non – covalently bound to the carbon nanotube surface, allowing for dispersion in an aqueous solution, but no change to the carbon nanotube surface and therefore keeping its properties as before.

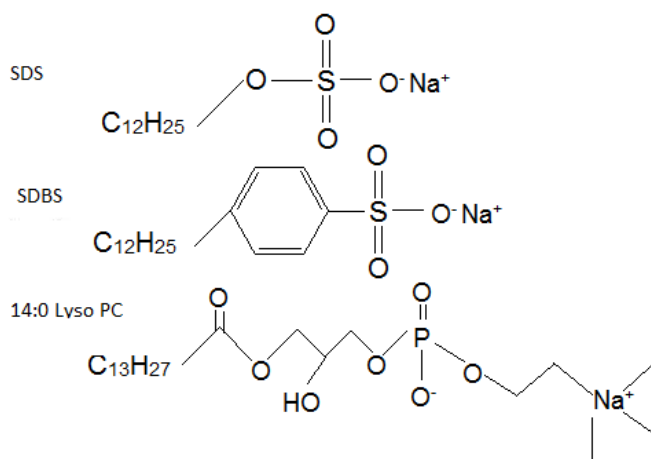


Figure 1.8: Structures of the three surfactants used in these studies to non – covalently disperse the carbon nanotubes. They are SDS, Sodium dodecylbenzenesulfonate (SDBS) and 1-ditetradecanoyl-sn-glycero-3-phosphocholine (MPC).

The way these carbon atoms are arranged gives rise to different conformations. These conformations are armchair, zigzag and chiral and are shown below in Figure 1.9 and Figure 1.10. The way the carbon nanotube is wrapped is represented by a pair of indices (n , m). The integer's n and m denote the number of unit vectors along two directions in the honeycomb crystal lattice (Brischetto et al., 2015).

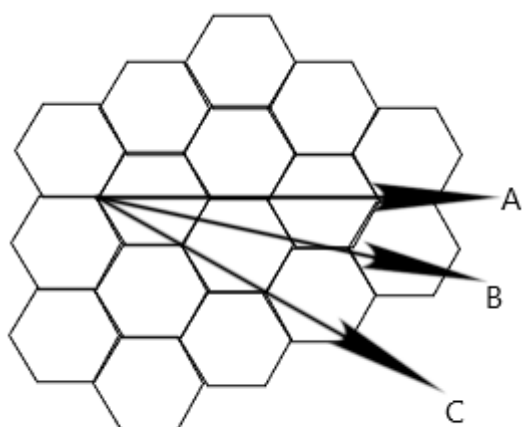


Figure 1.9: Chirality of carbon nanotubes with either A) armchair B) chiral) or C) zig zag conformation.

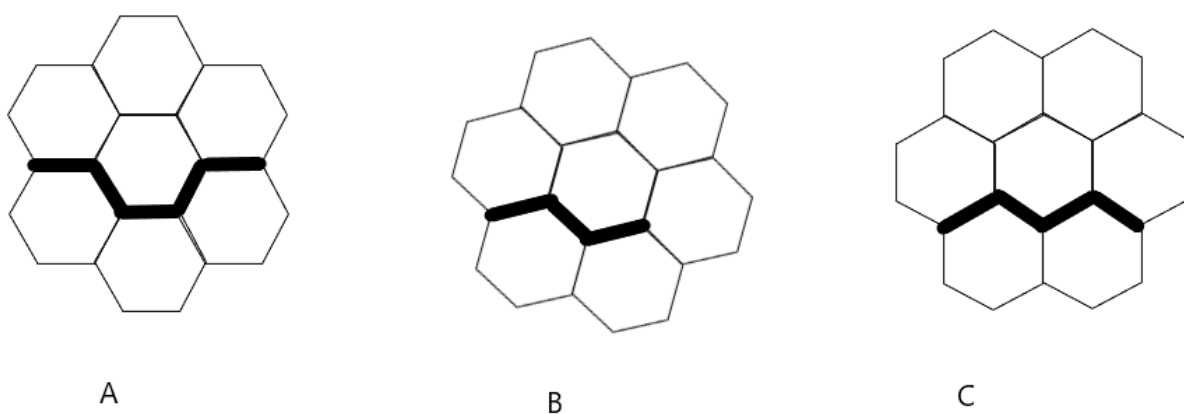


Figure 1.10: Carbon nanotube conformation showing the A) armchair B) chiral and C) zigzag conformations.

For the armchair conformation, the two vectors are defined as $n = m$, for zigzag they are $n, 0$ and for chiral they are n, m . These changes in vectors can cause differences in the conductance of the nanotube, its density, its lattice structure, and other properties. For example, a carbon nanotube is considered metallic if the value $n - m$ is divisible by three. Otherwise, the nanotube is semiconducting (Ganesh, 2013). What also has a great effect on the properties of a carbon nanotube is the extent of the curvature of the carbon nanotube relative to a graphene sheet (Jorio et al., 2007). These effects are dependent on the chirality of the carbon nanotube in question.

The length of a carbon nanotube is also known to affect its properties. For example Russ et al. were able to show that long carbon nanotubes were “highly conducting and were suitable for electromagnetic interference shielding as well as electrostatic dissipation applications” (Russ et al., 2013). The short carbon nanotubes were easier to process and were able to be used for electrostatic dissipation applications but were unsuitable for the electromagnetic interference shielding. Wang et al. were able to show that higher thermal and electrical conductivities were exhibited with longer multi – walled carbon nanotubes compared to their shorter counterparts but the tensile strength was not length dependent (Wang et al., 2013). This all shows that length, curvature and therefore width and the chirality of a carbon nanotube each effect its properties and therefore it’s potential in a given field.

Carbon nanotubes do have some properties that are not so useful though, especially for the biological field. Chief of these is its tendency to aggregate and not be miscible with water. “Physical approaches using amphiphilic surfactants have proven capable of debundling carbon nanotube bundles and stabilizing individual tubes while maintaining their integrity and intrinsic properties” (Wang et al., 2004). With the addition of surfactant, carbon nanotubes are able to be broken up into smaller and smaller bundles and even into individual tubes, with the surfactant surrounding it. They work by having both polar and non - polar groups which adsorb at the interface two immiscible phases, such as oil and water, air and

water or particles and solution (Vaisman et al., 2006). This acts to reduce the surface tension and therefore allow the dispersion in this case of the carbon nanotubes and overcome those high van der Waals forces.

1.3.2 Carbon nanotube analysis

The analysis of carbon nanotubes is vitally important and can be done through a variety of means including Ultra Violet – Visible – Near infra-red (UV – Vis – NIR) spectroscopy, Photoluminescence (PL), X-ray photoelectron spectroscopy (XPS), Raman spectroscopy and imaging techniques such as atomic force microscopy (AFM) and transmission electron microscopy (TEM) (Rance et al., 2010, Hamilton et al., 2013, Wepasnick et al., 2010, Piao et al., 2013, Dresselhaus et al., 2005, Safarova, 2007). This is because the biodistribution and pharmacokinetics of nanoparticles which are affected by many physicochemical characteristics such as shape, size, chemical composition, aggregation, solubility surface, and fictionalisation (Eatemadi et al., 2014).

Techniques such as UV – Vis – NIR spectroscopy and PL can be used to investigate the chirality and structure of the carbon nanotubes. The chirality and structure of the carbon nanotubes is important to know because their band gap can vary from zero to about 2 eV, their Youngs modulus and tensile strength can be affected, and their electrical conductivity can show metallic or semiconducting behaviour depending on the chirality of the carbon nanotube (Bellucci, 2005). Band gap refers to the energy range in which no electrons can exist within a solid. What this means for carbon nanotube properties is depending on whether a carbon nanotube is in the armchair, zig zag or some kind of chiral conformation, the carbon nanotube can be referred to as either a metallic or semiconducting carbon nanotube with each of the different types having different properties favourable for different electronic applications

(Liu and Cheng, 2016). Young's modulus and the tensile strength refer to the ability of the carbon nanotube to withstand a great amount of stretching and compression in one direction; in this case from either end of the tube. However, this reduces significantly when multiple tubes are involved such as with double or multi-walled carbon nanotubes. Carbon nanotubes are also not nearly as strong when pressure is applied across the tube or tubes due to their hollow structure.

XPS and Raman can be used to investigate the surface functionalisation of the carbon nanotubes which is an important way of determining how soluble the carbon nanotubes are likely to be in water, and how much modification has taken place of the carbon nanotube surface due to the addition of extra groups (Tsang et al., 1993). Imaging techniques such as AFM and TEM can be used to investigate the size and morphology of the carbon nanotubes. The size of a carbon nanotube can affect its application and the morphology, whether it is a single - walled carbon nanotube or multi - walled carbon nanotube, affects a number of properties including strength, electrical and thermal properties (Sinnott and Andrews, 2001). For this work, UV – Vis spectroscopy, PL, XPS, Raman spectroscopy and TEM will all be used to investigate the dispersion of the carbon nanotubes, the size of the carbon nanotubes post cutting and the chemical makeup of the surface post modification.

1.3.3 Carbon nanotubes uses today

Carbon nanotubes have been shown to stimulate the body's immune system. However the reasons for this are not so well known, and there is still a dispute as to whether this stimulation is a good thing or a bad thing for the body, and whether this stimulation is something specific to the carbon nanotube or simply because the carbon nanotube is seen as a particulate and therefore dealt with as such (Fadel and Fahmy, 2014). Carbon nanotubes properties are attractive for the next generation of immunotherapeutic platforms due to their ability to promote "efficient proliferation of antigen-specific effector cell populations, enhanced defence against

immuno-evasive or chronic pathogens, and successful immunisation with limited or minimal parenteral administration". carbon nanotubes can also be used to present antigens at a high density which enhances the immune systems response (Steenblock et al., 2009). They have also been shown to be a good platform to target antigen presenting cells and to translocate through the lipid bilayer for priming a cellular immune response (Konduru et al., 2009). These three routes are fluid phase pinocytosis and endocytosis and diffusion. Finally the tendency for carbon nanotubes to activate proinflammatory pathways and trigger the classic complement pathway may enhance the antigens proficiency (Demento et al., Rybak-Smith and Sim, 2011, Dumortier, 2013). Liu et al were able to show through (TEM) images confirmed that multi walled carbon nanotubes- NH_3^+ penetrate the cell membranes and are widely dispersed in the cell. The results showed that the multi walled carbon nanotubes- NH_3^+ : DNA complexes are able to transfect cells effectively at different charge ratio than naked DNA (Liu et al., 2016).

Carbon nanotubes have also been used for various other biological uses as shown in Figure 1.11 (He et al., 2013a). Carbon nanotubes can carry drug molecules to the nuclear membrane of a cell through the lipid bilayer within inducing a toxic effect. The drug can either enter through the membrane on its own or along with the carbon nanotube carrier, with the latter being more effective due to the lack of possible drug degradation of the drug prior to internalisation. Other uses include immunotherapy, cancer therapy, tissue regeneration, biological sensors and drug extractors. They have been first proven to be an excellent vehicle for drug delivery directly into cells without metabolism by the body (Zhang et al., 2011, He et al., 2013a, Al Faraj et al., 2016). Then other applications of carbon nanotubes have been extensively performed not only for drug and gene therapies but also for tissue regeneration (Veetil and Ye, 2009), biosensor diagnosis (Yang et al., 2015), enantiomer separation of chiral drugs (Tanaka et al., 2015) and extraction and analysis of drugs and pollutants (Pan et al.,

2005). They have also been found to instigate a specific immune response (Orecchioni et al., 2014) and act as an inherent adjuvant (Gottardi and Douradinha, 2013).

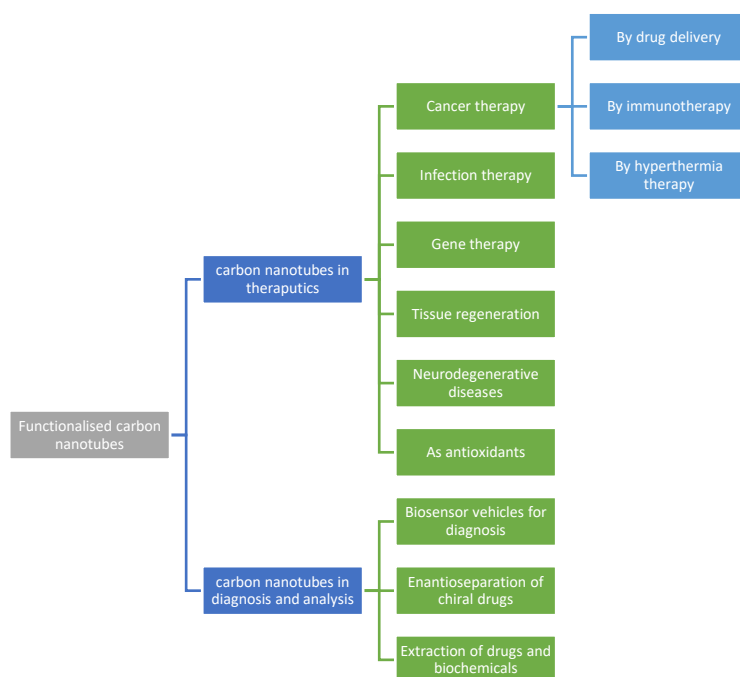


Figure 1.11: A schematic of the various pharmaceutical applications carbon nanotubes are used for (He et al., 2013a). These include delivery of drugs, tissue regeneration and as biosensor vehicles for diagnostics.

1.4 Current methods for the dispersion of carbon nanotubes in water for biological systems

1.4.1 Carbon nanotubes dispersed with surfactants

Carbon nanotubes are made up of carbon atoms in a graphite configuration rolled up into a tube (Meyyappan, 2004). These tubes can be concentric to form multi walled carbon nanotubes or on their own as single walled carbon nanotubes (Eatemadi et al., 2014). These

tubes have unique electrical, optical and mechanical properties and have also been shown to be useful for drug loading and as potential adjuvants, making them applicable for the biological and immunological fields (Peng et al., 2014, Sharma et al., 2015, Liu et al., 2012, Coleman et al., 2006, Heister et al., 2012, Tsai et al., 2013, Orecchioni et al., 2014, Fadel and Fahmy, 2014, Xing et al., 2016, Pondman et al., 2014). However the major drawback for these uses is that carbon nanotubes in their pristine form are practically insoluble (Dyke and Tour, 2004). This is due to the very high Van der Waals forces between the carbon nanotubes causing them to form large insoluble aggregates when introduced to water (Ansari et al., 2013, Zhbanov et al., 2010). These can be overcome using two different methods; covalent or non-covalent functionalisation.

Non-covalent functionalisation works by using an external compound such as SDS, SDBS or MPC to non-covalently attach to the carbon nanotube surface, as shown in Figure 1.9 (Yang et al., 2013, Fernandes et al., 2015, Dong Wook Chang, 2010, Wu et al., 2006). This works because compounds such as surfactants are amphiphilic. This means that they have a part of the molecule which is hydrophobic and a part which is hydrophilic. The hydrophobic part then interacts with the carbon nanotube surface and the hydrophilic part interacts with the water around. This then solubilises the carbon nanotube without affecting any of the carbon nanotubes other properties as this method does not directly affect the carbon nanotube structure.

Various methods of non-covalent functionalisation are used but most follow the same general premise. This being the carbon nanotubes and the dispersal agents are placed in water and then sonicated for a period of time. This disrupts the carbon nanotubes and dispersal agents allowing the carbon nanotubes to be solubilised. Generally, this is then followed by some form of centrifugation or filtration or both to remove any carbon nanotube aggregates which can cause the samples to reaggregate more quickly than they otherwise would. This is shown below in Figure 1.12 where using this method, neither the structure nor the length of the carbon nanotubes is affected during the process.

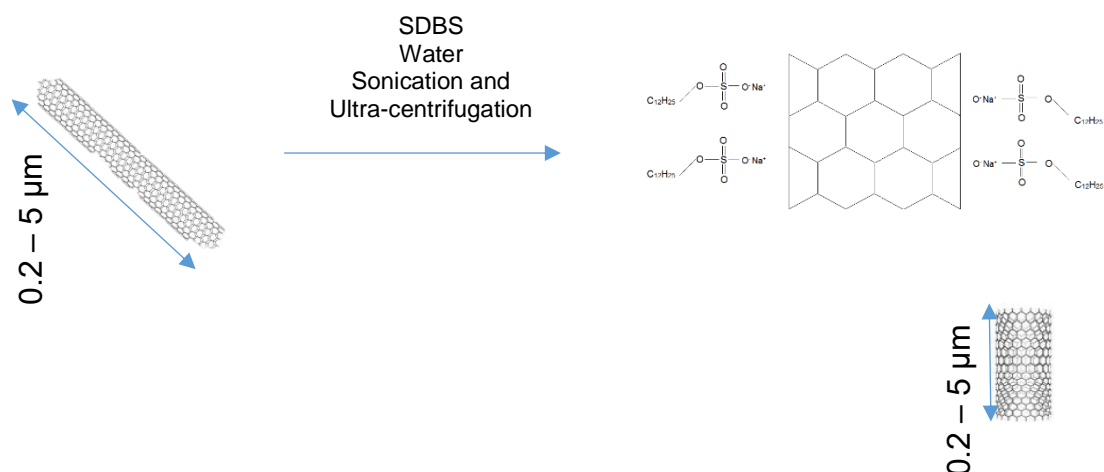


Figure 1.12: A) Method for dispersion of carbon nanotubes using SDS non – covalently so no damage to the carbon nanotube surface. B) Method for the dispersion of carbon nanotubes using a surfactant and bath sonication. Carbon nanotubes are placed in water with surfactant and then sonicated in a warmed water bath. These are then centrifuged and analysed using UV – Vis – NIR and PL.

1.4.2 Carbon nanotube carboxylation

Functionalisation and cutting of carbon nanotubes are required for bio-medical applications such as the loading of proteins and other biological molecules covalently to the surface and

increasing the hydrophilicity and decreasing the length of the carbon nanotube, without causing obvious toxicity to the cells around. An example methodology is shown below in Figure 1.13.

A limited number of defects can be tolerated by carbon nanotubes without losing their macroscopic electronic and mechanical properties (Balasubramanian and Burghard, 2005, Esplandiu et al., 2009, Aziz et al., 2007, Sánchez et al., 2008). In addition, the caps of the tubes, forming a hemispherical fullerene, have stronger reactivity than the sidewalls because of their higher curvature (Viswanathan et al., 2009, Malhotra et al., 2010). When treated with strong oxidizing agents such as nitric acid or sulfuric acid, carbon nanotubes can be opened and cut into short tubes (Malhotra et al., 2010, Yang et al., 2009, Munge et al., 2010). Moreover, oxygenated functional groups such as carboxylic acid, ketone, alcohol and ester groups can be generated by the oxidation process to the ends and the defect sites of the nanotubes (Shamsipur et al., 2010).

Using the nanotube-bound carboxylic acid groups introduced by oxidation treatment, further functionalisation can be performed via amidation, esterification or the zwitterion (COO-NH_3^+) formation. Before covalent modification, the carboxylic acids are often activated by thionyl chloride, carbodiimide [e.g. N-(3 - dimethylaminopropyl) - N'-ethylcarbodiimide (EDC), N, N'-dicyclohexylcarbodiimide (DCC)] or N-hydroxysuccinimide (NHS), to get highly reactive intermediate groups. Esterification can be achieved by the nucleophilic substitution reaction of nanotube carboxylate salt with alkyl halides (Jha and Ramaprabhu, 2010). Various lipophilic and hydrophilic compounds can then be attached to carbon nanotubes via amide or ester linkages, which significantly improved the solubility of carbon nanotubes in organic or aqueous solvents (Xu et al., 2008). These groups could be subsequently removed under basic or acidic hydrolysis conditions.

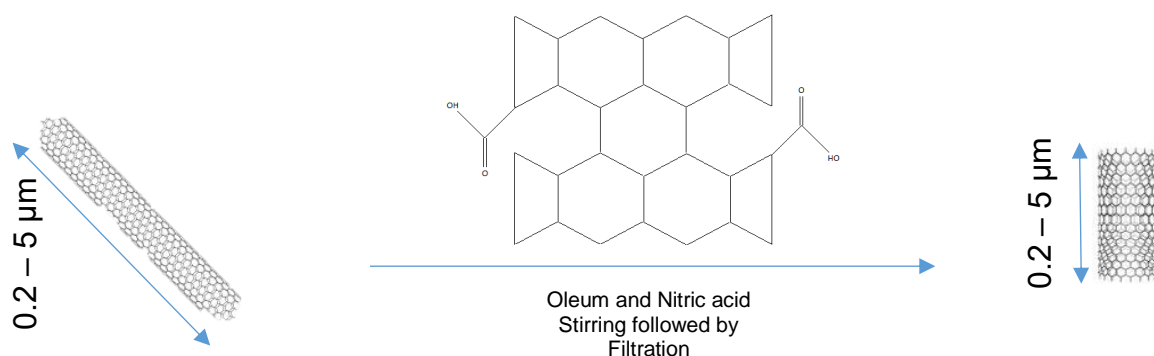


Figure 1.13: covalently functionalised carbon nanotube surface with carboxyl groups showing the disruption to the carbon nanotube structure and shortening that occurs with the addition of acid that causes defects in the carbon nanotube surface that eventually form larger defects and cause the carbon nanotube to become cut.

1.4.3 Carbon nanotube cutting

Carbon nanotubes are generally 200 to 5000 nm in length. However they can be made more homogenous and shorter by using a variety of methods including the use of neat acids, fluoridation followed by pyrolysis or the use of mechanical energy such as sonication, as shown in Figure 1.14 (Ashcroft et al., 2006, Donkor and Tang, 2014, Gao et al., 2015, Ma et al., 2013). All of the methods work on the basis of introducing defects into the carbon nanotube surface which can then be further broken and thereby cut the carbon nanotube. Through these methods, carbon nanotubes can be reduced down to the tens of nanometres in length.

Chen et al were able to form soluble, ultra-short (length < 60 nm), carboxylated, single-walled carbon nanotube by a scalable procedure that simultaneously cuts and functionalizes carbon nanotubes using a mixture of sulfuric and nitric acids (Chen et al., 2006). This process using oleum's (100% H_2SO_4 with excess SO_3) ability to intercalate between individual carbon

nanotubes inside carbon nanotube ropes. The solubility of these ultra-short carbon nanotubes in organic solvents, super acid and water is about 2 wt %. Li et al were able to successfully cut into different lengths multi walled carbon nanotubes, by controlling $\text{H}_2\text{SO}_4/\text{HNO}_3$ (5:3) oxidation time (Li and Zhang, 2006). During the cutting process H_2SO_4 and HNO_3 were added independently and the oxidation processes were carried out at a lower temperature to avoid excess weight loss and damage to carbon nanotube. The resulting shorted carbon nanotubes formed stable dispersions in the polar solvents without the help of surfactants that provided possibility for further functionalisation and application. Ziegler et al however were able to use slightly different solutions to try and get a more controlled cutting and functionalisation. The oxidation reaction of piranha solutions, a mixture of sulfuric acid and hydrogen peroxide, with purified HiPco carbon nanotubes was measured as a function of temperature (Ziegler et al., 2005a). At high temperatures, piranha is capable of attacking existing damage sites, generating vacancies in the graphene sidewall, and consuming the oxidised vacancies to yield short, cut nanotubes. Increased reaction time results in increasingly shorter nanotubes. However, significant sidewall damage occurs as well as selective cutting of the smaller diameter nanotubes. On the other hand, room-temperature piranha treatments show the capability of cutting existing damage sites with minimal carbon loss, slow cut rates, and little sidewall damage. Combined with a method of introducing controlled amounts of damage sites, these room-temperature piranha solutions have the potential to yield an efficient means of creating short, cut nanotubes. They were also able to run room-temperature piranha and ammonium persulfate solutions and show their ability to exploit the damage sites and etch single walled carbon nanotubes in a controlled manner. Despite the aggressive nature of these oxidizing solutions, the cut rate for carbon nanotubes is relatively slow and almost no new sidewall damage is introduced (Ziegler et al., 2005b).

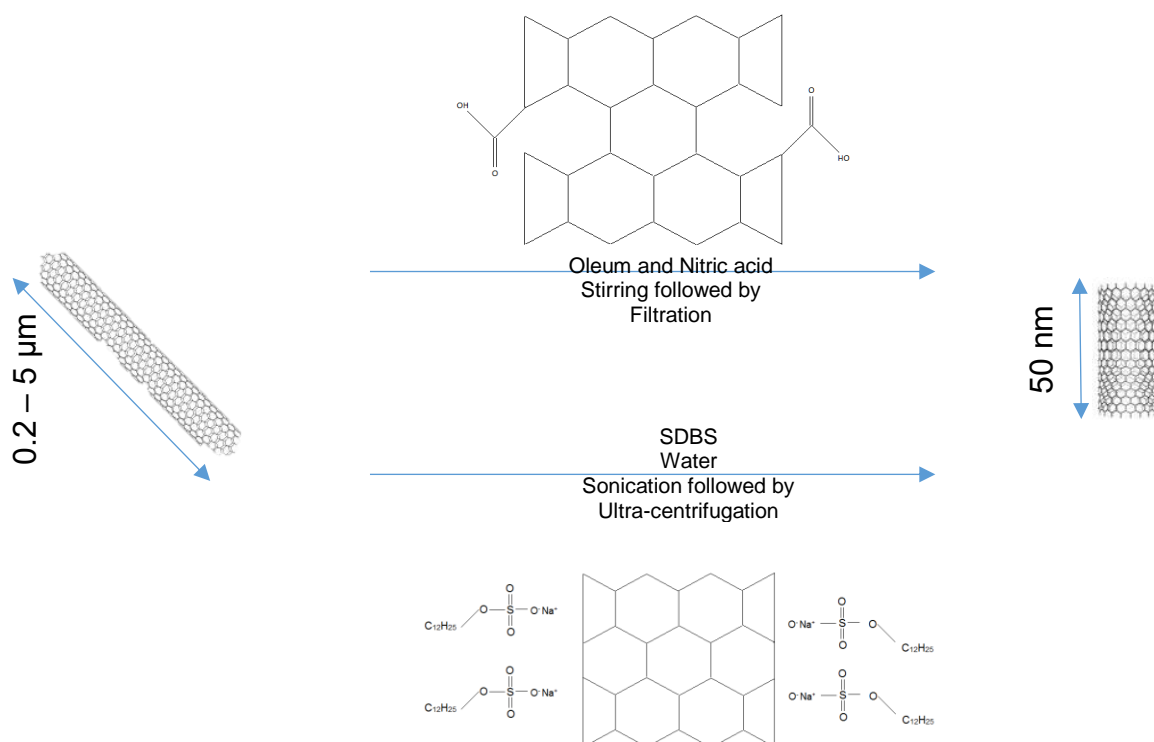


Figure 1.14: Cutting and functionalisation of carbon nanotubes using both covalent and non-covalent functionalisation methods. These use either harsh acids or mechanical power to cause defects in the carbon nanotube surface in such a way that causes bigger and bigger defects to occur that eventually results in the cutting of the carbon nanotube into shorter pieces.

1.4.4 Carbon nanotube separation

Once the carbon nanotubes have been cut, there remains the problem of presence the large variation in carbon nanotubes lengths including very small fragments of carbon. It is therefore important that there is some method of removing the very small and very large particles so to give the best chance of finding out what effect the ultra-short carbon nanotubes can have. These methods broadly separate into two. The first is using density gradient ultra-centrifugation, normally with iodixanol as a density gradient medium. For example, Fagan et

al were able to perform separation of single-wall carbon nanotube by length via centrifugation in a high density medium, in this case iodixanol. They also found that the distribution width was coupled to the rate of the separation. Less rapid separation was shown to produce narrower distributions (Fagan et al., 2008).

The second approach is using HPLC to separate the carbon nanotubes along a column and then take set amounts at the end for each size sample. Yang et al were able to perform purification and length separation of oxidatively shortened single-walled carbon nanotubes by size exclusion chromatography (SEC) without assistant reagents for dispersion using a PL aqua gel - OH column (300mm×7.5 mm). Almost all the carbonaceous impurities, such as carbonaceous particles, graphene fragments, were removed from the oxidatively shortened nanotubes materials. The short carbon nanotubes were separated into fractions according to nanotube lengths, and the length distribution of each fraction was relatively narrow (Yang et al., 2005). Liu et al were also able to perform size exclusion chromatography using size-exclusion columns (COSMOSIL carbon nanotube, Nacalai Tesque Inc). They used two types of columns (dimension: 7.5 mm × 300 mm, pore size: 300 and 1,000 Å) connected in series to separate both samples. Dispersed DNA – carbon nanotube solutions were filtrated through a 0.22-µm membrane and loaded (~0.5 ml) onto the column series. The hybrid was eluted with pH 7.0 buffer containing 40 mM Tris, 0.5 mM Ethylenediaminetetraacetic acid (EDTA) and 0.2 M NaCl (Liu et al., 2013).

1.5 Previous liposome – carbon nanotube work

1.5.1 Nano-trains

Some previous work on carbon nanotube – liposome complexes has already been done. For example, Miyako et al. were able to formulate what they called carbon nanotube – liposome supramolecular nanotrains formed of carbon nanotubes coated in avidin – polyethylene glycol (PEG₂₀₀₀) and then covered in temperature sensitive liposomes loaded with biotin and *N*-(7-nitrobenz-2-oxa-1,3-diazol-4-yl) dioleoyl phosphatidylethanolamine (NBD – F) (Miyako et al., 2012).

They have also been investigated where again liposomes are loaded onto carbon nanotubes with a drug loaded into the liposomes for drug delivery. In this case, multiple different drugs were loaded so as to deliver more than one agent at a time and so lead towards a more personalised medicine (Karchemski et al., 2012).

Another type of carbon nanotube – liposome complex was shown by Kim et al. where they formulated superlattices of carbon nanotubes and cationic liposomes which helps “provide a new insight into the interactions of functionalised carbon nanotubes in lipid membranes, which are essential for the biological or biomedical applications of carbon nanotubes such as drug delivery” (Kim et al., 2012).

1.5.2 Porins

Carbon nanotube porins are lengths of carbon nanotube that are short enough, generally sub 10 nm, to be inserted into the pore of a cell or liposome. These are then used for a variety of

reasons including investigating ultra-fast proton transport, the transport of other ions and uncharged particles and investigating bacterial porins through mimicking their structure using the carbon nanotube porins (Tunuguntla et al., 2017, Tunuguntla et al., 2016, Kim et al., 2014, Tran et al., 2016, Garcia-Fandino and Sansom, 2012). For example, Tunuguntla et al were able to show that carbon nanotube porins represent a “versatile nanopore building block for creating higher-order functional biomimetic materials”. They also showed that by using a combination of UV – Vis spectroscopy, Raman and DLS can be used to monitor the quality and progress of the carbon nanotube porin synthesis. Kim et al were able to show carbon nanotube porins can be used to transport and investigate the transport of ions and uncharged species through carbon nanotube porins embedded in a bilayer. Garcia – Fandino et al were able to design a set of cation – selective nanopores allowing to stress test” the understanding of design principles of nanopores and channels.

1.6 Bioruptor® applications

1.6.1 The need for a cheap and fast method of internally validating optimised sonication conditions

Currently to determine sonication efficiency, DNA shearing is used as the validation tool. It is robust method but is both expensive and time consuming. Therefore, a new method is required to reduce the cost and time taken whilst still maintaining the robustness of the DNA shearing method. Previous methods include chemical reactions (Kimura et al., 1996), elastic sphere Radiometry (Hasegawa and Yosioka, 1969), aluminium foil erosion (Pugin, 1987), calorimetric and optical methods (Majumdar et al., 1998, Kimura et al., 2007, Zieniuk and Chivers, 1976) and thermoprobes (Pugin, 1987). Previous work has shown how a

sonochemical reaction can be used to help placement of tubes within a sonication bath to best maximise efficiency using the potassium iodide coupled with ammonium molybdate reaction (Nascentes et al., 2001). The energy of ultrasound is not uniformly available from the ultrasonic bath. Only a small fraction of the total liquid volume in the immediate vicinity of the ultrasound source experiments the effects of cavitation. The intensity of ultrasound is continuously attenuated by the molecules present in the liquid due to various cohesive forces acting on the liquid (Majumdar et al., 1998). The ultrasonic intensity profile in the baths depends entirely on the design and location of the transducers. For commercially available ultrasonic baths a variety of transducers with different configurations are used (Mason, 1996).

1.6.2 The need for a new version of the Diagenode (Bioruptor® Pico)

Formalin-Fixed Paraffin-Embedded (FFPE) DNA kit to increase profitability

There are four commonly used extraction procedures for DNA extraction (Hoff-Olsen et al., 1999),

1. Organic extraction that uses liquid chemicals to produce clean high yield DNA although is very labour intensive (Moré et al., 1994).
2. Inorganic silica which uses just a one-tube extraction process to yield single stranded DNA (Walsh et al., 1991, Debra A. Dederich, 2002)
3. Solid phase extraction methods binding to beads made of compounds such as silica. Such kits include the Promega's DNA IQ (Eminovic et al., 2005), Applied Biosystems' PrepFiler (Brevnov et al., 2009) and Qiagen's QIAamp kits (Sefers et al., 2006).
4. Differential extraction: a multistep process used to separate sperm from other cells; used for analysing biological evidence from sexual assault cases (Vuichard et al., 2011)

Diagenode has developed and sold a kit for FFPE DNA extraction which is a silica-columns based purification approach (Diagenode). The first step in FFPE DNA extraction workflow is a paraffin removal. Traditional methods use toxic organic solvents (xylen or similar) followed by gradual rehydration of samples in ethanol solutions (from 100% EtOH down to 20%).

Xylen and ethanol steps are replaced by short sonication (Bioruptor®) of FFPE slices using FFPE extraction buffer in Diagenode protocol. This results in a paraffin emulsification (milky solution) that can be directly used in next steps. Proteinase K digestion to digest proteins and release DNA and then reversal of crosslinks (heating at 65°C). Sample filtration through DiaFilter columns to remove particles which may interfere with columns based DNA purification and DNA purification using silica-columns. This works very well as shown with the work by Bak et al (Bak et al., 2016). Using the kit they were able to propose that simple Polymerase chain reaction (PCR)-based quality control experiments at the genetic and DNA methylation level can be used for the best-performing FFPE samples. The apparent preservation of genetic and DNA methylation patterns in archival FFPE samples may be able to be used to identify genetic and epigenetic changes associated with brain-manifested diseases.

The production cost of the kit is quite high resulting in a very limited profitability but Diagenode wants to keep FFPE solution in its portfolio. At the time, Diagenode commercializes MicroChIP DiaPure columns/buffers which are very similar to the columns/buffers used in DNA FFPE kit.

1.7 Aims and objectives for this work

The aim of this work was to formulate a new liposome – carbon nanotube complex using the Bioruptor Bath sonication systems for vaccine and drug delivery development. The first objective of this work was to create liposome formation protocols for the Bioruptor bath sonication systems that would be comparable to other methods such as probe sonication and extrusion. These would have to be comparable or better in the speed of liposome size reduction, how small the liposomes are that are formed and the volume of liposomal solution that could be formed in a certain period of time. A number of different Bioruptor bath sonication systems were available and had a number of advantages and disadvantages which are shown below in Table 1.2. The second objective was to further investigate the sonication systems themselves and look into how they could be more efficiently used and look at new and cheaper ways of testing the machines output. The third objective was to investigate the current Bioruptor bath sonication systems to see if they could be used for carbon nanotube dispersion in water and if a biologically safe surfactant could be used instead of the standard SDS and SDBS. The final objective was to investigate covalently functionalizing the carbon nanotubes to make them hydrophilic without the need for a surfactant. This same process would be investigated to see whether it could be used to cut the carbon nanotubes in length down from microns in length to a few hundred nanometres or less. These would then be added to a liposome solution and sonicated to see how the two entities would interact.

Table 1.2: Advantages and disadvantages of each Bioruptor machine used in the formation and optimisation of the liposome size reduction protocols.

Bioruptor Machine	Advantages	Disadvantages
Bioruptor XL	<ul style="list-style-type: none"> • Can sonicate a range of volumes (0.1 mL up to 3 mL) allowing for a range of laboratory uses • 4 possible power outputs 	<ul style="list-style-type: none"> • Old model (not on the market)
Bioruptor Standard	<ul style="list-style-type: none"> • Can sonicate a range of volumes (0.1 mL up to 3 mL) allowing for a range of laboratory uses • 3 possible power outputs 	<ul style="list-style-type: none"> • Old model (not on the market)
Bioruptor Plus	<ul style="list-style-type: none"> • Currently on the market • Can sonicate a range of volumes (0.1 mL up to 3 mL) allowing for a range of laboratory uses • More powerful machine (40 kHz) 	<ul style="list-style-type: none"> • Only two power outputs available
Bioruptor Pico	<ul style="list-style-type: none"> • Currently on the market • Small sample volumes (down to 0.01 mL) allows for high throughput, low volume experiments • More powerful machine (40 kHz) 	<ul style="list-style-type: none"> • Unable to sonicate large volumes (0.5 mL plus)

2 Formation and optimisation of the process of
reducing liposome size through bath sonication using
the Bioruptor® bath sonicator systems

2.1 Aims and objectives

Previous work has focussed on using a probe sonicator to reduce the liposome size from the micron level to the nano level. This is important as smaller liposomes give a more homogeneous size mix which allows for a more homogeneous drug or vaccine concentration spread through the volume. This also allows for liposomes to be formed below 100 nm in diameter which is important especially for drug delivery. This is because below 100 nm, liposomes effectively hide from the immune system due to their size. They cannot be too small though as many delivery components are stored in the hydrophilic core of the liposome and if they are made too small, this core reduces in size too much, reducing the carrying capacity significantly.

For vaccines, the size of the liposome is less important as the antigen the liposome is delivering is meant to be found and used by the immune system. It is still important to try and achieve a small and consistent size range, however, to ensure a more homogeneous spread of the vaccine; this cannot be achieved through the use of MLVs formed through the lipid film hydration method, as they are extremely heterogeneous in size and as such have a very large PDI value. Also, the use of SUV as opposed to MLV allows for a more even dispersion of the payload as the drug or antigen or other component only has to translocate over one lipid bilayer and not several.

Therefore, the aim of this work is to formulate protocols using the various Bioruptor® bath sonicator systems to reduce liposome size effectively and consistently. The objectives of this work were first of all to create a protocol for reduction of DMPC and DMPC: Cholesterol liposomes using a probe sonicator and compare also to a high shear mixer; a different technique. The Bioruptor® systems were then investigated in turn to see how effective they are at reducing the liposome size compared to each other and to the probe sonicator. These

systems were also investigated to create protocols for reducing liposome size over a variety of lipids, volumes and other factors.

2.2 Materials and Methods

2.2.1 Lipid Film Hydration Method for the production of MLV

MLVs were prepared by the lipid hydration method. Weighed amounts of the required lipids were each dissolved in chloroform/methanol (9:1 v/v). These lipids were added together to a final concentration of either 8 mM DMPC or DMPC in combination with cholesterol 6:4 mM, 6:2mM and 4: 4mM respectively. The organic solvent was extracted using a roto-evaporator followed by flushing with N₂ to form a thin lipid film on the bottom of a round bottom flask. The lipid film was hydrated using 10 mM Tris or Phosphate Buffered Saline (PBS) buffer at pH 7.4 and at ~ 20 °C above the transition temperature for the main lipid in the formulation.

2.2.2 Formulation of size reduced liposomes using probe sonication

For each liposome formulation, the particle size was reduced using a sonication probe. The suspension of MLV was sonicated (at 10 amplitude for 6 minutes) using a titanium probe (MSE Soniprep 150 plus with MSE PG100 probe (UK)) slightly immersed into the solution. This sonication procedure causes the breaking of the lipid bilayer of liposomes, converting a slightly milky suspension of MLV into a clear suspension of size reduced liposomes. They were then placed in a centrifuge for 15 minutes at 25°C at 1393g (2500 revolutions per minute (RPM)). These vesicles were characterised for their size, PDI and zeta potential.

The amplitude level was then tested to see whether this would affect liposome size. An MLV liposome formation using DMPC of 8 mM was produced. The milky suspension was then placed in a small vial and sonicated at two different amplitude levels, 8 and 10 amplitude, for a total of 10 minutes each. A sample was taken at 1 minute and at every minute after that until the 10-minute limit had been reached. These were then analysed for their size and PDI.

Next the sonication time was tested. This time, 3 formulations were produced at either 8 mM DMPC or DMPC in combination with cholesterol 6:2 mM and 4:4 mM respectively. The milky suspension was then placed in vials and sonicated for a total of 10 minutes each. A sample was taken at 1 minute and at every minute after that until the 10-minute limit had been reached. These were then analysed for their size and PDI.

Concentration was also investigated to see whether this made a significant difference to liposome size reduction. An MLV liposome formation using DMPC of between 2 and 30 mM was produced for each concentration. The milky suspension was then placed in vials and sonicated for a total of 6 minutes each at 10 amplitude. They were then placed in a centrifuge for 15 minutes at 25°C at 2500rpm. These were then analysed for their size and PDI.

Finally, the optimised settings of 10 amplitude for 6 minutes at 8 mM were run. 3 formulations were produced using the above formulation method at either 8 mM DMPC or DMPC in combination with cholesterol 6:2 mM and 4:4 mM respectively. For each liposome formulation, the optimised method was used where the particle size was reduced using a sonication procedure. The suspension of MLV was sonicated at 10 amplitude for 6 minutes using a titanium probe (MSE PG100 probe) slightly immersed into the solution. They were then placed in a centrifuge for 15 minutes at 25°C at 2500rpm. These vesicles were characterised for their size, PDI and zeta potential.

2.2.3 Formulation of size reduced liposomes by the high shear mixing (HSM) homogenisation method studies

DMPC and DMPC: Cholesterol 6:2 MLV were formed using the lipid film hydration method and then Tris buffer (10 mM; pH 7.4) was added to the lipid film, which was then placed and mounted in a 60°C water bath on a Jenway 1000 hotplate and stirrer (UK). The use of a Heidolph silent crusher M (Germany) was used at a range of speeds (5,000, 10,000, 15,000, 20,000 and 25,000 rpm) and time (5 minutes increments up to 30 minutes). These vesicles were characterised for their size and PDI.

2.2.4 Formulation of size reduced liposomes using Bioruptor® XL studies

For each liposome formulation, the particle size was reduced using a bath sonicator Diagenode Bioruptor® XL (Belgium). Firstly, MLVs were made as part 2.1 states with DMPC and DMPC: Cholesterol 6: 2 formulations being made for investigation.

For the time experiment, DMPC and DMPC: Cholesterol 6:2 liposomes were produced using the Bioruptor® XL at 45°C using 1000 µL in 1.5 mL tubes. They were then sonicated at power M2 for different periods of time with various cycles. Each cycle had a 30 second delay before the next cycle began, and a 30 second delay at the end of each measurement was used too. These vesicles were characterised for their size and PDI.

For the power experiment, DMPC and DMPC: Cholesterol 6:2 liposomes were produced using the Bioruptor® XL at 45°C using 1000 µL in 1.5 mL tubes. They were then sonicated for 15 minutes of continuous sonication with a 30 second delay at the end, at the 4 different power levels of Low (L), Medium Low (M1), Medium High (M2) and High (H). These vesicles were characterised for their size and PDI.

For the volume experiment, DMPC and DMPC: Cholesterol 6:2 liposomes were produced using the Bioruptor® XL at 45°C using different volumes ranging from 100 to 1000 µL in 1.5 mL tubes. They were then sonicated at power level M2 for 15 minutes of continuous sonication with a 30 second delay at the end. These vesicles were characterised for their size and PDI.

For the concentration experiment, DMPC liposomes were produced using the lipid hydration method. Using the Bioruptor® XL, the samples were sonicated at 45°C using 300 µL in 1.5 mL tubes. They were sonicated at power level M2 for 15 minutes of continuous sonication with a 30 second delay at the end. These vesicles were characterised for their size and PDI.

2.2.5 Formulation of size reduced liposomes using Bioruptor® Standard studies

For each liposome formulation, the particle size was reduced using a bath sonicator Diagenode Bioruptor® Standard (Belgium). Firstly, MLVs were made as part 2.1 states with DMPC and DMPC: Cholesterol 4: 4 formulations being made for investigation.

For the power experiment, DMPC and DMPC: Cholesterol 4:4 liposomes were produced using the Bioruptor® Standard at 45°C using 300 µL in 1.5 mL tubes. They were then sonicated for 15 minutes of 30, 30 at the 3 different power levels of L, M and H. These vesicles were characterised for their size and PDI.

For the second power experiment, DMPC and DMPC: Cholesterol 4:4 liposomes were produced using the Bioruptor® Standard at 45°C using 300 µL in 1.5 mL tubes. They were then sonicated for 15 minutes of 30, 0 at the 3 different power levels of L, M and H. These vesicles were characterised for their size and PDI.

For the pulse experiment, DMPC and DMPC: Cholesterol 4:4 liposomes were produced using the Bioruptor® Standard at 45°C using 300 µL in 1.5 mL tubes. They were then sonicated for

15 minutes at power level L with a reduction in time off of 5 seconds per experiment from 30, 30 to 30, and 0. These vesicles were characterised for their size and PDI.

For the time experiment, DMPC and DMPC: Cholesterol 4:4 liposomes were produced using the Bioruptor® Standard at 45°C using 300 µL in 1.5 mL tubes. They were then sonicated at power M for different periods of time up to 15 minutes. Each cycle was 30 seconds on, 30 seconds off cycle. These vesicles were characterised for their size and PDI.

For the further time experiment, DMPC and DMPC: Cholesterol 4:4 liposomes were produced using the Bioruptor® Standard at 45°C using 300 µL in 1.5 mL tubes. They were then sonicated at power M for different periods of time from 15 to 30 minutes. Each cycle was 30 seconds on, 0 seconds off cycle. These vesicles were characterised for their size and PDI.

For the volume experiment, DMPC and DMPC: Cholesterol 4:4 liposomes were produced using the Bioruptor® Standard and then sonicated for 15 minutes of 30, 0 at the power level M. The volume was tested between 100 µL and 1000 µL in 1.5 mL tubes. These vesicles were characterised for their size and PDI.

For the next volume experiment, DMPC and DMPC: Cholesterol 4:4 liposomes were produced using the Bioruptor® Standard and then sonicated for 15 minutes of 30, 0 at the power level M. The volume was tested between 0.5 and 3 mL in 15 mL tubes. These vesicles were characterised for their size and PDI.

For the position experiment, DMPC and DMPC: Cholesterol 4:4 liposomes were produced using the Bioruptor® Standard and then sonicated for 15 minutes of 30, 0 at the power level M. Each position in the holder was assigned an arbitrary number between 1 and 6 and each ran 3 times to compare how much variability there was in the same position over multiple tests and between the 6 different positions available. These vesicles were characterised for their size and PDI.

For the temperature experiment, DMPC and DMPC: Cholesterol 4:4 liposomes were produced using the Bioruptor® Standard using 300 µL in 1.5 mL tubes. They were then sonicated for

15 minutes of 30, 0 at the power level M. The temperature was tested in 5 degree increments between 5 and 50 °C. These vesicles were characterised for their size and PDI.

The next few tests all involved using a Polypropylene (PP) tube instead of the previously provided Polytetrafluoroethylene (PTFE) tubes to see what difference the plastic choice makes. For the power experiment, DMPC and DMPC: Cholesterol 4:4 liposomes were produced using the Bioruptor® Standard at 45°C using 300 µL in 1.5 mL PP tubes. They were then sonicated for 15 minutes of 30, 30 at the 3 different power levels of L M, and H. These vesicles were characterised for their size and PDI.

For the time experiment, DMPC and DMPC: Cholesterol 4:4 liposomes were produced using the Bioruptor® Standard at 45°C using 300 µL in 1.5 mL PP tubes. They were then sonicated at power M for different periods of time. Each cycle was 30 seconds on, 30 seconds off cycle. These vesicles were characterised for their size and PDI.

For the small volume experiment, DMPC and DMPC: Cholesterol 4:4 liposomes were produced using the Bioruptor® Standard and then sonicated for 15 minutes of 30, 0 at the power level M. The volume was tested between 100 µL and 1000 µL in 1.5 mL PP tubes. These vesicles were characterised for their size and PDI.

For the larger volume experiment, DMPC and DMPC: Cholesterol 4:4 liposomes were produced using the Bioruptor® Standard and then sonicated for 15 minutes of 30, 0 at the power level M. The volume was tested between 0.5- and 2-mL PP tubes. These vesicles were characterised for their size and PDI.

For the formulation experiment, 6 formulations were investigated. DMPC, DMPC: Cholesterol 4:4, Phosphatidylcholine (PC): Cholesterol 4:4, DSPC: Cholesterol 4:4, DMPC: Cholesterol: 1, 2-Dimyristoyl-Sn-glycero-3-phospho-rac-(1-glycerol) sodium salt (DMPG) 4:4:1 and DMPC: Cholesterol: N-[1-(2, 3-Dioleoyloxy) propyl]-N, N, N-trimethylammonium chloride (DOTAP) 4:4:1 liposomes were produced using the Bioruptor® Standard and then sonicated for 15

minutes of 30, 0 at the power level M with a 100 μ L volume in a 1.5 mL TPX® tube. These vesicles were characterised for their size, PDI and zeta potential.

2.2.6 Formulation of size reduced liposomes using Bioruptor® Plus studies

For each liposome formulation, the particle size was reduced using a bath sonicator Diagenode Bioruptor® Plus (Belgium). Firstly, MLVs were made as part 2.1 states with DMPC and DMPC: Cholesterol 4: 4 formulations being made for investigation. All samples unless stated otherwise were sonicated in a TPX® tube.

For the cycles experiment, DMPC and DMPC: Cholesterol 4:4 liposomes were produced using the Bioruptor® Plus using 100 μ L in 1.5 mL tubes. They were then sonicated for up to 30 cycles in 5 cycle increments at H power or L power. These vesicles were characterised for their size and PDI.

For the concentration experiment, DMPC liposomes were produced using the Bioruptor® Plus using 100 μ L in 1.5 mL tubes using 8, 16- and 24-mM concentrations, sonicated for 15 cycles at the H power level. These vesicles were characterised for their size and PDI.

For the temperature experiment, DMPC and DMPC: Cholesterol 4:4 liposomes were produced using the Bioruptor® Plus using 100 μ L in 1.5 mL tubes. They were then sonicated for 15 cycles at L and H power levels. The temperature was tested in at 20, 30 and 40 °C. These vesicles were characterised for their size and PDI.

For the small volume experiment, DMPC and DMPC: Cholesterol 4:4 liposomes were produced using the Bioruptor® Plus and then sonicated for 15 cycles at H power level. The volume was tested between 100 μ L and 300 μ L in 1.5 mL TX tubes. These vesicles were characterised for their size and PDI.

For the small volume plastics experiment, DMPC liposomes were produced using the Bioruptor® Plus and then sonicated for 15 cycles at H power level using a 100 µL sample in either a TPX® or PP 1.5 mL tube. These vesicles were characterised for their size and PDI.

For the largest volume plastics experiment, DMPC liposomes were produced using the Bioruptor® Plus and then sonicated for 15 cycles at H power level using a 0.5, 1 or 2 mL sample in either a TPX®, Polycarbonate tubing (PCT), Polypropylene Co-polymer (PPCO) or PP 50 mL tube. These vesicles were characterised for their size and PDI.

For the larger volume plastics experiment, DMPC liposomes were produced using the Bioruptor® Plus and then sonicated for 15 cycles at L and H power levels using a 100 or 500 µL sample in either a TPX® or PP 15 mL tube. These vesicles were characterised for their size and PDI.

For the larger cholesterol ratio experiment, DMPC: Cholesterol liposomes were produced using the Bioruptor® Plus in 4:4, 5:3, 6:2 and 7:1 ratio and then sonicated for 15 cycles at L and H power levels using a 100 µL sample in a TPX® 1.5 mL tube. These vesicles were characterised for their size and PDI.

For the lipid concentration test, DMPC: Cholesterol 4:4 liposomes were produced with either 0, 1, 2 or 4 mM of either 1, 2-Dioleoyl-sn-glycero-3-phosphoethanolamine (DOPE), DOTAP or DMPG added. These were sonicated for 15 cycles at H power using a 100 µL sample in a TPX® 1.5 mL tube. These vesicles were characterised for their size, PDI and zeta potential.

2.2.7 Formulation of size reduced liposomes using Bioruptor® Pico studies

For each liposome formulation, the particle size was reduced using a bath sonicator Diagenode Bioruptor® Pico (Belgium). Firstly, MLVs were made as part 2.1 states with DMPC and DMPC: Cholesterol 4: 4 formulations being made for investigation.

For the cycles experiment, DMPC and DMPC: Cholesterol 4:4 liposomes were produced using the Bioruptor® Pico using 100 µL in 1.5 mL tubes. They were then sonicated for up to 10 cycles. These vesicles were characterised for their size and PDI.

For the small volume experiment, DMPC and DMPC: Cholesterol 4:4 liposomes were produced using the Bioruptor® Pico and then sonicated for 10 cycles. The volume was tested between 100 µL and 300 µL in 1.5 mL TX tubes. These vesicles were characterised for their size and PDI.

2.2.8 Characterisation of liposomes

The liposomes were then characterised using a Brookhaven Nanobrook (USA). A 100 µL sample was placed in a 4 clear sided cuvette. 1.9 mL of deionised water was added and the sample vortexed to ensure thorough mixing. The sample was then allowed to stand for a few minutes, and then placed in the machine. Each of the three batches was ran three times and the average and standard deviation calculated for both the size and PDI once outliers had been removed.

2.3 Results and discussion

2.3.1 A probe sonication study into liposome size reduction

Probe sonication was the first method to be investigated as it is very well established within the literature. Probe sonication has been used to reduce the size of liposomes since their first conception back in the 60s. Since then, hundreds of papers have been published using probe sonication as the means for reducing liposome size after initial formation using the lipid film hydration method. For example, compared to other methods such as extrusion and microfluidics, there has been consistently more papers published decade on decade using sonication than either of these two methods, as shown in Figure 2.1. This shows that this method is well used and well known within the scientific domain. This is due to a number of factors including how easy it is to use the equipment with no special skills required and how quick it reduces the liposomes size, generally within just a couple of minutes. Probe sonication far outweighs bath in number of publications with 376 publications specifying probe sonication for liposome work but only 70 specifying bath sonication. This again is due to how quick the probe reduces liposome size compared to a bath sonicator. Therefore, the probe sonicator is a good place to start and it is important to get a good baseline for comparison to the bath sonicator protocols that are later going to be formulated and optimised.

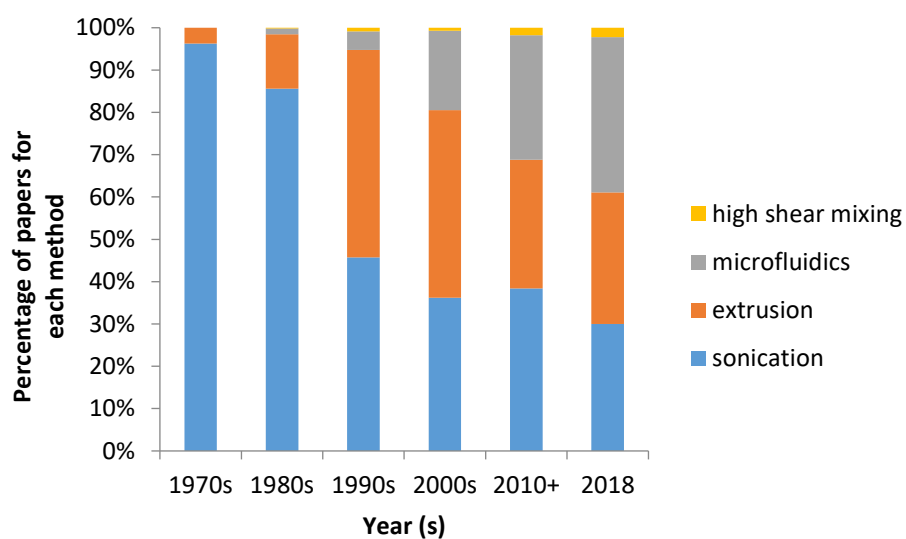
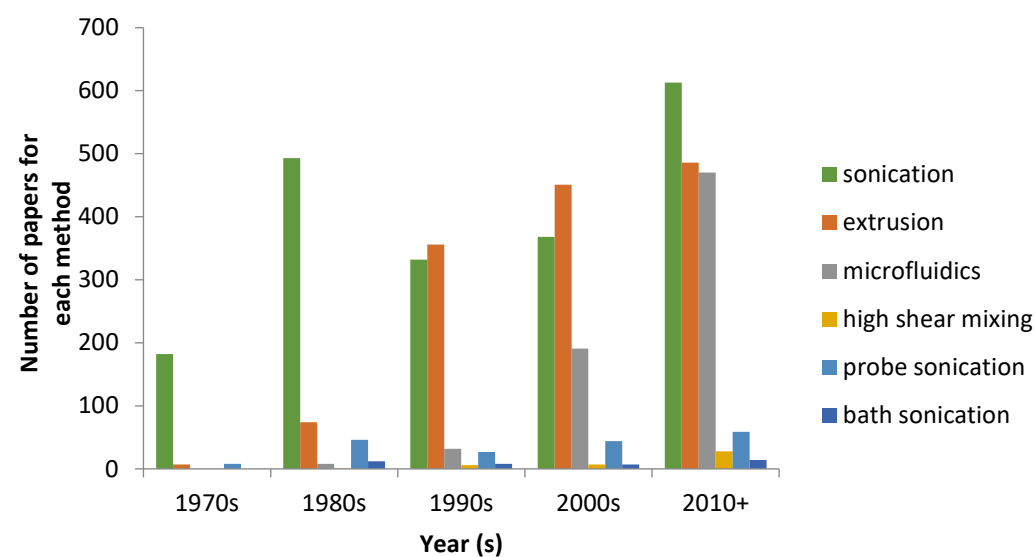


Figure 2.1: Number of publications for microfluidics, sonication and extrusion for liposome formation using the name of the method and the word liposome in their titles on all databases on web of science.

2.3.1.1 Initial probe sonication study

Initial experiments were run to form MLV by the lipid hydration method and then forming size reduced liposomes by sonication using DMPC and DMPC Cholesterol in a 6: 4 ratio. These results are shown below in Table 2.1. It was found that MLV liposomes were in the order of several microns, whereas once they had been sonicated and centrifuged under the initial conditions, they were much smaller with DMPC liposomes forming a size of 81.6 ± 5.9 nm and DMPC: Cholesterol 6:4 being 136 ± 30.5 nm. A reduction in PDI was also noted, with drops to 0.272 ± 0.014 for DMPC, and 0.307 ± 0.095 for DMPC Cholesterol 6:4. For the sonication method, a PDI of below 0.3 is seen as an acceptable PDI. For other methods such as extrusion and microfluidics, a lower PDI of below 0.15 can be achieved meaning the liposomes formed using these methods are more homogenous than those formed using sonication methods. The zeta potential for these lipids was also found to get more negative once they had been sonicated.

Table 2.1: Initial experimental results for DMPC and DMPC Cholesterol 6:4 using the lipid hydration and sonication methods.

FORMULATION	SIZE	Z AVERAGE SIZE	AVERAGE ZETA	PDI
	REDUCED/MLV	(D. NM)	POTENTIAL / MV	
DMPC	MLV	4713 ± 2412	-7.86 ± 12.1	0.344 ± 0.067
DMPC	Size reduced	81.6 ± 5.93	-17.6 ± 15.6	0.272 ± 0.014
DMPC: CHOLESTEROL	MLV	3321.5 ± 887.2	-1.36 ± 1.01	0.727 ± 0.198
DMPC: CHOLESTEROL	Size reduced	135.97 30.47	-30.1 ± 10.1	0.307 ± 0.095

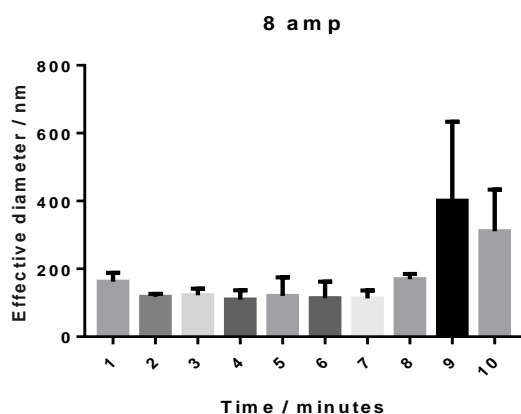
2.3.1.2 Probe sonication study into how amplitude level and time affects liposome size reduction

The level of sonication afforded to the liposomes with two different levels, 10 amplitude and 8 amplitude, being used was tested first. These showed very little difference in how long they took to form the size reduced liposomes, or how small the size reduced liposomes were, up until 8 minutes as shown in Figure 2.2. There was no significant difference shown between 3 and 7 minutes for the 8 amplitude size data and between 5 and 7 minutes for the 10 amplitude data. The smallest size achieved for 8 amplitude was at 7 minutes being 112.8 ± 23.8 nm and 88.9 ± 2.1 nm for 10 amplitude. After that, a significant increase in the size seen was noted

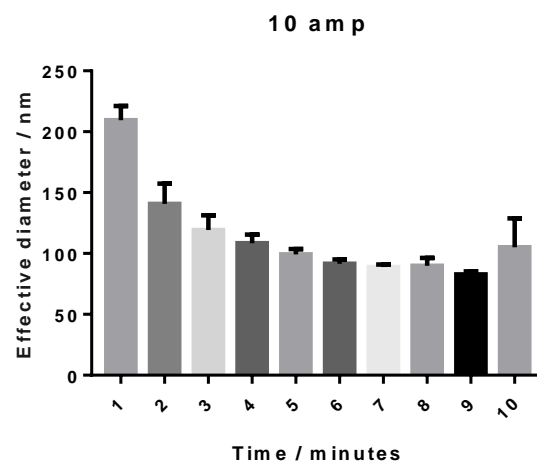
with both amplitudes, between 8 and 9 minutes for 8 amplitude using a t test with a p value of < 0.0001 and between 9 and 10 minutes for 10 amplitude with a p value of 0.0026. Although this is unclear why, it could be down to the liposomes being broken up and forming larger constructs or by being attacked by the free radicals that are formed (Maulucci et al., 2005). These results also showed that once the liposomes had been sonicated, a lower PDI was also found. However no significant difference was seen between any of the 8 amplitude PDI apart from between 1 and 8 minute marks with a p value of 0.0381. With the 10 amplitude data, significant differences were only seen between the 1 minute mark and several other time points, and between the 10 minute mark and several other time points. What this showed was that the PDI was decreased once sonicated was applied to the sample, but this would increase and decrease over time and not in a uniform pattern. This could be because as the liposomes are broken and reformed, the PDI of the mixture increases and decreases with this process.

It also showed that although there wasn't a significant difference between the size of polydispersities at 6 minutes between 8 and 10 amplitude, the tenfold increase in standard deviation seen with 8 amplitude compared to 10 amplitude showed that for a more consistent size, it is better to use 10 amplitude. The results for the 10 amplitude size were also lower, although not significantly so, compared to the 8 amplitude size data.

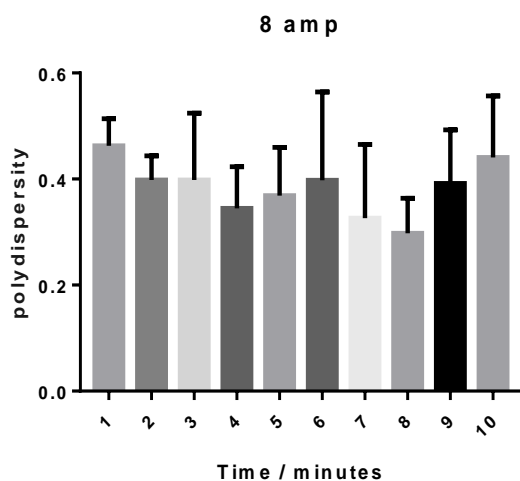
Overall what this shows is that the amplitude of sonication does not have a significant effect on the size of PDI of liposomes produced at the same time point. What this data did show was that by decreasing the amplitude, an increase in relative standard deviation was seen. It also showed that by sonicating for 6 minutes, this would allow for as small a size as possible to be achieved without the risk of over sonicating the sample and starting to break it down, thereby increasing the size result.



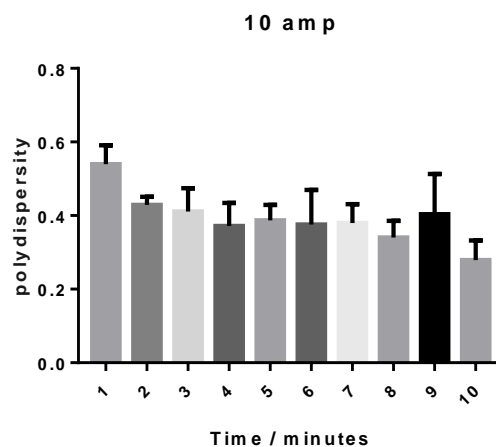
A)



B)



C)



D)

Figure 2.2: A and B) Size of probe sonicated DMPC liposomes sonicated over 10 minutes with samples taken every minute at either 8 (A) or 10 (B) amplitude. C and D) PDI of probe sonicated DMPC liposomes sonicated over 10 minutes with samples taken every minute at either 8 (A) or 10 (B) amplitude.

2.3.1.3 Probe sonication study into how cholesterol concentration affects liposome size reduction

Following this, 3 different formulations were then tried over a 10 minute period at 10 amplitude to see if the different formulations could require different sonication times. Each formulation was showed that once a sonication time of 6 minutes had been reached, a small and consistent size and a smaller PDI was seen, as shown in Figure 2.3. Also, at the 6 minute mark, there is a significant difference between the sizes seen for DMPC compared to its DMPC Cholesterol counterparts. DMPC: Cholesterol 6:2 and DMPC: Cholesterol 4:4 showed no significant difference. This showed that the size of the DMPC liposomes being produced were significantly smaller than their DMPC: Cholesterol counterparts and that although a different sonication time wouldn't be needed for the different formulations, that the DMPC: Cholesterol liposomes produced are significantly bigger than the DMPC liposomes.

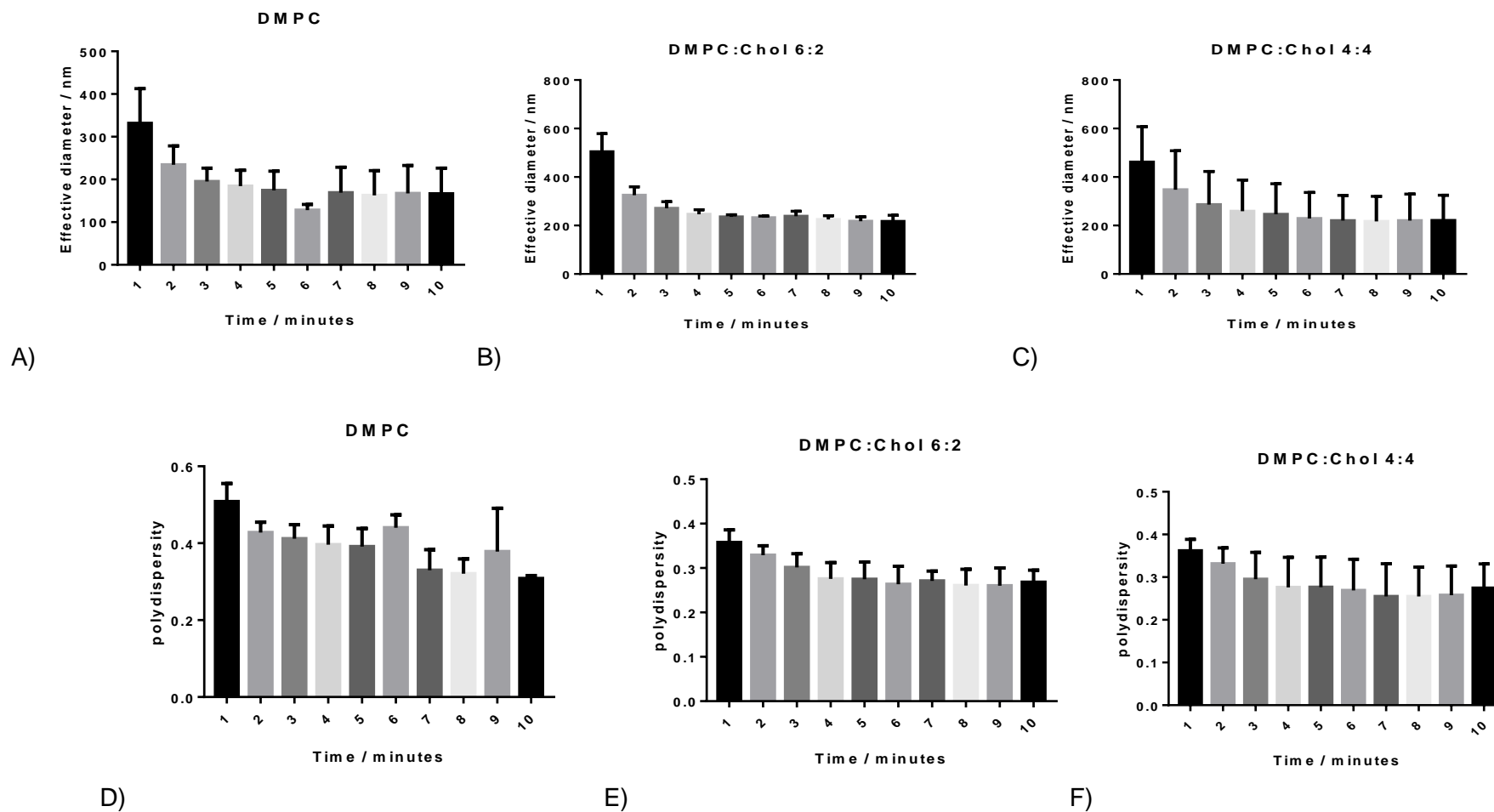


Figure 2.3: A – C) Size of 3 different formulations; DMPC (A), DMPC: Cholesterol 6:2 (B) and DMPC: Cholesterol 4:4 (C) sonicated over a 10 minute time period at 10 amplitude. D - F) PDI of 3 different formulations; DMPC (D), DMPC: Cholesterol 6:2 (E) and DMPC: Cholesterol 4:4 (F) sonicated over a 10 minute time period at 10 amplitude.

2.3.1.4 Probe sonication study into how concentration affects DMPC liposome size reduction

Concentration is also an important factor to test as a concentration change will affect the number of liposomes in any given volume and change factors such as viscosity and how much energy each individual liposome will receive in order to be broken down and reformed into the smaller liposomes. The results showed in Figure 2.4 showed no significant difference between 2 and 8 mM of with sizes all around 85 nm. There was a significant increase for 20 mM of 116.6 ± 1.7 nm and 30 mM of 120.4 ± 2.5 nm. There were statistically significant differences for PDI but no increase above 0.3 or below 0.25 so not significant for this work. What this showed is that concentration only begins to affect size reduction slowly over a large range, in this case from 2 to 30 mM.

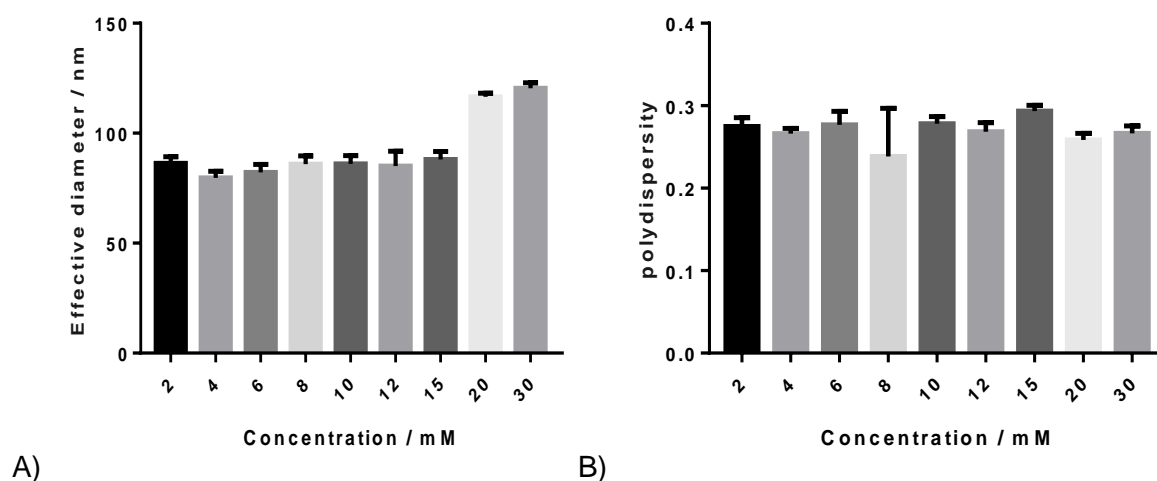


Figure 2.4: A) Size of sonicated DMPC liposomes at a range of concentrations from 2 to 30 mM sonicated at 10 amplitude for 6 minutes. B) PDI of sonicated DMPC liposomes at a range of concentrations from 2 to 30 mM sonicated at 10 amplitude for 6 minutes.

2.3.1.5 Probe sonication study using the optimised conditions

The amplitude, concentration and time optimisation were put together to form the final probe sonication results as shown in Figure 2.5. It was found that there was a significant difference between each formulation size. DMPC had a size of 85.9 ± 3.8 nm up to 110 ± 0.6 nm for DMPC: Cholesterol 6:2 and up to 134 ± 1.7 nm for DMPC: Cholesterol 4:4. PDI showed no significant difference between the Cholesterol forms, 0.202 ± 0.013 and 0.209 ± 0.011 for 6:2 and 4:4 respectively. DMPC had a statistically higher PDI at 0.239 ± 0.058 . What these showed is that as cholesterol was added to the formulation, the size increased but the PDI dropped, showing the liposomes were reduced in size less but there was an increase in uniformity. Though these increases in size were significant, they weren't large as they only increase by tens of nanometres. Therefore, the method could easily be modified slightly, with an increase in time for example, to take into account the different formulation to then produce smaller liposomes comparable to the DMPC liposomes produced.

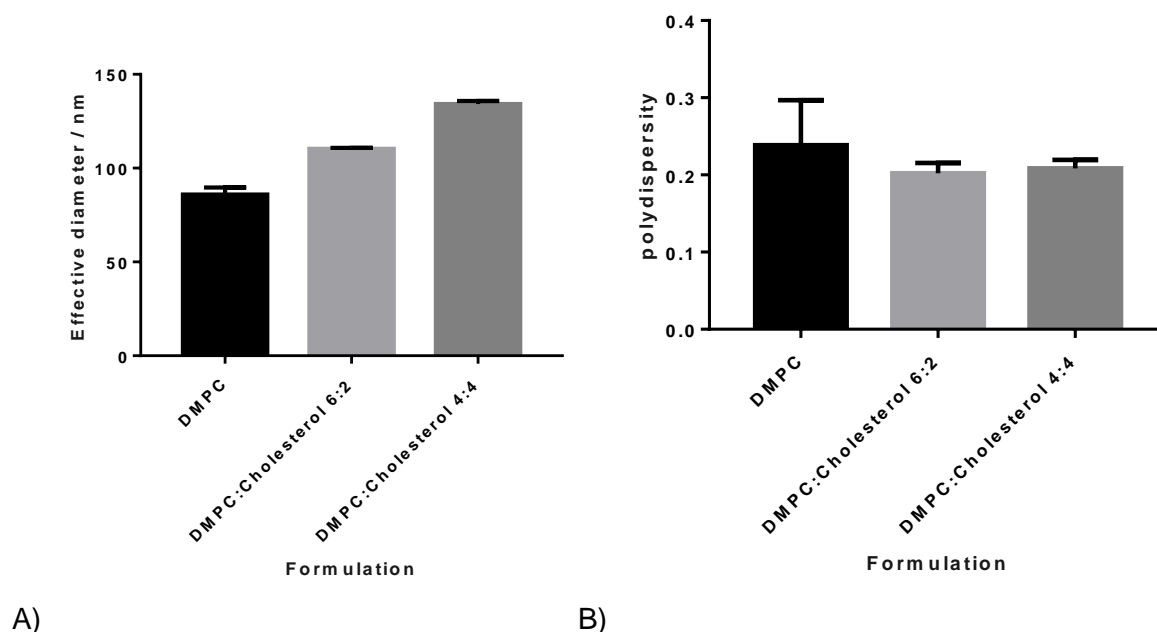


Figure 2.5: A) Size of final formulations of DMPC, DMPC: Cholesterol 6:2 and DMPC: Cholesterol 4:4 made using optimised sonication conditions of 10 amplitude for 6 minutes. B) PDI of final formulations of DMPC, DMPC: Cholesterol 6:2 and DMPC: Cholesterol 4:4 made using optimised sonication conditions of 10 amplitude for 6 minutes.

2.3.1.6 Discussion

What these results mean is that there is now a good baseline for probe sonicated DMPC and DMPC: Cholesterol liposomes which can then be used as a direct comparison to other methods such as high shear mixing and bath sonication. It was shown that amplitude did not have a significant effect on the probes ability to reduce liposome size although 10 amplitude was chosen as it gave smaller standard deviations. It was also shown that time is an important factor as the longer the samples were sonicated for, the smaller the size of the liposomes.

However, this size reduction was limited after 6 minutes of sonication and therefore this was the time point chosen. Formulation was also shown to have an effect on the finished liposome size with samples of DMPC, DMPC: Cholesterol 6:2 and DMPC: Cholesterol 4:4 liposomes ran under the same conditions showing significant differences in both size and PDI. It was shown that as you increased the cholesterol concentration, the liposome size increases and the PDI decreases. This shows that if you require liposomes to be a certain size, the formulation has to be taken into account and if any changes are made to that formulation, then the other factors such as time may have to be changed as well.

2.3.2 Developing and optimising a protocol for the production of SUV using DMPC and DMPC: Cholesterol lipid formulations using high shear mixing

HSM has been used for production of liposomes previously, with some success (Vemuri et al., 1990, Foged et al., 2014). HSM is used a lot more within the industrial sector because of its scalability compared to many of the other liposome size reduction methods currently used (Wagner and Vorauer-Uhl, 2011). High shear mixing works differently to sonication where instead of using sonic energy to disrupt the bilayers and reduce the size of the liposomes, a milling effect is employed (Khadka et al., 2014). Therefore, the aim of this study was to see whether DMPC and DMPC: Cholesterol liposomes could be also used by the HSM method using laboratory high shear mixers.

2.3.2.1 High shear mixing study into the effect of rpm parameters on vesicle size reduction

Each of the three formulations DMPC 8 mM, DMPC: Cholesterol 6:2 mM and DMPC: Cholesterol 4: 4 mM, was tested at different rpm ranging from 5k rpm to 25k rpm in increments of 5k. Figure 2.6 shows that at the slowest speed of 5,000 rpm, there is no size reduction of the liposomes at all. DMPC 8 mM liposomes came out at 3192 ± 273 nm, DMPC: Cholesterol 6:2 came out at 7404 ± 3111 nm and DMPC: Cholesterol 4:4 came out at 10046 ± 8235 nm. A decrease in size was seen as an increase in rpm occurred, with a minimum size of 1223 ± 269 nm, 1467 ± 81 nm and 1027 ± 133 nm being achieved respectively for each formulation. With PDI, an increase was seen with DMPC 8 mM liposomes, but decreases were seen with both DMPC: Cholesterol formulations. DMPC 8 mM increased from 0.252 ± 0.086 at 5000

rpm to 0.317 ± 0.019 at 25000 rpm, DMPC: Cholesterol 6:2 decreased meanwhile from 0.453 ± 0.078 down to 0.360 ± 0.028 between 5000 and 25000 rpm and DMPC: Cholesterol 4:4 reduced from 0.592 ± 0.221 to 0.352 ± 0.024 . This showed that even at the highest rpm that this model can achieve, the size of the liposomes produced is still far larger and with larger polydispersities compared to the probe sonicated liposomes.

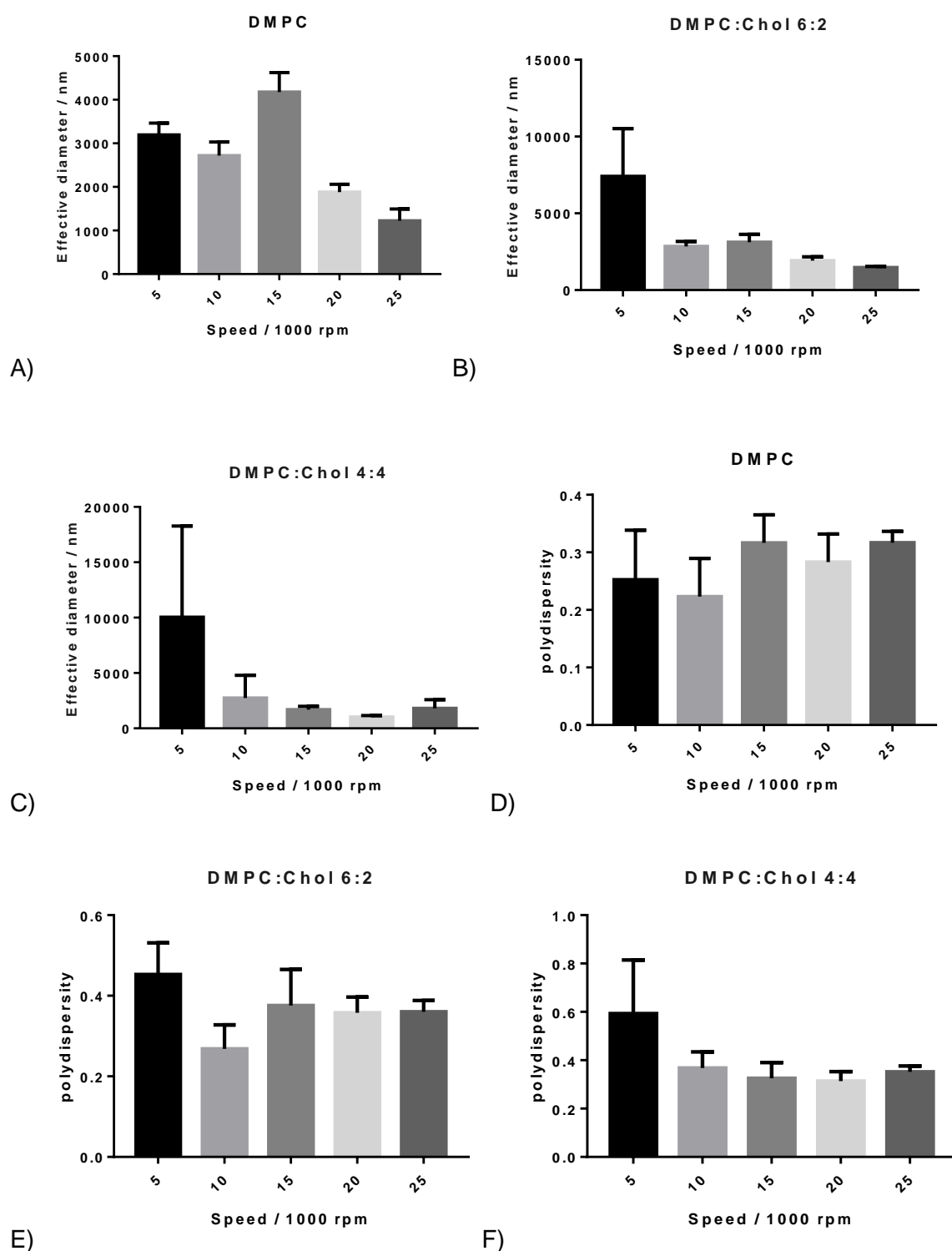


Figure 2.6: A – C) Size of 3 different formulations; DMPC (A), DMPC: Cholesterol 6:2 (B) and DMPC: Cholesterol 4:4 (C) high shear mixed over 5000 to 25000 rpm. D – F) PDI of 3 different formulations; DMPC (D), DMPC: Cholesterol 6:2 (E) and DMPC: Cholesterol 4:4 (F) high shear mixed over 5000 to 25000 rpm.

2.3.2.2 High shear mixing study into the effect of time on liposome size reduction

Each of the three formulations DMPC 8 mM, DMPC: Cholesterol 6:2 mM and DMPC: Cholesterol 4: 4 mM, were subject to times ranging from 5 to 30 minutes at 5 minute time points to see if HSM the samples for longer would make a difference to their size. As shown in Figure 2.7, all three liposome formulations were still above a micron in size after 5 minutes of high shear mixing, with a size for DMPC 8 mM of 1497 ± 193 nm, DMPC: Cholesterol 6:2 of 1193 ± 155 nm and DMPC: Cholesterol 4:4 of 2166 ± 816 nm. Each then further reduced in size down to a minimum of 517 ± 142 nm, 581 ± 104 nm and 691 ± 30.6 nm respectively. There were mixed results for the polydispersities. DMPC 8 mM actually rose from 0.332 ± 0.024 to 0.375 ± 0.037 from 5 to 30 minutes of high shear mixing (Figure 3.3B). DMPC: Cholesterol 6:2 did not see any notable change, reducing from 0.355 ± 0.023 to 0.354 ± 0.025 (Figure 3.3B). DMPC: Cholesterol 4:4 saw a reduction in PDI, down from 0.383 ± 0.065 to 0.283 ± 0.035 (Figure 3.3B). Even after half an hour of high shear mixing, the size of the liposomes could not be reduced down to a size that was comparable with probe sonication. This could be down to the milling effect not being as effective at reducing the size of these lipid formulations under these conditions compared to the sonic energy using with probe sonication.

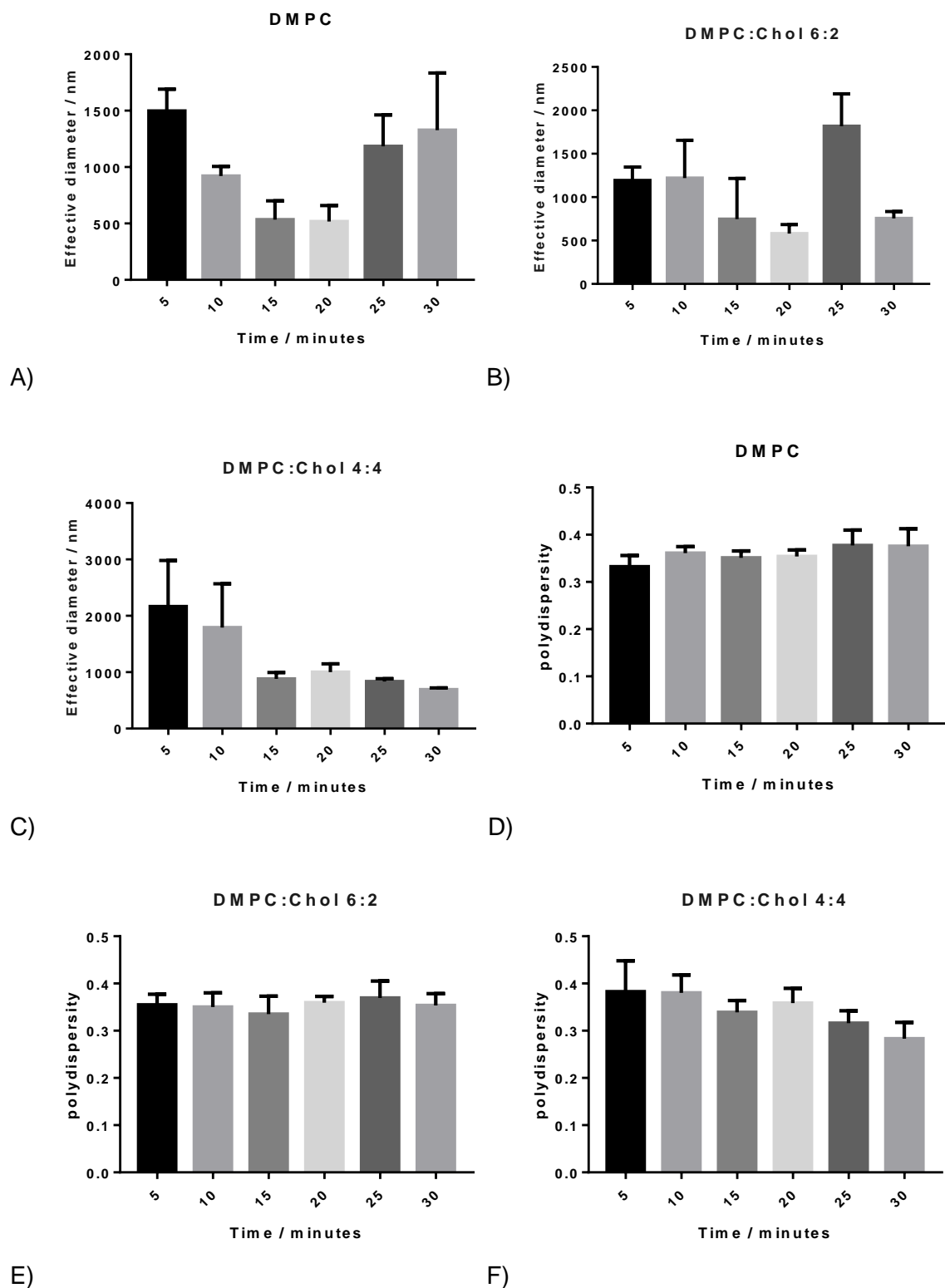


Figure 2.7: A – C) Size of 3 different formulations; DMPC (A), DMPC: Cholesterol 6:2 (B) and DMPC: Cholesterol 4:4 (C) high shear mixed over 5 to 30 minutes. D – F) PDI of 3 different formulations; DMPC (D), DMPC: Cholesterol 6:2 (E) and DMPC: Cholesterol 4:4 (F) high shear mixed over 5 to 30 minutes.

2.3.2.3 Discussion

So even though with this method and these lipids the size reduction wasn't as great as desired, high shear mixing has been used to make liposomes and other nanoparticles well within the nano range before. For example, Trotta et al investigated using a high shear mixer to form solid nanoparticles using glyceryl monostearate nanodispersions. They succeeded in forming sub-micron nanoparticles with a smallest size of 205 nm. What this shows was that by using an emulsifier at least, it is possible to form nanoparticles in the nano size range by just using a high shear mixer (Trotta et al., 2003). Another study by Zakeri-Milani et al also showed that by using a high shear mixer, it is possible to form solid lipid nanoparticles in a 200 – 500 nm size range by using c (Zakeri-Milani et al., 2014).

Other studies have been carried out where the high shear mixer has been used as a precursor element, and then the liposomes reduced to their optimum size using other methods such as sonication. For example, Mohammadi et al was able to produce liposomes using lecithin and cholesterol with a particle size range of 82 to 89 nm. This worked by producing the liposomes using the lipid film hydration method, and then high shear mixing them for 15 minutes at 60 °C. They were then probe sonicated for 5 minutes and sized (Mohammadi et al., 2014). What this shows is that high shear mixing can be used to produce SUV, in conjunction with another size reduction method, something this study did not look in to. High shear mixing has also been shown to be able to produce small liposomes on their own, using different lipid formulations as to those used in this study. Dietrich et al was able to form liposomes Dimethyldioctadecylammonium (Bromide Salt) (DDA), D-(+)-trehalose 6, 6'-dibehenate (TDB) and a high shear mixer at 60 – 80 °C for 15 minutes after the liposomes had been formed using the lipid film hydration method. These liposomes came out to be approximately 203 nm in size, growing slightly larger to 267 nm once the inactivated polio virus vaccine had been bound to the liposome (Dietrich et al., 2014). Therefore, how this study fits in is that even though you can form lipid nanoparticles and liposomes using high shear mixing alone, you

cannot form DMPC and DMPC: Cholesterol liposomes in the required size range using high shear mixing alone.

2.3.3 Bioruptor® XL liposome size reduction studies

Previous studies have looked into reducing the size of liposomes using bath sonication (Hadian et al., 2014, Kim, 2015). However, none have gone into much detail which is why this study was needed. Also, no studies have been done that look at optimisation of DMPC liposome size using bath sonication, and no studies have been done to look at the Bioruptor® systems as a way of reducing liposome size. Therefore, a number of different factors were investigated using a DMPC and DMPC: Cholesterol formulation looking at the Bioruptor® XL system. The factors that were investigated were time, pulse, power, volume and concentration.

2.3.3.1 Bioruptor® XL study into how the number of cycles affects liposome size reduction

Various time periods were tested from 5 to 20 minutes, using a different number of cycles, with the result shown below in Figure 2.8. These show that just by adding more cycles on top of one another doesn't necessarily lead to smaller liposome formation. Each time for example an extra 5 minute cycle was added to the first 5 minute cycle, up to 15 minutes total, a significant difference was seen as the size increased. What the results do show is that long periods of sonication is the best way to reduce the size of liposomes, with 15 minutes of continuous sonication giving the smallest significant results over the shortest period of time

for both formulations in question. DMPC: Cholesterol liposomes were smaller for 2 cycles of 10 minutes, but this was not significant. The PDI results followed a roughly similar pattern with the smallest PDI for DMPC liposomes being for 15 minutes of continuous sonication which came to 0.279 ± 0.031 . There was no significant difference between any of the DMPC: Cholesterol liposomes PDI results. Therefore, 15 minutes of continuous sonication was the chosen time period for this study.

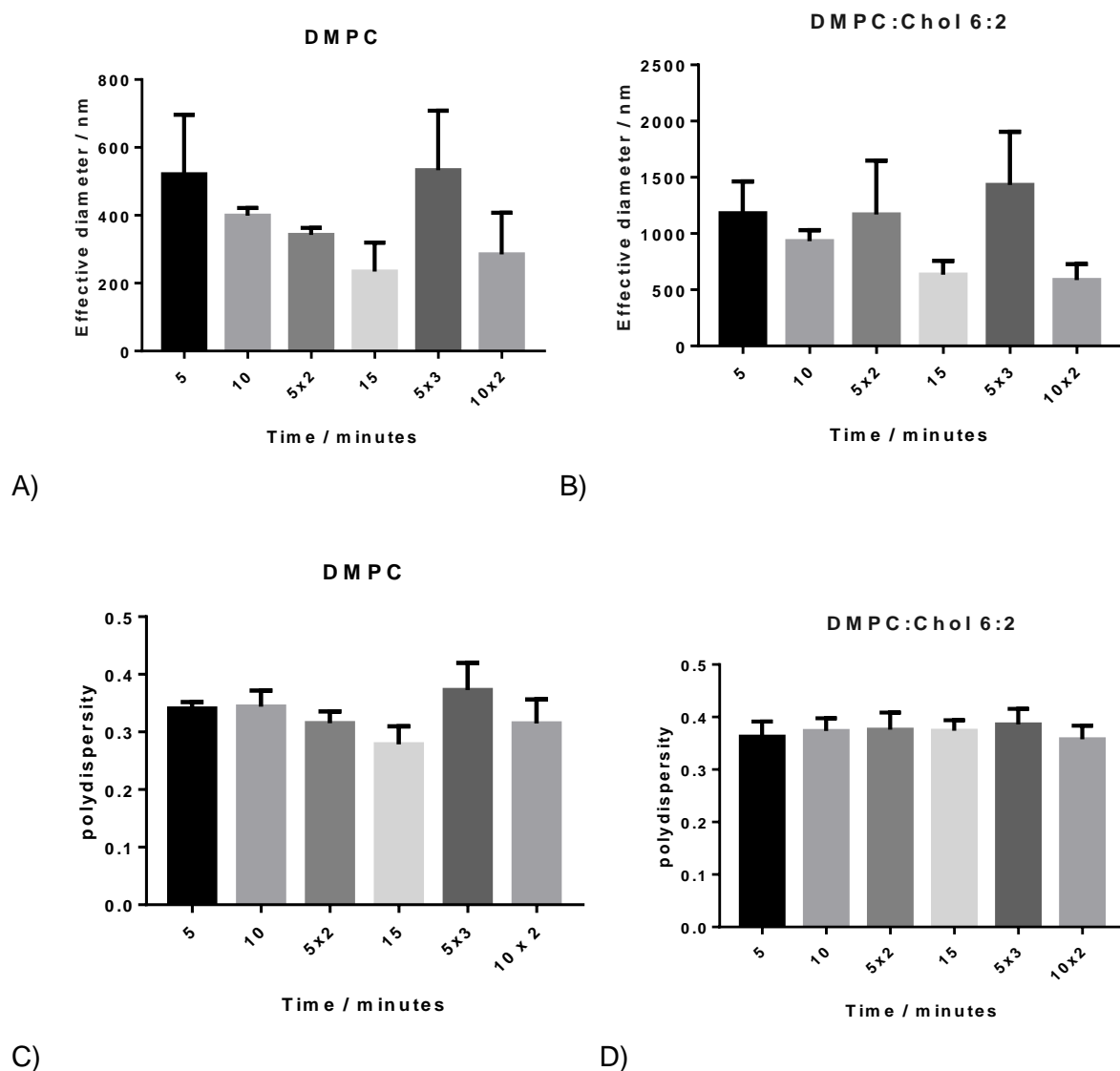


Figure 2.8: A – B) Size of sonicated liposomes over various time and cycle settings up to a maximum of 20 minutes for DMPC (A) and DMPC: Cholesterol 6:2 (B) sonicated at power level M2 at 45°C using 1000 μ L in 1.5 mL tubes. C – D) PDI of sonicated liposomes over various time and cycle settings up to a maximum of 20 minutes for DMPC (A) and DMPC: Cholesterol 6:2 (B) sonicated at power level M2 at 45°C using 1000 μ L in 1.5 mL tubes.

2.3.3.2 Bioruptor® XL study into how the power level affects liposome size reduction

Next the four different power levels were tested with the machine, L, M1, M2 and H (130W, 200W, 250W and 300W respectively). What these results show in Figure 2.9 is that it doesn't make too much of a difference how much power you put into, so long as it's enough. This can clearly be seen with the low power tests, with sizes of 8787 ± 6483 nm for DMPC liposomes and 4384 ± 1836 nm for DMPC: Cholesterol liposomes. PDI was also high with values of 0.391 ± 0.157 for DMPC liposomes at low power and 0.4 ± 0.117 for DMPC: Cholesterol liposomes on the same power level. The other power levels had no significant differences to one another when run under the same conditions with lows of 256 ± 79 nm in size and a PDI of 0.302 ± 0.036 for DMPC liposomes and a size of 616 ± 92 nm and PDI of 0.367 ± 0.015 for DMPC: Cholesterol liposomes. Therefore, the middle power level of M2 was chosen as it would reduce the liposomes sufficiently.

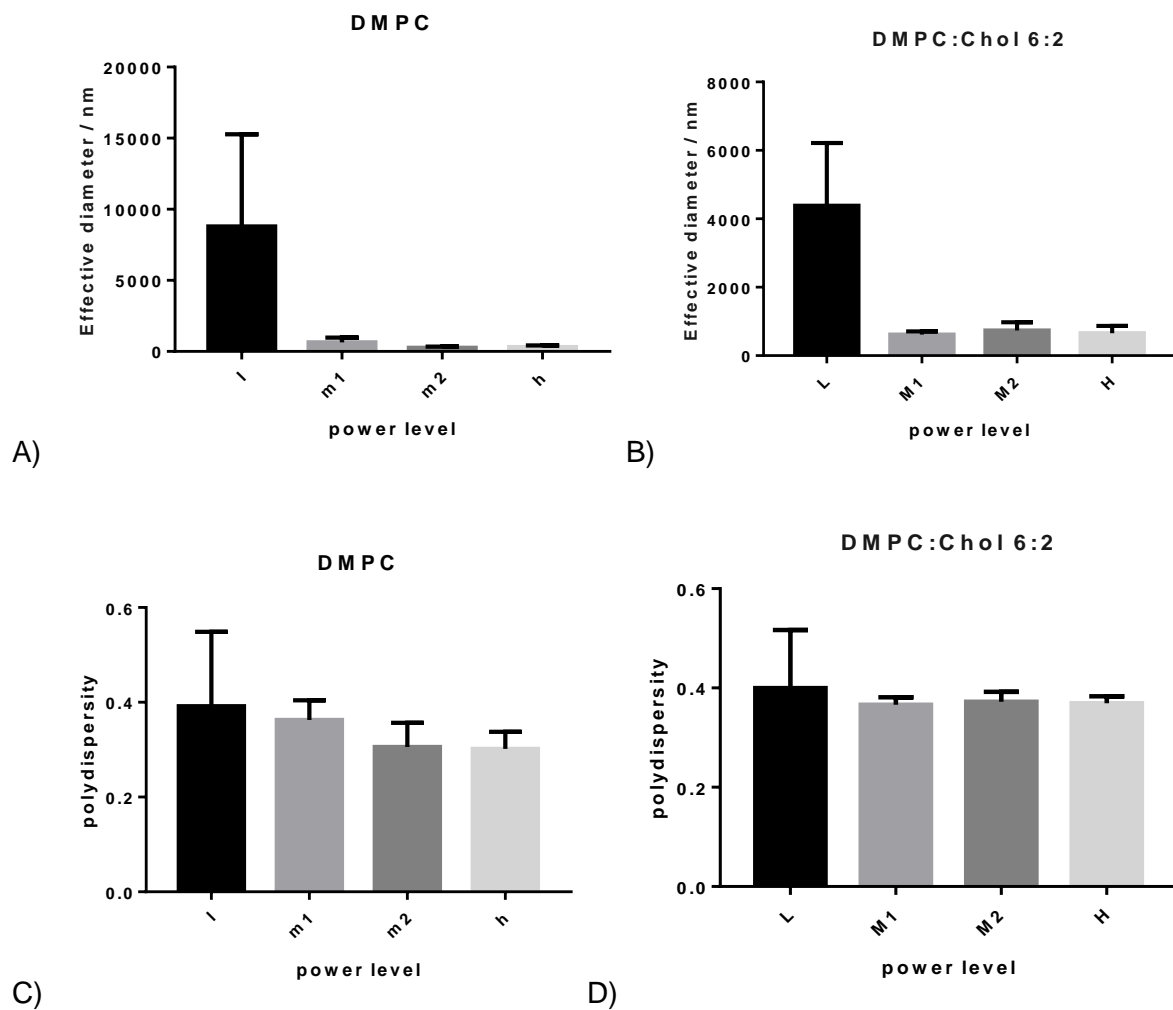


Figure 2.9: A – B) Size of DMPC (A) and DMPC: Cholesterol 6:2 (B) liposomes sonicated using the 4 different power levels over 15 minutes of continuous sonication at 45°C using 1000 μ L in 1.5 mL tubes. C – D) PDI of DMPC (A) and DMPC: Cholesterol 6:2 (B) liposomes sonicated using the 4 different power levels over 15 minutes of continuous sonication at 45°C using 1000 μ L in 1.5 mL tubes.

2.3.3.3 Bioruptor® XL study into how volume affects liposome size reduction

What we can see is that the sizes of these liposomes produced are still much larger than those formed by probe sonication, 200 nm + compared to 100 nm approximately. However, once volume had been taken into account, things began to look a lot better. As shown below in Figures 2.10, the original volume of 1000 μ L was far too large, and the sonicator was unable to sonicate the entire sample, leading to the larger sizes recorded. However, once volume had dropped below 500 μ L, and particularly 300 μ L, it was seen that sizes of liposomes could now be produced that were comparable to those found with probe sonication. PDI too was seen to reduce markedly and reduce further in fact than that found with probe sonication. Using the smaller volumes, the smallest vesicle size for DMPC liposomes of 89.7 ± 4.1 nm and PDI 0.269 ± 0.005 was achieved for a 0.1 mL sample volume. For DMPC: Cholesterol 6:2, the lowest vesicle size and PDI achieved were 65.3 ± 2.9 nm and 0.182 ± 0.012 respectively, this time for a 0.2 mL sample, although there was no significant difference between these results and those for the 0.1 mL sample. A significant difference was seen once the volume had been raised above 300 μ L for DMPC: Cholesterol, and above 500 μ L for DMPC liposomes. Therefore, a volume of 300 μ L was chosen for the optimisation because even though smaller sizes were noted with 100 μ L and 200 μ L, the aim is to produce as much of the size reduced liposomes as possible as for this work it is not imperative that the liposomes are reduced below 100 nm.

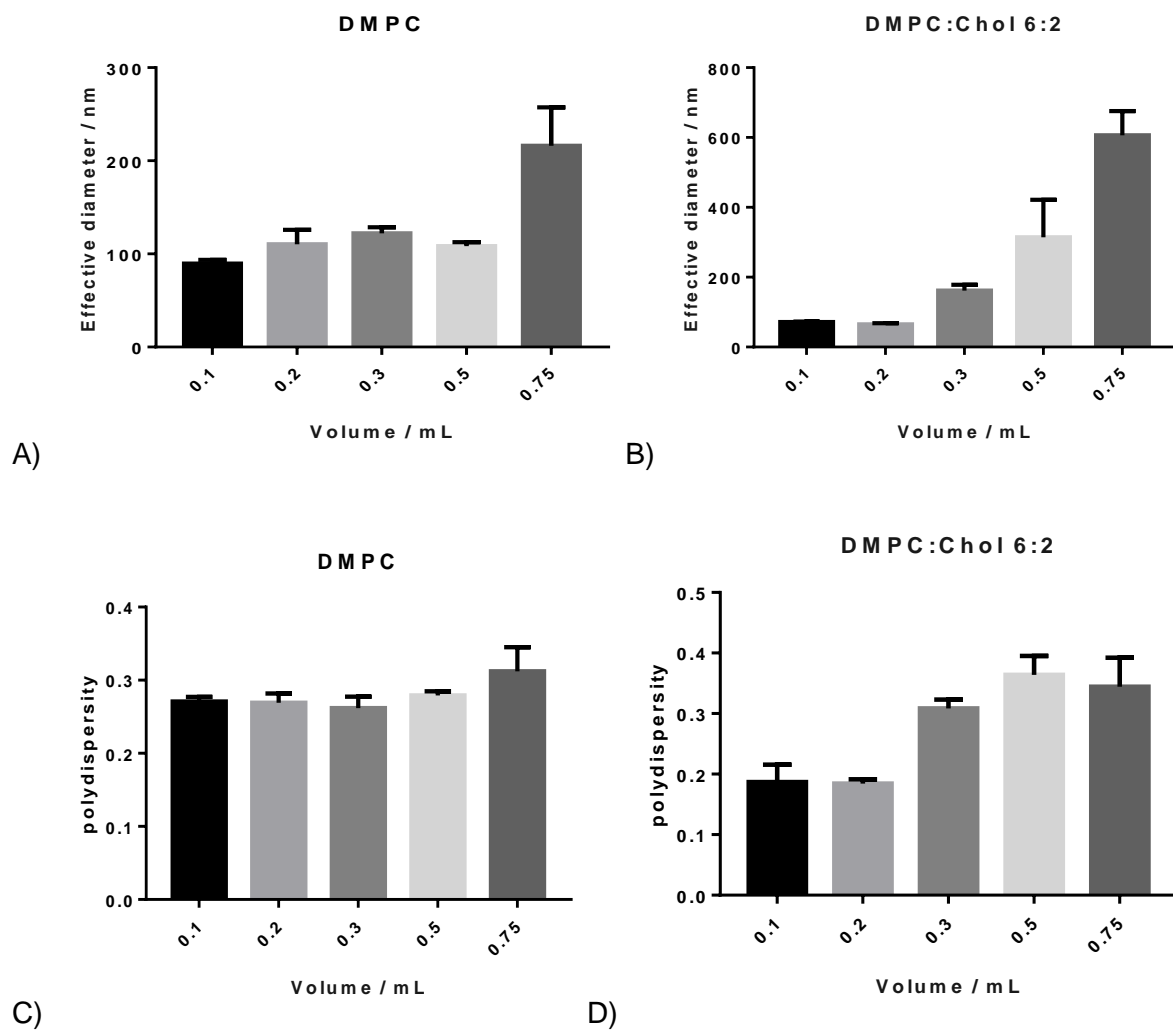
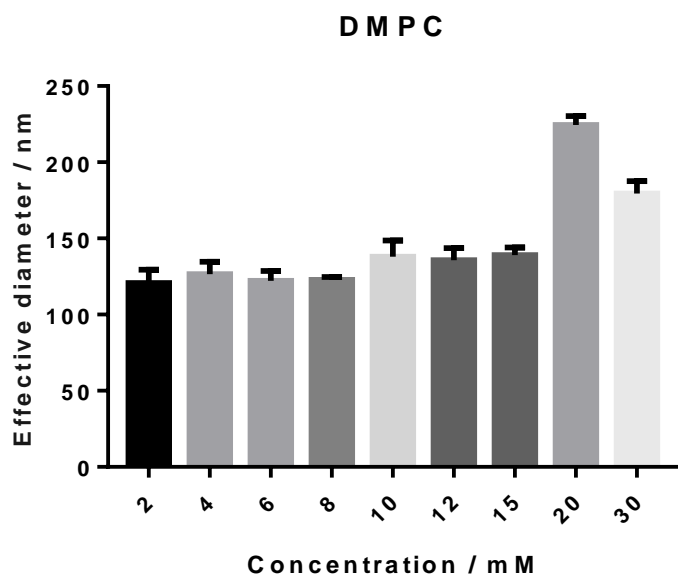


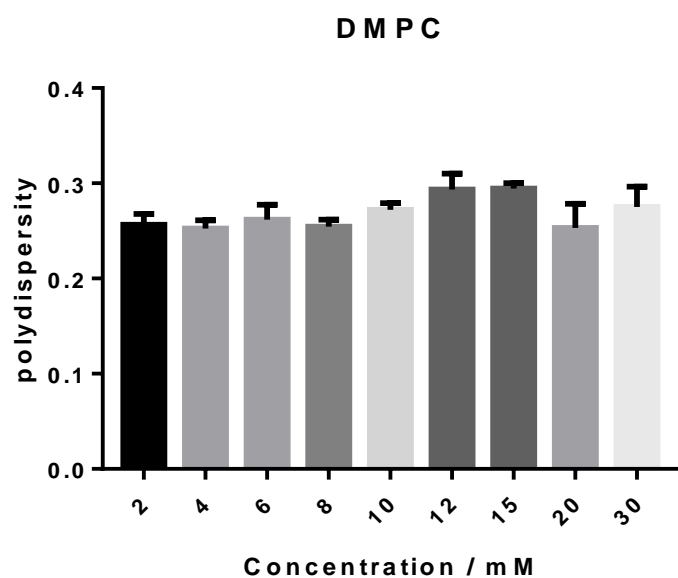
Figure 2.10: A – B) Size of DMPC (A) and DMPC: Cholesterol 6:2 (B) liposomes sonicated using a range of volumes from 0.1 to 0.75 mL over 15 minutes of continuous sonication at 45°C using 1000 μ L in 1.5 mL tubes at power level M2. C – D) PDI of DMPC (A) and DMPC: Cholesterol 6:2 (B) liposomes sonicated using a range of volumes from 0.1 to 0.75 mL over 15 minutes of continuous sonication at 45°C using 1000 μ L in 1.5 mL tubes at power level M2.

2.3.3.4 Bioruptor® XL study into how concentration affects liposome size reduction

Concentration for bath sonication was tested using the lipid DMPC at various concentrations. The results are shown below in Figure 2.11. What they show is that very little difference between the various concentrations for either method, until the concentrations reach 20mM and 30mM. There were some significant differences, but these can be discounted because of the very small standard deviations and that the sizes of the liposomes do not increase above 150 nm for bath sonication until they reach 20 mM and above. What these show is that at these levels, you begin to saturate the method, meaning that only so many size reduced liposomes can be produced within a given volume. However, it also showed that the concentration currently used of 8 mM is perfectly fine and so kept for the optimisation.



A)



B)

Figure 2.11: Size (A) and PDI (B) of DMPC liposomes sonicated at power level M2 at 45°C using 300 μ L in 1.5 mL tubes for 15 minutes of continuous sonication.

2.3.3.5 Discussion

What these results showed was that all factors need to be investigated to optimise the method for producing small liposomes. The need for small liposomes is important for drug delivery but liposome size modification is important for other uses including vaccine delivery. For example, even though the number of cycles and time sonicated was optimised first, this still left the DMPC and DMPC: Cholesterol liposomes in the several hundred nanometres range. It also showed that even with the same sonication time, the way the cycles are formulated does have a significant bearing on the size reduction. For example, 15 minutes of continuous sonication gave liposomes that were half the size of the liposomes formed by 3 cycles of 5 minutes of sonication each. The power level also showed that there is a minimum amount of power required to reduce liposome size and if this threshold is not crossed, then the liposomes will stay as MLVs and within the micron range as opposed to the nanometre range for a power level above this threshold. The volume data is what really showed that the Bioruptor® could be used to produce liposomes of a similar size to those produced by probe sonication. At volumes of 0.1 mL in a 1.5 mL tube, liposomes formed of both DMPC and DMPC: Cholesterol were found to be below 100 nm, an important factor as it is generally understood that liposomes of below 100 nm can evade the bodies innate immune system without the need for masking agents such as PEG. However, for this work, it was more important to produce sufficient liposomes of a small size rather than of the smallest size which is why 0.3 mL was chosen as the volume to take forward. Finally, concentration was again shown to have a small but significant effect with increases in size and PDI above 15 mM. What this showed is that similar to probe sonication, a finite amount of energy is put into the system over a set amount of time and the more concentrated the liposomes are, the less able they are to reduce in size using that set amount of energy over the same amount of time.

2.3.4 Bioruptor® Standard liposome size reduction studies

The Bioruptor® Standard is the precursor to the machines currently marketed by Diagenode, the Plus and the Pico. Therefore, it is important to investigate and optimise the various factors associated to see how small these liposomes can be produced, and how quickly. To this end, many factors including time, power level, temperature, volume, plastic and size of tube were all investigated.

2.3.4.1 Bioruptor® Standard study into how power level affects liposome size reduction

The first parameter tested was the three different power levels, L, M and H, as shown in Figure 2.12. These equate to 160, 200 and 320 W and showed something really interesting. There was no significant difference across the board between any of the DMPC: Cholesterol 4:4 samples with sizes of $187.2 \pm 33.9\text{nm}$, $184.7 \pm 21.9\text{ nm}$ and $190.3 \pm 20.7\text{ nm}$ respectively and polydispersities of 0.292 ± 0.014 , 0.29 ± 0.015 and 0.298 ± 0.019 . However, with DMPC 8 mM, there was a significant increase seen for both size and PDI at the Medium and High power. Between L and M, an increase in size was noted from $194 \pm 9.7\text{ nm}$ to $221 \pm 10.5\text{ nm}$ and an increase in PDI from 0.23 ± 0.024 to 0.254 ± 0.015 respectively. A further increase in size and PDI up to $295.9 \pm 44.9\text{ nm}$ and 0.35 ± 0.026 was noted for H power. These increases could be attributed to the increase in power starting to break apart the liposomes that have been formed, causing some aggregation and generally not allowing the DMPC liposomes to form as small as they would want (Lankin et al., 2002). Because of the significant differences seen with DMPC liposomes, the Low power was the level chosen for optimisation.

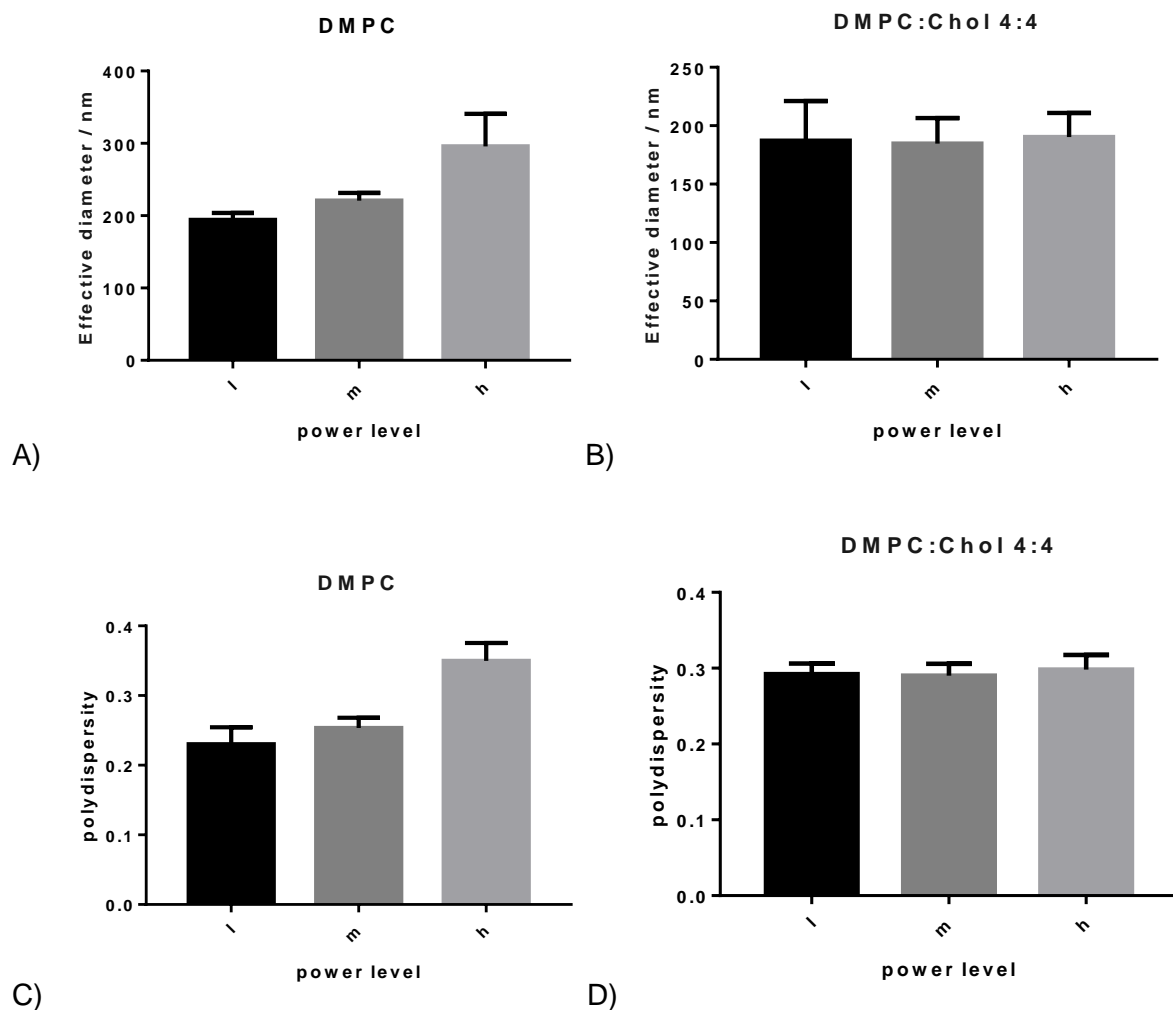


Figure 2.12: A – B) Size of DMPC (A) and DMPC: Cholesterol 4:4 (B) liposomes were produced using the Bioruptor® Standard at 45°C using 300 μ L in 1.5 mL tubes. They were then sonicated for 15 minutes of 30, 30 at the 3 different power levels of L, M and H. C – D) PDI of DMPC (A) and DMPC: Cholesterol 4:4 (B) liposomes were produced using the Bioruptor® Standard at 45°C using 300 μ L in 1.5 mL tubes. They were then sonicated for 15 minutes of 30, 30 at the 3 different power levels of L, M and H.

2.3.4.2 Bioruptor® Standard study into how power level with continuous sonication affects liposome size reduction

As shown in Figure 2.13, the power level was run again using continuous sonication. A significant rise in both size and PDI was seen with DMPC 8 mM liposomes when using the highest power of 320W but there was no significant difference this time between Low and Medium power. This increase in size and PDI was from 177.5 ± 4.2 nm to 219.3 ± 33.3 nm and from 0.207 ± 0.016 to 0.283 ± 0.04 respectively. The same pattern as before was seen with DMPC: Cholesterol 4:4 liposomes, with no significant difference between any of the power levels for either size or PDI. There was a significant difference also between the best sizes attained for both formulations using the M power compared to when there was no continuous sonication. Using continuous sonication saw a reduction in size for DMPC 8 mM liposomes from 221 ± 10.5 nm down to 177.5 ± 4.2 nm and a reduction in PDI from 0.256 ± 0.012 down to 0.207 ± 0.016 , compared to when the samples had 30 seconds on, 30 seconds off cycle. A reduction was also noted for DMPC: Cholesterol 4:4, from 184.7 ± 21.9 nm down to 155.2 ± 13.6 nm and a reduction in PDI from 0.290 ± 0.015 down to 0.241 ± 0.026 respectively. Therefore, the M power was chosen now as the optimal power level because of this minimal size and PDI data.

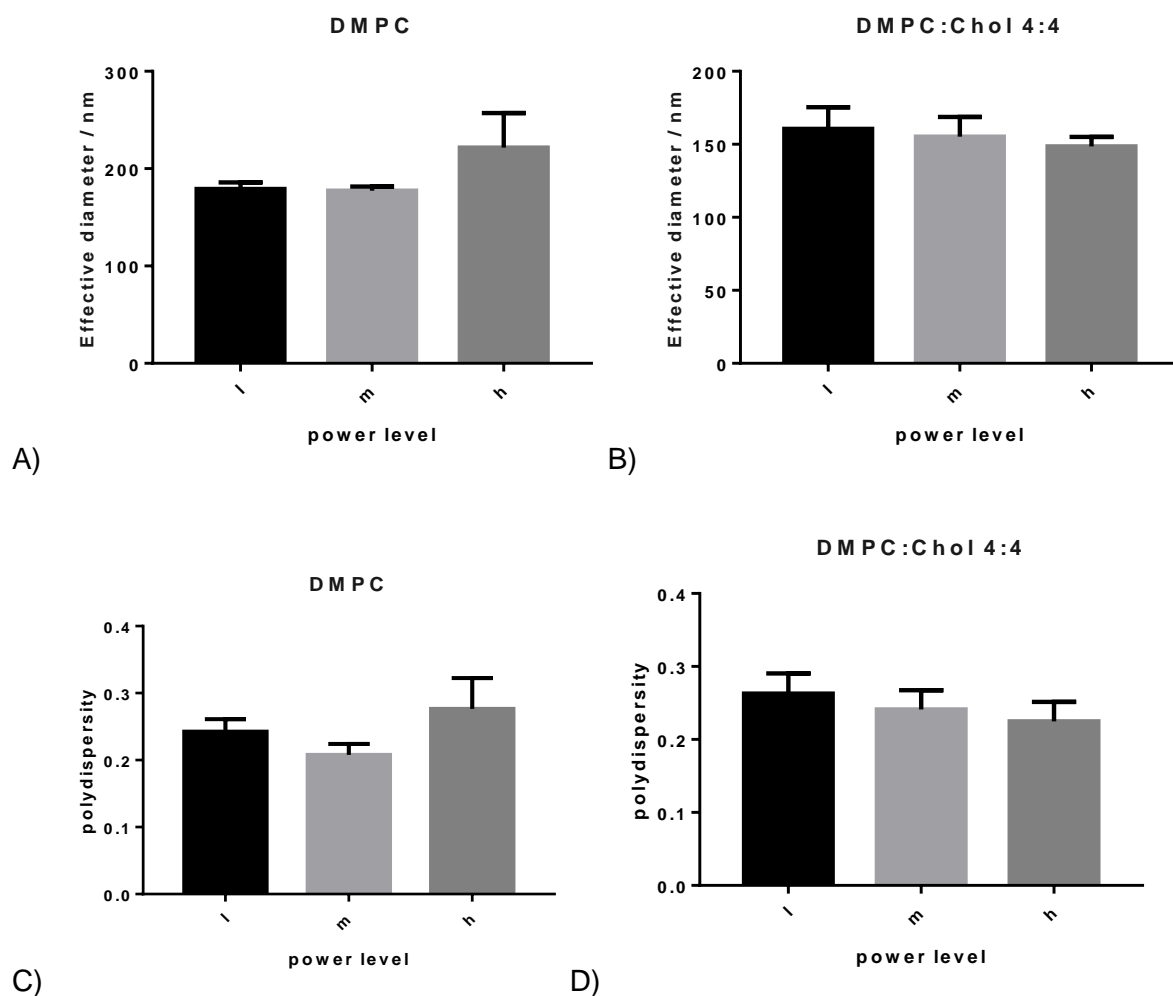


Figure 2.13: A – B) Size of DMPC (A) and DMPC: Cholesterol 4:4 (B) liposomes were produced using the Bioruptor® Standard at 45°C using 300 μ L in 1.5 mL tubes. They were then sonicated for 15 minutes of 30, 0 at the 3 different power levels of L, M and H. C – D) PDI of DMPC (A) and DMPC: Cholesterol 4:4 (B) liposomes were produced using the Bioruptor® Standard at 45°C using 300 μ L in 1.5 mL tubes. They were then sonicated for 15 minutes of 30, 0 at the 3 different power levels of L, M and H.

2.3.4.3 Bioruptor® Standard study into how pulse settings affect liposome size reduction

The next parameter tested was the different pulse levels as shown in Figure 2.14. For this what was found was that for both formulations an overall decrease in size was seen as you reduced the amount of time off. For DMPC 8 mM, a reduction in size was seen between 30 seconds off and 0 seconds off from 199.1 ± 9.7 nm down to 179.1 ± 6.8 nm. For DMPC: Cholesterol 4:4, a reduction was also seen from 199.6 ± 52.8 nm down to 158.5 ± 12 nm. A slight increase in PDI was noted for DMPC 8 mM, from 0.231 ± 0.023 to 0.241 ± 0.017 and a slight decrease in PDI was noted for DMPC: Cholesterol 4 4:4 from 0.294 ± 0.017 down to 0.263 ± 0.022 . What this showed was that as you decrease the amount of time off, and therefore increase the amount of sonication time overall, you get a further decrease in size for both formulations. Therefore, a continuous sonication was chosen.

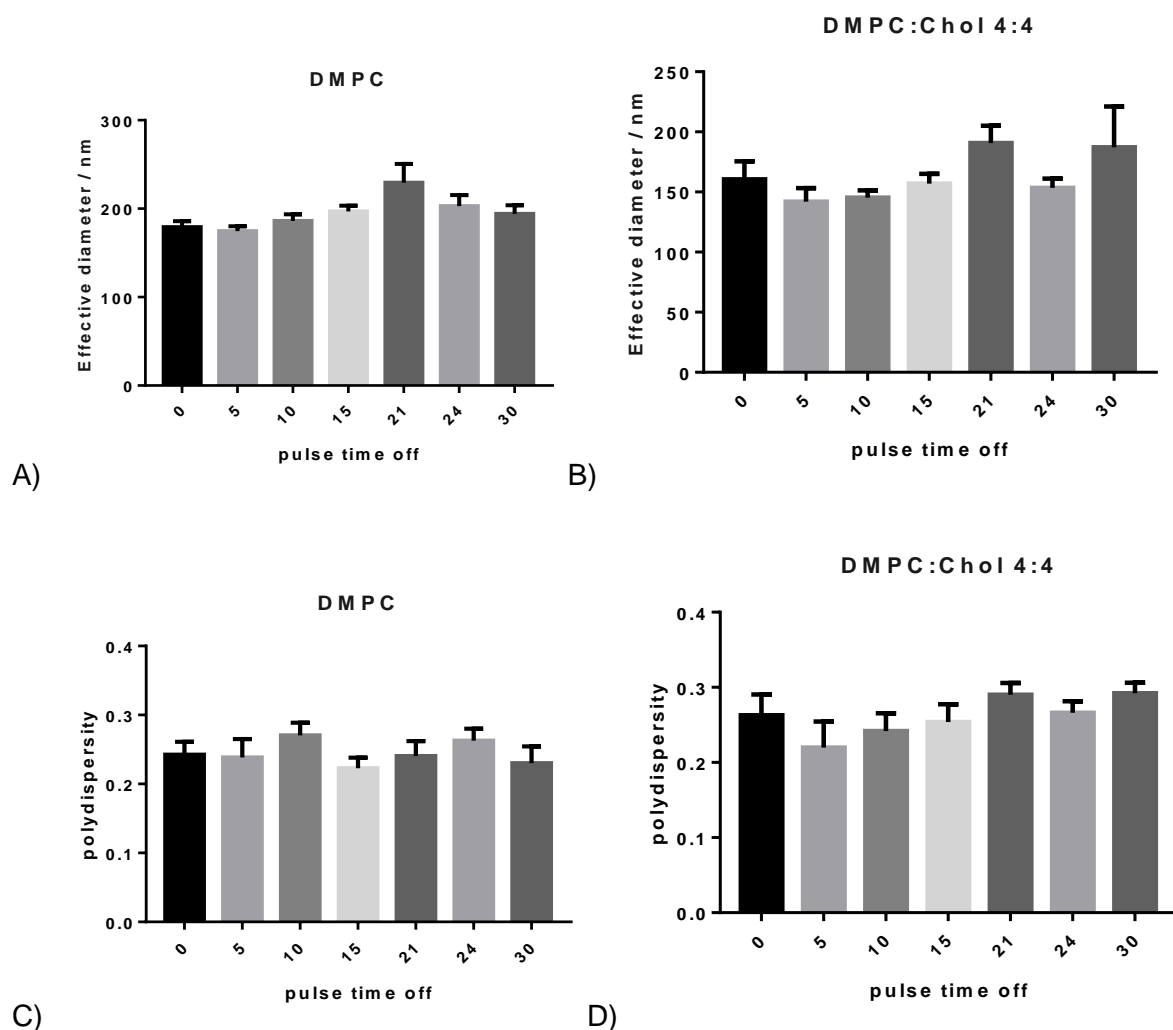


Figure 2.14: A – B) Size of DMPC (A) and DMPC: Cholesterol 4:4 (B) liposomes were produced using the Bioruptor® Standard at 45°C using 300 μ L in 1.5 mL tubes. They were then sonicated for 15 minutes at power level L with time on kept constant at 30 seconds and time off ranging from 0 to 30 seconds. C – D) PDI of DMPC (A) and DMPC: Cholesterol 4:4 (B) liposomes produced using the Bioruptor® Standard at 45°C using 300 μ L in 1.5 mL tubes. They were then sonicated for 15 minutes at power level L with time on kept constant at 30 seconds and time off ranging from 0 to 30 seconds.

2.3.4.4 Bioruptor® Standard study into how time affects liposome size reduction

As shown in Figure 2.15, a reduction in size and PDI was seen as time increased. For DMPC 8 mM, a reduction in size from 5 to 15 minutes from 349.1 ± 63.8 nm down to 221 ± 10.5 nm was seen, and a reduction in PDI from 0.304 ± 0.022 down to 0.256 ± 0.012 was seen respectively. For DMPC: Cholesterol 4:4, a reduction in size from 5 to 15 minutes was seen from 361.9 ± 26 nm down to 184.7 ± 21.9 nm and a reduction in PDI over the same time frame from 0.341 ± 0.016 down to 0.29 ± 0.015 . These results therefore showed that as you increase the time a liposome sample is sonicated, you reduce both the size and PDI of that formulation (Woodbury et al., 2006).

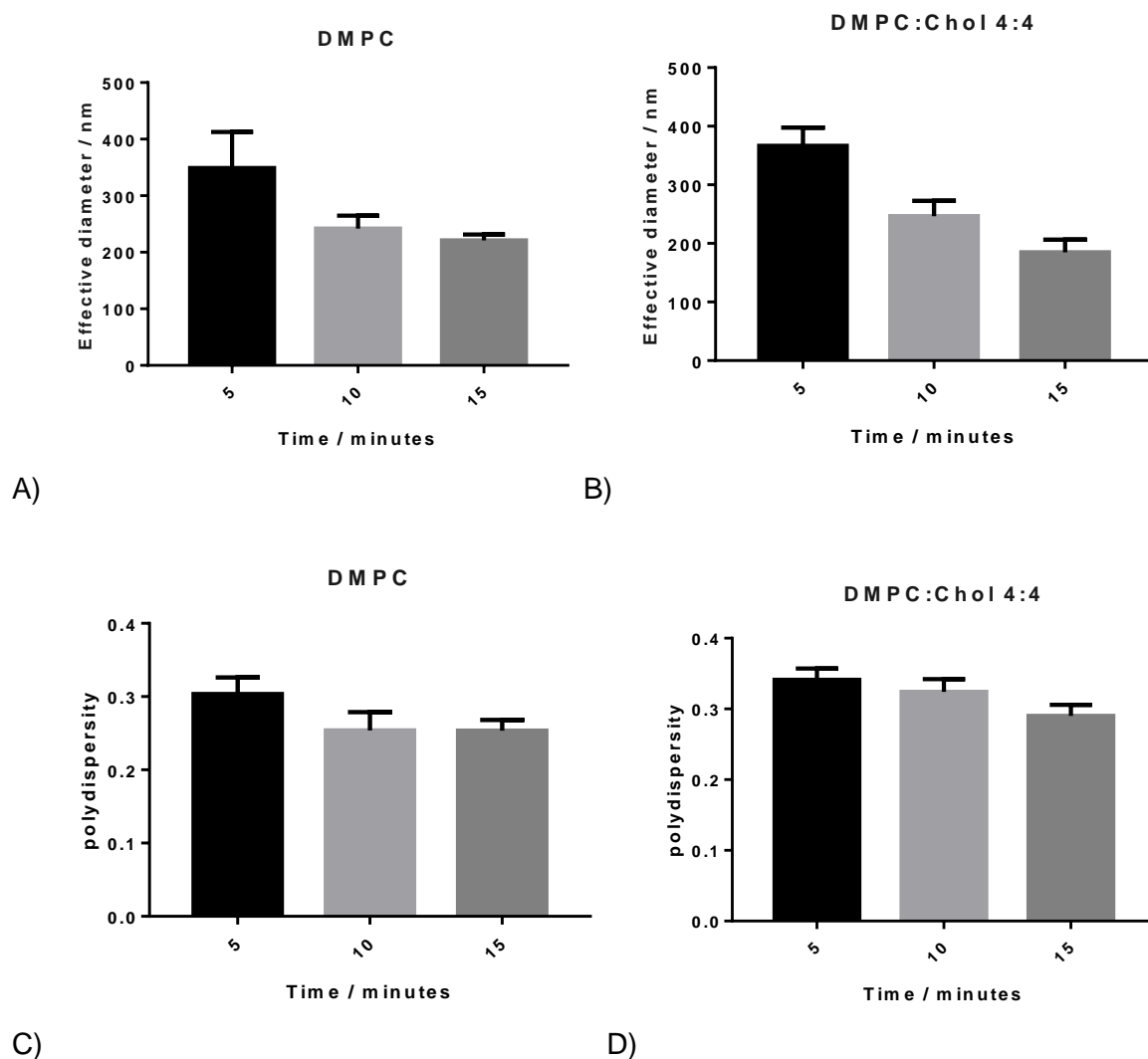


Figure 2.15: A – B) Size of DMPC (A) and DMPC: Cholesterol 4:4 (B) liposomes produced using the Bioruptor® Standard at 45°C using 300 μ L in 1.5 mL tubes. They were then sonicated at power level L for 30 seconds on, 30 seconds off for between 5 and 15 minutes. C – D) PDI of DMPC (A) and DMPC: Cholesterol 4:4 (B) liposomes produced using the Bioruptor® Standard at 45°C using 300 μ L in 1.5 mL tubes. They were then sonicated at power level L for 30 seconds on, 30 seconds off for between 5 and 15 minutes.

2.3.4.5 Bioruptor® Standard study into how a longer period of time affects liposome size reduction

Time had been investigated up to 15 minutes so a further increase in these parameters was used to see whether sonicating for even longer would lead to statistically smaller liposomes. The results showed in Figure 2.16 showed a significant decrease between 15 and 20 minutes for DMPC, 179 ± 6.8 nm down to 158 ± 3.5 nm. No significant difference for 25 or 30 minutes was seen. DMPC: Cholesterol had a small but significant decrease 15 to 20 minutes of 161 ± 14.8 nm down to 149 ± 7.8 nm, but back up for 25 minutes, up to 186 ± 21 nm. No sig difference for DMPC for PDI, all around 0.24. DMPC: Cholesterol saw again a significant decrease from 15 to 20 mins from 0.262 ± 0.028 to 0.235 ± 0.016 . It then statistically increased for 25 minutes with a PDI of 0.286 ± 0.017 . What these showed is that by increasing the time to 20 minutes, there was a significant decrease in size of both DMPC and DMPC: Cholesterol liposomes with either a decrease or no difference seen with the PDI. However, when increased to 25 minutes, there were no significant decreases and in fact some of the results had started to increase, although not significantly. Therefore, sonicating for too long lead to overall liposome size increasing and PDI increasing, leading to larger liposomes with decreased uniformity or aggregation of liposomes increasing the overall size of the sample.

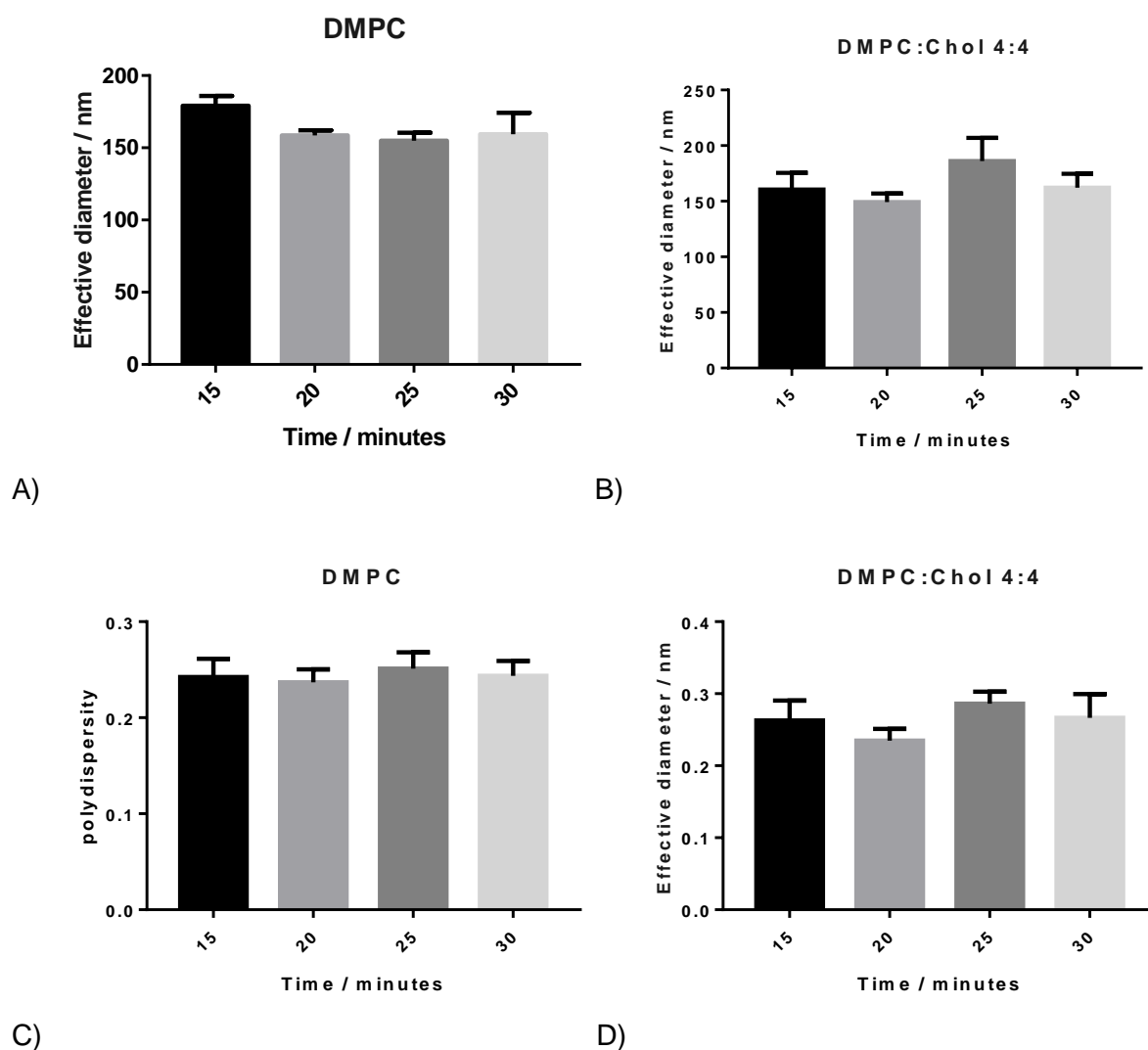


Figure 2.16: A – B) Size of DMPC (A) and DMPC: Cholesterol 4:4 (B) liposomes produced using the Bioruptor® Standard at 45°C using 300 μ L in 1.5 mL tubes. They were then sonicated at power level L for 30 seconds on, 30 seconds off for between 15 and 30 minutes. C – D) PDI of DMPC (A) and DMPC: Cholesterol 4:4 (B) liposomes produced using the Bioruptor® Standard at 45°C using 300 μ L in 1.5 mL tubes. They were then sonicated at power level L for 30 seconds on, 30 seconds off for between 15 and 30 minutes.

2.3.4.6 Bioruptor® Standard study into how volume affects liposome size reduction

With the different volumes with the PTFE 1.5 mL tube, it was found that a size reduction for both formulations could be achieved, if the volume was set to 100 μ L, as shown in Figure 2.17. The results attained for the DMPC 8 mM formulation were a smallest size of 114.6 ± 2.3 nm and PDI of 0.259 ± 0.013 . While for the DMPC: Cholesterol 4:4 liposomes, a smallest size of 128.8 ± 1.7 nm and PDI of 0.171 ± 0.023 were attained. As you increased the volume, the sizes and polydispersities of both formulations increased until at 1000 μ L, DMPC 8 mM had a size and PDI of 430.3 ± 120.5 nm and 0.353 ± 0.029 respectively and DMPC 4:4 had a size and PDI of 550.1 ± 295 nm and a PDI of 0.345 ± 0.015 . What these showed was that like the Bioruptor® XL, the smallest sizes and polydispersities can be achieved using the minimum volume of sample, 100 μ L.

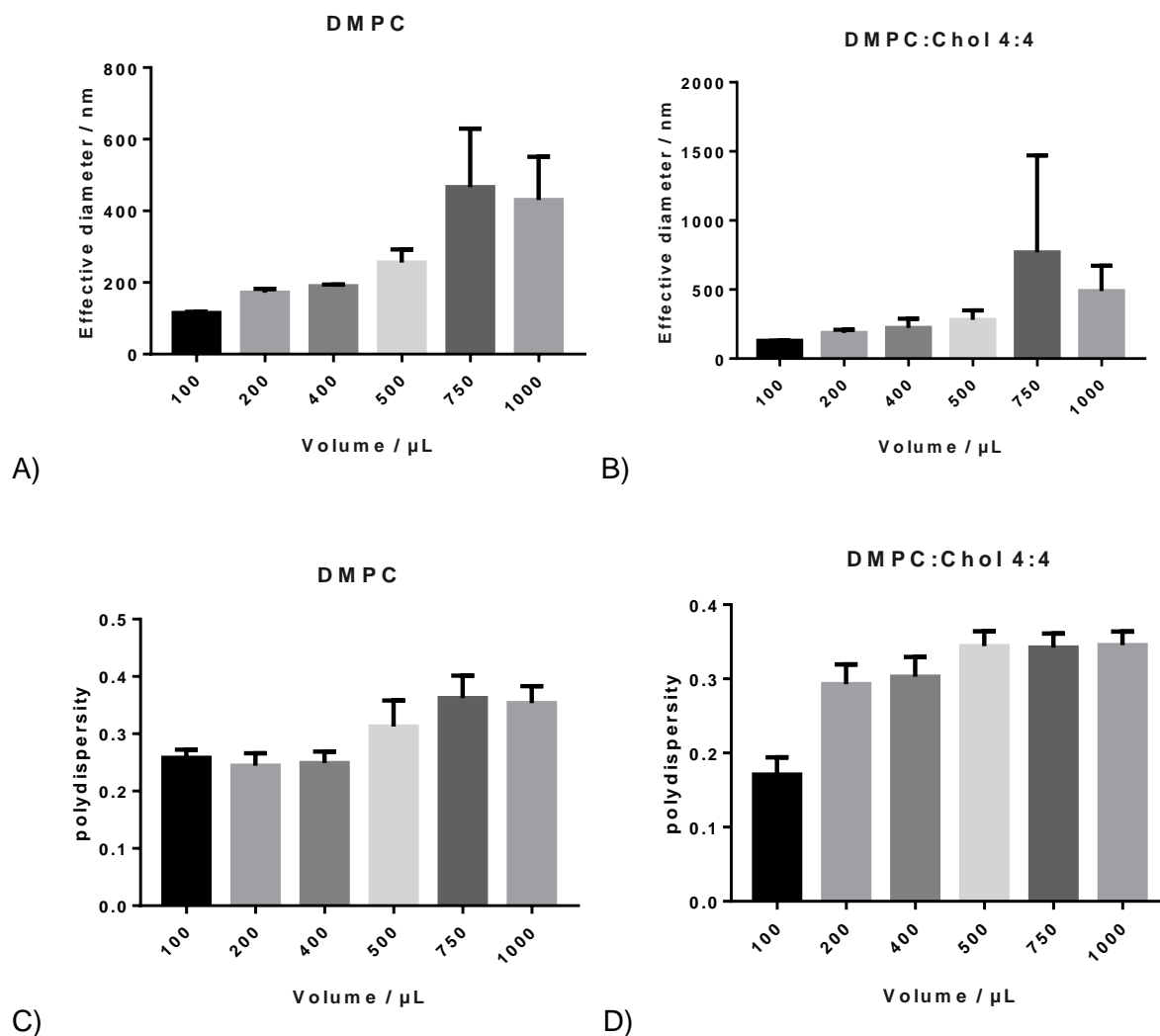


Figure 2.17: A – B) Size of DMPC (A) and DMPC: Cholesterol 4:4 (B) liposomes produced using the Bioruptor® Standard at 45°C using a range of volumes from 0.1 to 1 mL in a 1.5 mL tube. They were sonicated at power level M for 15 minutes of 30 seconds on, 0 seconds off cycle. C – D) PDI of DMPC (A) and DMPC: Cholesterol 4:4 (B) liposomes produced using the Bioruptor® Standard at 45°C using a range of volumes from 0.1 to 1 mL in a 1.5 mL tube. They were sonicated at power level M for 15 minutes of 30 seconds on, 0 seconds off cycle.

2.3.4.7 Bioruptor® Standard study into how the use of larger tubes affects liposome size reduction

With the different volumes with the PTFE 15 mL tube, it was found that a size reduction for both formulations could be achieved, if the volume was set to 0.5 mL, as shown in Figure 2.18. The results attained for the DMPC 8 mM formulation were a smallest size of 137.8 ± 9.4 nm and PDI of 0.304 ± 0.01 . While for the DMPC: Cholesterol 4:4 liposomes, a smallest size of 163 ± 10.8 nm and PDI of 0.294 ± 0.009 were attained. As you increased the volume, the sizes and polydispersities of both formulations increased. For DMPC 8 mM, the maximum size and PDI of 548 ± 50.9 nm and 0.357 ± 0.016 was attained for the 2 mL sample and for DMPC 4:4 had a size and PDI of 913.2 ± 125.6 nm and a PDI of 0.369 ± 0.015 at 3 mL of sample. What these showed was that like the 1.5 mL tubes, the smallest sizes and polydispersities can be achieved using the minimum volume of sample, 0.5 mL.

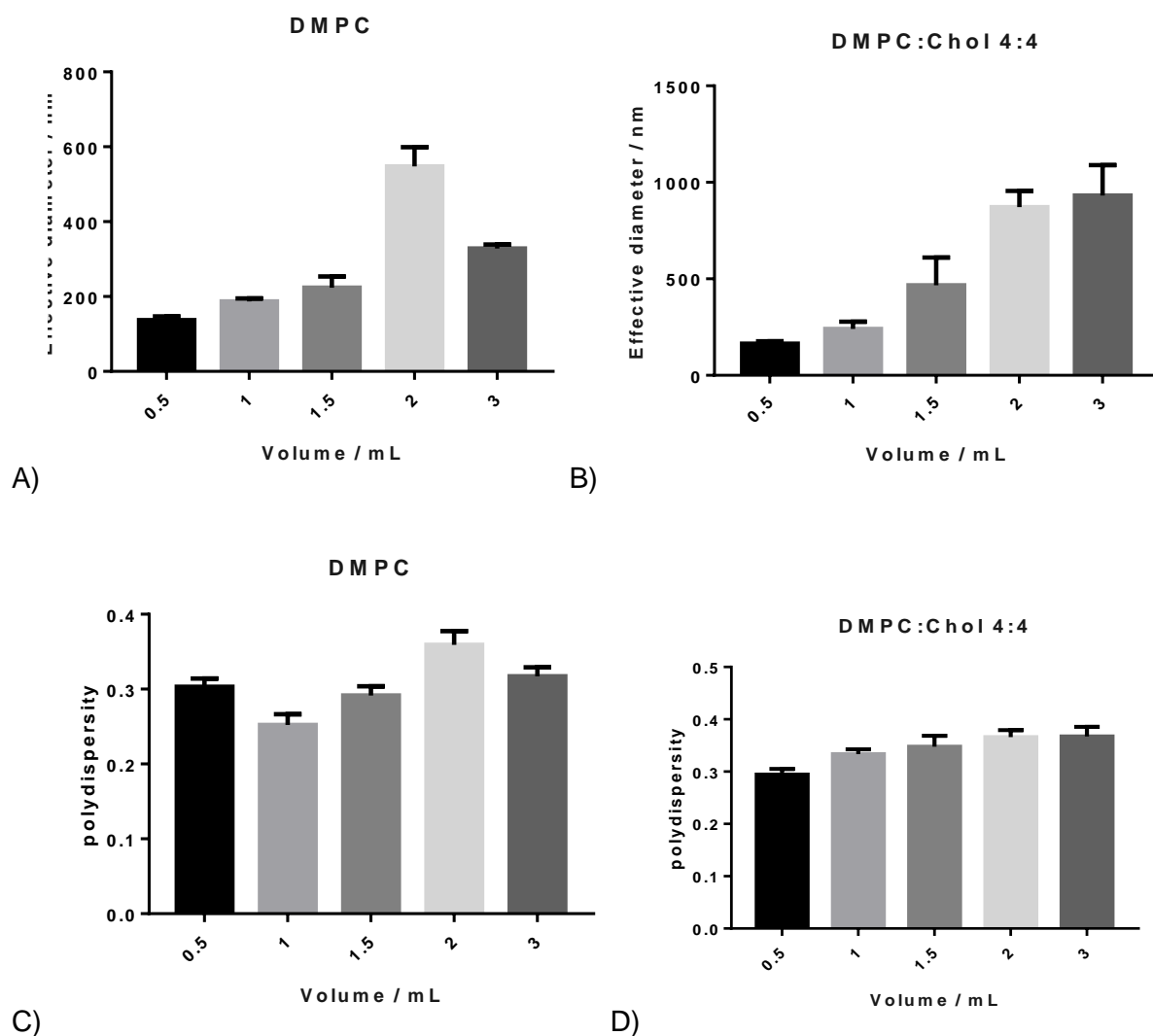


Figure 2.18 A – B) Size of DMPC (A) and DMPC: Cholesterol 4:4 (B) liposomes produced using the Bioruptor® Standard at 45°C using a range of volumes from 0.5 to 3 mL in a 15 mL tube. They were sonicated at power level M for 15 minutes of 30 seconds on, 0 seconds off cycle. C – D) PDI of DMPC (A) and DMPC: Cholesterol 4:4 (B) liposomes produced using the Bioruptor® Standard at 45°C using a range of volumes from 0.5 to 3 mL in a 15 mL tube. They were sonicated at power level M for 15 minutes of 30 seconds on, 0 seconds off cycle.

2.3.4.8 Bioruptor® Standard study into how position within the water bath affects liposome size reduction

With the different position test, it was found that there was some variability within the different positions as shown in Figure 2.19. For DMPC 8 mM, these ranged from 93.5 ± 3.6 nm to 141 ± 46 nm in size and from 0.257 ± 0.025 to 0.289 ± 0.028 for PDI. While for the DMPC: Cholesterol 4:4 liposomes, the size ranged from 172 ± 15 nm to 252 ± 30 nm and PDI from 0.27 ± 0.018 to 0.322 ± 0.017 . For DMPC 8 mM, the only significantly different position however was position 1. For the DMPC: Cholesterol 4:4 liposomes, positions 1, 4 and 6 were significantly different from 2, 3 and 5. The average size and PDI for DMPC 8 mM was 117.7 ± 29.6 nm and 0.269 ± 0.03 respectively. While for the DMPC: Cholesterol 4:4 liposomes, the average size and PDI were 210.1 ± 51.3 nm and 0.295 ± 0.029 respectively. What this shows is that there is inter variability between the different positions, although the reason behind this is unclear. It could be that the water bath temperature isn't uniform across the different positions, although the motor that turns the system should alleviate this problem. The other reason could be that the liposomes are not given enough time to reduce in temperature after sonication before they are sized.

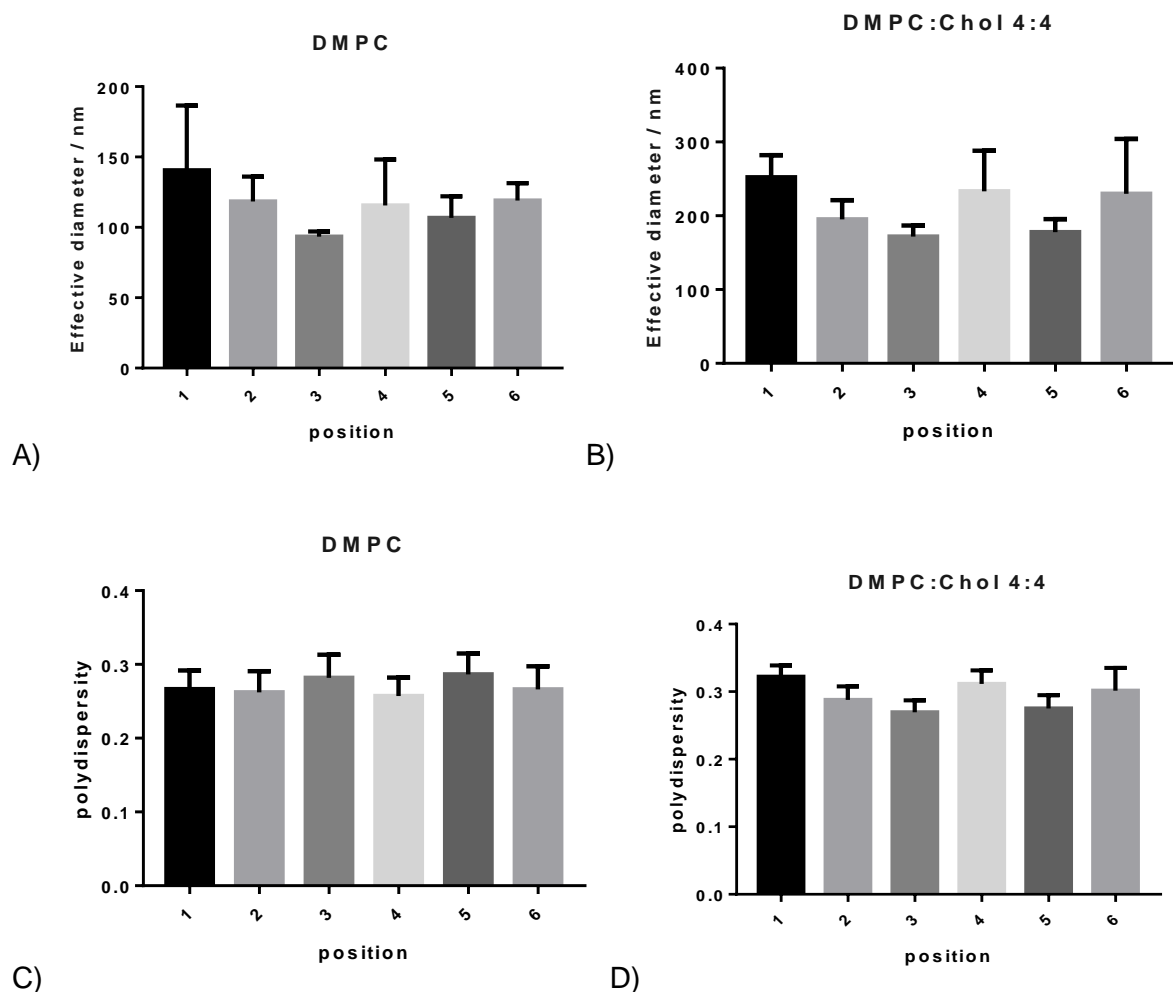


Figure 2.19: A – B) Size of DMPC (A) and DMPC: Cholesterol 4:4 (B) liposomes produced using the Bioruptor® Standard and then sonicated for 15 minutes of 30, 0 at the power level *M* using a 0.1 mL sample. Each position in the holder was assigned an arbitrary number between 1 and 6 and each ran 3 times to compare how much variability there was in the same position over multiple tests and between the 6 different positions available. C – D) PDI of DMPC (A) and DMPC: Cholesterol 4:4 (B) liposomes produced using the Bioruptor® Standard and then sonicated for 15 minutes of 30, 0 at the power level *M* using a 0.1 mL sample. Each position in the holder was assigned an arbitrary number between 1 and 6 and each ran 3 times to compare how much variability there was in the same position over multiple tests and between the 6 different positions available.

2.3.4.9 Bioruptor® Standard study into how temperature affects liposome size reduction

With temperature, as temperature was reduced then the size and PDI increased of both formulations as shown in Figure 2.20. This increase was particularly acute when the temperature was dropped below the 24 °C transition temperature of DMPC. However, this was not immediate or total as the reduced temperature makes it more difficult but not impossible for the liposome size to be reduced and the temperature within the tube is known to be several degrees higher than the overall water bath during sonication.

DMPC 8 mM liposomes had a minimum size at 35 °C of 164.9 ± 6.2 nm and minimum PDI at 50 °C of 0.224 ± 0.015 . The best size and PDI combined was at 45 °C with a slightly bigger size of 179.1 ± 6.8 nm and a PDI of 0.268 ± 0.02 . The size and polydispersities then increased as the temperature reduced, with a maximum size and PDI at 5 °C of 1562 ± 308 nm and 0.381 ± 0.025 respectively. Meanwhile, DMPC 4:4 liposomes had a minimum size at 50 °C of 157.4 ± 20.4 nm and minimum PDI of 0.198 ± 0.05 . The best size and PDI at 45 °C were a size of 158.5 ± 12 nm and a PDI of 0.263 ± 0.022 . The size and polydispersities then increased as the temperature reduced, with a maximum size and PDI at 25 °C of 608.7 ± 184 nm and 0.373 ± 0.046 respectively. This clearly shows that as you decrease the temperature, then the size increases for both formulations, especially once you drop below the transition temperature as this is vital in keeping the bilayer in a disordered phase so it can be modified (Duzgunes, 2003). What Figure 4.4A also shows is that even below the transition temperature, you can still reduce the size of your liposomes, although not to the smallest sizes achieved at the higher temperatures. It also shows that the addition of cholesterol stabilises the membrane, meaning both at the low temperatures like 5 or 10 °C you get smaller liposomes because when they are first formed as MLV they are smaller, and that at the temperatures around the transition temperature of DMPC, you don't get as much of a size

reduction compared to the formulation made with DMPC. This could be down to cholesterol having the effect of abolishing the transition temperature of the lipid system as seen in previous work by Bajoria et al (Bajoria and Contractor, 1997).

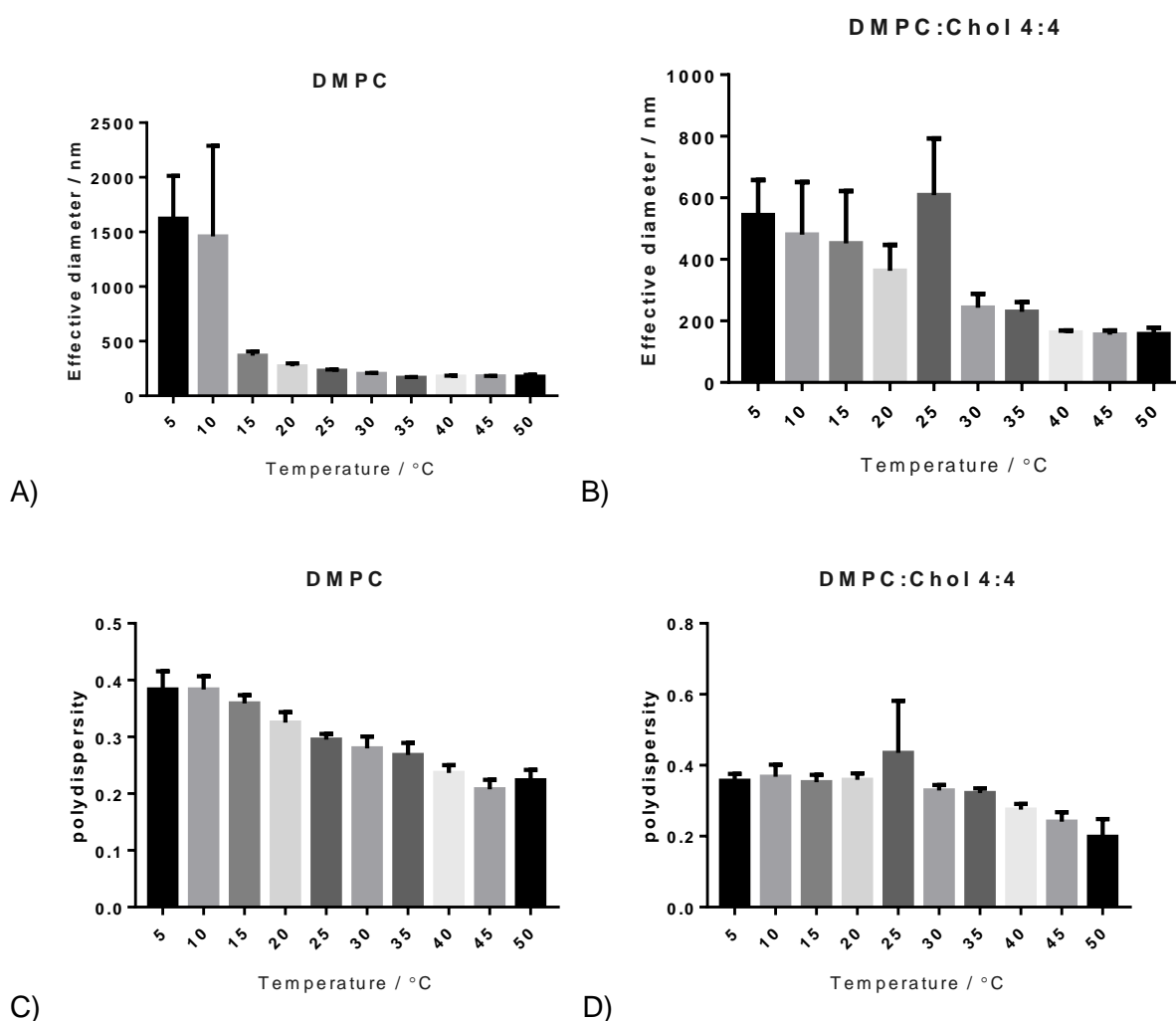


Figure 2.20: A – B) Size of DMPC (A) and DMPC: Cholesterol 4:4 (B) liposomes produced using the Bioruptor® Standard at 45°C using a range of volumes from 0.5 to 3 mL in a 15 mL tube. They were sonicated at power level M for 15 minutes of 30 seconds on, 0 seconds off cycle. C – D) PDI of DMPC (C) and DMPC: Cholesterol 4:4 (D) liposomes produced using the Bioruptor® Standard at 45°C using a range of volumes from 0.5 to 3 mL in a 15 mL tube. They were sonicated at power level M for 15 minutes of 30 seconds on, 0 seconds off cycle.

2.3.4.10 Bioruptor® Standard study into how the use of PP tubes and power level affects liposome size reduction

Power was the first parameter to be tested with the results below in Figure 2.21. These show that as you increase the power to power level M, you either increase or make no difference to the size and PDI of your formulations. For DMPC 8 mM liposomes, the size decreases slightly between L and M power from 139.6 ± 11 nm down to 132.7 ± 30.8 nm but PDI increases from 0.257 ± 0.012 to 0.295 ± 0.014 . For DMPC: Cholesterol 4:4, size again decreases from 183.6 ± 18.8 nm to 177.8 ± 12.4 nm and PDI also drops from 0.304 ± 0.016 to 0.286 ± 0.016 . However, as you then increase the power level to H, you see a significant increase in the size of DMPC 8 mM liposomes up to 157.4 ± 4 nm but a decrease in the PDI down to 0.246 ± 0.011 . For DMPC: Cholesterol 4:4 there is no significant change in either the size or PDI. What this shows is that again if you put too much power into the system, and you do not have a stabilising agent such as cholesterol in your formulation, then you will see an increase in size and PDI as the lipids become damaged. Therefore, M power was chosen as the optimal value.

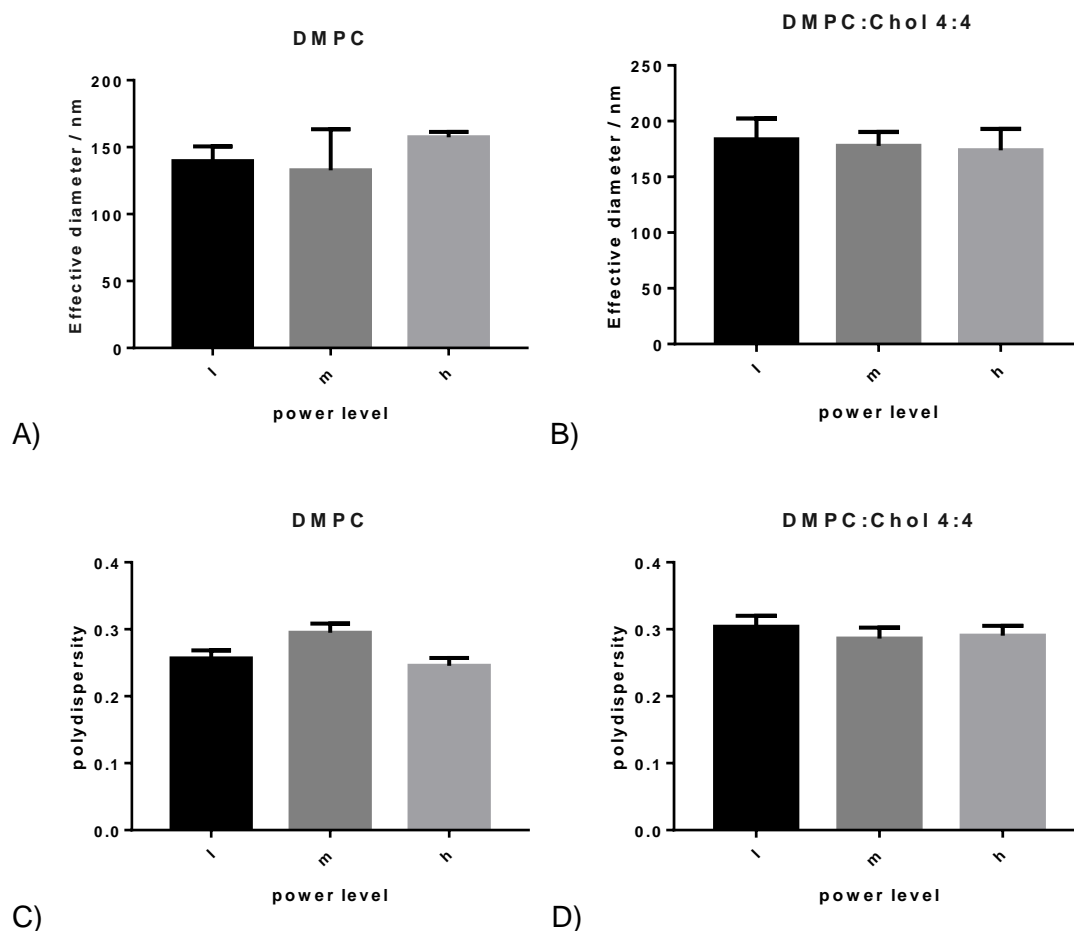


Figure 2.21: A – B) Size of DMPC (A) and DMPC: Cholesterol 4:4 (B) liposomes were produced using the Bioruptor® Standard at 45°C using 300 μ L in 1.5 mL PP tubes. They were then sonicated for 15 minutes of 30, 30 at the 3 different power levels of L, M and H. C – D) PDI of DMPC (A) and DMPC: Cholesterol 4:4 (B) liposomes were produced using the Bioruptor® Standard at 45°C using 300 μ L in 1.5 mL PP tubes. They were then sonicated for 15 minutes of 30, 30 at the 3 different power levels of L, M and H.

2.3.4.11 Bioruptor® Standard study into how the use of PP tubes and time affects liposome size reduction

Time was the next parameter to be tested, with the results below in Figure 2.22. These show that as you increase the time, you decrease the size and PDI of your formulations, as seen before. The best results attained for the DMPC formulation were at 15 minutes and were a best size of 111.6 ± 4.4 nm and PDI of 0.295 ± 0.011 . While for the DMPC: Cholesterol 4 4:4, a size of 177.8 ± 12.4 nm and PDI of 0.286 ± 0.016 were achieved at 15 minutes. For DMPC: Cholesterol 4:4 liposomes, this size and PDI is comparable to that achieved using the PTFE tubes, while for DMPC 8 mM it is significantly smaller, reduced down from 221 ± 10.5 nm but with a higher PDI than that attained with PTFE tubes. The tube type affects size and polydispersity because the different plastics have different attributes such as hardness and how well it transfers the sonic energy through the plastic to the liposomes inside.

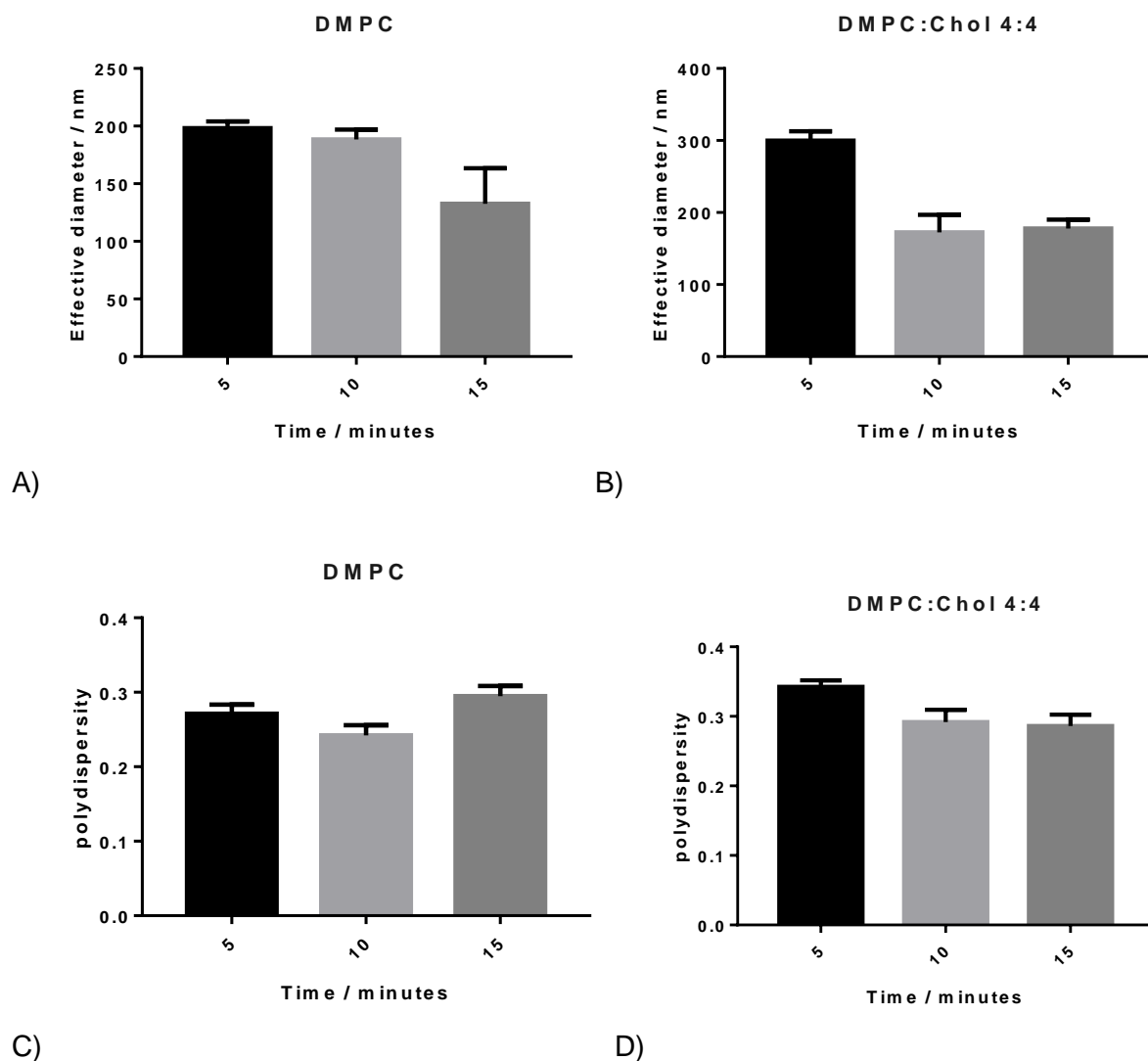


Figure 2.22: A – B) Size of DMPC (A) and DMPC: Cholesterol 4:4 (B) liposomes were produced using the Bioruptor® Standard at 45°C using 300 μ L in 1.5 mL PP tubes. They were then sonicated for 5 to 15 minutes of 30, 30 at power level M. C – D) PDI of DMPC (A) and DMPC: Cholesterol 4:4 (B) liposomes were produced using the Bioruptor® Standard at 45°C using 300 μ L in 1.5 mL PP tubes. They were then sonicated for 5 to 15 minutes of 30, 30 at power level M.

2.3.4.12 Bioruptor® Standard study into how the use of PP tubes and volume affects liposome size reduction

With the different volumes with the PP 1.5 mL tube, it was found that a size reduction for both formulations could be achieved, if the volume was set to 100 μ L, as shown in Figure 2.23. The results attained for the DMPC 8 mM formulation were a smallest size of 108.6 ± 9.3 nm and PDI of 0.24 ± 0.016 . While for the DMPC: Cholesterol 4:4 liposomes, a smallest size of 146.2 ± 16.1 nm and PDI of 0.31 ± 0.02 were attained. As you increased the volume, the sizes and polydispersities of both formulations increased. For DMPC 8 mM, the biggest values occurred with 750 μ L which had a size and PDI of 1239 ± 553 nm and 0.334 ± 0.03 respectively and DMPC 4:4 had the biggest values occur at 1000 μ L with a size and PDI of 3378 ± 1495 nm and a PDI of 0.41 ± 0.068 . What these showed was that like the Bioruptor® XL, the smallest sizes and polydispersities can be achieved using the minimum volume of sample, 100 μ L. What these also showed was that the results attained for the PP tubes compared to the PTFE tubes were mixed. For DMPC 8 mM a slightly smaller size and PDI was attained but for DMPC: Cholesterol 4:4, the opposite was true.

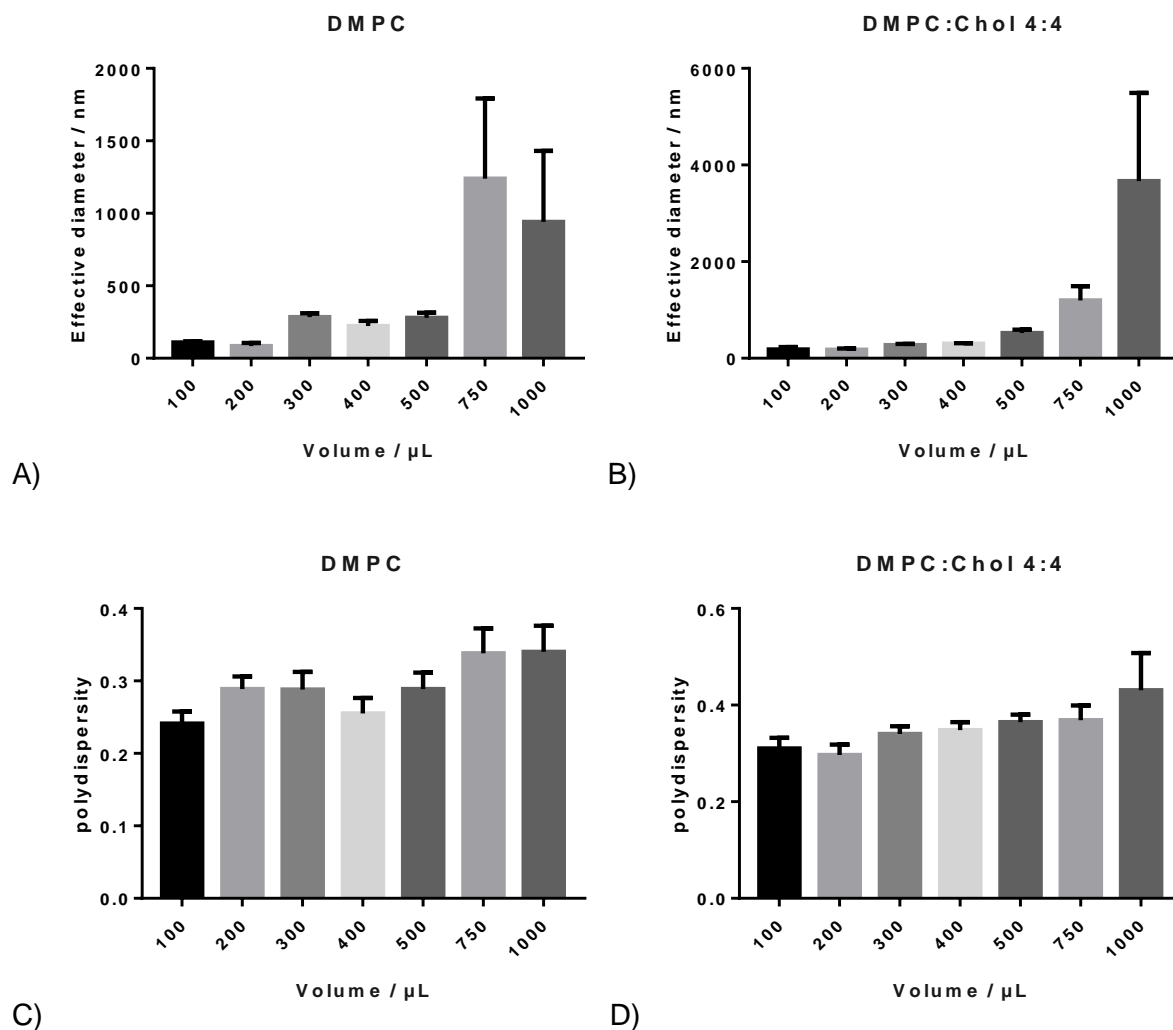


Figure 2.23: A – B) Size of DMPC (A) and DMPC: Cholesterol 4:4 (B) liposomes were produced using the Bioruptor® Standard at 45°C using 100 to 1000 μL in 1.5 mL PP tubes. They were then sonicated for 15 minutes of 30, 0 at power level M. C – D) PDI of DMPC (A) and DMPC: Cholesterol 4:4 (B) liposomes were produced using the Bioruptor® Standard at 45°C using 100 - 1000 μL in 1.5 mL PP tubes. They were then sonicated for 15 minutes of 30, 0 at power level M.

2.3.4.13 Bioruptor® Standard study into how the use of larger PP tubes affects liposome size reduction

With the different volumes with the PP 15 mL tube, it was found that a size reduction for both formulations could be achieved, if the volume was set to 0.5 mL, as shown in Figure 2.24. The results attained for the DMPC 8 mM formulation were a smallest size of 108.9 ± 4.6 nm and PDI of 0.321 ± 0.005 . While for the DMPC: Cholesterol 4:4 liposomes, a smallest size of 148.4 ± 14 nm and PDI of 0.316 ± 0.025 were attained. As you increased the volume, the size increased but polydispersities either decreased or were not significantly different of both formulations. For DMPC 8 mM, the maximum size and PDI of 263.1 ± 111.1 nm and 0.27 ± 0.048 was attained for the 2 mL sample and for DMPC 4:4 had a size and PDI of 287.1 ± 165.4 nm and a PDI of 0.32 ± 0.021 at 2 mL of sample. What these showed was that like the 1.5 mL tubes, the smallest sizes and polydispersities can be achieved using the minimum volume of sample, 0.5 mL.

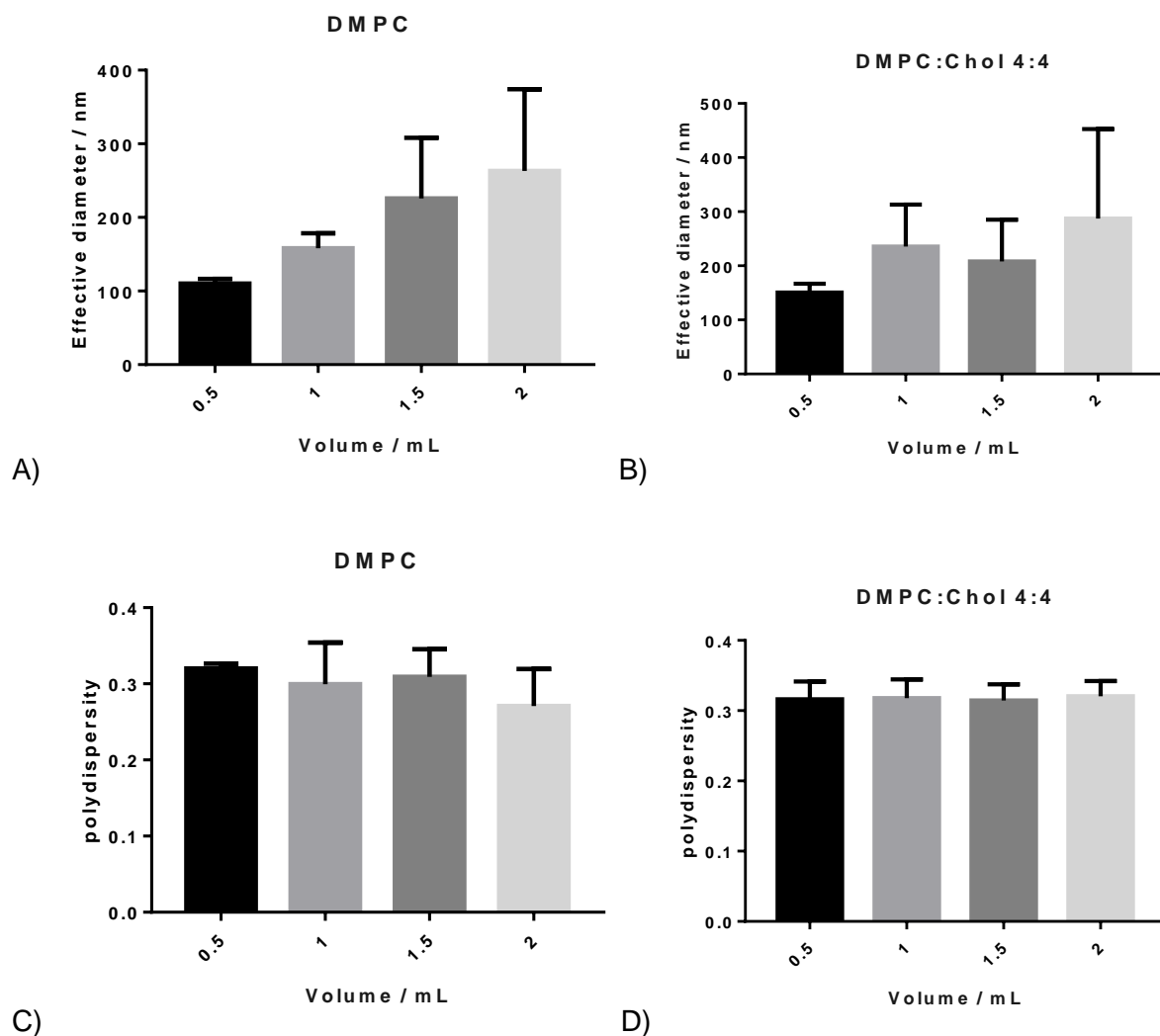


Figure 2.24: A – B) Size of DMPC (A) and DMPC: Cholesterol 4:4 (B) liposomes were produced using the Bioruptor® Standard at 45°C using 0.5 to 2 mL in 15 mL PP tubes. They were then sonicated for 15 minutes of 30, 0 at power level M. C – D) PDI of DMPC (A) and DMPC: Cholesterol 4:4 (B) liposomes were produced using the Bioruptor® Standard at 45°C using 0.5 to 2 mL in 15 mL PP tubes. They were then sonicated for 15 minutes of 30, 0 at power level M.

2.3.4.14 Bioruptor® Standard study into how formulation affects

liposome size reduction

4 different formulations along with the 2 already looked at, DMPC and DMPC: Cholesterol, were investigated using the same conditions with each sample run at the same time as each other. The conditions used were the optimised conditions for the DMPC and DMPC: Cholesterol liposomes and the results are shown below in Figure 2.25. Firstly, when DMPC liposomes had cholesterol added to them, the size increased from 169.7 ± 9.5 nm to 472.5 ± 24.8 nm. However, once DMPG or DOTAP had been added, a significant decrease in size was seen when either the anionic or cationic lipid were added with drops down to 106.6 ± 6.8 nm and 111.2 ± 20.4 nm respectively. DMPG has a transition temperature of 23 °C and DOTAP has a transition temperature of 0 °C. The same pattern was also noted with the PDI.

For the use of a higher transition temperature lipid, DSPC, there was no significant difference between the sizes achieved compared to the lower transition temperature lipid of DMPC. For DSPC, a size of 417.2 ± 39.3 nm was achieved which is comparable to the 472.5 ± 24.8 nm achieved for the DMPC: Cholesterol liposomes. However, when using an even lower transition temperature, PC, a drop in size was achieved down to 155.5 ± 38.5 nm. DSPC has a transition temperature of 55 °C and PC has a transition temperature of -15 °C. Again, the same pattern was seen in the PDI.

For the zeta potential, each of the formulations that do not contain any charged lipids the zeta potential was found to be near neutral. DMPC, DMPC: Cholesterol, DSPC: Cholesterol and PC: Cholesterol had zeta potentials of -4.6 ± 2.01 mV, -9.48 ± 1.2 mV, -0.68 ± 1.35 mV and -3.72 ± 1.93 mV respectively. When an anionic lipid is added, the zeta potential drops to -18.16 ± 1.32 mV whilst when a cationic lipid is added, the zeta potential increases to 23.53 ± 1.21 mV. This is all in line with what was expected.

Therefore, in conclusion the bath sonicator is able to be used to produce liposomes of various transition temperatures and charges and reduce their size sufficiently down to the nanometre range. These liposomes are able to be produced at the same time using exactly the same conditions, a big plus compared to the probe sonication method.

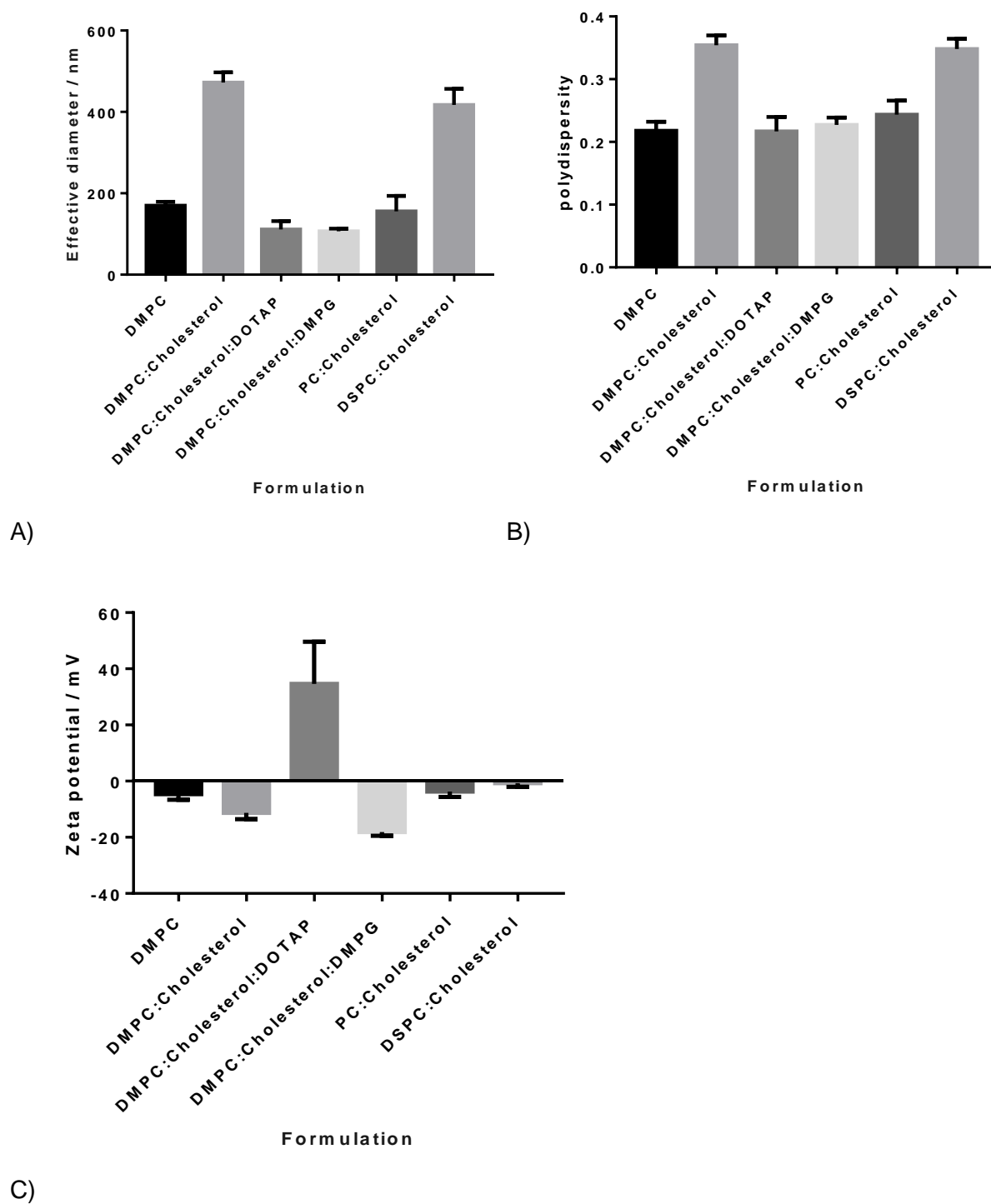


Figure 2.25: Size (A), PDI (B) and zeta potential (C) for 6 formulations that were investigated. DMPC, DMPC: Cholesterol 4:4, PC: Cholesterol 4:4, DSPC: Cholesterol 4:4, DMPC: Cholesterol: DMPG 4:4:1 and DMPC: Cholesterol: DOTAP 4:4:1 liposomes were produced using the Bioruptor® Standard and then sonicated for 15 minutes of 30, 0 at the power level M with a 100 μ L volume in a 1.5 mL TPX® tube.

2.3.4.15 Discussion

The Bioruptor® Standard data shows that liposome production using a bath sonicator system relies on a large number of factors. All the factors investigated showed some effect on the size and PDI of the liposomes produced. These ranged from the usual time and power levels being investigated and it being shown that the longer the liposomes are sonicated for and the higher the power level, the smaller the liposomes are produced. It was also shown that if the sonication time stays the same but the off time in between cycles is reduced, this leads to smaller liposomes compared to those with larger time off between cycles. Volume for both the large and small tubes was investigated, and it was found that the lower the volume, the smaller the liposomes. It was also shown that the system could be up scaled somewhat within the laboratory setting by increasing the tube size from 1.5 mL to 15 mL. This would allow more liposomes to be reduced in size over the same time period, in this case instead of 0.6 mL (6 x 0.1 mL), 3 mL (6 x 0.5 mL) can be produced over the same time period to a similar size and PDI using the same formulation.

The position test gave some really interesting data as it showed there was some variability between each position over a number of tests. However, this could be due to a number of factors such as the size of the MLVs that were placed in each tube which will have varied and therefore required a different amount of energy to reduce them to the same size. Therefore, this shows that by increasing the size of the tube, the size variance would be reduced as less tubes would be required to reduce the same volume of liposomes in size. Temperature data showed the importance of the transition temperature when sonicating liposomes. For DMPC liposomes, the decrease in size as the temperature was increases was easy to see and also showed that even if the water bath was at a set temperature below the transition temperature, there was still size reduction. This is due to there still being energy applied and also the temperature within the sample tube is usually higher compared to the water bath as a whole. The DMPC: Cholesterol liposomes reduced in size too although at a slower rate. This is due

to the addition of the cholesterol which increases the rigidity of the liposome bilayer, making it harder to be broken apart and reduced in size. Previous data for the Bioruptor® XL and probe sonicator back this up as under the same conditions, DMPC: Cholesterol liposomes formed larger liposomes compared to their DMPC counterparts. The PP tubes used, which are not Diagenode specific, showed similar results for all the optimisation categories like power, time and volume.

Finally, the choice of formulation was also shown to be vital in how well the liposomes are reduced in size. For example, the addition of cholesterol showed an increase in size but the further addition of a positive or negative lipid showed a decrease in the end size. This could be due to a reduction in aggregation and in overall transition temperature. The use of a smaller phospholipid saw a decrease in size, i.e. PC but the use of a much larger lipid, DSPC, saw a further increase in size compared to the original DMPC: Cholesterol formulation. All formulations containing just neutral lipids showed zeta potentials of near 0 with the addition of a negative lipid causing a negative zeta potential and the addition of a positive lipid causing the opposite as expected.

2.3.5 Bioruptor® Plus liposome size reduction studies

The Bioruptor® Plus is one of Diagenodes machines that is currently on the market to its customers. This makes it imperative that the Bioruptor® Plus is tested to make sure it can produce the liposome size reduction required and is comparable to the other Bioruptor® models previously and to the probe sonicator. This is important as the plus points of using a bath sonicator, the ability for it to be ran in sterile conditions, more than one sample at once and the lack of titanium contamination, do not mean a lot if the machine does not deliver the size reduction required in a good enough time period.

2.3.5.1 Bioruptor® Plus study into how the length of sonication and power level affects liposome size reduction

Length of sonication and power level are known to be important factors in the effectiveness of the reduction of liposome size using the bath sonicator. Therefore, it was important to investigate using the new Bioruptor® Plus exactly what combination of power level and length of sonication gave the smallest liposomes.

Figure 2.26 and 2.27 shows the size and PDI of DMPC and DMPC: Cholesterol 4:4 liposomes sonicated at both low and high power up to 30 cycles in increments of 5 cycles. After just 5 cycles, the size of the liposomes produced using high power was found to be significantly smaller than those formed with low power for DMPC: Cholesterol liposomes and this significant increase was seen up to 20 cycles. DMPC liposomes had no significant differences in size until 15 cycles whereby the high-powered liposomes were significantly smaller, and this trend continued up to 30 cycles. For all samples bar the high powered DMPC liposomes, the smallest size obtained was after 20 cycles, after which no significant decrease in size was

seen. However, DMPC high power sonicated liposomes continued to reduce in size up to the 25 cycle mark, and then no significant decrease was seen either. The size obtained for the DMPC liposomes at these cycles were for low power, 110 ± 11 nm, and for high power 85 ± 9 nm. For DMPC: Cholesterol 4:4 liposomes, the size obtained at the 20 cycle point were for low power, 147 ± 8 nm and for high power, 137 ± 5 nm. The data shows that the polydispersities of the formulations do initially decrease for all the formulations. However, some do begin to increase again, particularly the high powered samples after approximately 20 cycles. For DMPC liposomes, the PDI obtained at the 20 cycle point were for low power, 0.241 ± 0.02 and after 25 cycles for high power, 0.297 ± 0.012 . For DMPC: Cholesterol 4:4 liposomes, the PDI obtained at the 20 cycle point were for low power, 0.242 ± 0.026 and for high power, 0.219 ± 0.02 .

So, what these results show is that by running the sonication for a longer period of time at the higher power level, significantly smaller liposomes can be made. However, there can sometimes be an increase in PDI with the higher power level and this could be due to the power being too much and causing the liposomes to break apart. The cholesterol containing liposomes were also found to be significantly larger than their non-cholesterol containing counterparts.

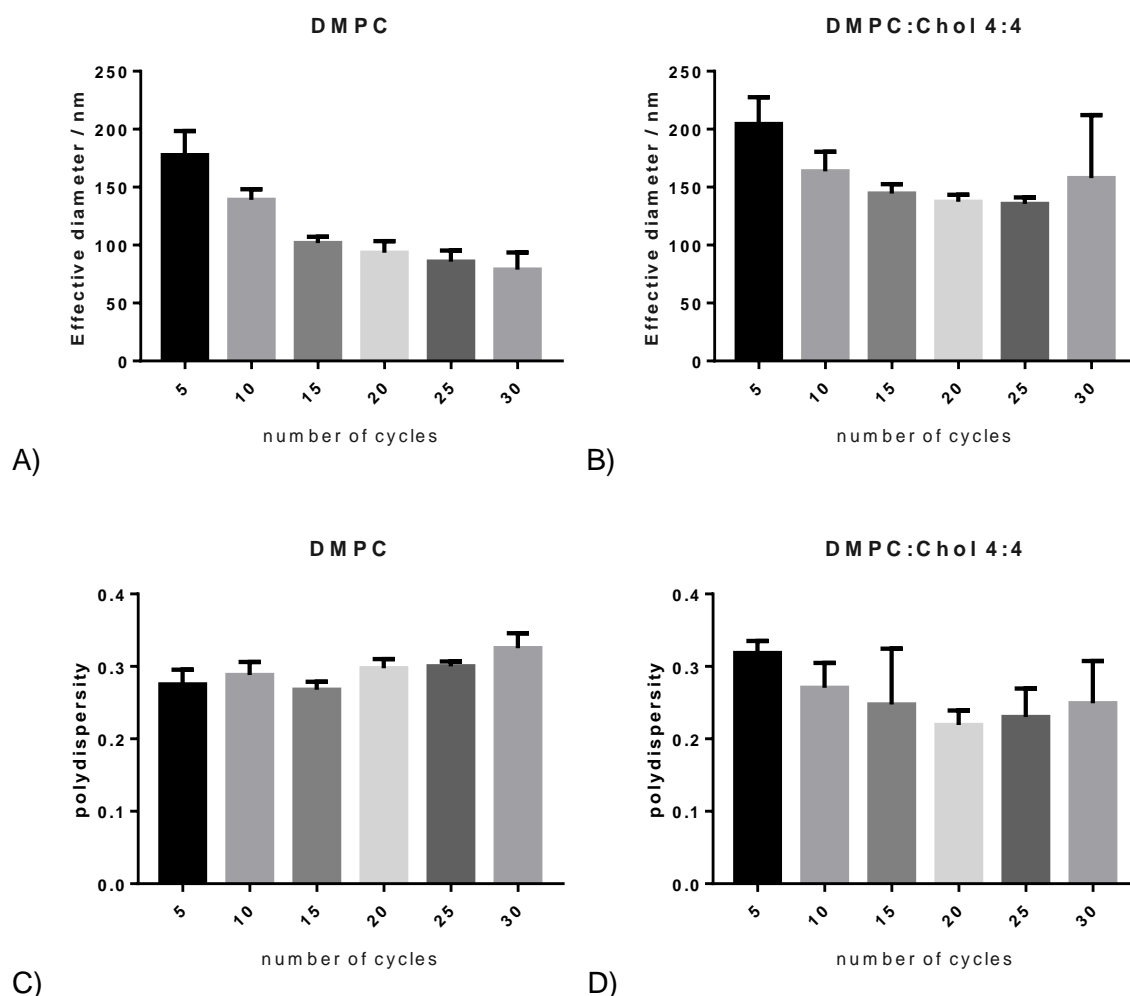


Figure 2.26: A – B) Size of DMPC (A) and DMPC: Cholesterol 4:4 (B) liposomes produced using the Bioruptor® Plus at 40°C using 0.1 mL of sample in 1.5 mL tubes. They were then sonicated for 5 to 30 cycles at H power. C – D) PDI of DMPC (C) and DMPC: Cholesterol 4:4 (D) liposomes were produced using the Bioruptor® Plus at 40°C using 0.1 mL of sample in 1.5 mL tubes. They were then sonicated for 5 to 30 cycles at H power.

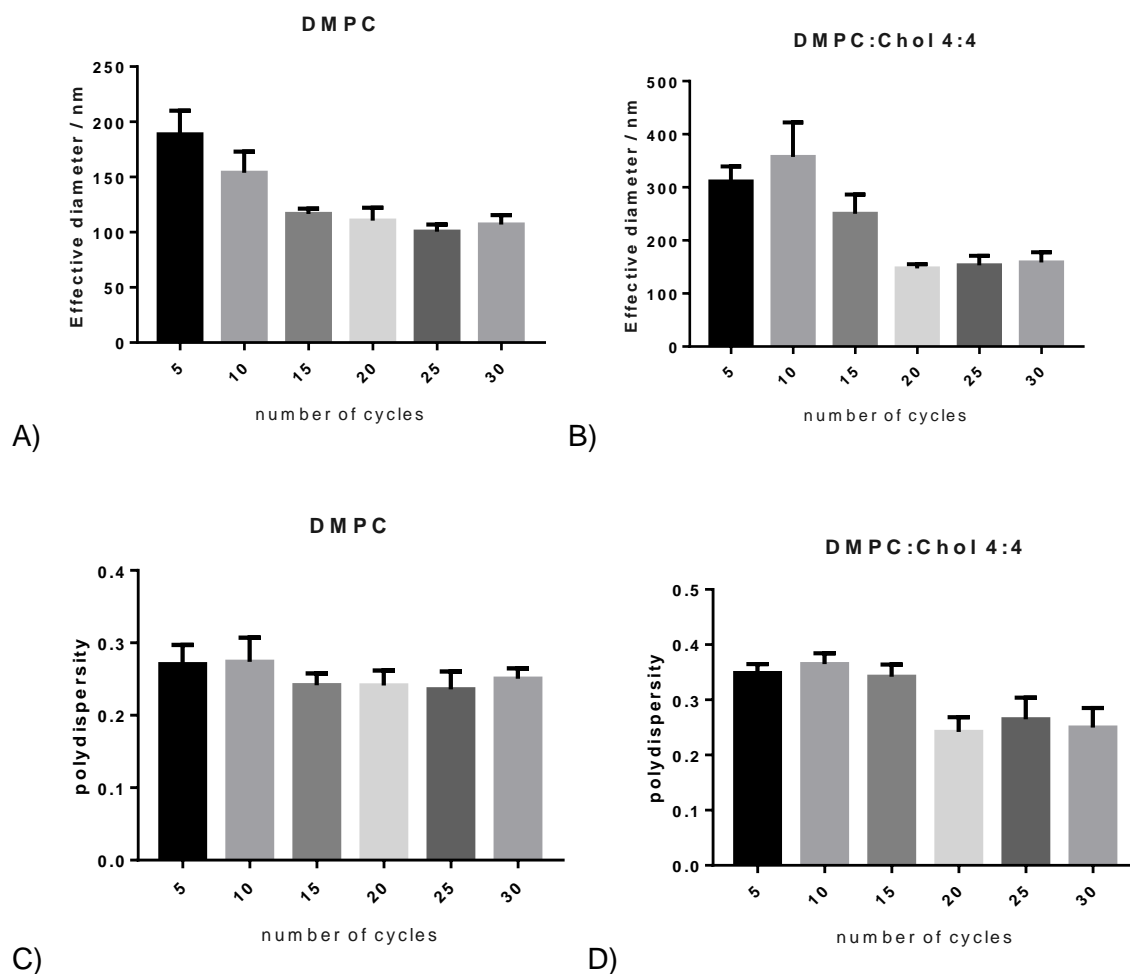
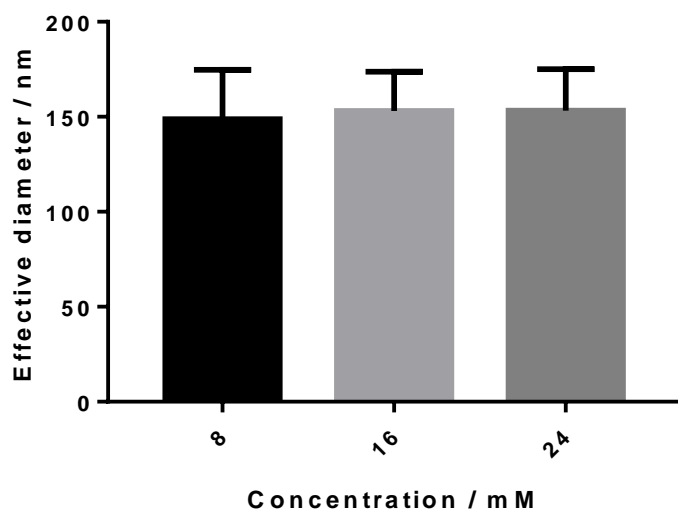


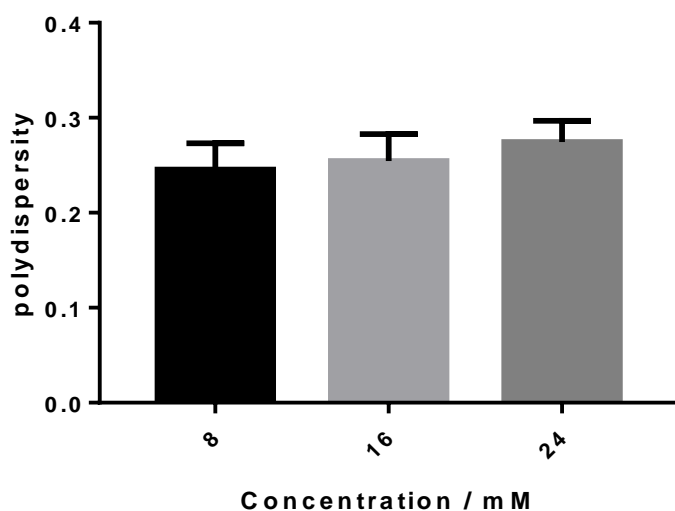
Figure 2.27: E - F) Size of DMPC (E) and DMPC: Cholesterol 4:4 (F) liposomes produced using the Bioruptor® Plus at 40°C using 0.1 mL of sample in 1.5 mL tubes. They were then sonicated for 5 to 30 cycles at L power. G - H) PDI of DMPC (G) and DMPC: Cholesterol 4:4 (H) liposomes were produced using the Bioruptor® Plus at 40°C using 0.1 mL of sample in 1.5 mL tubes. They were then sonicated for 5 to 30 cycles at L power.

2.3.5.2 Bioruptor® Plus study into how concentration affects liposome size reduction

The results in Figure 2.28 show that for the different concentrations a 2 mL sample of 8 mM DMPC: Cholesterol liposomes was compared to a 2 mL sample of 16 mM and a 2 mL sample of 24 mM DMPC: Cholesterol liposomes and no significant changes were seen in either the size or PDI of either the 16 mM or 24 mM samples when compared to the 8 mM sample or when compared to each other.



A)



B)

Figure 2.28: A) Size of DMPC liposomes at 8, 16 and 24 mM produced using the Bioruptor® Plus at 40°C using 0.1 mL of sample in 1.5 mL tubes. They were then sonicated for 15 cycles at H power. B) PDI of DMPC liposomes at 8, 16 and 24 mM produced using the Bioruptor® Plus at 40°C using 0.1 mL of sample in 1.5 mL tubes. They were then sonicated for 15 cycles at H power.

2.3.5.3 Bioruptor® Plus study into how temperature affects liposome size reduction

Temperature is known to be an important factor due to the liposomes transition temperature as the results in Figure 2.29 show. These results showed that for both low and high power, DMPC liposomes behaved as expected whereas temperature increased, size decreased, from 104.7 nm down to 86.7 nm for low power and from 128.1 nm down to 82.4 nm for high power. PDI also generally followed the same pattern dropping from 0.396 down to 0.264 for low power and from 0.324 down to 0.240 for high power. DMPC: Cholesterol however showed an increase in size from 20 to 30 °C for both high and low power and a further increase at 40 °C for low power. The reasons for this are unclear although a similar pattern was seen for the PDI.

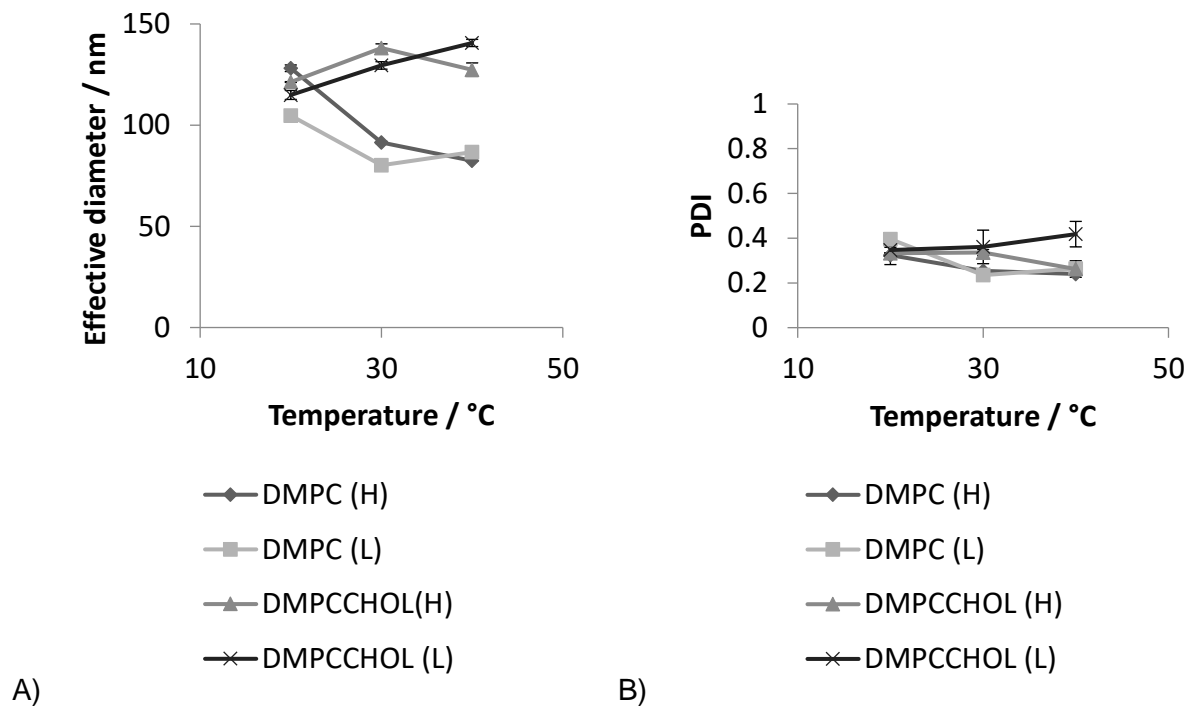


Figure 2.29: A) Size of DMPC and DMPC: Cholesterol 4:4 liposomes produced using the Bioruptor® Plus at 20, 30 and 40°C using 0.1 mL of sample in 1.5 mL tubes. They were then sonicated for 15 cycles at L and H power. B) PDI of DMPC and DMPC: Cholesterol 4:4 liposomes produced using the Bioruptor® Plus at 20, 30 and 40°C using 0.1 mL of sample in 1.5 mL tubes. They were then sonicated for 15 cycles at L and H power.

2.3.5.4 Bioruptor® Plus study into how volume affects liposome size reduction

Volume is also an important factor as shown with the previous Bioruptor® models as shown in Figure 2.30. In this case, DMPC and DMPC: Cholesterol liposomes were tested for their size reduction using low and high power from 0.1 to 0.3 mL of sample in a 1.5 mL tube. What these results showed was that as you decreased the volume, there was a corresponding decrease in size and PDI for both formulations at both power levels. DMPC liposomes saw size reductions from 139.2 to 90.9 nm and 135.6 to 96.5 nm for low and high power respectively. DMPC: Cholesterol saw size reductions from 224.6 to 129.9 nm and from 191.1 to 149.3 nm for low and high power respectively. DMPC liposomes saw a PDI reduction from 0.377 to 0.255 and from 0.356 to 0.229 for low and high power respectively. DMPC: Cholesterol liposomes saw a PDI reduction from 0.746 to 0.336 and from 0.657 to 0.352 for low and high power respectively.

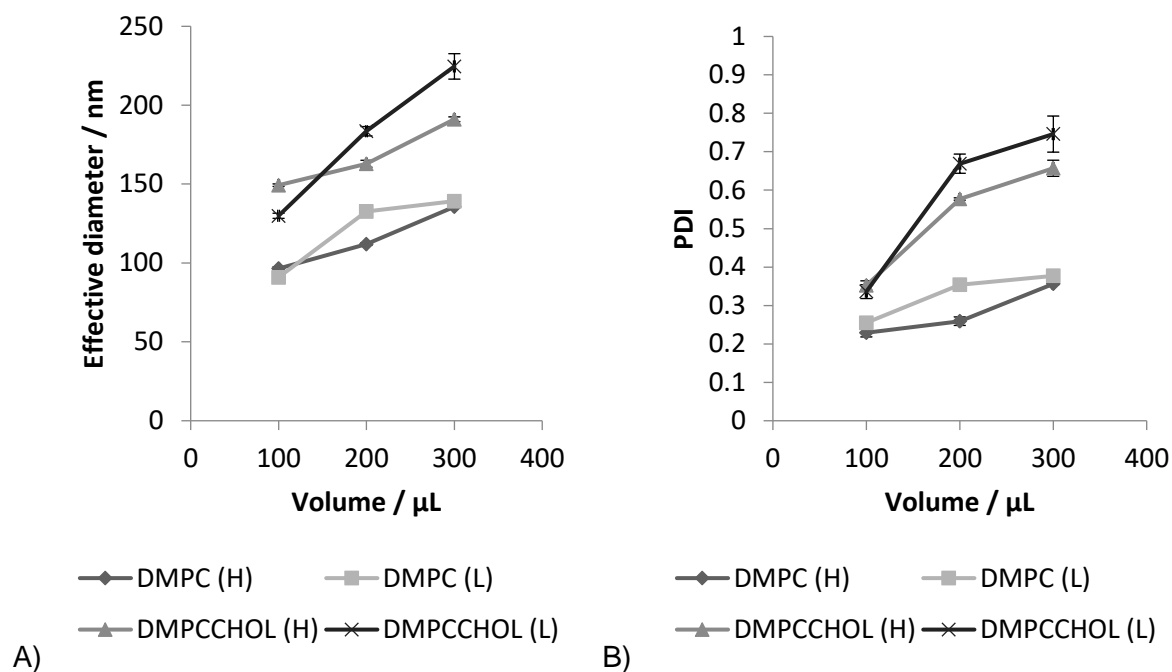


Figure 2.30: A) Size of DMPC and DMPC: Cholesterol 4:4 liposomes produced using the Bioruptor® Plus at 40°C using 0.1, 0.2 or 0.3 mL of sample in 1.5 mL tubes. They were then sonicated for 15 cycles at L and H power. B) PDI of DMPC and DMPC: Cholesterol 4:4 liposomes produced using the Bioruptor® Plus at 40°C using 0.1, 0.2 or 0.3 mL of sample in 1.5 mL tubes. They were then sonicated for 15 cycles at L and H power.

2.3.5.5 Bioruptor® Plus study into how different plastics using a 1.5 mL tube affects liposome size reduction

The plastic composition was investigated to see whether different plastics would give different results. Initially the 1.5 mL tubes were tested using the Diagenode supplied TPX® plastic and PP Eppendorf tubes. The results in Figure 2.31 showed a significant difference between the two plastics for both size and PDI. TPX® DMPC liposomes had a size and PDI of 96.6 nm and 0.234 respectively. PP tubes however showed a significantly larger size and PDI of 138.5 nm and 0.267 respectively. This showed that plastic can be a factor in how well the liposomes are reduced in size and therefore was investigated further.

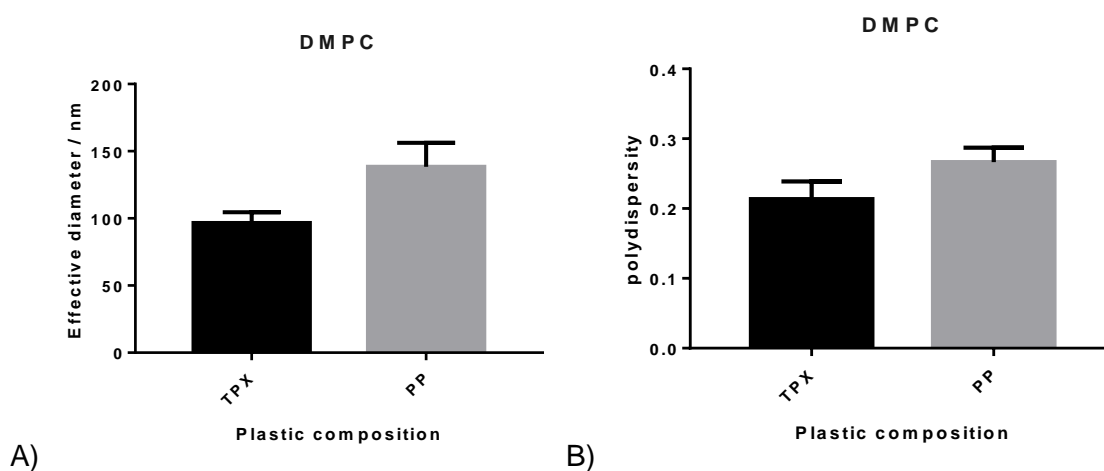


Figure 2.31: A) Size of DMPC liposomes produced using the Bioruptor® Plus at 40°C using 0.1 mL of sample in TPX® or PP 1.5 mL tubes. They were then sonicated for 15 cycles at H power. B) PDI of DMPC liposomes produced using the Bioruptor® Plus at 40°C using 0.1 mL of sample in TPX® or PP 1.5 mL tubes. They were then sonicated for 15 cycles at H power.

2.3.5.6 Bioruptor® Plus study into how different plastics using a 50 mL tube affects liposome size reduction

The plastic used to sonicate the liposomes could be an important factor in how well the liposomes are reduced in size. This is because the plastic composition will react differently to the sonication energy and will transfer different amounts of energy to the liposomes inside. Also, the TPX and PP tubes were narrower and taller than the PP and PPCO tubes and this different shape could also affect how much the liposomes are reduced in size.

Figure 2.32 show four different 50 mL plastic tubes sonicated with 0.5 mL of DMPC liposomes. Previous work had used the PCT tubes which gave a liposome size and PDI of 76.1 ± 7.5 nm and 0.317 ± 0.016 respectively. With PPCO, there was no significant increase in size and a small drop on PDI with size and PDI of 82.9 ± 6 nm and 0.272 ± 0.012 respectively. TPX® and PS however show a significant increase in size compared to both PCT and PPCO, and a significant increase in PDI compared to PPCO liposomes. TPX® had a size and PDI value of 236 ± 114 nm and 0.305 ± 0.025 respectively and PS had a size and PDI value of 158 ± 18.7 nm and 0.298 ± 0.02 respectively.

The data also shows PCT and PPCO plastic tubes being used to form samples of 0.5 mL, 1 mL and 2 mL. Both plastics showed a significant increase in size when sonicating the larger volumes. For PCT and PPCO, the PDI firstly significantly increased and then significantly decreased from 0.5 mL to 1 mL, and then 1 mL to 2 mL. For PCT, the 1 mL and 2 mL samples had sizes and PDIs of 146 ± 10 nm and 112 ± 13 nm, and 0.338 ± 0.02 and 0.314 ± 0.015 respectively. For PPCO, the 1 mL and 2 mL samples had sizes and PDIs of 110 ± 11 nm and 172 ± 12 nm, and 0.35 ± 0.008 and 0.257 ± 0.027 respectively.

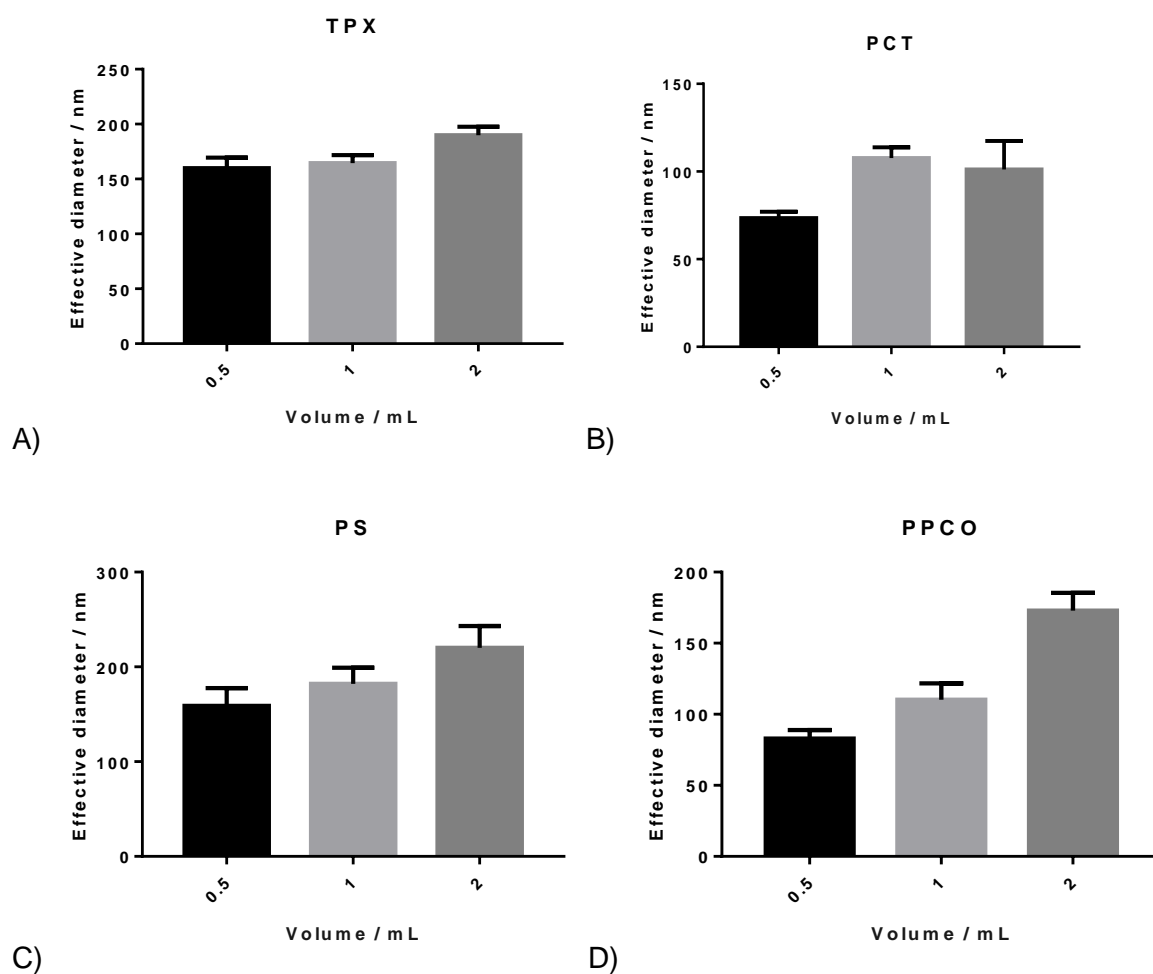


Figure 2.32: A - D) Size of DMPC liposomes produced using the Bioruptor® Plus at 40°C using 0.5, 1 or 2 mL of sample in a TPX® (A), PCT (B), PS (C) or PPCO (D) 50 mL tube. They were then sonicated for 15 cycles at H power.

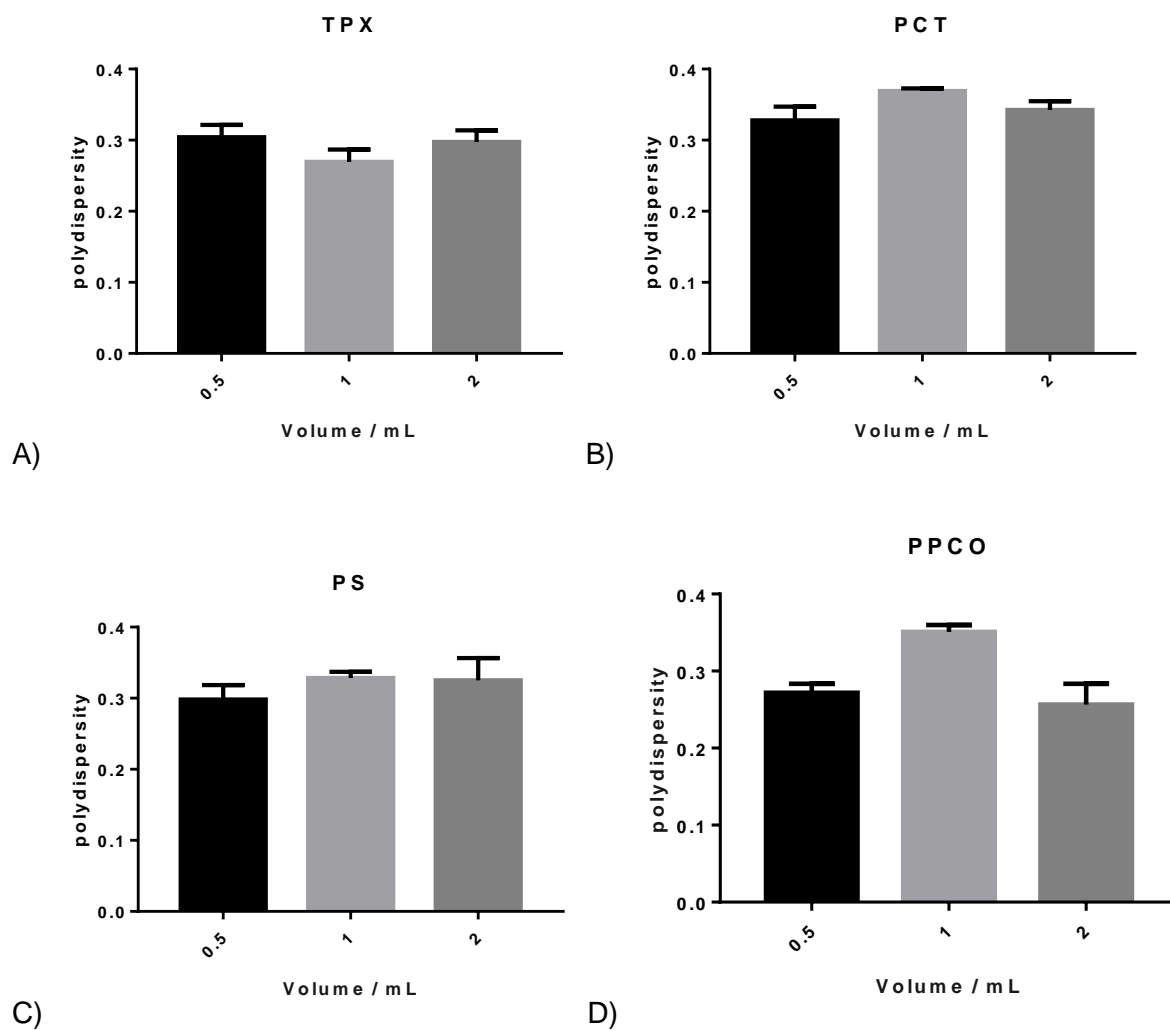


Figure 2.33: A - D) PDI of DMPC liposomes produced using the Bioruptor® Plus at 40°C using 0.5, 1 or 2 mL of sample in a TPX® (A), PCT (B), PS (C) or PPCO (D) 50 mL tube. They were then sonicated for 15 cycles at H power.

2.3.5.7 Bioruptor® Plus study into how different plastics using a 15 mL tube and power level affects liposome size reduction

Figure 2.34 show the use of PP and TPX® 15 mL tubes sonicated with 0.5 mL DMPC liposomes run on both low and high power. TPX® showed a significant decrease from low power to high power in both size and PDI. Size dropped from 253 ± 43 nm to 175 ± 8 nm and PDI dropped from 0.359 ± 0.024 to 0.311 ± 0.009 . However, PP showed no significant change in size or PDI. Low power had a size of 270 ± 53 nm and a PDI of 0.329 ± 0.04 and high power had a size of 323 ± 102 nm and a PDI of 0.359 ± 0.033 . Figure 5.5.5 E shows the use of the same tubes sonicated with 0.1 mL DMPC liposomes run on both power levels. This time there was no significant difference between the TPX® samples for low and high power. Low power had a size of 183 ± 6 nm and a PDI of 0.306 ± 0.026 and high power had a size of 178 ± 25 nm and a PDI of 0.293 ± 0.027 . However, there was a significant size decrease from low to high power for the PP sonicated liposomes, although no significant change was seen with the PDI. Low power had a size of 252 ± 29 nm and a PDI of 0.32 ± 0.019 and high power had a size of 132 ± 7 nm and a PDI of 0.322 ± 0.012 .

What this shows is that PPCO can be used as another plastic for the formation of DMPC size reduced liposomes as it gave a similar size and a lower PDI compared to the PCT tubes. However, TPX® and PS were not as suitable as they gave larger sizes and were not able to reduce the size of the liposomes as well as the others. This could be due to the way the tubes are put together whereby the sonication aid within the tube doesn't reach all the way to the bottom as found with the PCT and PPCO tubes. This could therefore significantly reduce the sonication energy being able to be input into the liposomes. It was also seen that a rise in the volume increases the size of the liposomes significantly and that the use of the 15 mL tubes did also result in size reduction, although not as much as the 50 mL PCT and PPCO tubes.

Finally, the use of power is also important because with both tubes it was found that a further size reduction could be obtained by using the higher power level.

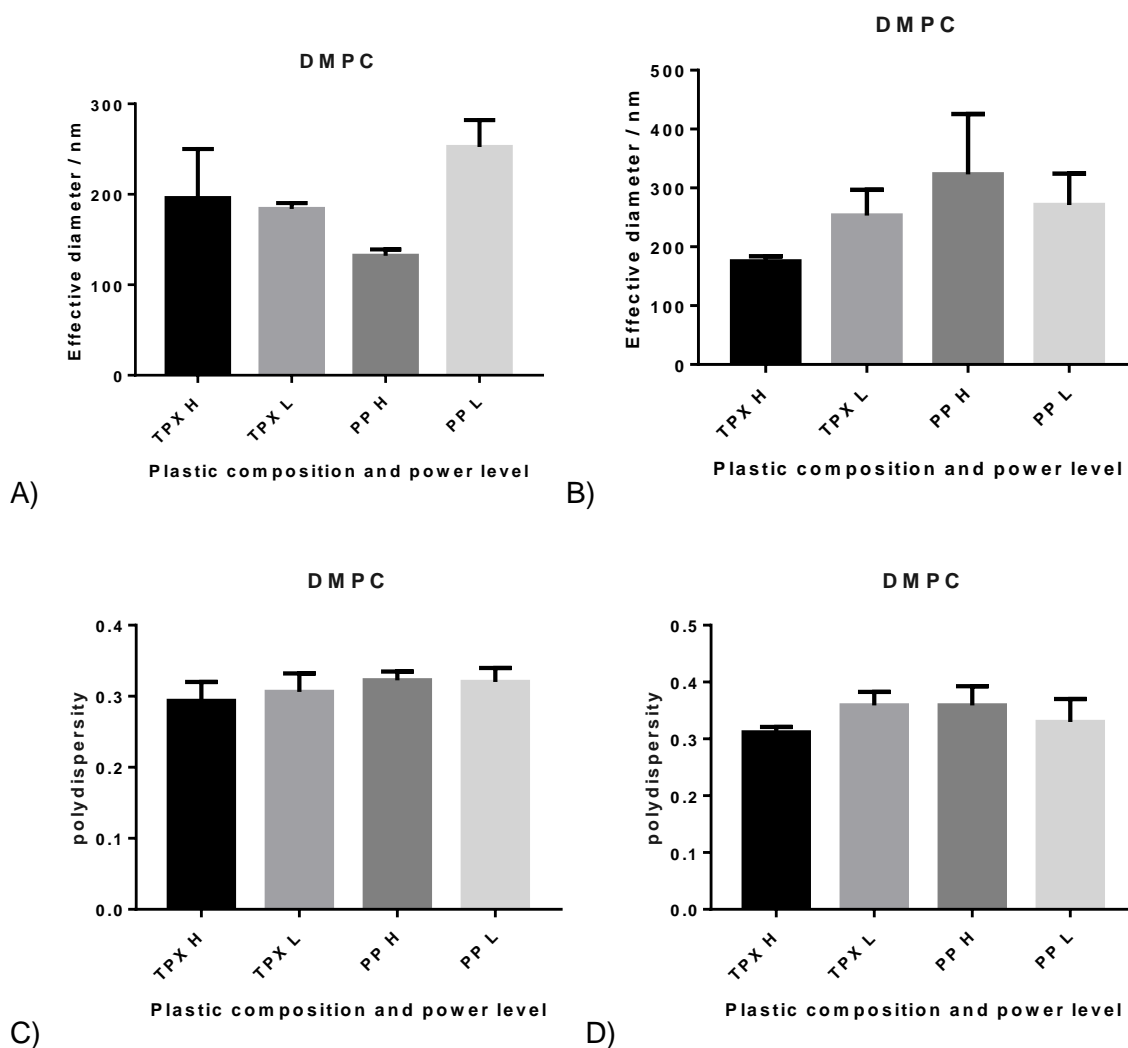


Figure 2.34: A – B) Size of DMPC liposomes produced using the Bioruptor® Plus at 40°C using 0.1 mL (A) or 0.5 mL (B) of sample in 15 mL TPX® or PP tubes. They were then sonicated for 15 cycles at L and H power levels. C – D) PDI of DMPC liposomes produced using the Bioruptor® Plus at 40°C using 0.1 mL (C) or 0.5 mL (D) of sample in 15 mL TPX® or PP tubes. They were then sonicated for 15 cycles at L and H power levels.

2.3.5.8 Bioruptor® Plus study into how DMPC: Cholesterol ratio affects liposome size reduction

Cholesterol is an important part of many liposomal formulations due to its stabilizing effect on the lipid bilayer and ability to prevent lipid exchange (Socaciu et al., 2000, Sulkowski et al., 2005). Up to 66 mol% of cholesterol can be incorporated into a liposome bilayer depending on the lipid used, although 50 mol% is more common (Huang et al., 1999). Therefore, it is important to see whether the addition of the cholesterol has any effect on the size of the liposomes formed.

The results in Figure 2.35 show that with any addition of cholesterol to the DMPC liposomal formulation, an increase in size is seen. For the low power sonicated liposomes, DMPC liposomes were 110 ± 11.6 nm in size but when cholesterol was added in a ratio of 7:1, an increase was seen up to 148 ± 12.6 nm. However no further significant increases in size were seen with the 6:2, 5:3 and 4:4 ratios having sizes of 139 ± 9.6 nm, 143 ± 10.2 nm and 147 ± 8 nm respectively. A similar pattern was seen with the high power sonicated liposomes. DMPC liposomes were 93.4 ± 10 nm in size, but with the addition of cholesterol in the ratio 7:1, an increase in size was seen up to 154 ± 8.8 nm. Further increases in cholesterol content did not cause any further increases in size with the ratios 6:2, 5:3 and 4:4 having sizes of 152 ± 11.8 nm, 144 ± 15.7 nm and 137 ± 6 nm respectively.

There is a small drop in the PDI with the high power sonicated liposomes, but no significant change with the low power sonicated liposomes. The high power sonicated liposomes saw a PDI value for the DMPC liposomes of 0.297 ± 0.013 . However, with the addition of cholesterol, this dropped so for the 7:1, 6:2, 5:3 and 4:4 ratios, a PDI value of 0.236 ± 0.028 , 0.261 ± 0.025 , 0.273 ± 0.024 and 0.219 ± 0.02 were achieved respectively. However no significant change was seen with the low power sonicated liposomes with PDI values for the DMPC, 7:1, 6:2, 5:3

and 4:4 liposomes being 0.241 ± 0.02 , 0.25 ± 0.027 , 0.247 ± 0.022 , 0.248 ± 0.026 and 0.242 ± 0.026 respectively.

What these results show is that any addition of cholesterol to the DMPC formulation elicits an increase in size but can cause a decrease in PDI. This is important because it shows that even with the same lipid and method; different sizes of liposomes can be obtained simply with the addition or exclusion of cholesterol from the formulation.

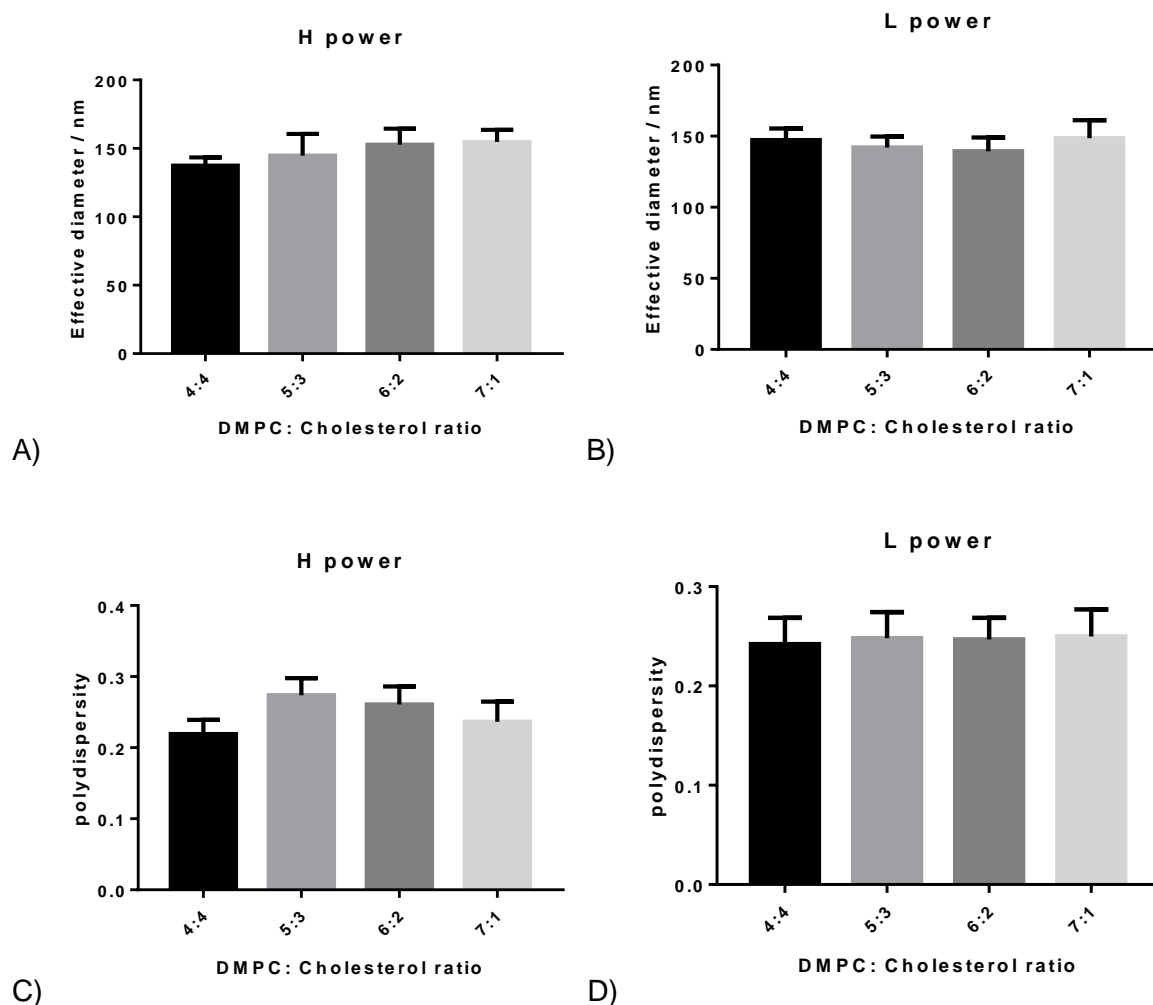


Figure 2.35: A – B) Size of DMPC: Cholesterol liposomes produced using a range of ratios using the Bioruptor® Plus at 40°C using 0.1 mL sample in a 1.5 mL TPX® tube. They were then sonicated for 15 cycles at L (A) and H (B) power levels. C – D) PDI of DMPC: Cholesterol liposomes produced using a range of ratios using the Bioruptor® Plus at 40°C using 0.1 mL sample in a 1.5 mL TPX® tube. They were then sonicated for 15 cycles at L (C) and H (D) power levels.

2.3.5.9 Bioruptor® Plus study into how lipid concentration affects liposome size reduction

Liposomes are made up of lipids, which can be anionic, cationic or zwitterionic. It is therefore important to see how the charge or lack of charge affects the size, PDI and zeta potential of the liposomes. It is also important to see how varying the concentration of the charged lipid affects the size, PDI and zeta potential.

The results in Figure 2.36 and 2.37 show that liposomes made up of just DMPC have a charge of -7.8 ± 5.7 mV and with the addition of cholesterol saw it increase in negativity down to -24.8 ± 3.8 mV. Figure 7.9 also shows what happened to the zeta potential with the addition of a cationic lipid, DOTAP. With the addition of 1 μ mole of DOTAP saw an increase in zeta potential to 32.7 ± 5.8 mV and with the addition of 2 and 4 mM, no significant increase was seen in the zeta potential with results of 29.9 ± 8.1 mV and 36.7 ± 6.8 mV respectively. With the addition of a zwitterionic lipid, DOPE, there was no significant difference between any of the formulations to the zeta potential, as seen in Figure 5.8 C. With the addition of 1, 2 and 4 mM of DOPE, the zeta potential was -18.2 ± 19.5 mV, -22.8 ± 15.8 mV and -15.2 ± 1.5 mV respectively. Finally, in Figure 5.7 D, the addition of the anionic lipid DMPG saw a decrease in the liposomes charge. There was a significant decrease with the addition of 1 μ mole of DMPG, down to -69.4 ± 4.2 mV. There was no significant change between 1 and 2 mM with a zeta potential of -67.8 ± 6.1 mV. The addition of more DMPG, up to 4 mM, saw a further significant decrease down to -89 ± 3 mV.

The data also shows that the addition of 1 μ mole of DOTAP, there was no significant change in the size or PDI with results of 154.6 ± 27.1 nm and 0.222 ± 0.035 respectively. The addition of 2 mM saw a significant decrease in both size and PDI down to 101.7 ± 3.1 nm and 0.110 ± 0.042 respectively. The addition of 4 mM of DOTAP saw no significant change in either the size or PDI with a size of 99.1 ± 5.2 nm and a PDI of 0.148 ± 0.037 . The addition of 1 μ mole

of DOPE there was a significant drop in both size and PDI down to 102.1 ± 5.6 nm and 0.157 ± 0.018 respectively. However, the addition of 2 mM of DOPE saw a small but significant increase in size to 114.3 ± 5.9 nm although no significant change was seen with the PDI, with a result of 0.121 ± 0.027 . The addition of 4 mM of DOPE saw a significant decrease down to 87.7 ± 3.2 nm although again no significant change with the PDI, with a result of 0.141 ± 0.018 . The addition of DMPG is shown in Figures 5.8 I and J. The addition of 1 μ mole of DMPG saw a significant decrease in both size and PDI, down to 89.3 ± 5.8 nm and 0.197 ± 0.026 respectively. The addition of 2 mM of DMPG saw a further significant decrease in the size down to 72.1 ± 4.6 nm although no significant change was seen with the PDI, with a result of 0.215 ± 0.012 . The addition of 4 mM of DMPG saw no significant change for either the size or PDI, with values of 75.1 ± 5.1 nm and 0.203 ± 0.031 respectively.

What these results show is that adding a negative or positive lipid to the neutral DMPC: Cholesterol formulation decreases both the size and PDI of the formulations. The zeta potential followed the expected pattern of increasing with a cationic lipid and decreasing with an anionic lipid. The addition of DOPE, a zwitterionic lipid, did have an effect on the size but no significant effect on the zeta potential, as expected. This is important because for vaccine to work well, a positive liposome allows the depot effect to occur. The depot effect allows for an increase in the amount of time in which liposomes and therefore the antigen stays at the site of injection. This therefore increases the overall immune response because the immune system has a longer period of time in which to interact with and take up the antigen. Therefore for vaccine work, the liposomes should be positively charged so they can interact with the mostly negative human cells and cause the depot effect to occur (Henriksen-Lacey et al., 2010).

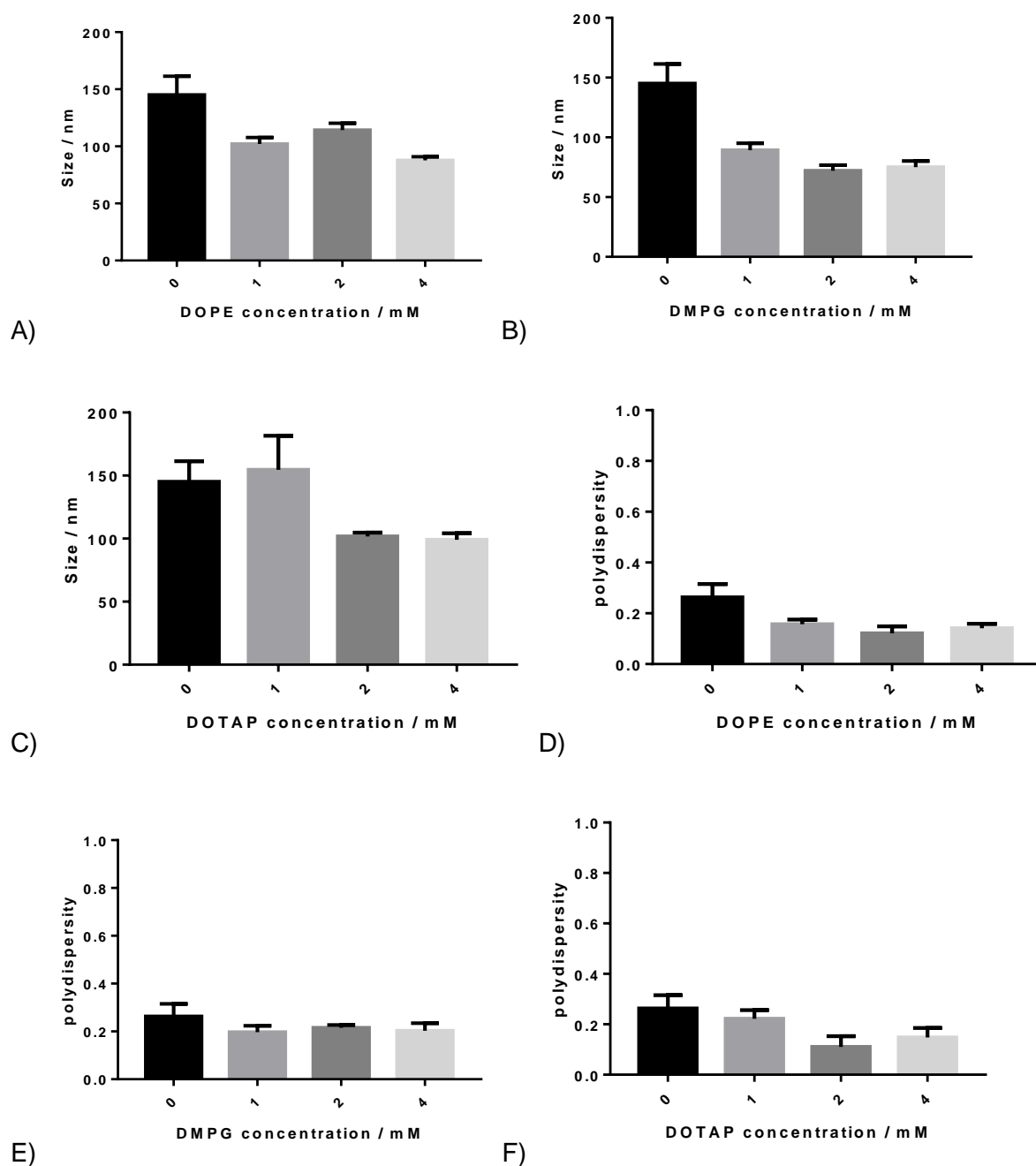


Figure 2.36: A – C) Size of DMPC: Cholesterol liposomes produced with the addition of 1, 2 or 4 mM of DOPE (A), DMPG (B) or DOTAP (C) lipid. The Bioruptor® Plus was used at 40°C using 0.1 mL sample in a 1.5 mL TPX® tube. They were then sonicated for 15 cycles at H power level. D - F) PDI of DMPC: Cholesterol liposomes produced with the addition of 1, 2 or 4 mM of DOPE (D), DMPG (E) or DOTAP (F) lipid. The Bioruptor® Plus was used at 40°C using 0.1 mL sample in a 1.5 mL TPX® tube. They were then sonicated for 15 cycles at H power level.

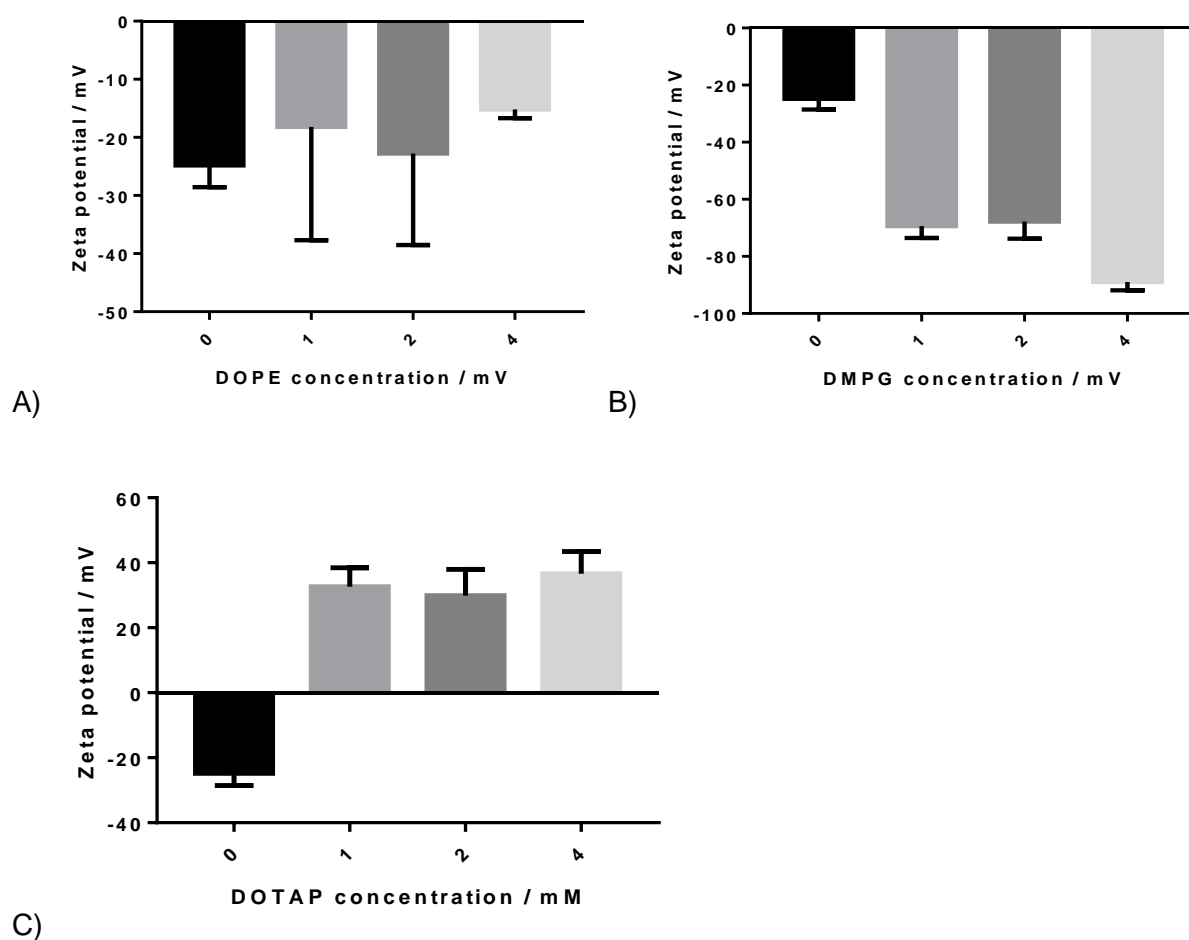


Figure 2.37: A - C) Zeta potential of DMPC: Cholesterol liposomes produced with the addition of 1, 2 or 4 mM of DOPE (A), DMPG (B) or DOTAP (C) lipid. The Bioruptor® Plus was used at 40°C using 0.1 mL sample in a 1.5 mL TPX® tube. They were then sonicated for 15 cycles at H power level.

2.3.5.10 Discussion

The results showed that the Bioruptor® Plus system can be used to produce SUVs and that it is comparable to the probe sonication results. The cycles and power data showed that as expected, an increase in the number of cycles lead to a decrease in liposome size, and that the use of the higher power level gave a bigger size reduction compared to the low power. The concentration data again tallied with previous data showing that up to in this case 24 mM, there was no significant difference in size or PDI. The temperature data did show that for DMPC liposomes at least, the previous data held true showing that as you increase temperature, you decrease the size of your finished liposomes. Volume followed previous data showing that a smaller volume gave a smaller liposome. The cholesterol ratio also showed the expected data, filling in the gaps between DMPC, DMPC: Cholesterol 6:2 and DMPC: Cholesterol 4:4 showing that as you increase Cholesterol concentration, you increase the finished size of your liposome but decrease its PDI. The plastics data showed that plastic is an important factor to consider when producing these liposomes. TPX® showed to be better able to reduce liposome size compared to PP for the 1.5 mL tubes and also in the most part for the 15 mL tubes. However, when comparing the 50 mL tubes, TPX® did not appear to work as well. TPX® did not reduce the liposome size as much as others under the same conditions, namely PPCO and PCT. This could be due to the tubes being a different shape and having a different sonication aid used although this would require further investigation. However, what this data did show was that 50 mL tubes could be used to produce mL of liposomes at a reasonable size under the same conditions used for the much smaller tubes. Finally the formulation data showed that as you add additional lipid to a formulation, you are liable to change how well that formulation reduces in size, and need to be prepared to change the method if a certain size is required.

2.3.6 Bioruptor® Pico liposome size reduction studies

The Bioruptor® Pico is another machine currently on the market from Diagenode. This is a smaller machine but does have other advantages. In particular, its compact nature means that the space it requires in a lab environment is smaller. However its use of only one power level could be a problem, and it cannot be used with larger tubes due to the shallow nature of the sonication bath itself.

2.3.6.1 Bioruptor® Pico study into how number of cycles affects liposome size reduction

The Bioruptor® Pico is another machine used by Diagenode and so it was important to test whether liposomes could be made using this machine also. Number of cycles was first investigated as the Pico has no opportunity to change the power output. The data in Figure 2.38 showed that as the number of cycles, and therefore sonication time, increased, there was a decrease in size and PDI for DMPC liposomes from 3 to 10 cycles of 105.2 down to 75.1 nm and from 0.426 to 0.268 respectively. DMPC: Cholesterol liposomes showed a dissimilar pattern for size and PDI, with decreases from 3 to 10 cycles of 114.7 to 108.5 nm and 0.456 to 0.434 respectively. Both of these drops were not seen to be statistically significant. What this showed is that for DMPC liposomes, size reduction comes relatively easily with increased sonication time but with the addition of cholesterol, the liposomes are harder for the Pico to reduce in size over time.

2.3.6.2 Bioruptor® Pico study into how volume affects liposome size reduction

Volume as shown before with previous Bioruptor® systems, is known to be important in how well the sonicator works at reducing liposome size. However this data in part seemed to contradict this as shown in Figure 2.38. DMPC liposomes sonicated with 0.1, 0.2 or 0.3 mL of sample in showed no significant difference in size or PDI across the board with sizes of 80.2, 94.6 and 80.0 nm and polydispersities of 0.346, 0.396 and 0.387 respectively. DMPC: Cholesterol liposomes showed a decrease in size with smaller volumes, down from 159.6 to 107.7 nm but no significant difference in PDI from 0.41 to 0.397 respectively.

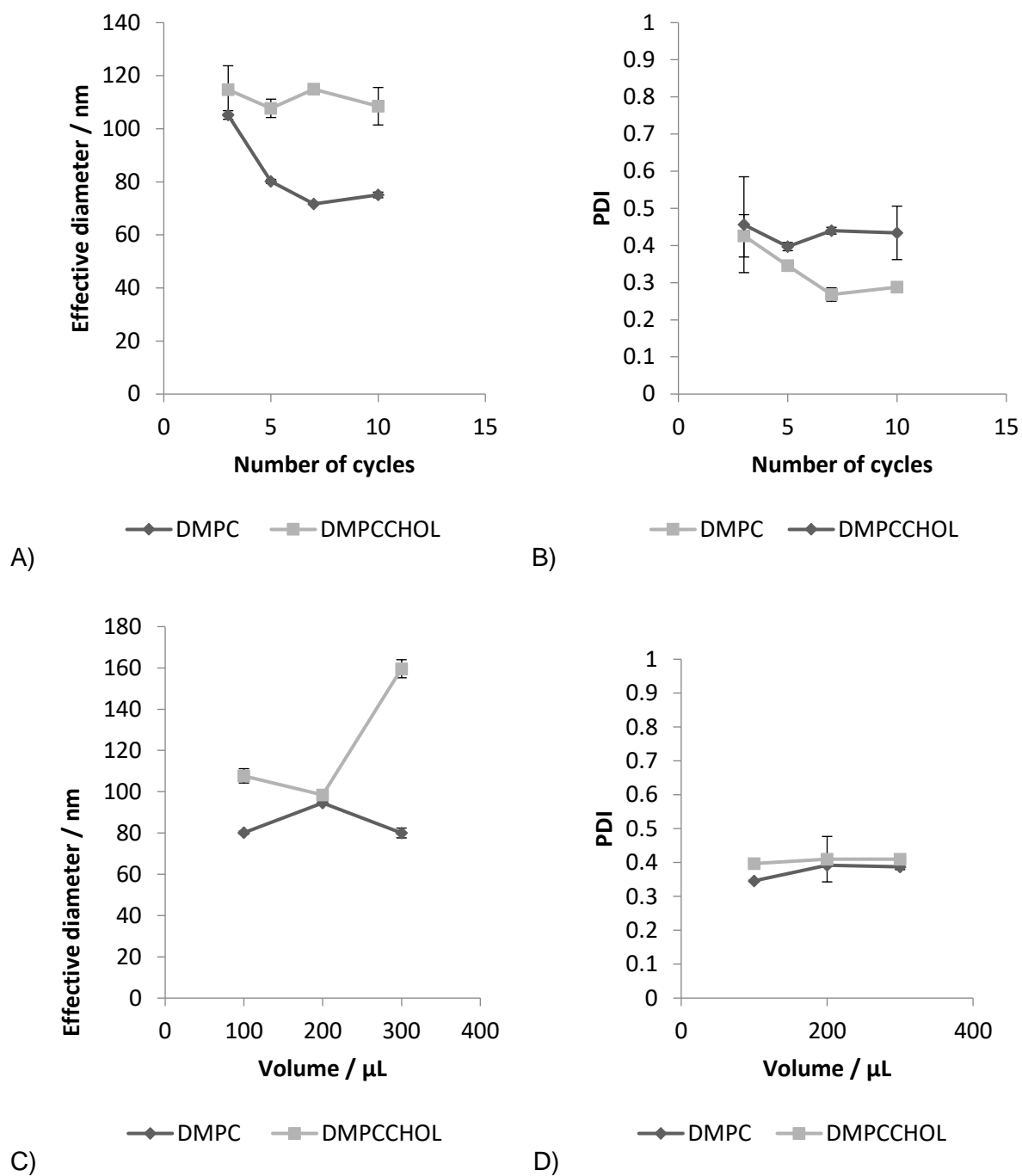


Figure 2.38: A – B) Size (A) and PDI (B) of DMPC and DMPC: Cholesterol liposomes produced using the Bioruptor® Pico at 40°C using 0.1 mL sample in a 1.5 mL TPX® tube. They were then sonicated for up to 10 cycles. C – D) Size (C) and PDI (D) of DMPC and DMPC: Cholesterol liposomes produced using the Bioruptor® Pico at 40°C using 0.1 to 0.3 mL sample in a 1.5 mL TPX® tube. They were then sonicated for 10 cycles.

2.3.6.3 Discussion

Liposomes were formed using the Bioruptor® Pico, although only two factors were investigated. These showed however that it is another viable machine to be used for liposome size reduction and that with further work, it could be used for liposome size reduction. In particular, its small size and compact nature would lend itself well to a lab environment with the sonicator and control mechanism all included in one machine.

2.4 Conclusion

In conclusion, DMPC and DMPC: Cholesterol liposomes were successfully reduced in size using both the probe sonicator and each of the bath sonicators; the XL, the Standard, the Plus and the Pico. The probe sonicator performed as expected compared to the literature and reduced the liposome size to below 100 nm in just a couple of minutes. However this process is difficult to control in regards to temperature, cannot be done under sterile conditions and required further processing post sonication by using a centrifuge to remove the titanium particles that break off from the probe itself during the sonication process. What each of the bath sonicators does is allow for the liposomes to be sonicated in a temperature controlled sterile environment without the need for further processing. This process does require longer to sonicate compared to the probe sonicator, up from approximately 6 minutes of probe sonication to 15 – 20 minutes of bath sonication, but the ability to sonicate multiple samples at once allows for overall more sample to be sonicated at any one time. Each Bioruptor® was individually optimised as subtle changes in the designs and power levels means that such parameters as time and pulse need to be calibrated depending upon the machine.

It was shown that all factors need to be taken into consideration. These include time, power level, concentration, volume, temperature, and pulse. For example, the choice of plastic for

the liposomes to be sonicated in was shown to play an important role when optimised through the Bioruptor® Plus and the Bioruptor® Standard. The choice of plastic was also different depending on the size of the tube as it was found that for the 1.5 mL tube, TPX® was the best performing plastic at liposome size reduction. However, for the larger 50 mL tube, it was found that PCT was the better performing plastic. Formulation was also an important factor in how much the liposomes were reduced in size. For example, the addition of just 1 mM of a positive or negative lipid to an 8 mM formulation reduced the liposome size significantly to below 100 nm. This is important because many formulations that are on the market or being researched, require a mix of multiple lipids and other parts to form the final liposome. It is also known that a negatively charged liposome is more efficient than a neutral liposome for internalisation into the cells by endocytosis process (Mishra et al., 2011). However cationic liposomes have been shown to be useful for both drug and vaccine delivery due to their interactions with the negatively charged human cells (Schwendener, 2014, Vitiello et al., 2015).

There are some limits to this process however. The first is that there is not much chance of further scale up beyond the lab as a bath sonicator machine generally cannot be up scaled enough to meet the demands of an industrial setting. This is also true for probe sonication but other methods such as microfluidics can be scaled up to the litre scale. Also the transition temperature of the lipid is paramount as a higher transition temperature lipid of for example 1, 2-Distearoyl-sn-glycero-3-phosphoethanolamine (DSPE) of 75 °C would simply not be possible with the water bath associated with the Bioruptor® systems (Avanti, 2018). Also, it is known that as temperature increases, sonication efficiency decreases and therefore it will reach a point where it simply is no longer efficient to use the bath sonicator. On one hand, high temperatures can help to disrupt solvent-solute interactions, which involve Van der Waals forces, H-bonding and dipole interaction, also faster diffusion occurs at higher temperature. But on the second hand, a too high temperature can also lead to “vaporous” cavitation where acoustic bubbles can do coalescence with natural bubbles of vapour, decreasing the efficiency of the ultrasonic effects (Mason, 1991, Niemczewski, 2007, Ali et al., 2014).

However, the Bioruptor® bath sonicator systems are very good for producing small quantities of most liposomal formulations and is especially useful for the lower transitional temperature lipids as the water bath allows for a much more controlled temperature which allows the smaller liposomes to form without damaging the lipid due to a high temperature.

- 3 Bioruptor bath sonicator systems: applications in the spheres of liposomes, DNA extraction and sonicator efficiency

3.6 Aims and objectives

The Bioruptor® bath sonication systems can be used for a variety of different techniques including DNA extraction, DNA shearing, protein and chromatin analysis. The second objective was to improve DNA extraction through improving the kit currently being offered through the company Diagenode. The final objective was to improve the sonication efficiency tests done by the company by using a different technique involving the use of potassium iodide and the cavitation effect that occurs during the sonication process.

3.2.1 Investigating more cost effective methods of demonstrating bath sonicator efficiency

At the start of each day, fresh solutions of Potassium Iodide (KI) 0.29 Mol/L and Ammonium molybdate (AM) 3.67 mM/L were formulated. Before using, 5 parts of KI were mixed with 0.1 part of ammonium molybdate (e.g. 5 ml plus 0.1 ml) and scaled accordingly to the number of samples per day. The KI/AM mix was kept at room temperature (RT) before use. 2 Bioruptor® models will be used in the study: Bioruptor® Pico and the Bioruptor® Plus. The Bioruptors were used with a cooling system set at 4°C for initial trials as specified below. *To note that salts can precipitate in samples at 4°C. If salt are observed, use 10°C (or higher T if needed) but be sure that the temperature is controlled.* After sonication, the sample was measured at 352 nm (yellow colour due to I₂ formation) on the Smart SpecPlus. A blank was included which is KI/AM without sonication.

3.2.1.1 Conditions to test on the Bioruptor® Pico:

Each of the following experiments was ran with the following cycle settings and size of samples:

3 cycles 30"On/30" OFF x12 samples

5 cycles 30"On/30" OFF x12 samples

10 cycles 30"On/30" OFF x12 samples

15 cycles 30"On/30" OFF x12 samples

Experiment 1: Use 0.65 ml microtubes (ref C30010011) and a corresponding tube holder filled with 100 µl of KI/AM mix and sonicate for

Experiment 2: Use 0.65 ml microtubes (ref C30010011) and a corresponding tube holder filled with 200 µl of KI/AM mix and sonicate

Experiment 3: Use 0.5 ml microtubes (refC30010013) filled with 100 µl of KI/AM mix and sonicate

Each of the following experiments was ran with the following cycle settings and size of samples:

3 cycles 30"On/30" OFF x6 samples

5 cycles 30"On/30" OFF x6 samples

10 cycles 30"On/30" OFF x6 samples

15 cycles 30"On/30" OFF x6 samples

Experiment 4: Use 1.5 ml microtubes with caps (ref C30010016) and a corresponding tube holder filled with 300 µl of KI/AM mix and sonicate for

Experiment 5: Use 1.5 ml TPX microtubes (refC30010010) and a corresponding tube holder filled with 100, 200 or 300 µl of KI/AM mix and sonicate for

3.2.1.2. Conditions to test on the Bioruptor® Plus

Each of the following experiments was ran with the following cycle settings and size of samples:

3 cycles 30"On/30" OFF x6 samples

5 cycles 30"On/30" OFF x6 samples

10 cycles 30"On/30" OFF x6 samples

15 cycles 30"On/30" OFF x6 samples

Experiment 6: Use 1.5 ml TPX® microtubes (ref C30010010) and a corresponding tube holder filled with 300 µl of KI/AM mix and sonicate at high power

Experiment 7: Use 1.5 ml TPX® microtubes (ref C30010010) and a corresponding tube holder filled with 300 µl of KI/AM mix and sonicate at low power

Experiment 8: Use 1.5 ml BioSigma microtubes and a corresponding tube holder filled with 300 µl of KI/AM mix and sonicate at high power

Experiment 9: Use 1.5 ml BioSigma microtubes and a corresponding tube holder filled with 300 µl of KI/AM mix and sonicate at low power

Experiment 10: Use 1.5 ml TPX® microtubes (ref C30010010) and a corresponding tube holder filled with 100 µl of KI/AM mix and sonicate at high power

Experiment 11: Use 1.5 ml TPX® microtubes (ref C30010010) and a corresponding tube holder filled with 200 µl of KI/AM mix and sonicate at high power

Experiment 12: Use 1.5 ml BioSigma microtubes and a corresponding tube holder filled with 100 µl of KI/AM mix and sonicate at high power

Experiment 13: Use 1.5 ml BioSigma microtubes and a corresponding tube holder filled with 200 µl of KI/AM mix and sonicate at high power

Experiment 14: Use 1.5 ml BioSigma microtubes and a corresponding tube holder filled with 100 µl of KI/AM mix and sonicate at high power at 10 °C

Experiment 15: Use 1.5 ml BioSigma microtubes and a corresponding tube holder filled with 200 µl of KI/AM mix and sonicate at high power at 10 °C

Experiment 16: Use 1.5 ml BioSigma microtubes and a corresponding tube holder filled with 100 µl of KI/AM mix and sonicate at high power at 20 °C

Experiment 17: Use 1.5 ml BioSigma microtubes and a corresponding tube holder filled with 200 µl of KI/AM mix and sonicate at high power at 20 °C

3.2.2 Investigating more cost effective materials for DNA extraction using the Bioruptor® Pico

Protocol:

Before starting, ethanol (100 %) was added to the wash buffer and labelled as such. The Bioruptor® Pico was turned on and left at room temperature. A thermomixer was preheated to 56 °C and another to 37 °C with the appropriate amount of extraction buffer placed in to preheat to the required 37 °C. The elution buffer was also equilibrated to room temperature.

The sections of DNA were placed in a 1.5 mL Bioruptor® tubes and 180 µl of pre-warmed FFPE extraction buffer was added. The sections were cut up when required to ensure they were completely immersed in the buffer. Each sample was then incubated for 10 minutes at 37 °C. Each sample was then vortexed and then sonicated using Bioruptor® Pico for 3-5 cycles 30"On/30"Off at room temperature until the paraffin had been emulsified and dissociated from the tissue section with the solutions turning milky once complete. These were then briefly spun down and transferred to a new 1.5 ml tube. 20 µl of Diagenode proteinase K was then added. Each sample was incubated for 1 hour at 56 °C in a Thermomixer with shaking at 1300 rpm. 4 µl of reversal crosslink buffer was added and then each sample was incubated at 65°C for 4h or overnight with shaking at 1300 rpm.

Each sample was then span down and the supernatant carefully transferred to a DiaFilter column to remove paraffin if required. These were the centrifuged for 2 minutes at 8000 rpm at room temperature. The filter unit was discarded and the collection tube containing the flow-through was kept. 1 ml of binding buffer and 20 µl of precipitant was then added to the flow-through or the sample that had not been filtered. A DiaPure Spin column was placed in a collection tube, 600 µl of the mixture from the previous step was loaded and then centrifuged for 1 min at 8000 rpm at RT. The flow-through was discarded and then tube reused with the second half of each sample, 600 µl, was added to the column and then centrifuged under the same conditions. The spin columns were then washed twice with 400 µL of washing buffer,

following the sample centrifuge protocol as before. After washing, the spin column was placed in a clean 1.5 ml tube and 50 µl of Elution buffer at room temperature was added to the centre of the membrane. This was then left to incubate at room temperature for 3 minutes and then centrifuged for 1 minute at 14000 rpm at room temperature. The eluate contained the purified DNA. This was then quantified and analysed.

3.2.2.1 Assay 1.

Sample 1: test the protocol for FFPE DNA extraction replacing original columns and buffers r by MicroChIP DiaPure columns and buffers as specify below.

Sample 2: as sample 1/2 but omitting DiaFilter column at step 8.

3.2.2.2 Assay 2:

Compare 3 different compositions of FFPE extraction buffer (buffer 1 vs buffer 2 vs buffer 3) using the protocol for FFPE DNA extraction as above replacing original columns and buffers r by MicroChIP DiaPure columns and buffers as specify below and

- Sample 1 FFPE extraction buffer 1
- Sample 2 FFPE extraction buffer 2
- Sample 3 FFPE extraction buffer 3

3.2.2.3 Assay 3.

Choose the best experimental condition from assay 1 and 2 and compare the efficiency of decrosslinking (step 7)

- 4h at 65°
- Overnight at 65°C
- 15 min at 95°C

3.2.2.4 Analysis of DNA ran with DNA fragment analyser

DNA was analysed using the Advanced analytical fragment analyser. The inlet buffer was measured into each well 1 mL at a time and changed daily. TE buffer was also measured into each well, 0.2 mL at a time and again changed daily. 0.022 mL of diluent marker was added to each well a sample was to be added to as well as the final well, #12. 0.002 mL of the ladder was added to well #12 only and then 0.002 mL of sample was added to each well with diluent marker in. In the wells without sample, a blank solution of 0.024 mL was added. The gel was added with the addition of the dye (add 0.001 ml of dye for 10 ml of gel) and conditioning solution was topped up. Each required 5 mL for each lane being ran.

3.7 Results and discussion

3.3.2 Investigating more cost effective methods of demonstrating bath sonicator efficiency

3.3.2.1 Bioruptor® Pico

For experiment 1, 0.65 ml tubes were sonicated with 0.1 ml samples in Pico for 3, 5, 10, 15 cycles of 30 seconds on, 30 seconds off. Results were expected to be the best as small tubes with smallest volume to back up what the DNA results show. Results below show a good R value of 0.993 with RSD steadily decreasing to 24 % in Figure 3.1. The data shows the results generally stays fairly close to the mean and the steady increase is clear. Finally the p values all show significant differences across with board meaning that as the number of cycles increased, the reaction increased so more of the iodine was converted to I₂ formation.

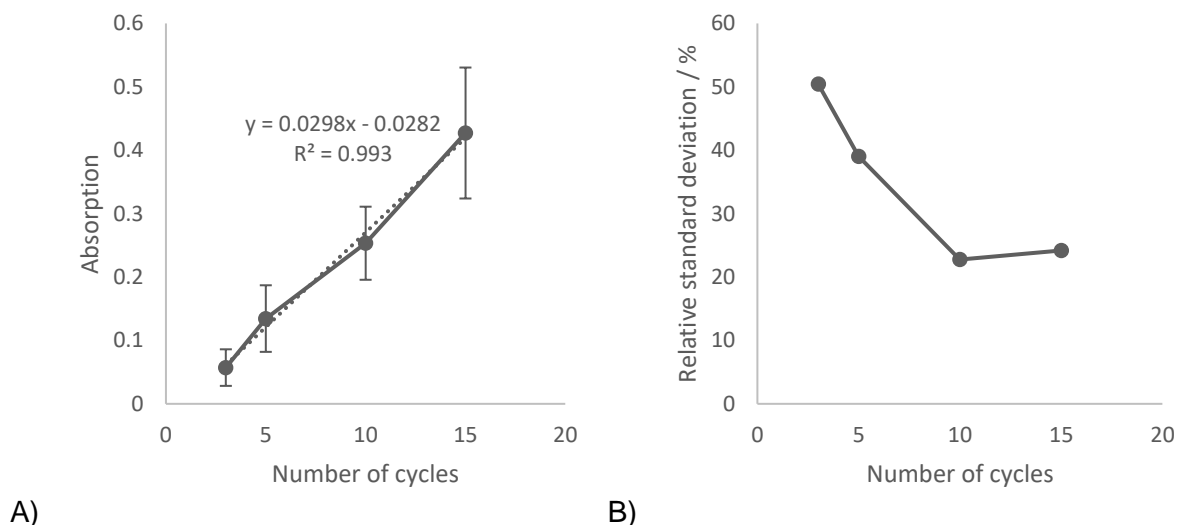


Figure 3.1: A) Average absorption for Experiment 1 settings, 0.65 ml tubes were sonicated with 0.1 ml samples in Pico, from 3 to 15 cycles with standard deviation. B) Relative standard deviation for Experiment 1 from 3 to 15 cycles.

Experiment 2 was done under the same conditions but used a 0.2 ml sample volume and showed that doubling the volume did not just decrease the values by half. The data in Figure 3.2 shows a significantly smaller absorbance and a much larger scatter over that absorbance. The R value is poor at 0.87 and even though the RSD does drop, it drops from above 200 % to 44 %, so still pretty high. Finally the p values show no significant difference between any samples apart from between 3 and 15 cycles. This showed that an increase in volume can dramatically reduce the efficacy of sonication to such an extent that it almost completely stops the I_2 formation.

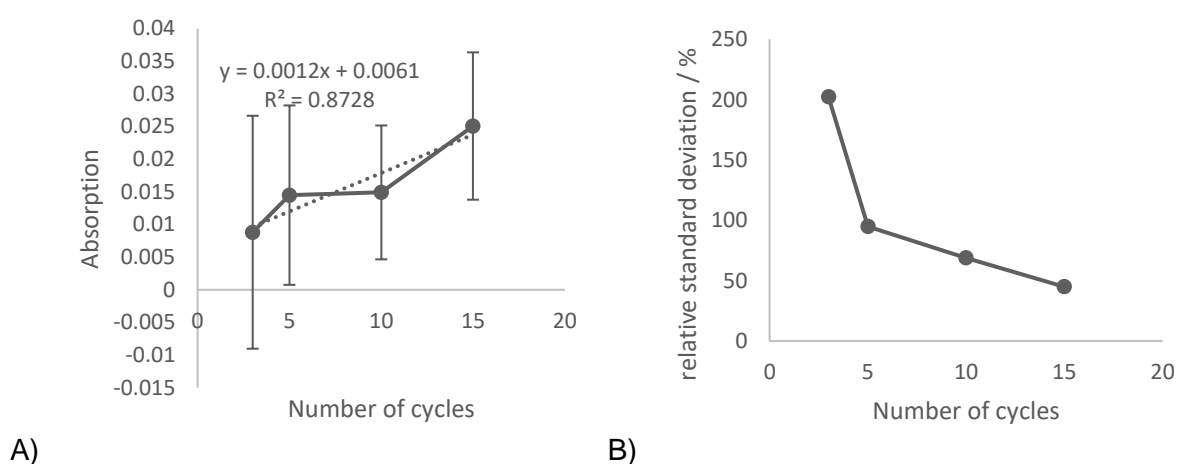


Figure 3.2: A) Average absorption for Experiment 2 settings, 0.65 ml tubes were sonicated with 0.2 ml samples in Pico, from 3 to 15 cycles with standard deviation. B) Relative standard deviation for Experiment 2 from 3 to 15 cycles.

Experiment 3 used 0.5 ml tubes with 0.1 ml sample with the smaller tubes comes an overall increased percentage volume and therefore a reduction was expected. The R value was again not good at 0.9 and the overall absorbance was lower than the 0.65 ml tube with a 0.1 ml sample as shown below in Figure 3.3. The RSD stayed fairly constant between 58 and 29 %. There appeared to be a saturation whereas the cycles were increased, the increase in absorption became smaller and smaller in comparison. Although this is difficult to be sure of as the spread of the data, particularly at the 15 cycles, is very large. There were a few significant differences between 3 and 10 to 15 cycles. What this shown is that as you increase the volume of tube to sample volume ratio, there is a decrease in sonication efficacy.

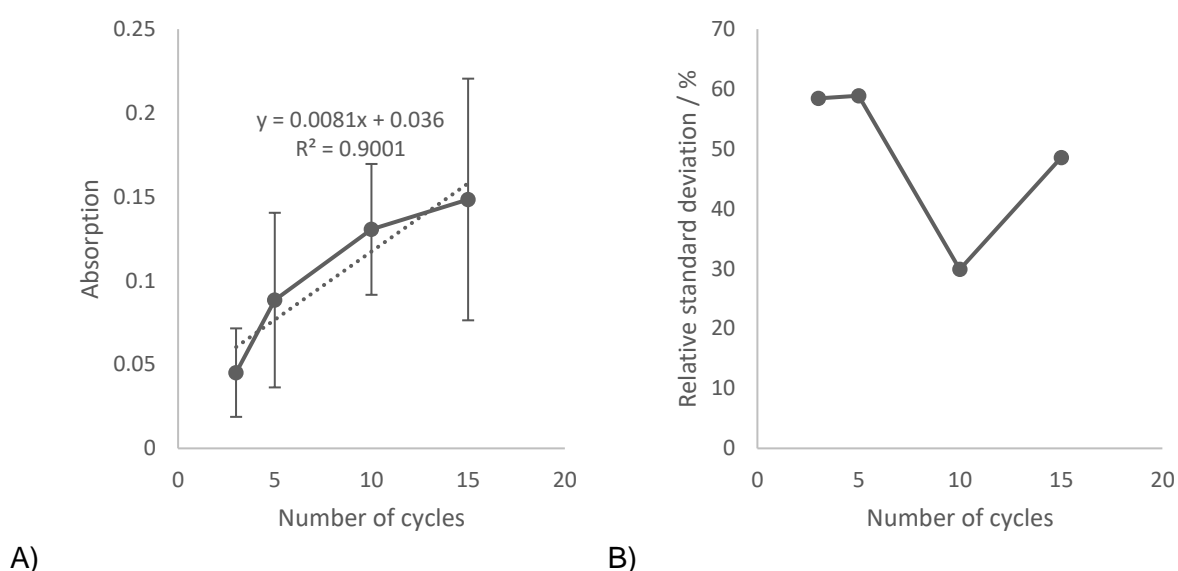


Figure 3.3: A) Average absorption for Experiment 3 settings, 0.5 ml tubes were sonicated with 0.1 ml samples in Pico, from 3 to 15 cycles with standard deviation. B) Relative standard deviation for Experiment 3 from 3 to 15 cycles.

Experiment 4 used the larger 1.5 ml tubes with caps with 0.3 ml sample with the results shown below in Figure 3.4. This was expected to be better than the equivalent TPX® tubes. This showed good r value of 0.994 and gave a good RSD down to below 30 % and there were some significant differences.

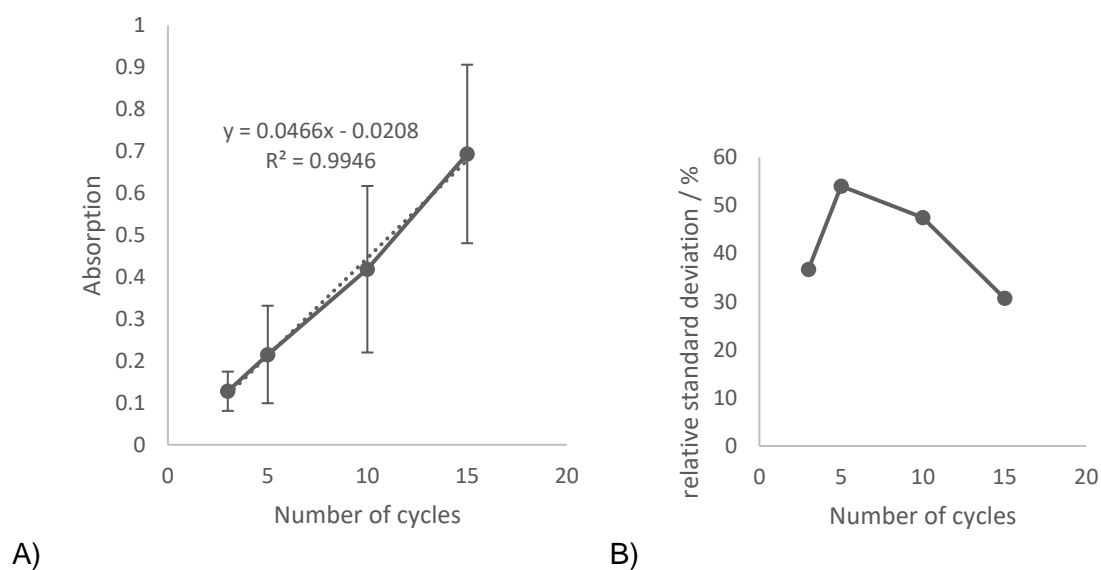


Figure 3.4: A) Average absorption for Experiment 4 settings, 1.5 ml tubes were sonicated with 0.3 ml samples in Pico, from 3 to 15 cycles with standard deviation. B) Relative standard deviation for Experiment 4 from 3 to 15 cycles.

Experiment 5a used the TPX® 1.5 ml tubes with 0.1 ml sample in. This data shows a more confusing picture. The expectation was that a reduced volume would give a better absorption and that this would be up with experiment 1 and 4. However, the reduction was large compared to these two previous experiments as shown in Figure 3.5. The increase from 3 to 5 cycles actually saw a small reduction in mean absorption. There was an increase at 15 cycles but it was still significantly lower than the other two experiments mentioned. The r value is again poor at 0.91. This could be due to the different position of the tube within the bath due to a lack of cap which can be seen below. Too little sample means the sonic energy sweet spot is too high and therefore does not interact with the sample. The addition of another 0.1 ml however means this sweet spot is reach and is shown below in 5b. This shows that the use of the sonication efficiency kit is vital in being able to determine the parameters for the research before it is actually carried out. This means no loss of research samples trying to ascertain these parameters.

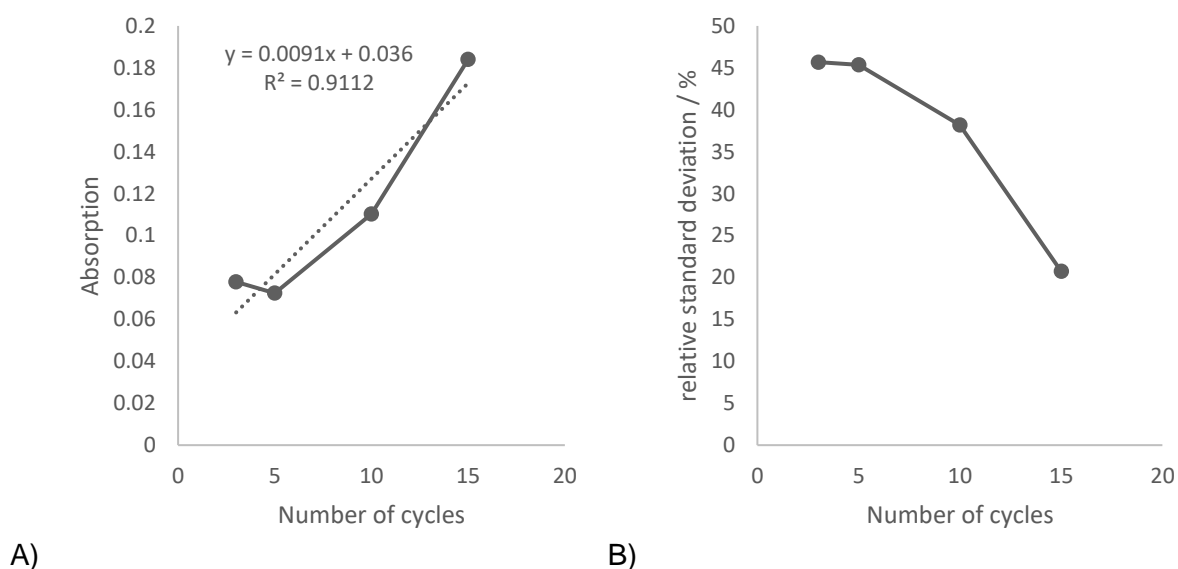


Figure 3.5: A) Average absorption for Experiment 5a settings, 1.5 ml TPX® tubes were sonicated with 0.1 ml samples in Pico, from 3 to 15 cycles with standard deviation. B) Relative standard deviation for Experiment 5a from 3 to 15 cycles.

Experiment 5b used the same tube as before with 0.2 ml sample. An increase in sample volume was expected to decrease further the absorption but instead the complete opposite was seen in Figure 3.6. The increase in volume saw a large significant increase in absorption and with a perfect r value of 1. There were significant differences across the board apart from between 3 and 5 cycles where no significant difference was seen. This large increase, as mentioned before, is because the sample is now in the sonicators sweet spot and therefore is getting the maximum sonication and therefore maximum absorption.

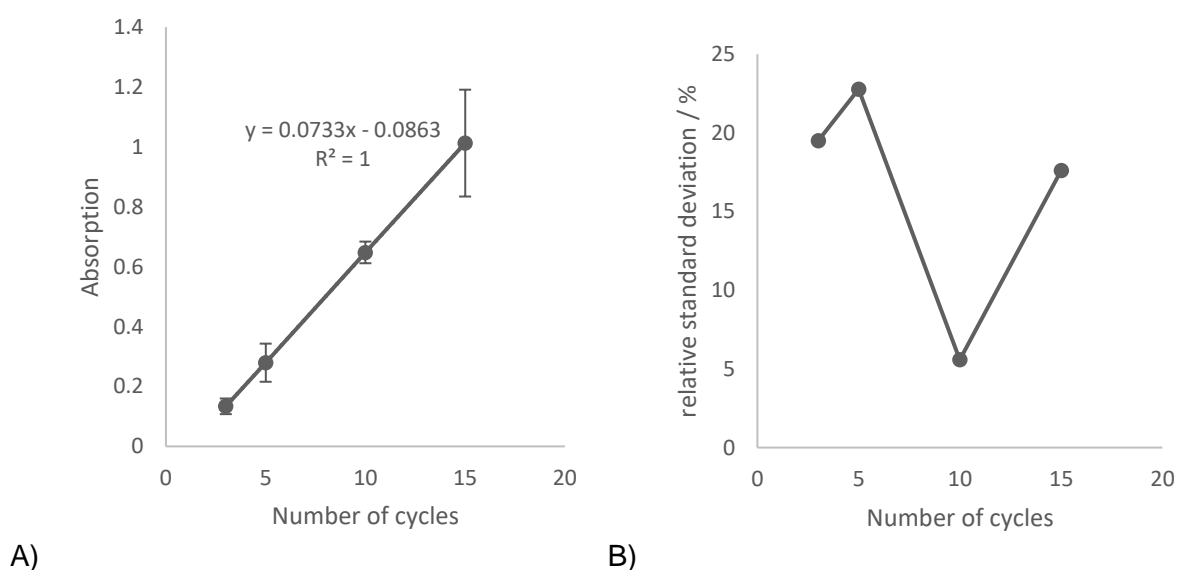


Figure 3.6: A) Average absorption for Experiment 5b settings, 1.5 ml TPX® tubes were sonicated with 0.2 ml samples in Pico, from 3 to 15 cycles with standard deviation. B) Relative standard deviation for Experiment 5b from 3 to 15 cycles.

Experiment 5c used the same tubes as before with 0.3 ml sample and compared directly with the tubes with caps in experiment 4. Here a similar pattern emerges as before with a good increase and an r value of 0.988 as shown below in Figure 3.7. The RSD were relatively good at around 30 % although 10 cycles gave a really good reading of below 6 %. The p values show no significant difference between 3 and 5 or between 10 and 15 cycles but the rest were significant increases and the overall data showed a decrease compared to the 0.2 mL samples.

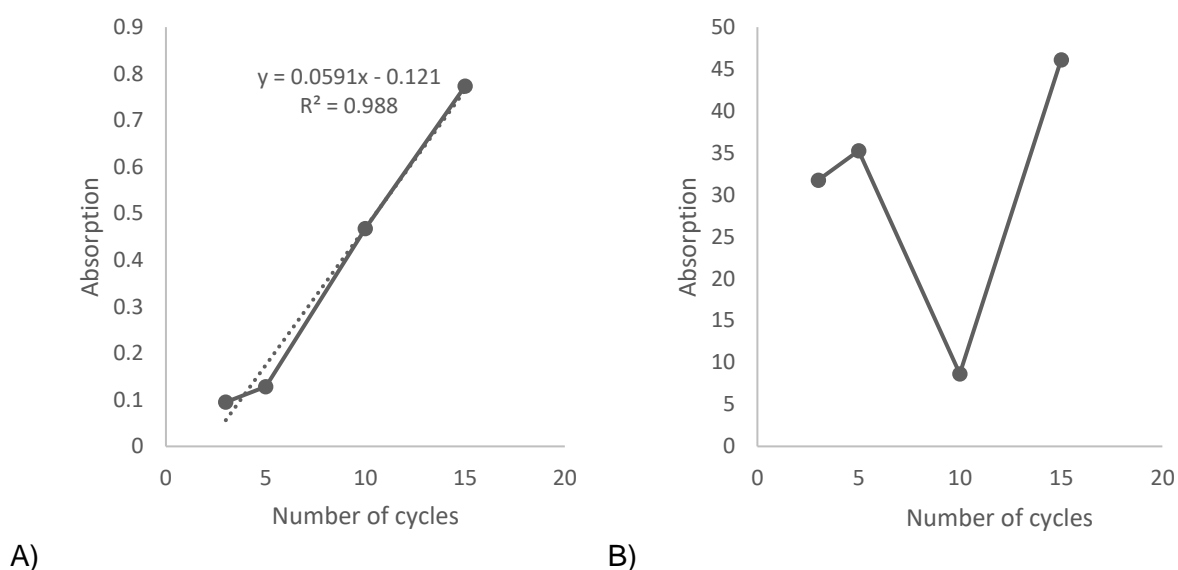


Figure 3.7: A) Average absorption for Experiment 5c settings, 1.5 ml TPX® tubes were sonicated with 0.3 ml samples in Pico, from 3 to 15 cycles with standard deviation. B) Relative standard deviation for Experiment 5c from 3 to 15 cycles.

Figure 3.8 below shows the combination of experiments 1 to 5. What these show is that as you increase volume of sample in a tube, the absorption decreases. This is true if you decrease the sample volume to tube volume ratio. However this was not true for the larger 1.5 mL tubes whereby a capped tube showed a large absorption for a 0.1 mL sample, the TPXC tube had a largest absorption for a 0.2 mL sample. This shows that the size of the cap and the effect this has on where the tube is placed in the water bath has an effect on the sonication efficiency.

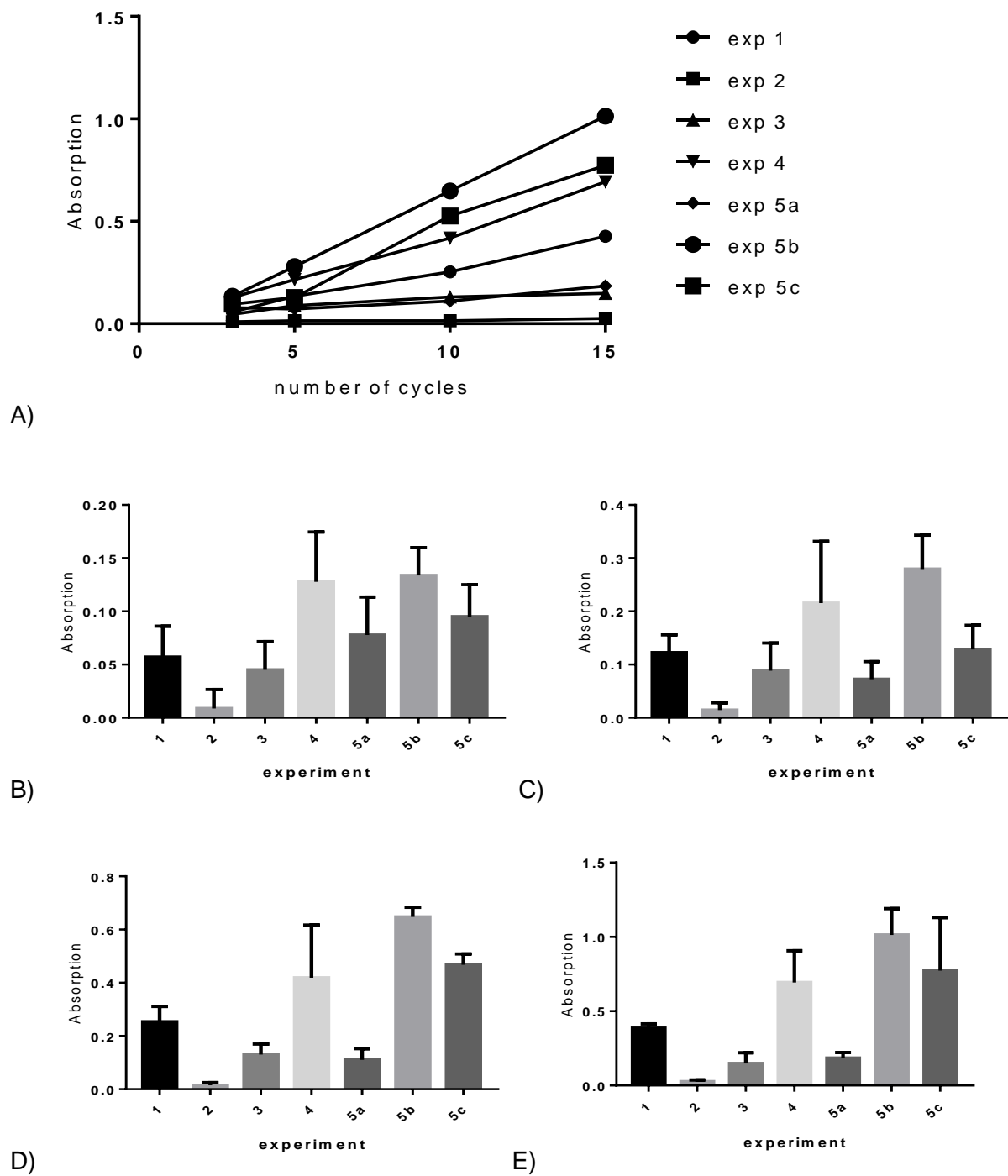


Figure 3.8: (A) Overall line plot showing absorption of the different Pico experiments absorption averages. Absorption peak heights for (B) 3, (C) 5, (D) 10 and (E) 15 cycles.

3.3.2.2 Bioruptor® Plus data

Experiment 6 used TPX® 1.5 ml tubes with 0.3 ml sample using the Bioruptor® Plus sonicator on high power showed a good absorption at the 3 cycle mark although no significant increase was seen with 5 cycles in Figure 3.9. An increase was seen up to 10 cycles but then again at 15 cycles, no significant increase was seen. The RSD were all good at below 30 % and the r value was 0.968.

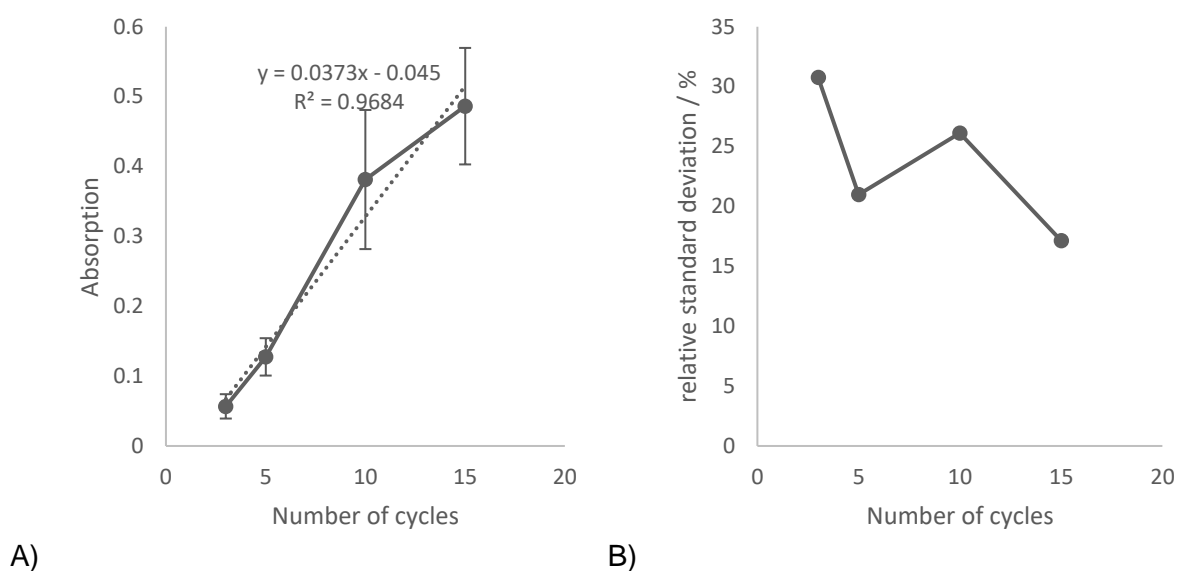


Figure 3.9: A) Average absorption for Experiment 6 settings, 1.5 ml TPX® tubes were sonicated with 0.3 ml samples at H power in Plus, from 3 to 15 cycles with standard deviation. B) Relative standard deviation for Experiment 6 from 3 to 15 cycles.

Experiment 7 used the same tubes, volume and machine as before with low power and had a similar story as shown below in Figure 3.10. No significant difference was seen between 3 and 5 cycles with significant increases for the rest of the samples. The RSD was again at or below 30 % throughout and the r value was near perfect at 0.9998. There was no significant difference between the samples of low and high power showing that the power level does not affect sonication efficacy for the type of tube and sample volume used in the experiment.

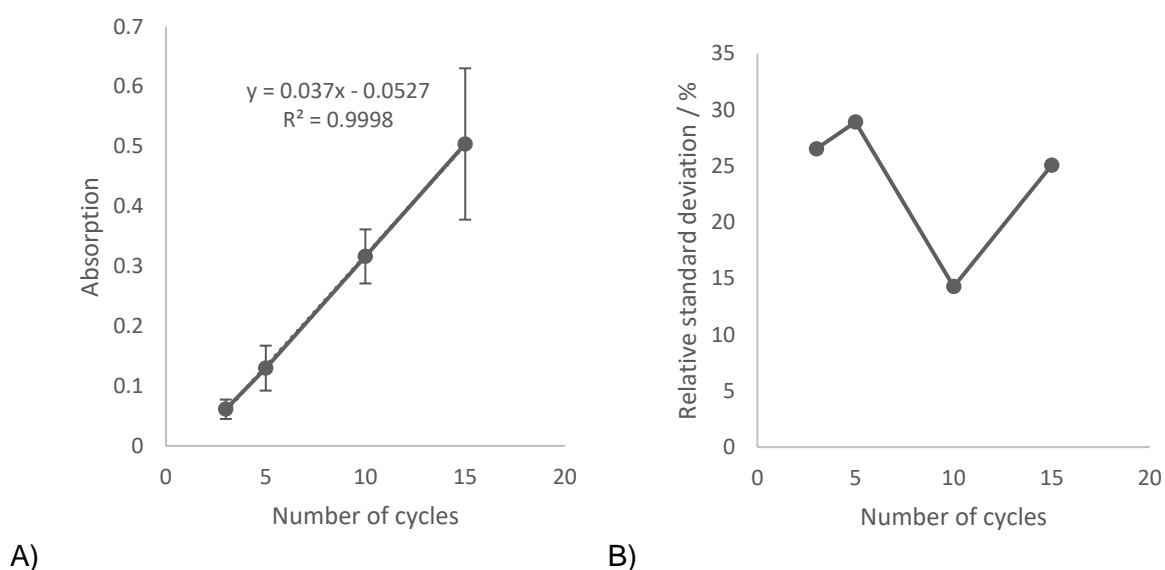


Figure 3.10: A) Average absorption for Experiment 7 settings, 1.5 ml TPX® tubes were sonicated with 0.3 ml samples at L power in Plus, from 3 to 15 cycles with standard deviation. B) Relative standard deviation for Experiment 7 from 3 to 15 cycles.

Experiment 8 used the 1.5 mL BioSigma tubes with a 0.3 ml sample at high power. This was expected to form poorly compared to the TPX® tubes but the initial signs were promising. There was again no significant difference between the 3 and 5 or 10 and 15 cycles but significant difference between the others as shown below in Figure 3.11. The RSD was again at or below 30 % and the r value not bad at 0.9833. However by the time the number of cycles increased to 15, the BioSigma tubes had a reduced sonication efficacy compared to the TPX® tubes.

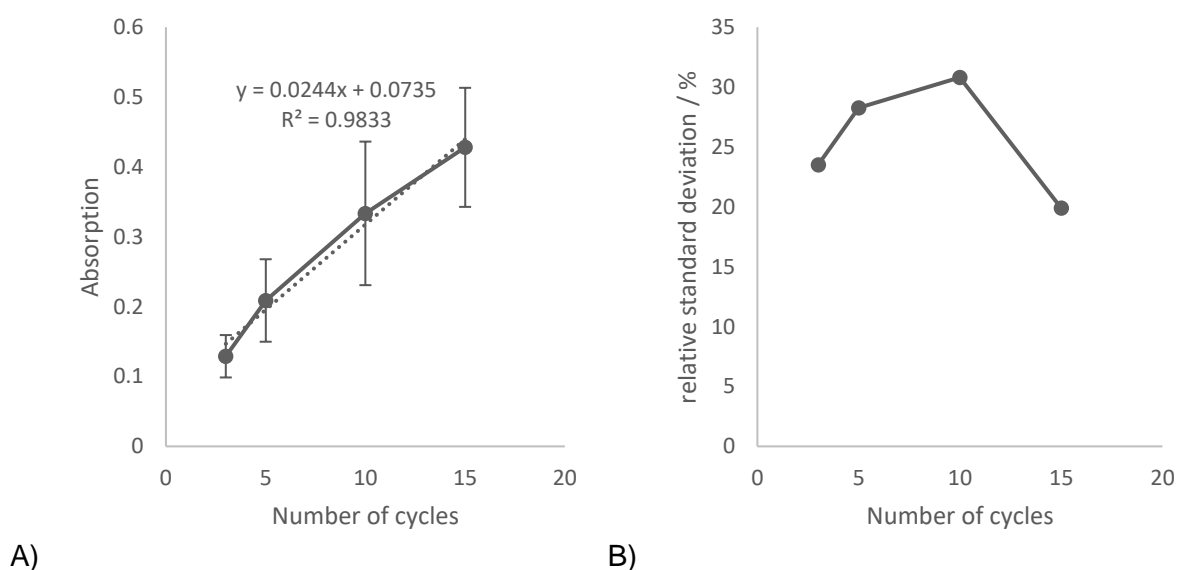


Figure 3.11: A) Average absorption for Experiment 8 settings, 1.5 ml BioSigma tubes were sonicated with 0.3 ml samples at H power in Plus, from 3 to 15 cycles with standard deviation. B) Relative standard deviation for Experiment 8 from 3 to 15 cycles.

Experiment 9 used the same tubes, volume and machine as before with low power. Again there was no significant difference between 3 and 5 cycles with significant differences after this between 5 and 15 cycles as shown below in Figure 3.12. The RSD was again around or below 30 % and the r value was poor at 0.953. There was no significant difference between the low and high power samples again so for this tube at this volume, the power level does not significantly affect sonication efficacy.

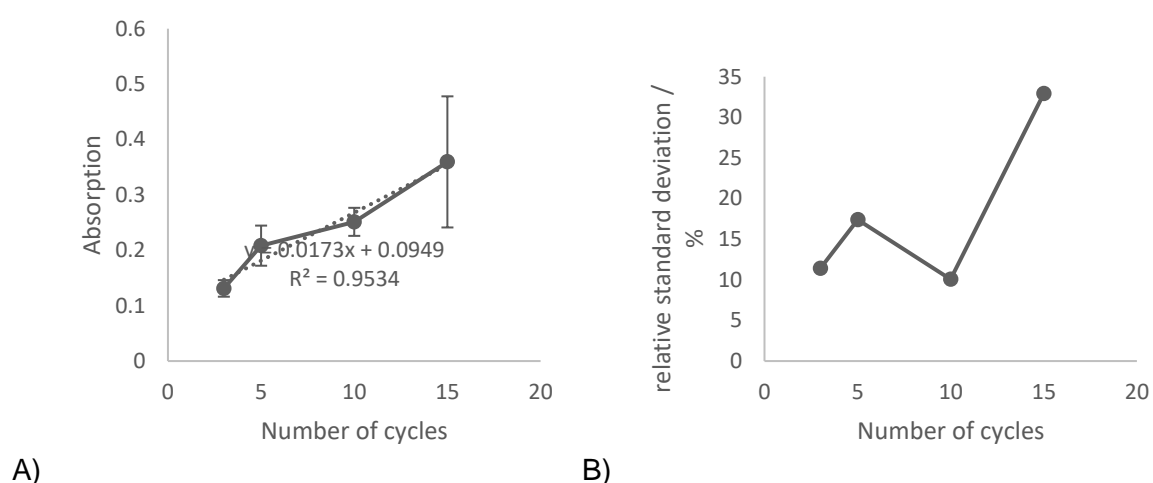


Figure 3.12: A) Average absorption for Experiment 9 settings, 1.5 ml BioSigma tubes were sonicated with 0.3 ml samples at L power in Plus, from 3 to 15 cycles with standard deviation. B) Relative standard deviation for Experiment 9 from 3 to 15 cycles.

Experiment 10 used a TPX® 1.5 mL tube with a Bioruptor® Plus at high power with a 0.1 ml sample. Reducing the volume here caused the same problem as before, with a sharp drop in the efficiency and overall no significant differences between any of the number of cycles as shown below in Figure 3.13. The r value was poor and the RSDs were not good, especially for the later cycles. This showed that both Bioruptor® systems have a sweet spot where as the volume of sample is reduced too much, the sonication energy cannot reach it as well and therefore the I_2 formation is reduced.

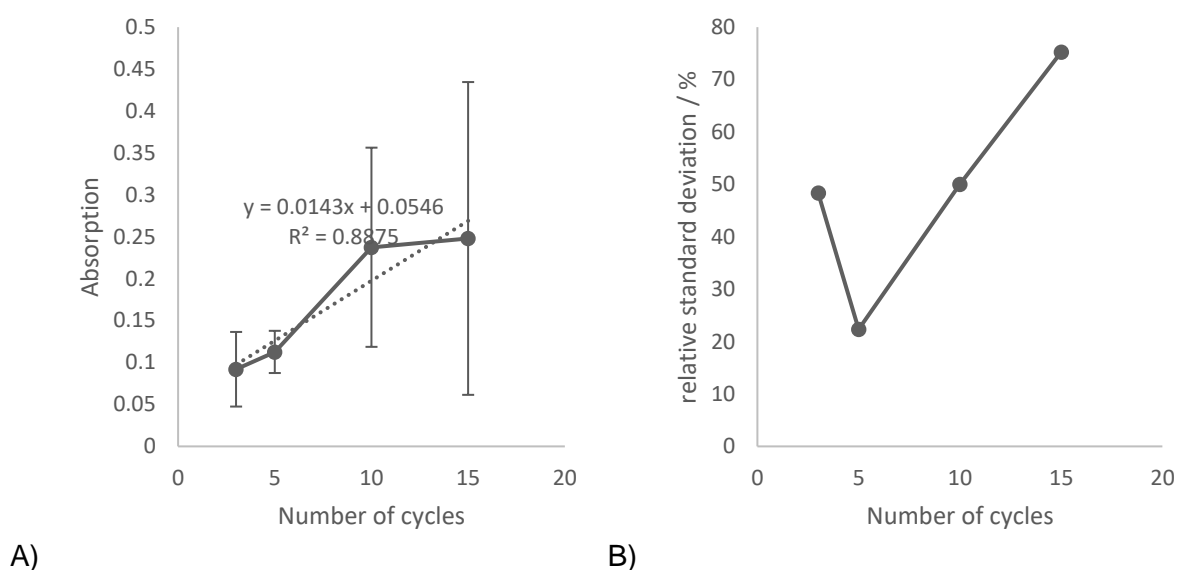


Figure 3.13: A) Average absorption for Experiment 10 settings, 1.5 ml TPX® tubes were sonicated with 0.1 ml samples at H power in Plus, from 3 to 15 cycles with standard deviation. B) Relative standard deviation for Experiment 10 from 3 to 15 cycles.

Experiment 11 used the same parameters as before with a 0.2 ml sample. An increase in volume this time appeared to show an increase in absorption although this was not significant compared to the 0.1 ml sample and not as large as the 0.3 mL sample as shown below in Figure 3.14. Cycle on cycle, the only significant increase was between 10 and 15 cycles. The r value was good at 0.998 and the RSD was good at around or below 30 %.

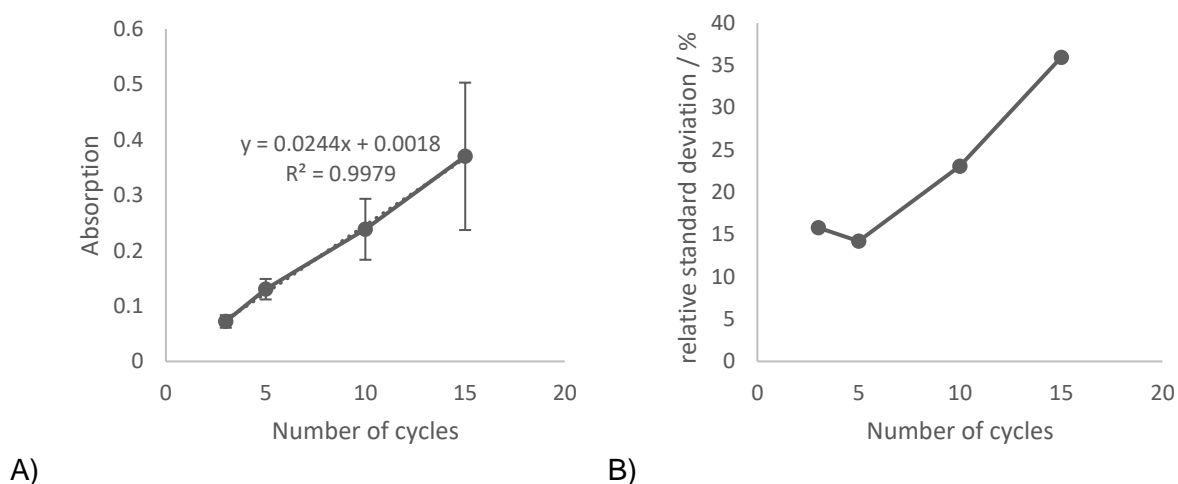


Figure 3.14: A) Average absorption for Experiment 11 settings, 1.5 ml TPX® tubes were sonicated with 0.2 ml samples at H power in Plus, from 3 to 15 cycles with standard deviation. B) Relative standard deviation for Experiment 11 from 3 to 15 cycles.

Experiment 12 used BioSigma 1.5 ml tubes with a 0.1 ml sample on high power. The use of the different tube did not see a significant increase or decrease in the absorption seen as seen in Figure 3.15. The small sample size did give an r value of 0.99 although the RSD were higher than before. This showed that it was the volume and not the plastic composition of the tube in this case which affects sonication efficacy.

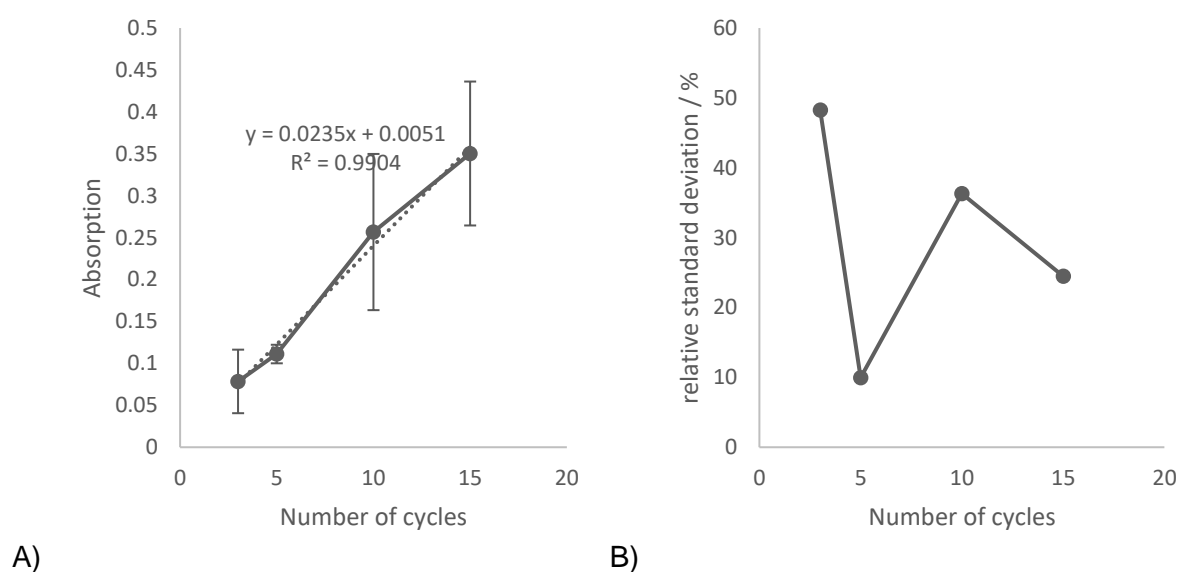


Figure 3.17: A) Average absorption for Experiment 12 settings, 1.5 ml BioSigma tubes were sonicated with 0.1 ml samples at H power in Plus, from 3 to 15 cycles with standard deviation. B) Relative standard deviation for Experiment 12 from 3 to 15 cycles.

Experiment 13 used the same criteria as before with a 0.2 ml sample. Only a significant cycle on cycle difference was seen between 5 and 10 cycles as shown in Figure 3.16. These results were significantly smaller than the 0.1 or 0.3 mL sample which was not expected. The r value was good at 0.998 and the RSD were at or below 40 %.

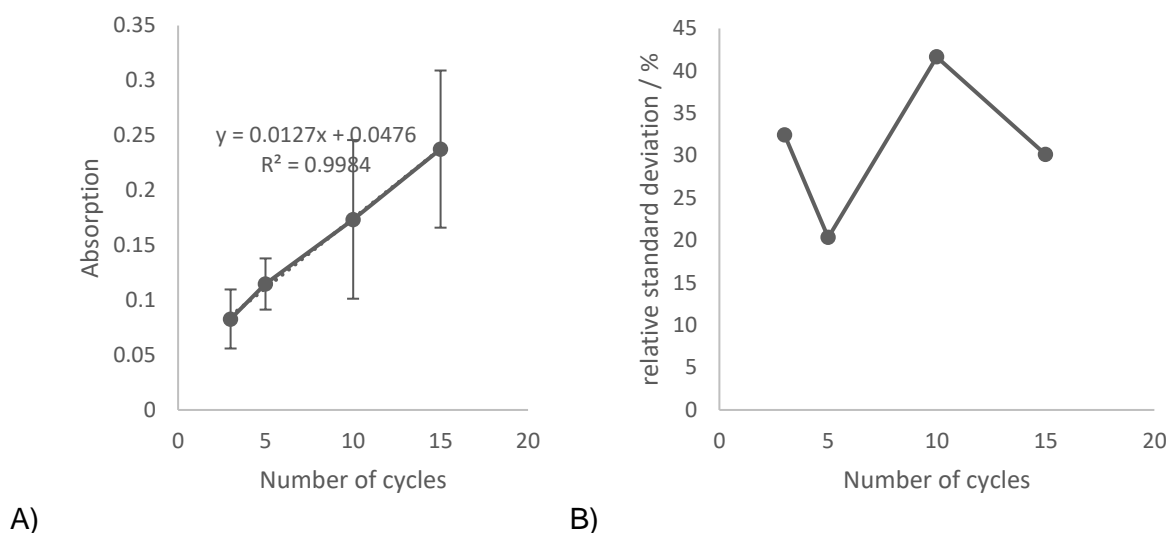
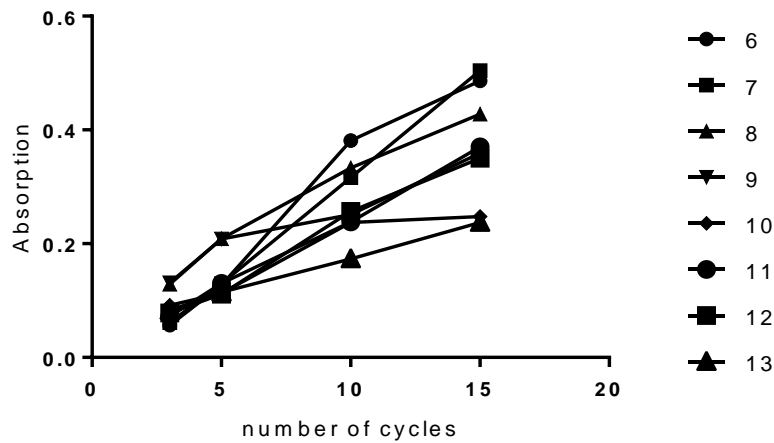
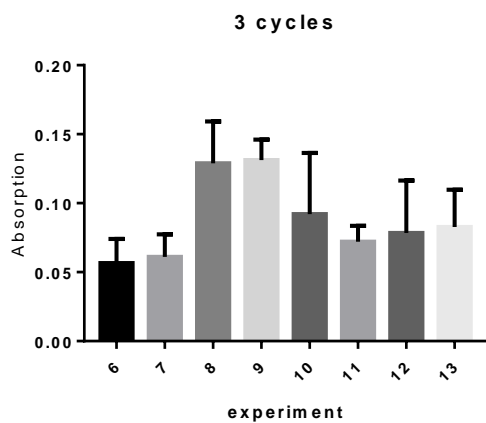


Figure 3.16: A) Average absorption for Experiment 13 settings, 1.5 ml BioSigma tubes were sonicated with 0.2 ml samples at H power in Plus, from 3 to 15 cycles with standard deviation. B) Relative standard deviation for Experiment 13 from 3 to 15 cycles.

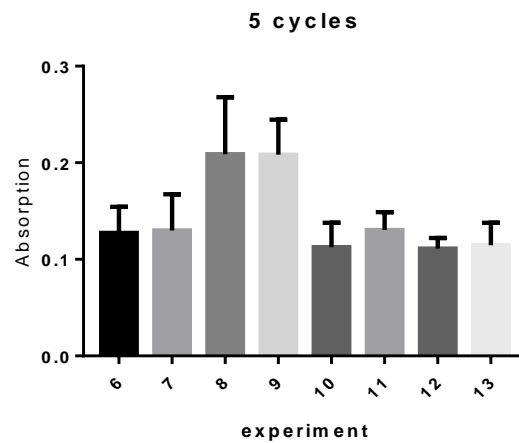
Figure 3.17 below shows the combined results for experiments 6 to 13. What these show firstly is that there is no significant difference between the absorption seen for low and for high power. However the BioSigma tubes used for experiments 8 and 9 showed an increased absorption compared to TPX® tubes. What experiments 10 to 13 showed was that as you decreased the volume from 0.3 mL to 0.2 mL you had an increase in absorption and a further increase was seen when reducing the volume from 0.2 mL to 0.1 mL.



A)

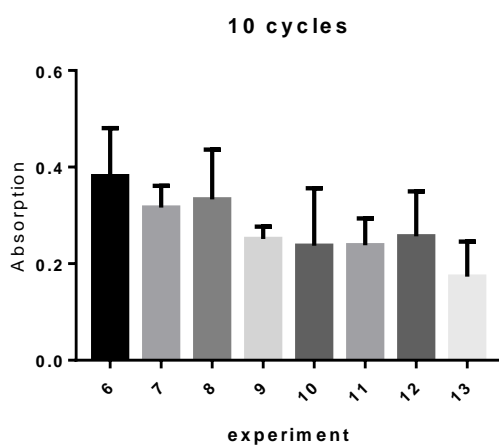


B)



C)

D)



E)

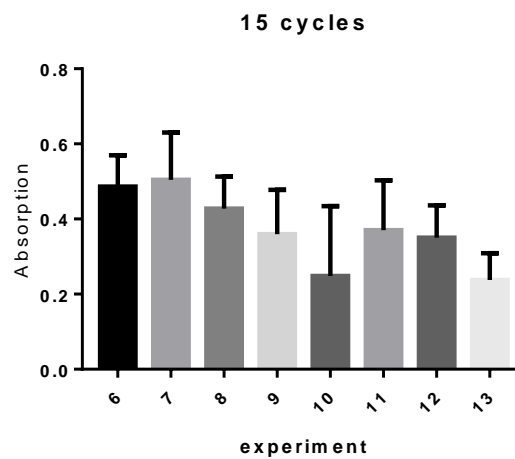


Figure 3.17: (A) Overall line plot showing absorption of the experiments 10 to 13 absorption averages. Absorption peak heights for (B) 3, (C) 5, (D) 10 and (E) 15 cycles.

Experiment 14 used BioSigma 1.5 ml tubes with a 0.1 ml sample at high power at 10 °C. The increase in temperature saw a decrease in the absorption compared to 4 °C, although this was not significant as shown below in Figure 3.18. There was a tailing off at the upper end of the cycles, which saw a poor r value of 0.86 and RSD values ranging between 15 and 50 %.

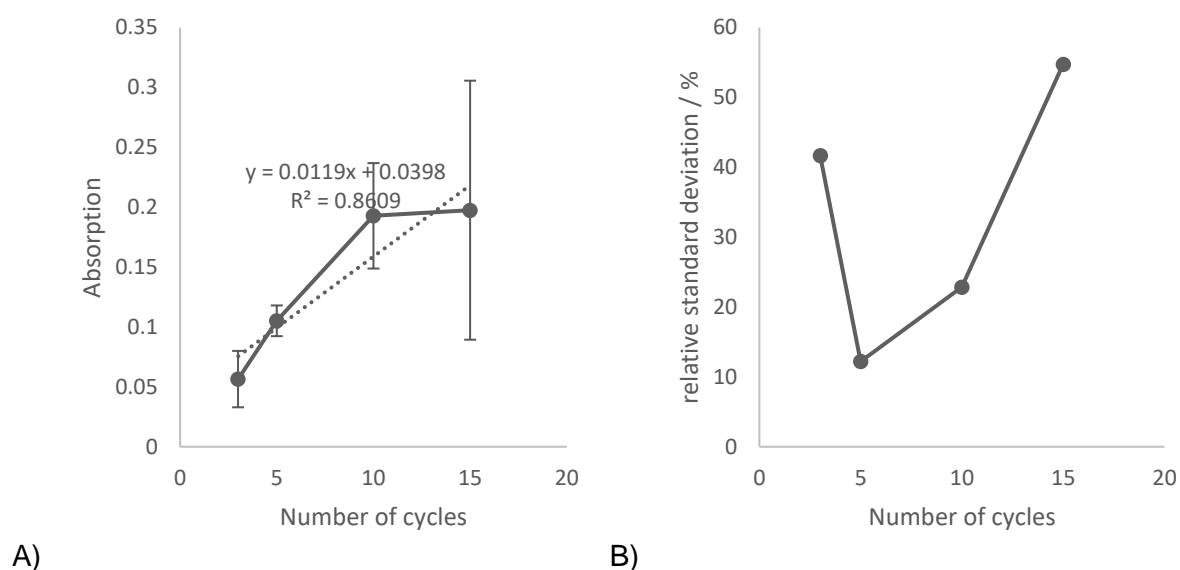


Figure 3.18: A) Average absorption for Experiment 14 settings, 1.5 ml BioSigma tubes were sonicated with 0.1 ml samples at H power at 10 °C in Plus, from 3 to 15 cycles with standard deviation. B) Relative standard deviation for Experiment 14 from 3 to 15 cycles.

Experiment 15 used the same parameters as above with 0.2 ml sample as shown below in Figure 3.19. The increase in volume this time appeared to have a negative impact on the absorption with a significantly reduced absorption compared to the 0.1 ml 4 °C sample, although not compared to the equivalent 0.2 mL 4 °C sample. The r value was good though at 0.995 although the RSD was relatively high at between 40 and 60 %.

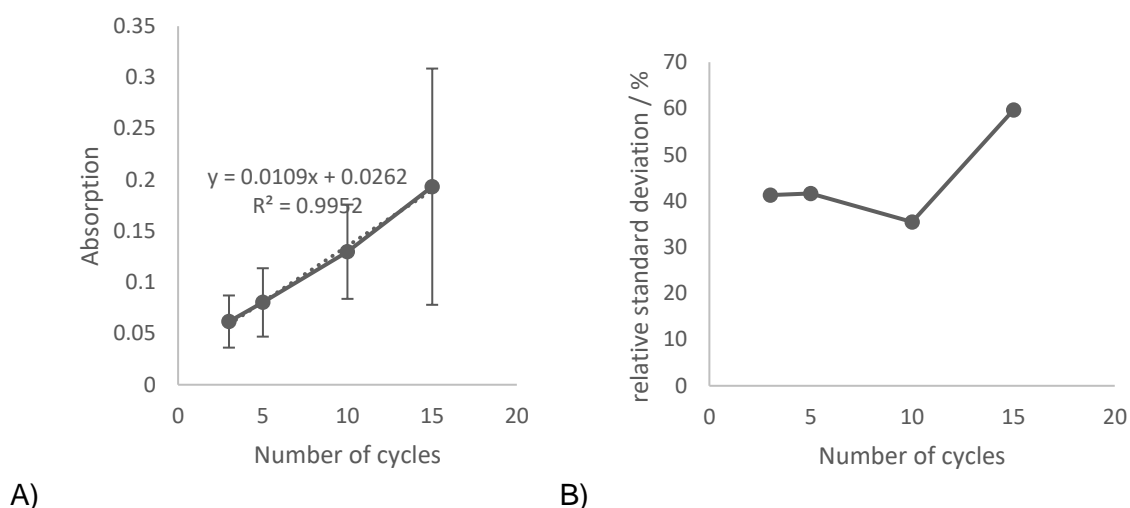


Figure 3.19: A) Average absorption for Experiment 15 settings, 1.5 ml BioSigma tubes were sonicated with 0.2 ml samples at H power at 10 °C in Plus, from 3 to 15 cycles with standard deviation. B) Relative standard deviation for Experiment 15 from 3 to 15 cycles.

Experiment 16 used the same parameters as above with a 0.1 ml sample at 20 °C as shown below in Figure 3.20. The further increase in temperature saw a further decrease in absorption for the 0.1 mL sample. There was no significant difference due to the high RSD and low absorption across the board and the r value being 0.04.

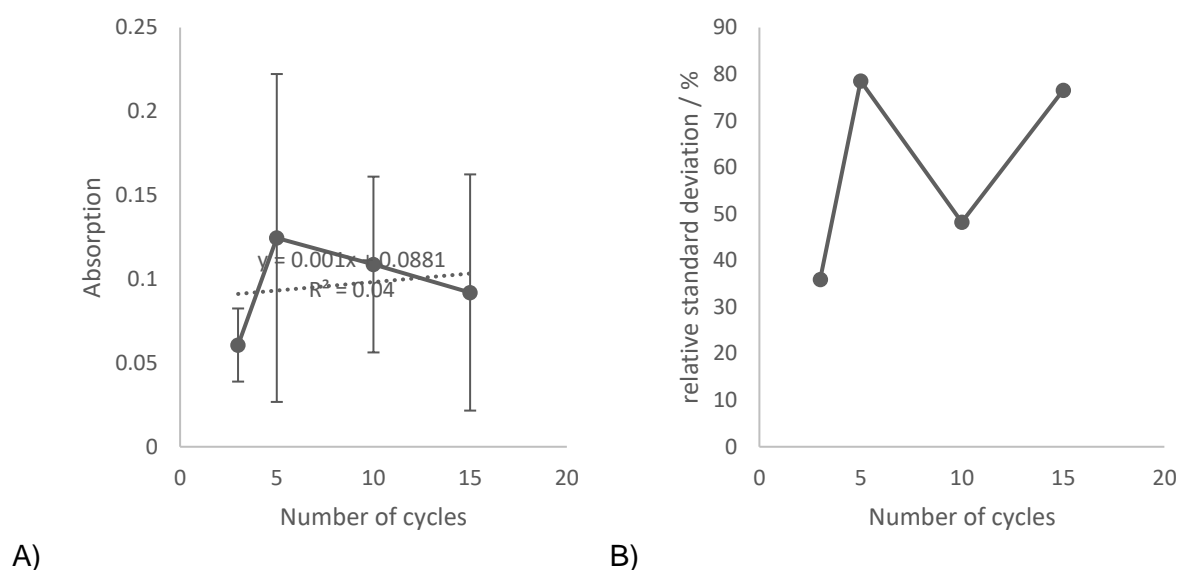


Figure 3.20: A) Average absorption for Experiment 16 settings, 1.5 ml BioSigma tubes were sonicated with 0.1 ml samples at H power at 20 °C in Plus, from 3 to 15 cycles with standard deviation. B) Relative standard deviation for Experiment 16 from 3 to 15 cycles.

Experiment 17 used the same parameters as before with a 0.2 ml sample as shown below in Figure 3.21. Some significant differences were seen between the 5 and 10 cycle runs, although there was again a saturation of the absorption after this as no increase was seen at 15 cycles. The r value was poor again at 0.838 and a steady increase up to above 60 % was seen in the RSD.

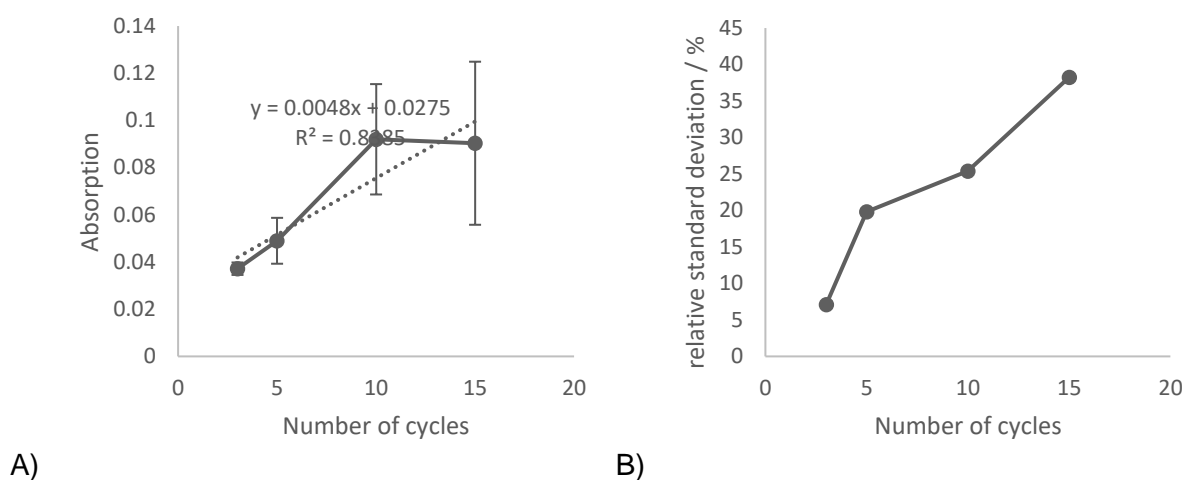


Figure 3.21: A) Average absorption for Experiment 17 settings, 1.5 ml BioSigma tubes were sonicated with 0.2 ml samples at H power at 20 °C in Plus, from 3 to 15 cycles with standard deviation. B) Relative standard deviation for Experiment 17 from 3 to 15 cycles.

Figure 3.22 shows that as you increase temperature of the water bath, absorption is shown to decrease. This shows that sonication power level decreases as the water bath temperature increases.

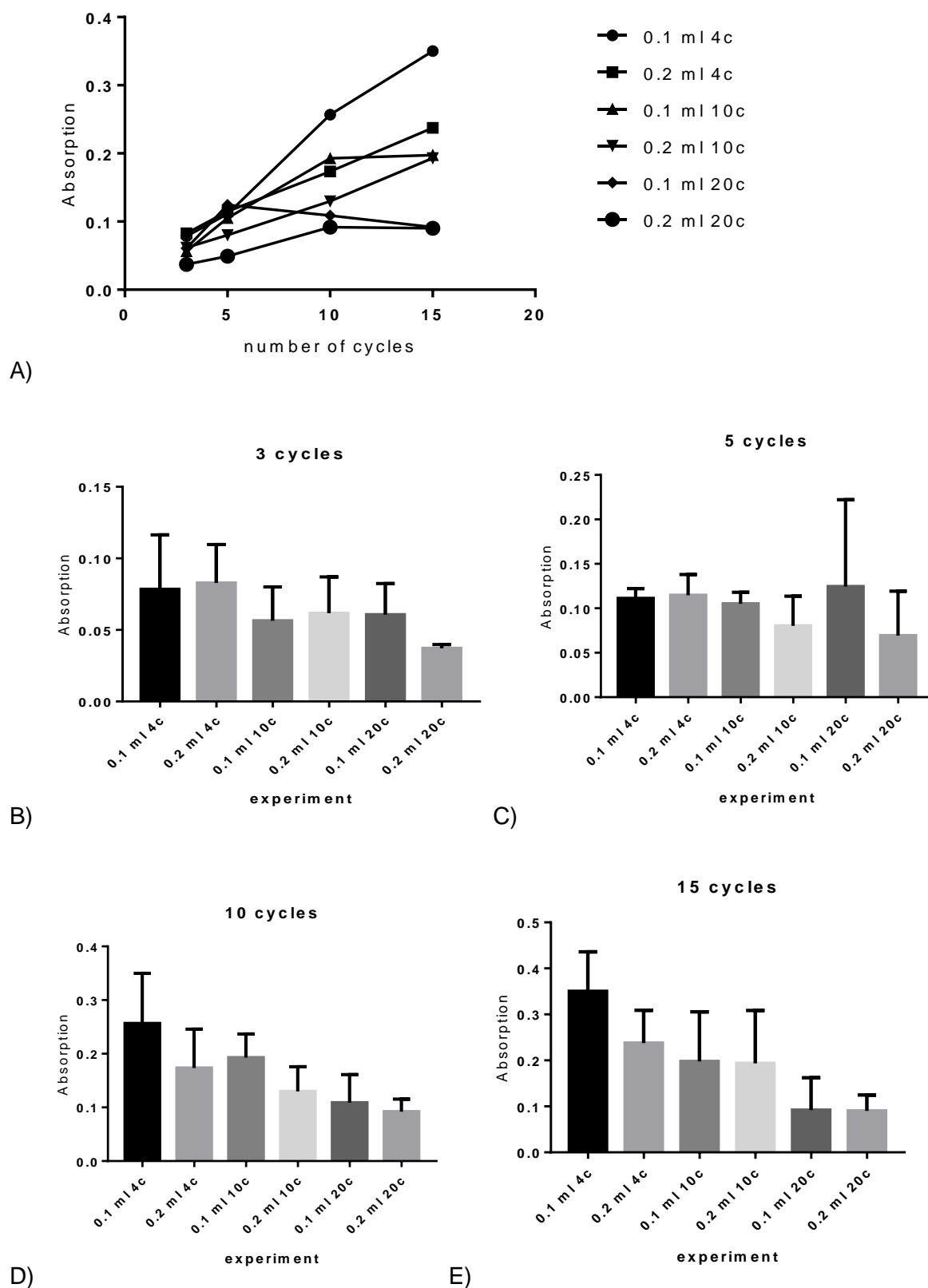


Figure 3.22: (A) Overall line plot showing absorption of the experiments 14 to 17 absorption averages. Absorption peak heights for (B) 3, (C) 5, (D) 10 and (E) 15 cycles.

3.3.2.3 Discussion

The overall data compared to one another showed some important results. Firstly, the top experiments we had in terms of absorption were those with the 1.5 ml tubes and with the best volumes. The samples also all showed an increase when sonicated for up to 15 cycles compared to the absorption seen with 3 cycles.

Some significant differences were seen however using the Bioruptor® Pico bath sonicator system. Between experiments 1 and 2, a significant difference was seen from 3 to 15 cycles and therefore a significant increase in absorption when using 0.1 ml compared to 0.2 ml. Between experiments 1 and 3, no significant difference was seen until 10 cycles and therefore no significant difference between using the 0.65 ml or the 0.5 ml tubes until a larger number of cycles is used for the same volume. Between experiments 4 and 5, no significant difference across the board was seen between 0.3 ml sample in tubes with caps and TPX® tubes without caps which shows that the position in the bath, whilst important, does not exert enough of an effect to be significant. However volume does have a significant effect with the smallest volume showing significant difference after 5 cycles and the larger volume of 0.3 ml showing a significant difference at 10 cycles.

All the Bioruptor® Plus experiments together showed a similar pattern throughout and that the difference between low and high power and between TPX® and BioSigma tubes were there. At 3 cycles, no significant difference was seen between the low and high power samples, but significant differences were seen across the board between TPX® and BioSigma tubes, although not in the way that was expected. It was expected that the TPX® tubes would perform better, but this data shows that at 3 cycles, it is the BioSigma tubes that perform the best. At 5 cycles, the exact same pattern is seen, except the significant difference had dropped. At 10 cycles, almost no differences are seen whatsoever with the only one being between TPX® high power and BioSigma low power. This is the first time however a

significant difference is seen whereby the TPX® tube significantly better performs compared to the BioSigma tubes. At 15 cycles however, no significant differences are seen whatsoever across the board. So at 15 cycles, the tube type and power level makes no significant difference to the absorption value seen.

For the second set of Bioruptor® Plus bath sonicator results, no significant differences were found across the board and so with this set up, the use of a different tube or the use of a smaller volume did not make a difference. At 3 cycles, the only significant difference seen was between 4 °C and 20 °C for 0.2 mL sample. At 5 cycles, no significant differences. At 10 cycles, some significant differences were found between the 0.1 mL 4 °C sample and the 0.1 mL 20 °C sample and the 0.2 mL 10 and 20 °C samples. At 15 cycles, some significant differences were found between 0.1 mL 4 °C sample and the 0.1 and 0.2 mL 10 and 20 °C samples.

3.3.3 Investigating more cost effective materials for DNA extraction using the Bioruptor® Pico

DNA extraction is useful for a number of different areas and is done through a number of ways. These include organic multistep liquid chemical process, inorganic silica methods, solid phase extraction methods or differential extraction. Diagenode developed a silica based method of DNA extraction however this is not cost effective. Therefore the use of a Bioruptor® to not necessitate the use of traditional methods using toxic organic solvents is investigated as well as the use of DiaPure columns and buffers to try and keep the production in house and therefore cheaper.

3.3.3.1 Assay 1

Assay 1 data is shown below in Figure 3.23. These show the difference between using a DiaFilter column or not. A DiaFilter column is simply a column that fits into the 1.5 mL tube provided and removes larger chunks of DNA and paraffin that were not removed during the previous processes, giving a purer sample of DNA extracted. This could be seen as an important step to aid in the removal of the paraffin after the use of the Bioruptor® Pico but could be seen as a disadvantage whereby it could remove DNA as well. This data showed just that with a reduced concentration of DNA for those samples that used the filter column. The samples with the filter gave a concentration of 20.15 ng/ μ L and the samples without the filter column gave a concentration of 38.19 ng/ μ L, but with a p value of 0.19, this was not statistically significant. However in its favour, it did not require any extra time on the centrifuge whereby those samples that didn't use the filter column did require at times an extra minute or two on the centrifuge. This could be due to the paraffin blocking the filter increasing the time needed to filter the liquid through the filter.

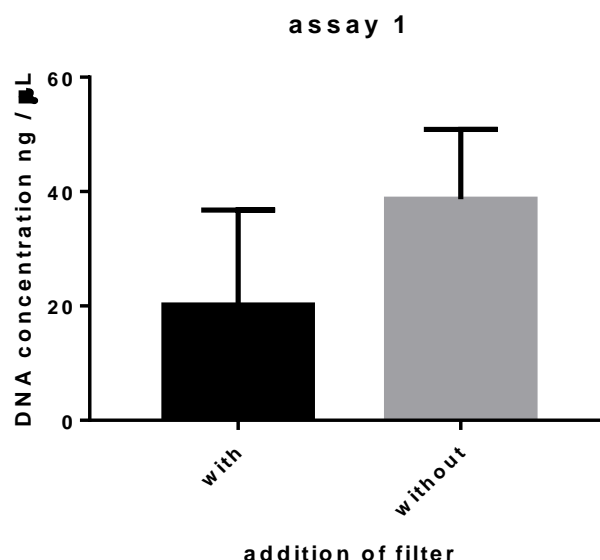


Figure 3.23: Assay 1 results showing the difference in DNA concentration achieved with or without a filter stage.

3.3.3.2 Assay 2

Assay 2 looked into the use of three different buffers for the DNA extraction numbered 1 to 3 with results shown below in Figure 3.24. Buffer number 1 is the buffer normally used with the kit and showed good DNA extraction and buffer number 2 showed similar results. Buffer number 3 showed a much greater DNA extraction although not significant due to the high standard deviations.

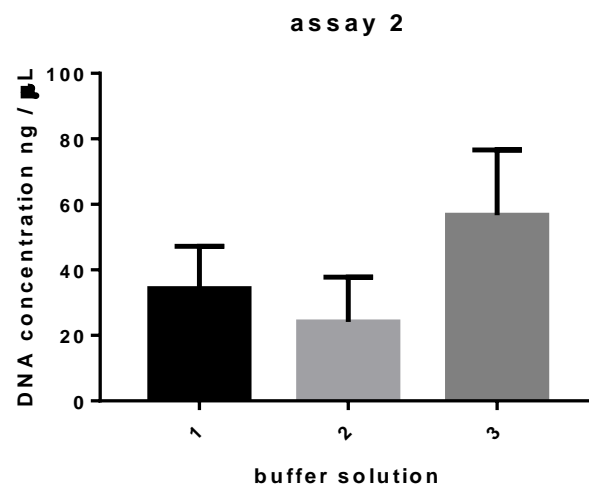


Figure 3.24: Assay results showing DNA concentration results for each of the 3 chosen buffers.

3.3.3.3 Assay 3

Assay 3 was used to compare extraction conditions with changes to how long and at what temperature the samples are shaken after being sonicated. The three conditions showed that temperature was not an important factor as even though the first conditions had the highest temperature, it also had the lowest DNA extraction concentration as shown below in Figure 3.25. What the results did show was that the longer the samples were left to shake, the more DNA was extracted with an increased concentration from 15 minutes to 4 hours and from 4 hours to overnight.

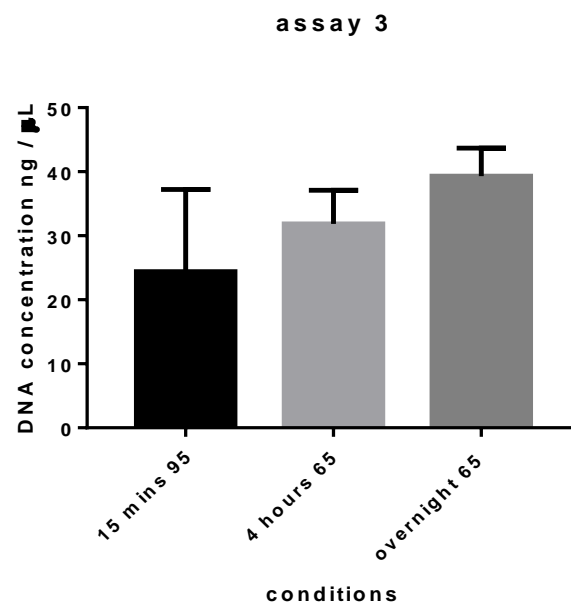


Figure 3.25: Assay results showing DNA concentration for three different conditions.

3.4 Conclusion

Using the Bioruptor® Plus bath sonication system, it was also shown that for lipophilic drugs, methods 2 and 3 whereby the lipid film hydration part of the methodology was bypassed showed a much better drug loading ability. However, the amount of drug incorporated would not be concentrated enough for a clinically relevant dosage for any of the three drugs used in this study. Further work would have to be carried out to see if increasing the concentration up to a clinically relevant dosage could be possible without having to increase the volume of the formulation to something that would be too large for a child to take. This is due not only to the increase in drug concentration being required, but also the subsequent increase in lipid concentration which could affect the ability of the Bioruptor® Plus to form the smaller liposomes and load the drug into the lipid bilayer.

It was also shown that certain drugs such as propofol could have unexpected side effects during the process causing them to be unusable for this particular method such as destroying the plastic tubes the samples are sonicated in. Albendazole too was shown not to be able to be used for this process due to its ability to aggregate and come out of solution as soon as the sonication process was complete.

Characterisation of the ultrasonic bath is very important for sonochemical reactions. The conditions of maximum cavitation intensity can be different for each ultrasonic bath and, due to this behaviour, it is very difficult to compare the results obtained with different ultrasonic baths even using the same conditions. In analytical chemistry, when reproducible and accurate results are required, the experimental conditions (such as water volume, temperature, detergent concentration, vertical and horizontal positions, number of tubes, sonication time) must be studied, established and rigorously reproduced for each experiment. An innovative way to study these conditions was employed in the present work by spectrophotometrically following the I₂ formation from free radical of iodine (I·) obtained after sonication of a KI solution.

In conclusion, for the 0.65 ml tubes, clearly the 0.1 ml sample is the better volume giving a significantly better result compared to the 0.2 mL sample and it performs better than the 0.5 ml tube. For the 1.5 ml tubes, there was no significant difference between the tubes with caps and the TPX® tubes. A decrease in volume to 0.1 ml saw a drop in efficiency with the 1.5 ml TPX® tubes under a variety of conditions and a similar pattern was seen with the BioSigma tubes. No significant difference was seen between the low and high power samples. A decrease in temperature saw a decrease in efficiency of the sonochemical reaction. High relative standard deviations means repeatability is the main issue. Also some results did not go the same as previous DNA results and therefore need to be investigated further.

What the DNA extraction results show is that the addition of a filter does reduce sample prep time but does also reduce DNA extraction concentration. The choice of buffer was also shown to have an effect on DNA concentration as did the conditions in which the samples were left to shake and extract. However from these results, none of these differences were statistically significant and so more work will need to be done to see whether these are indeed significant differences.

4. Water dispersion of carbon nanotubes

4.1 Aims and Objectives

Carbon nanotubes are inherently insoluble in water due to high Van Der Waals forces. The carbon nanotube surface is made up of benzene rings and need some kind of modification to increase their solubility. This can be through either covalent or non – covalent functionalisation. This study focussed on non – covalent functionalisation which occurs through mixing the carbon nanotubes with a surfactant such as SDS, SDBS or a phospholipid in water. Sonication is used to disrupt the surfactant and carbon nanotube molecules which allows for them to interact and for the surfactant to non – covalently bond with the carbon nanotube surface.

The aim of this work was to create protocols for the Bioruptor® systems to disperse carbon nanotubes. The objectives were to first of all create protocols for dispersing carbon nanotubes using SDS and SDBS using the current Bioruptor® systems. The second objective was to investigate the use of a non – toxic surfactant, MPC, to disperse the carbon nanotubes and compare directly to SDS and SDBS.

4.2 Materials and methods

4.2.1 Dispersion of carbon nanotubes using the Bioruptor® Plus

CoMoCat single walled carbon nanotubes, SDBS and SDS were purchased from Sigma Aldrich (Sigma Aldrich, Dorset, UK) (Nish et al., 2007). These were dispersed in deionised water at initial concentrations of 0.1 % SDS or SDBS and 0.01 % carbon nanotubes (Yang et al., 2013). 10 mL of dispersion was placed into a 50 mL Nalgene™ Polycarbonate tube and a metallic bar was placed inside to aid in the dispersion process by reflecting sound waves to

produce a better dispersion efficiency. Sonication was undertaken using the Bioruptor® Plus (Diagenode, Liège, Belgium) at power level L which equates to 130 W and at a temperature of range between 5 and 40 °C. This was kept constant through the use of a temperature regulator. Sonication took place over 60 cycles of 60 seconds on and 15 seconds off. Once sonication was complete, the dispersion was centrifuged for 150 minutes at 40, 000 G at 17 °C. The supernatant was then removed from the samples and analysed using UV – Vis spectroscopy and PL.

4.2.1.1 Temperature studies

Carbon nanotubes were made as described previously at 5, 13, 20, 30 and 40 °C. The samples were then analysed using UV – Vis spectroscopy and PL.

4.2.1.2 Cycles study

Carbon nanotubes were made as described previously using a number of different cycle settings detailed below in Table 4.1. The samples were then analysed using UV – Vis.

Table 4.1: Bioruptor® Plus bath sonicator system cycle settings used for this study keeping the total time as similar as possible.

Time on /seconds	Time off / seconds	Number of cycles	Total time / minutes
60	15	60	75
50	13	75	78.75
40	10	90	75
30	8	120	76
20	5	180	75
10	5	300	75

4.2.1.3 DMPC study

Carbon nanotubes were made as described previously using 1, 2-dimyristoyl-sn-glycero-3-phosphocholine (DMPC) as the surfactant. The samples were then ran on the UV – Vis spectrometer.

4.2.1.4 Dilution study

Carbon nanotubes were made as described previously at 5, 13 and 20 °C. The samples were then diluted 1 in 2 and 1 in 10 and ran on the UV – Vis spectrometer.

4.2.1.5 Surfactant study

Surfactant choice is known to have a great effect on how efficacious the dispersion of carbon nanotubes is using the Bioruptor® bath sonication system. SDS and SDBS are both standards used within the carbon nanotube field but both are toxic to the human body and are therefore unsuitable for dispersion of carbon nanotubes for biological purposes. Other surfactants that could be used include lysophospholipids. MPC was investigated to see whether it could be used to disperse carbon nanotubes, at what concentrations and how it compares to the other surfactants. Therefore each surfactant was sonicated at concentrations ranging from 0.1 to 1 mg / mL with a constant concentration of 0.1 mg / mL of carbon nanotubes.

4.2.1.6 Carbon nanotubes stability study

Carbon nanotubes were made as described previously at two separate sonication temperatures of 13 and 40 °C dispersed in SDBS and at 13 °C with SDS and MPC. Samples were then analysed using UV – Vis spectroscopy over a period of 6 months to see if there was any change in the spectra. The samples were left on the benchtop under the same conditions to allow direct comparison between the samples.

4.2.2 Dispersion of carbon nanotubes using the probe sonicator

1 mg of carbon nanotubes were dispersed with 10 mL of distilled water and 10 mg of SDBS in a glass vial. The vial was placed on the probe sonicator (MSE Soniprep 150 plus with MSE PG100 probe (UK)) in an ice bath that was refreshed every 20 minutes. The probe was set to 5 amps and ran for either 15, 30, 60, 90 and 120 minutes. The samples were then ultra-

centrifuged as described previously and then analysed using UV – Vis spectroscopy and DLS. These were also analysed using PL.

4.2.3 Analysis of carbon nanotubes

Analysis was conducted using the UV – Vis – NIR spectrometer (Lambda 1050, Perkin Elmer, USA). The wavelength scanning range for the UV – Vis spectrometer was from 270 to 1100 nm using a plastic clear sided cuvette. The scan interval was set to 1 nm for the UV – Vis spectrometer. 3 mL of sample was placed into the cuvette and analysed after a blank of deionised water had been ran. Samples were ran in triplicate.

PL analysis of carbon nanotubes has previously been described by Lutsyk et al and Tan et al (Lutsyk et al., 2016, Tan et al., 2007). Briefly, the fluorescence emission spectra at various excitation wavelengths were recorded using a Horiba NanoLog excitation–emission spectrofluorometer equipped with a nitrogen-cooled InGaAs array detector to generate PL excitation-emission maps, with the X-axis representing the wavelength of the PL emission, λ emission (EM), and the Y-axis representing the excitation wavelength, λ excitation (EX). Entrance/exit slits of 14 nm in width were used for both the excitation and emission monochromators in the NIR PL measurements. The PL experiments in the visible range were performed using a silicon detector and 2 nm entrance/exit slits for the monochromators.

4.3 Results and discussion

4.3.1 Dispersion of carbon nanotubes with the Bioruptor® Plus

4.3.1.1 Water dispersion of carbon nanotubes using SDS as the surfactant compared to SDBS

Diagenodes Bioruptor® sonicator systems have been used in studies previously to aid in the dispersion of carbon nanotubes (Scardaci et al., 2007, Hasan et al., 2014). Scardaci et al were able to show that after 4 hours of sonication with the addition of SDBS successful dispersion was achieved. Hasan et al were able to show that after the same sonication time and using the same surfactant, double – walled carbon nanotubes (DW carbon nanotubes) were successfully dispersed. An important analysis tool is that of PL. PL comprises both fluorescence and phosphorescence processes and originates from an excitation/emission process between different electronic energy levels in the material. PL can be used to gain a variety of information such as the diameter of the carbon nanotubes, presence of small bundles, quantity of semi – conducting carbon nanotubes in the sample and their chirality (He et al., 2013b). However it has limited use for DW carbon nanotubes and cannot be used at all for MW carbon nanotubes as the nanotube – nanotube interactions cause the PL signal to be quenched (Satishkumar et al., 2007). For this work involving single walled carbon nanotubes though it is a highly useful tool.

All the results showed that the samples were too concentrated for PL analysis and therefore needed to be diluted. Figure 4.1 A shows that carbon nanotubes dispersed using SDS at 13 °C needed to be diluted by a factor of 10 and gave a strong reading for PL excitation at approximately 580 nm and emission at approximately 980 nm which corresponds to the 6,5

chirality which is the majority chirality found in the original pristine carbon nanotubes. Figure 4.1 (B) shows that carbon nanotubes dispersed using SDS at 5 °C also needed to be diluted by a factor of 10 and showed a similar dispersion of carbon nanotube chiralities. Figure 4.1 (C) shows that carbon nanotubes dispersed using SDBS at 13 °C needed a much larger dilution by a factor of 35 and showed an increased affinity for the dispersion of the 6,5 chirality compared to the others. Figure 4.1 (D) shows that carbon nanotubes dispersed using SDBS at 5 °C again needed a larger dilution factor of 20 and showed an increased affinity for dispersal of other chiralities.

The results show that by using SDBS as opposed to SDS, a much better dispersion of carbon nanotubes can be achieved which is shown by the need to increase the dilution factor of the SDBS dispersions compared to the SDS. The increase is required because SDBS at the concentrations formulated is too high for the detector to quantify. This is due to the SDBS molecule containing an extra benzene ring which allows aromatic stacking to occur between the carbon nanotubes and the SDBS (Guldi and Martín, 2010).

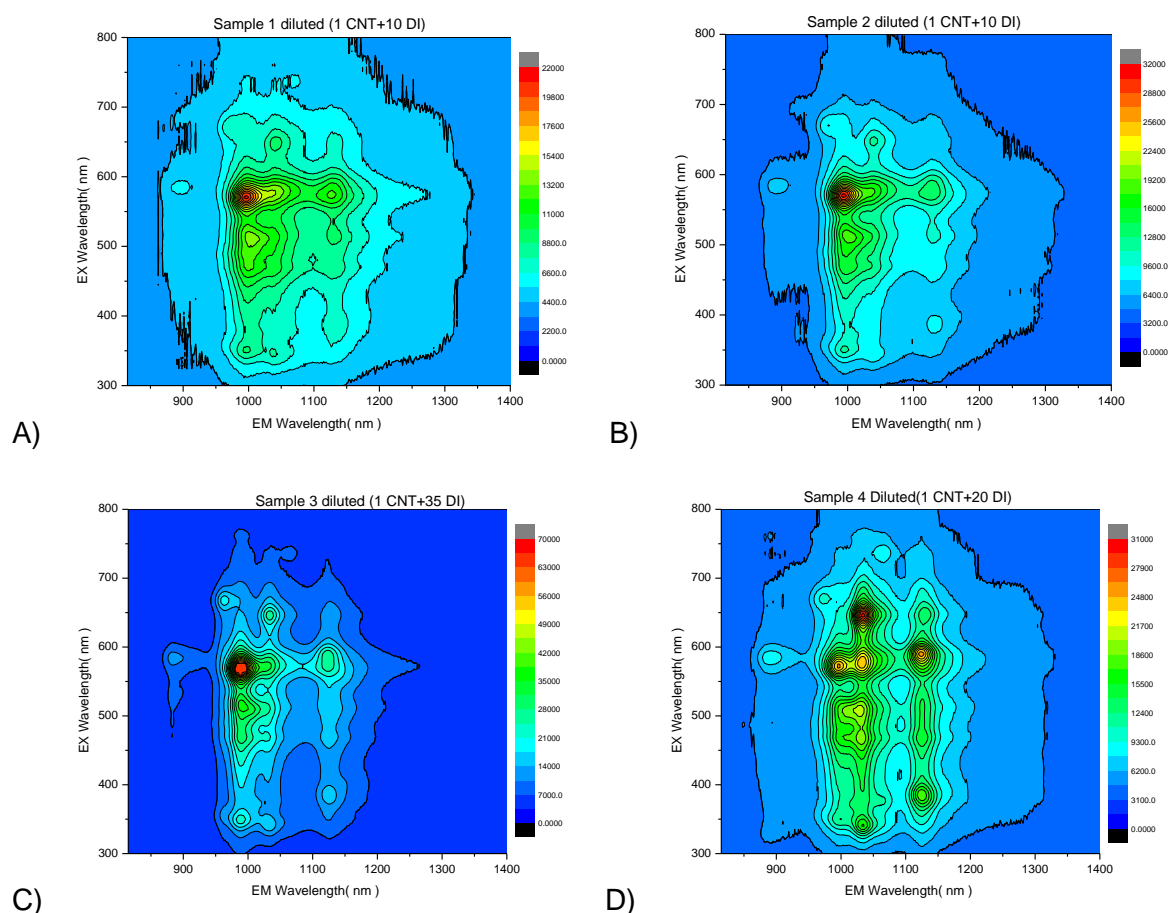


Figure 4.1 All runs were with Bioruptor® Plus, 0.01 % carbon nanotube concentration, 0.1 % surfactant concentration, 5 or 13°C water bath temperature, 2 mL sample size, Nalgene™ Polycarbonate tubes, cycle set up of 60 cycles of 60 seconds on, 15 seconds off, L power level. Ultracentrifugation for 150 minutes at 40, 000 G at 17°C. A) SDS dispersed carbon nanotubes at 13 °C. B) SDS dispersed carbon nanotubes at 5 °C. C) SDBS dispersed carbon nanotubes at 13 °C. D) SDBS dispersed carbon nanotubes at 5 °C.

4.3.1.2 Water dispersion of carbon nanotubes using SDBS as the dispersal surfactant

4.3.1.2.1 SDBS dispersed carbon nanotubes sonicated at different temperatures

Previous work by Shi et al was able to show that at temperatures at or above 30 °C, SDS has a tendency to lapse and to desorb from the carbon nanotube surface (Shi, 2013). This in turn leads to reaggregation of the carbon nanotubes. However, when they used a sonication temperature of 24 °C, the SDS did not lapse and reaggregation did not occur. Due to the ability of the Bioruptor® bath sonicator systems being able to really control the sonication temperature, sonication temperature was investigated over a range of temperatures from 5 °C up to 40 °C using UV – Vis spectroscopy as it is known that dispersion directly corresponds to absorbance strength (Njuguna et al., 2015).

The results in Figure 4.2 A - C show that initially there is an increase in the dispersion of the carbon nanotubes as shown by the increase in the UV – Vis spectrum of the 13 °C (orange) sonicated dispersion compared to the 5 °C (grey) sonicated dispersion. With further increases in sonication temperature, a significant drop is seen in the UV – Vis spectrum of the 20 °C (blue) and 30 °C (yellow) sonicated dispersions with no further drop seen with the 40 °C (green) sonicated dispersion.

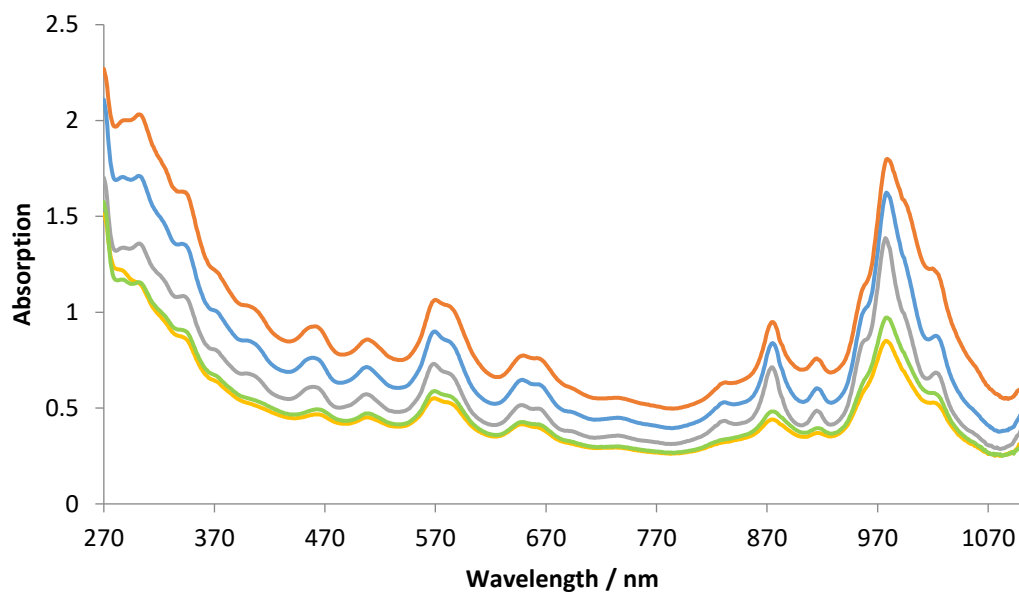
The results show that sonication temperature does have a significant effect on the quality of the dispersion of carbon nanotubes using the surfactant SDBS. With a lower sonication temperature of 5 °C, the drop in carbon nanotube dispersion compared to 13 °C could be down to the sonication temperature being too low and not inputting enough energy into the system. This means that after the 75 minutes of sonication, not all aggregations had been

debundled and SDBS adsorbed onto the carbon nanotube surface as debundling is a dynamic process. Once sonication had stopped, it meant there were more aggregates left over that were then subsequently removed during the centrifugation process.

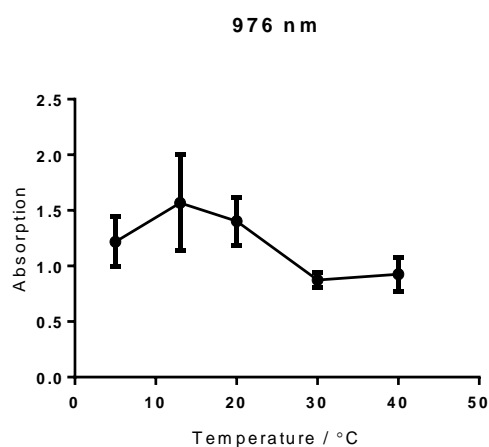
This could be due to the fact that over a long sonication time, in this case 75 minutes, the sonication process increases the temperature in the water bath by several degrees as noted in the Bioruptor® manual (Diagenode, 2015). Dumée et al for example also saw that the sonication temperature of their water bath went up from 17 to 25 °C over the sonication process (Dumée et al., 2013). This increase in temperature could be enough to cause the SDBS to lapse, as seen by Shi et al, and so cause the decrease in carbon nanotube dispersion. Also the increase in temperature can increase the frequency of collisions and contacts between the carbon nanotubes due to Brownian motion and decrease the dispersions stability (Dumée et al., 2013, Wong et al., 2009). It is possible that a combination of these processes is what lead to the reduction in the carbon nanotube dispersion. What this shows is that sonication temperature is vital for good carbon nanotube dispersion using a surfactant, and that by going either too high or too low, you can get sub optimal carbon nanotube dispersion using surfactants such as SDBS.

PL data from the initial runs is shown below in Figure 4.3 A – E. It shows a reduced dispersion concentration at higher temperatures and some electron transfer. Further runs were conducted, as shown in Figures 4.4 A - E, no significant changes were seen in any other PL plots and the UV data showed that the carbon nanotubes were broadly of similar dispersion efficiencies apart from at 40 °C whereby a reduction in efficiency was seen, correlating with previous work which showed that above 30 °C, there is a significant increase in lapsing of the surfactant away from the carbon nanotube surface and therefore increasing the hydrophobicity of the carbon nanotubes.

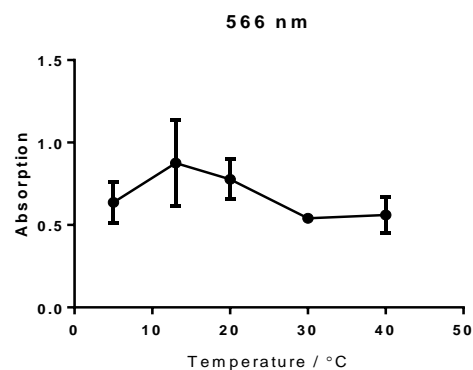
The decrease in dilution factor once the sonication temperature is increased above 13 °C could be due to SDBS lapsing and reuniting together, which allows the carbon nanotubes to then reaggregate and be removed during the centrifugation phase (Shi, 2013). This means that sonication temperature is a vital part of the method optimisation for the dispersion of carbon nanotubes and that bath sonication is an excellent piece of equipment for this due to the water bath being able to keep the temperature at near constant. The slight downside is that it is known that the temperature within the tube being sonicated is known to increase by a few degrees due to the sonication energy being imparted, and this could be the reason why the 20 °C samples showed signs of reduced dispersion, even though the literature states it happens when temperatures exceed 30 °C (Shi, 2013).



A)



B)



C)

Figure 4.2 A: All runs were with Bioruptor® Plus, 0.01 % carbon nanotube concentration, 0.1 % SDBS concentration, 2 mL sample size, Nalgene™ Polycarbonate tubes, cycle set up of 60 cycles of 60 seconds on, 15 seconds off, L power level. Ultracentrifugation for 150 minutes at 40, 000 G at 17°C. Results represent $n = 3$. Sonication temperature of 5 °C (grey), 13 °C (orange), 20 °C (blue), 30 °C (yellow), 40 °C (green). B) Absorption peak averages for the three runs at 976 nm for the 5 temperatures investigated. C) Absorption peak averages for the three runs at 566 nm for the 5 temperatures investigated.

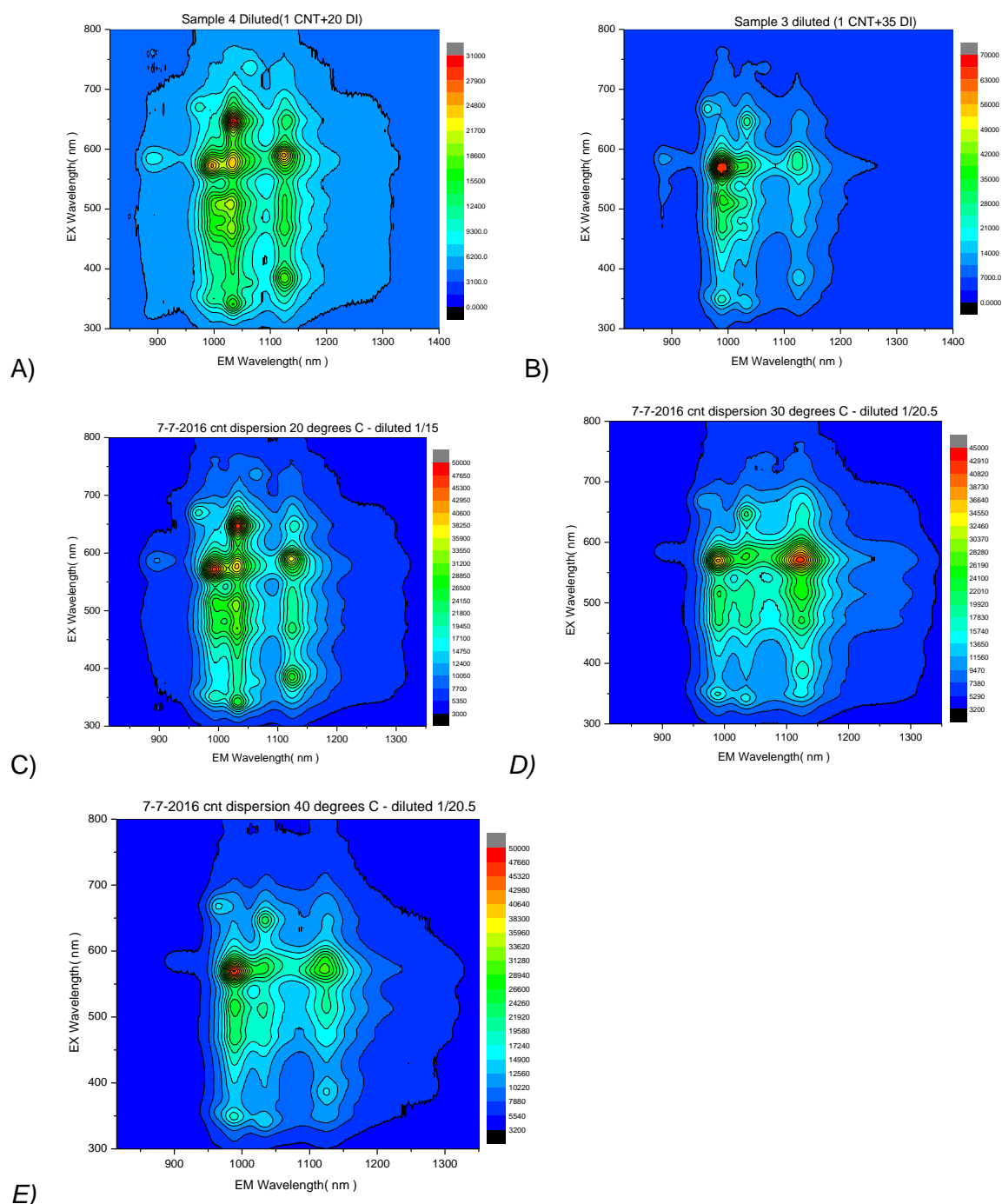


Figure 4.3 All runs were with Bioruptor® Plus, 0.01 % carbon nanotube concentration, 0.1 % surfactant concentration, 5 or 13°C water bath temperature, 2 mL sample size, Nalgene™ Polycarbonate tubes, cycle set up of 60 cycles of 60 seconds on, 15 seconds off, L power level. Ultracentrifugation for 150 minutes at 40, 000 G at 17°C. A) SDBS dispersed carbon nanotubes at 5 °C B) SDBS dispersed carbon nanotubes at 13 °C C) SDBS dispersed carbon nanotubes at 20 °C D) SDBS dispersed carbon nanotubes at 30 °C. E) SDBS dispersed carbon nanotubes at 40 °C.

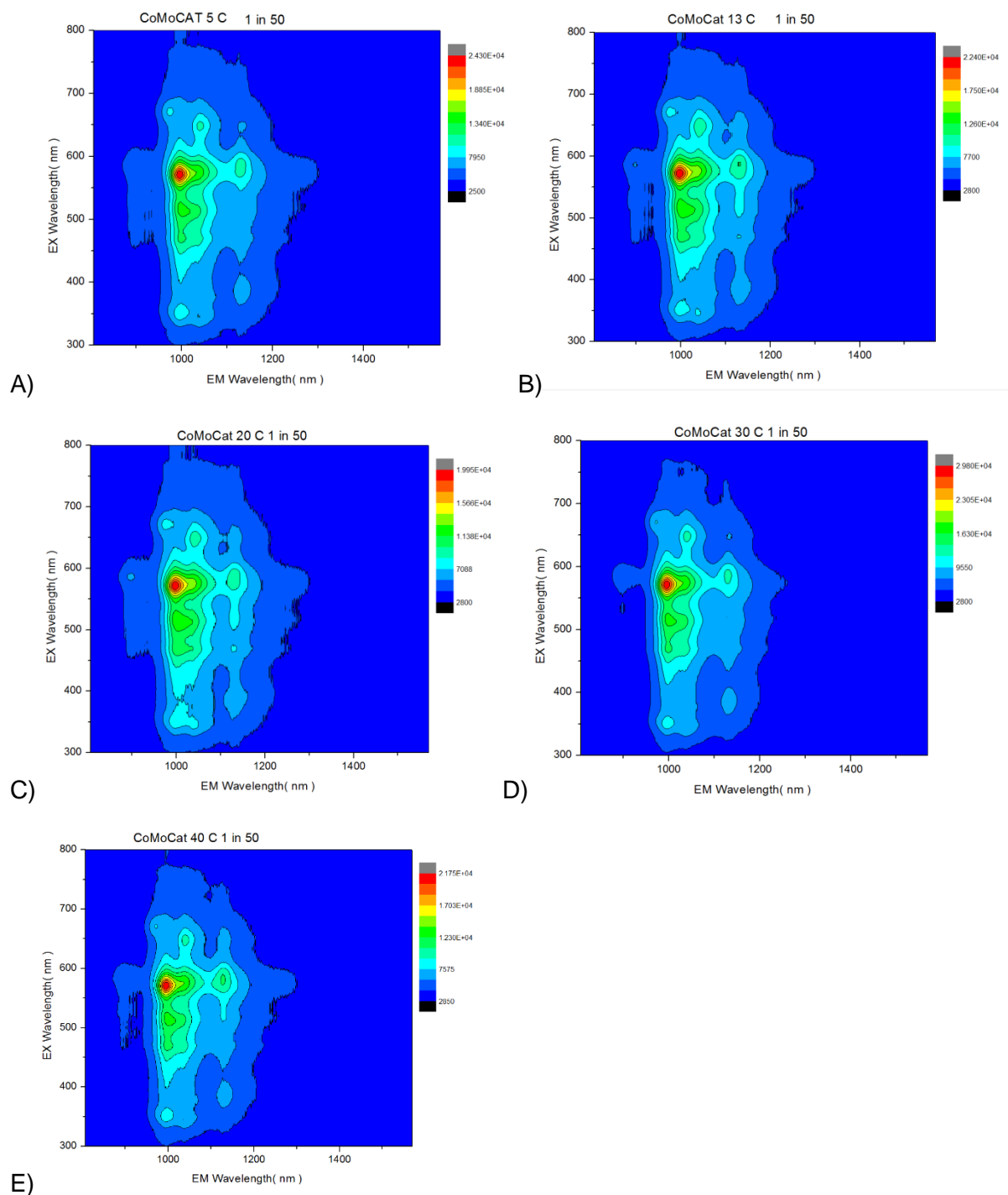


Figure 4.4 All runs were with Bioruptor® Plus, 0.01 % carbon nanotube concentration, 0.1 % surfactant concentration, 2 mL sample size, Nalgene™ Polycarbonate tubes, cycle set up of 60 cycles of 60 seconds on, 15 seconds off, L power level. Ultracentrifugation for 150 minutes at 40, 000 G at 17°C. A) PL plot of 5 °C sample. B) PL plot of 13 °C sample. C) PL plot of 20 °C sample. D) PL plot of 30 °C sample. E) PL plot of 40 °C sample.

4.3.1.2.2 Dispersion of carbon nanotubes at a number of different cycle settings using the Bioruptor Plus

Dispersion of carbon nanotubes is done through multiple cycles of sonication on and off set by the Bioruptor® system being used. Previous work has generally focussed on using 20 seconds on and 5 seconds off up to 180 cycles. However with the new machine, the Bioruptor® Plus, the number of cycles is limited to 99. Therefore the cycle settings were changed to accommodate this up to 60 cycles of 60 seconds on and 15 seconds off which would allow for only one session to be set rather than the 2 or 3 it would take using the old on and off times. This study investigated whether this change caused a difference in the carbon nanotube dispersion concentration.

Figure 4.5 A shows the average UV – Vis spectroscopy data for each of the cycle settings in question that were investigated. What they show is pretty identical spectra with no significant differences between them. This is further compounded in Figure 4.5 B and C which show the average peak heights at 566 and 976 nm for these CoMoCat carbon nanotubes.

What this data therefore shows is that cycle setting doesn't have a significant effect on the concentration of the carbon nanotubes post dispersion using sonication. I believe this is because the sonication process takes 75 minutes and that the amount of sonication time is the important factor, not how often the sonicator is turned on and off. This is particularly important for this work as it shows that there is no significant difference between the 60 seconds on and 15 seconds off used for this work and the 20 seconds on and 5 seconds off used for previous work using other Bioruptor® systems. This shows that this data can be compared to that previous work.

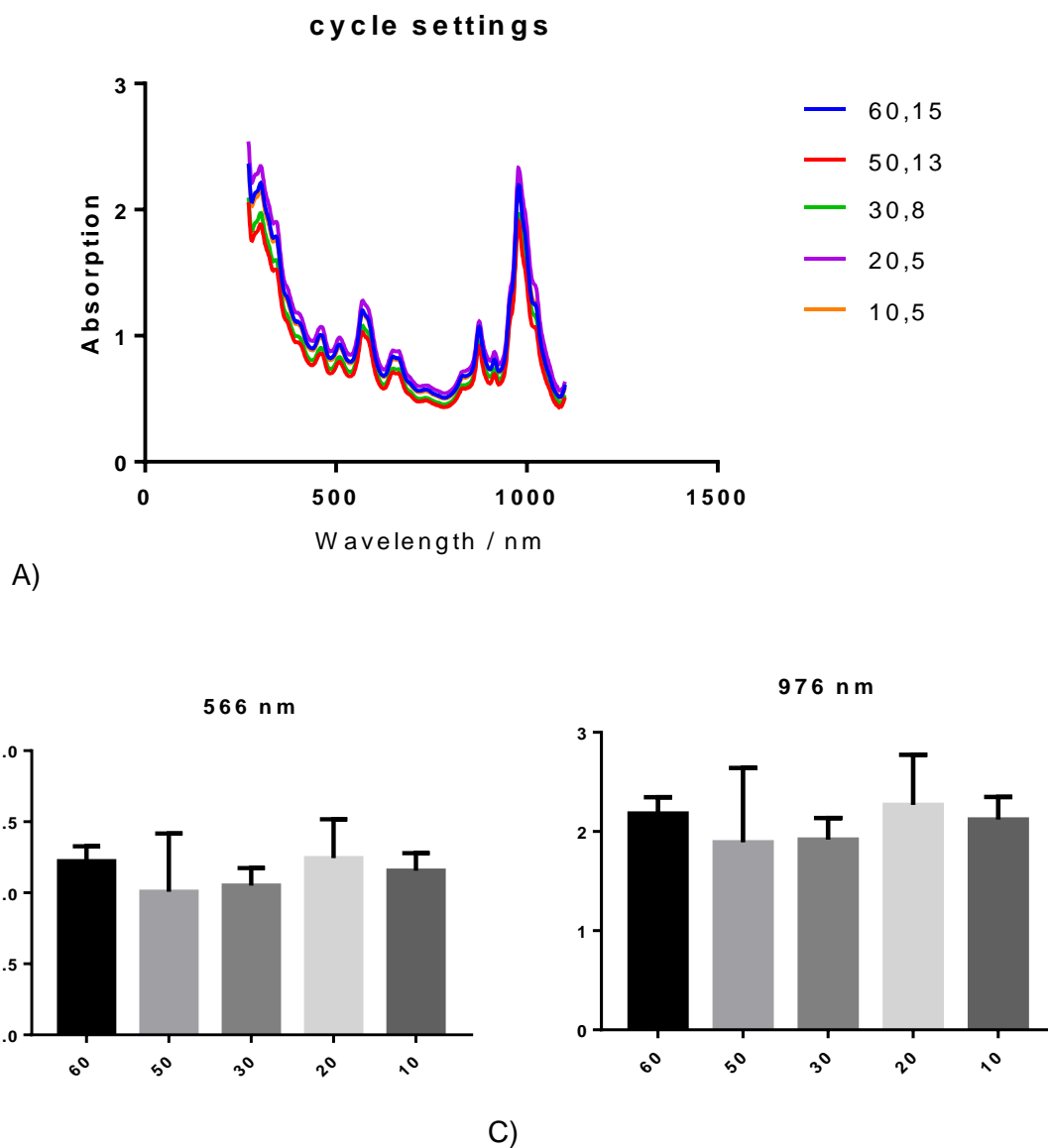


Figure 4.5 A) Average UV –Vis spectra showing dispersion of carbon nanotubes using different cycle settings. B) Average peak height at each cycle setting at 566 nm. C) Average peak height at each cycle setting at 976 nm.

4.3.1.2.3 Dilution study of dispersed carbon nanotubes in SDBS

The concentration of carbon nanotubes can be inferred by the strength of the absorption of the UV – Vis spectrum (Attal et al., 2006). The concentration is an important factor in determining the efficiency of the method of solubilisation of the carbon nanotubes using a surfactant such as SDBS. Therefore it is important that if a carbon nanotube sample is diluted, it can be inferred from the diluted sample what the concentration would be of the starting sample.

Using three samples of carbon nanotubes sonicated at 5, 13 and 20 °C, the samples were each diluted 1 in 2 and 1 in 10 with deionised water. These were then each compared to the original 1 in 1 sample to see how close the experimental results were to the theoretical 50 % and 10 % values. Figures 4.6 A, B and C show the spectrum achieved for the three different temperatures at the three dilution factors. Taking the two peaks associated with the 6, 5 chirality of 566 and 976 nm, the absorption peaks of the three dilution factors for the three temperatures were compared. These results are shown in Figures 4.7 A and B. What these results show in Figure 4.7 A is that the 1 in 2 dilutions were each very close to the 50 % value and the 1 in 10 were really close to the 10 % value.

Quantitatively, this is shown in Figure 4.7 B. Here the percentage difference between the experimental value and the theoretical value are shown. Each of the values is shown to be less than 1 % away from the theoretical value with an average of just 0.49 %. This means that when samples are diluted, it can be inferred from the absorption values what the original peaks would be, and therefore the concentration of the carbon nanotubes.

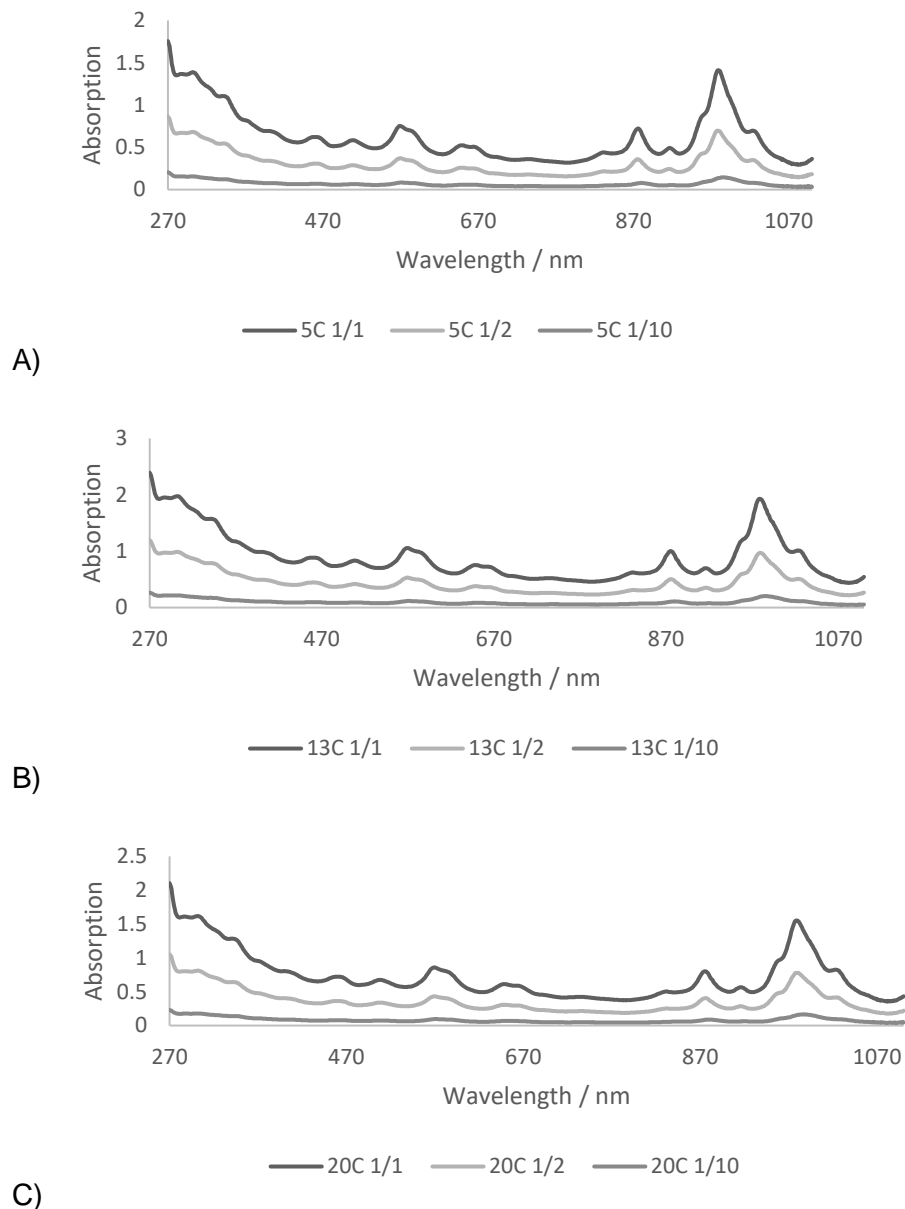
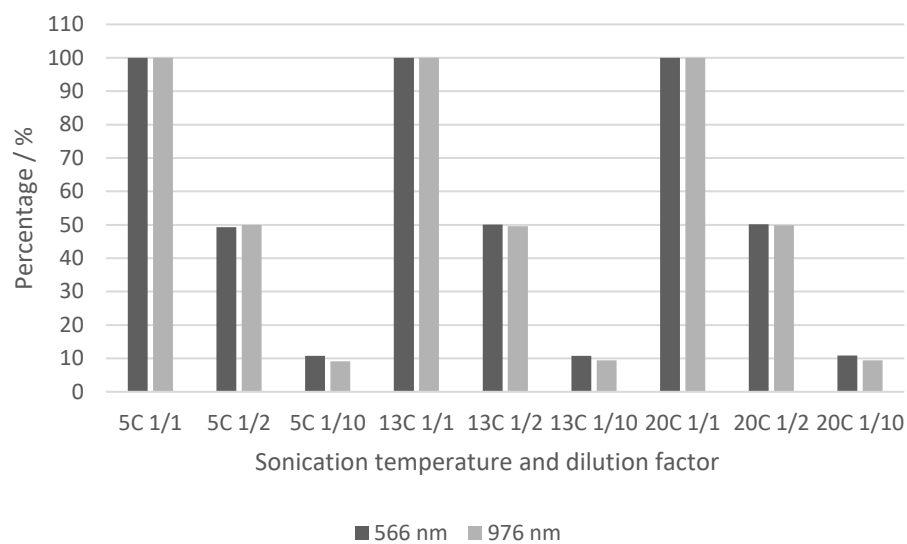
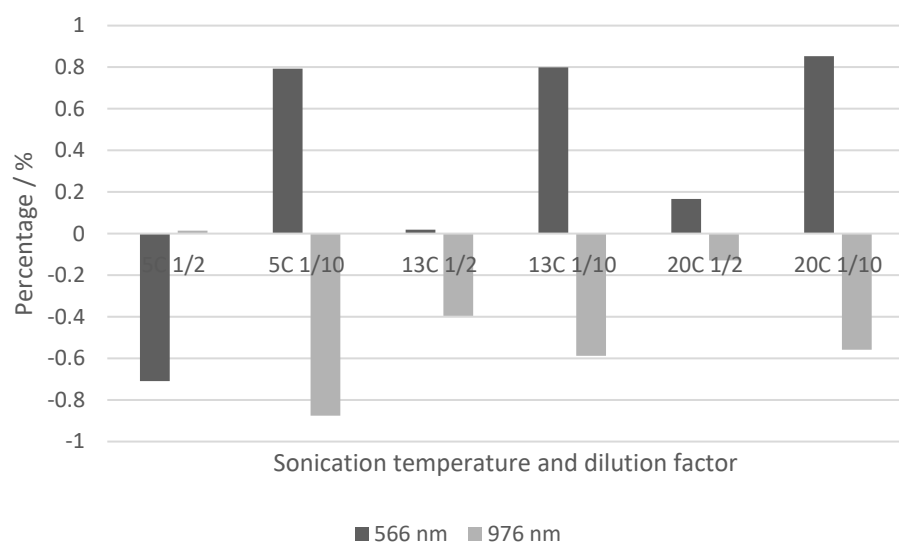


Figure 4.6 All runs were with Bioruptor® Plus, 0.01 % carbon nanotube concentration, 0.1 % surfactant concentration, 5 or 13°C water bath temperature, 2 mL sample size, Nalgene™ Polycarbonate tubes, cycle set up of 60 cycles of 60 seconds on, 15 seconds off, L power level. Ultracentrifugation for 150 minutes at 40, 000 G at 17°C. A) Carbon nanotubes sonicated at 5 °C with no dilution, diluted 1 in 2 and 1 in 10. B) Carbon nanotubes sonicated at 13 °C with no dilution, diluted 1 in 2 and 1 in 10. C) Carbon nanotubes sonicated at 20 °C with no dilution, diluted 1 in 2 and 1 in 10.



A)



B)

Figure 4.7 A) 566 and 976 nm peak heights for diluted samples compared to theoretical peak height for 50 % and 10 % of initial peak height. B) Difference from the theoretical value for the peak height for the 1/2 and 1/10 dilutions.

4.3.2 Probe sonication of carbon nanotubes with SDBS

Probe sonication works in a similar way to bath sonication, and has been shown to also disperse carbon nanotubes. Therefore it is important to compare the two methods to see which disperses carbon nanotubes the best. Previous work has shown that carbon nanotubes can be dispersed with a probe sonicator (Tunuguntla et al., 2017, Gao et al., 2015). Therefore the probe sonicator was investigated using a variety of time periods of sonication to see how well it compares to the Bioruptor® plus bath sonicator.

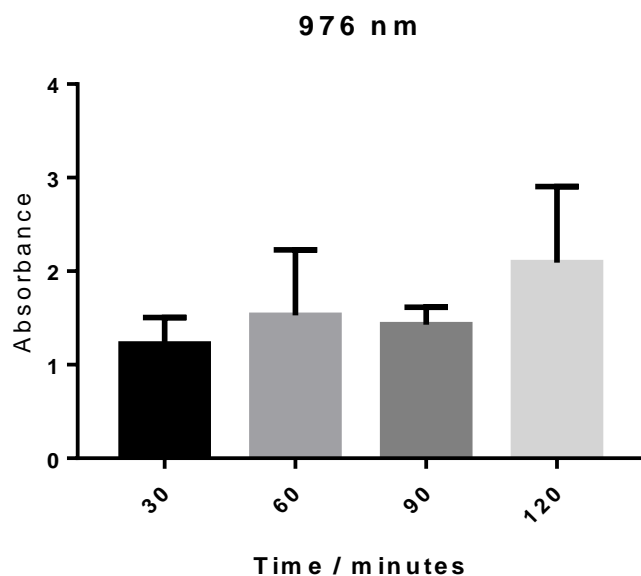
The results in Figure 4.8 A and B show that the probe over the same time period as the bath is not quite as efficacious at carbon dispersion. This is because for the 90 minutes of probe sonication, at 976 nm the peak height is 1.281 compared to the standard at 1.567 as shown in Figure 4.3. The same pattern is seen with 566 nm with the peak height of 0.653 compared to the standard at 0.875. However both showed an increase to above the standard after 2 hours of sonication up to 2.844 and 1.468 for 976 and 566 nm respectively. This could be down to a general increase in concentration caused by the extra half an hour of sonication.

Figure 4.9 A and B show the samples ran on the DLS. These show that over the 2 hours of sonication, there is no significant change in the size of PDI of the samples, indicating that there is no significant changes occurring to the length of the carbon nanotube carbon nanotubes. This correlates with other work which shows that probe sonication needs to occur for up to 10 hours or above before the carbon nanotubes are cut short enough to be shown on a DLS (Tunuguntla et al., 2017). However what it does show is that carbon nanotubes can be dispersed using the probe in a similar time frame to that of that Bioruptor® Plus bath sonicator.

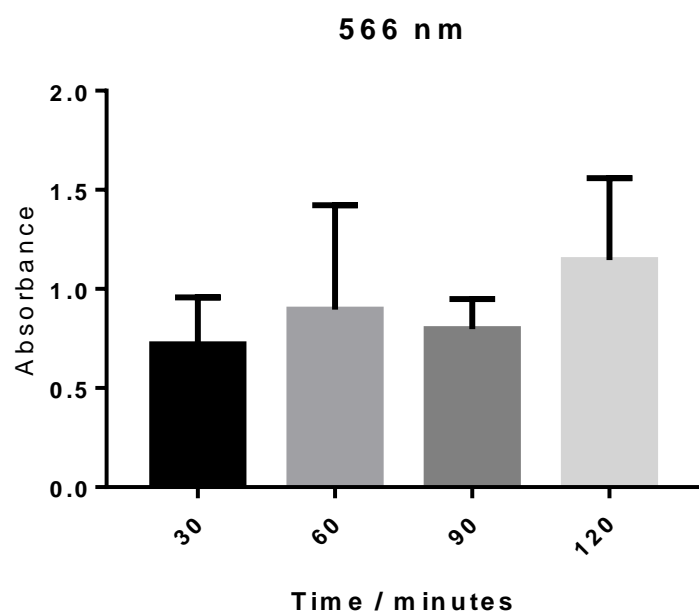
Figures 4.10 A - D show the PL map for the probe sonicated carbon nanotubes after each time point. After half an hour, Figure 4.10 A shows that increasing the time increases the concentration of carbon nanotubes successfully dispersed as the count goes up from 13,350

to 15,950. There is also some excitation energy transfer beginning to appear next to the 6, 5 chirality peak at excitation of 575 nm and emission of 1025 nm. After 1 hour however, as shown in Figure 4.10 B, this appears to have diminished once again and another general increase in concentration is seen with the count going up to 25,600. After 1.5 hours, as shown in Figure 4.10 C, the dilution factor had to be increased to 1 in 50. This sample also showed again an increase in the excitation energy transfer seen at emission 1025 nm. This was further seen in Figure 4.10 D where an increase in the count was seen up to 23,400 and an increase in the intensity was seen with the electron transfer peak to make it the second most intense peak after the 6, 5 peak.

What these showed was that carbon nanotubes can be successfully dispersed using the probe sonicator as well as the Bioruptor® bath sonicator. These carbons increase in dispersion efficiency the longer they are sonicated and due to the use of an ice bath, there is no significant decrease in dispersion due to the surfactant lapsing away from the carbon nanotube surface.

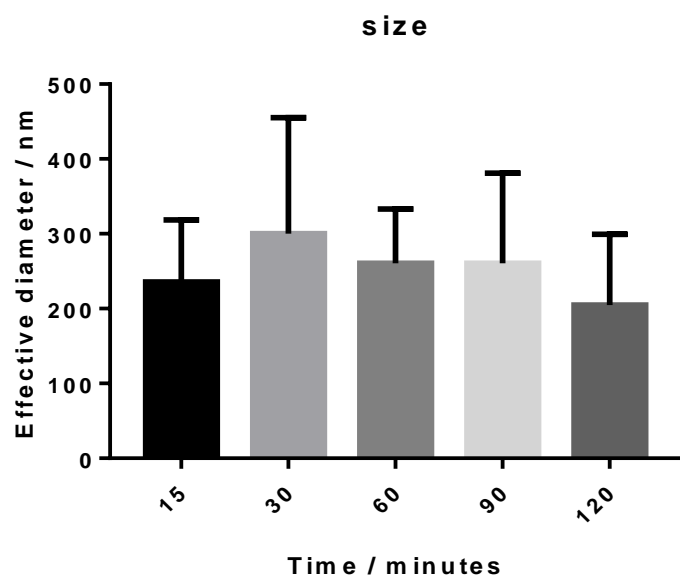


A)

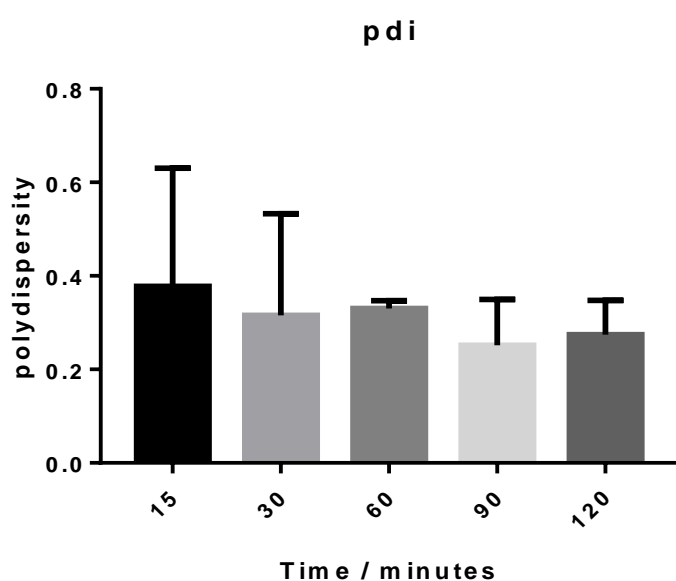


B)

Figure 4.8 All runs were with probe sonicator, 0.01 % carbon nanotube concentration, 0.1 % surfactant concentration, in an ice bath, 2 mL sample size, 10 amp power level. Ultracentrifugation for 150 minutes at 40, 000 G at 17°C. A) Carbon nanotubes dispersed in SDBS over time using the probe sonicator. Absorption peak height at 976 nm. B) Carbon nanotubes dispersed in SDBS over time using the probe sonicator. Absorption peak height at 566 nm.



A)



B)

Figure 4.9 All runs were with probe sonicator, 0.01 % carbon nanotube concentration, 0.1 % surfactant concentration, in an ice bath, 2 mL sample size, 10 amp power level. Ultracentrifugation for 150 minutes at 40, 000 G at 17°C. A) Carbon nanotube size dispersed with SDBS at varying times using the probe sonicator. B) Carbon nanotube PDI dispersed with SDBS at varying times using the probe sonicator

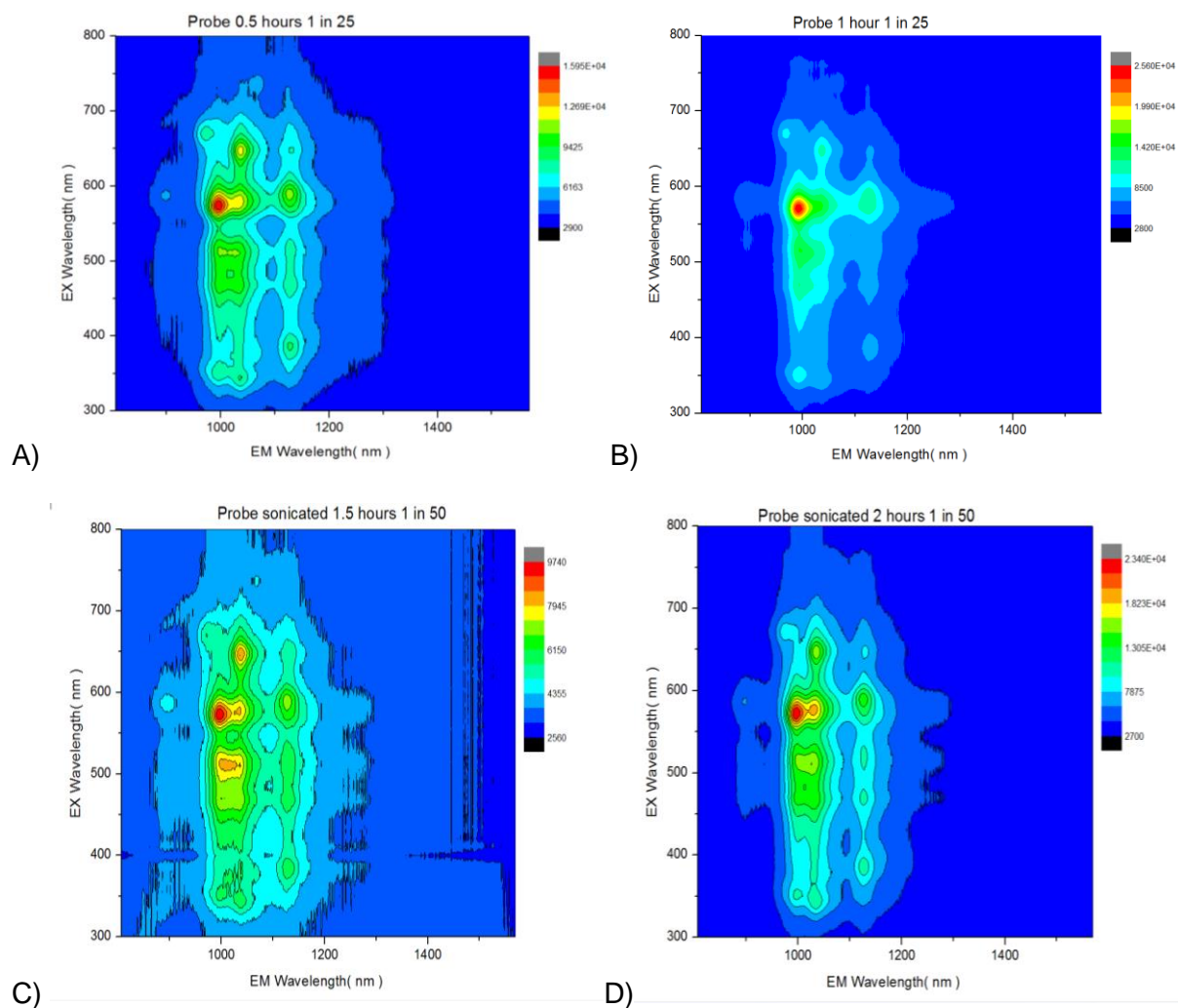


Figure 4.10: All runs were with probe sonicator, 0.01 % carbon nanotube concentration, 0.1 % surfactant concentration, in an ice bath, 2 mL sample size, 10 amp power level. Ultracentrifugation for 150 minutes at 40, 000 G at 17°C. A) PL plot of probe sonicated carbon nanotubes after 30 minutes. B) PL plot of probe sonicated carbon nanotubes after 60 minutes. C) PL plot of probe sonicated carbon nanotubes after 90 minutes. D) PL plot of probe sonicated carbon nanotubes after 120 minutes.

4.3.3 Water dispersion of carbon nanotubes using biologically safe surfactants

4.3.3.1 Dispersion of carbon nanotubes using MPC as a surfactant

Biologically safe surfactants are an important part of being able to use carbon nanotubes within a biological system. This is because the usual surfactants used, SDS and SDBS, are both toxic to the human body and are therefore unsuitable. The structure of phospholipids could lend itself to carbon nanotube dispersion and indeed previous work has shown that these could be used. This work focussed on using MPC and DMPC as the surfactants in question due to them being the same lipids used in the previous liposome work. This would mean that if these carbon nanotubes were to be taken forward into liposome complex work, the lipid in use would not have a bearing on properties such as liposome charge or immune response. This work therefore focussed on using the MPC and DMPC lipids in the same way as SDS and SDBS before so a direction comparison could be made to determine whether they could be used going forward.

Figure 4.11 A and B show the average peak heights for MPC at 566 and 976 nm compared to SDS and SDBS. What these show is that MPC is comparable to SDS in its ability to disperse carbon nanotubes with no significant difference shown between the two peak heights at either wavelength. However they both are much reduced compared to SDBS as expected as they do not contain the benzene ring which allows for a much better interaction between the carbon nanotube surface and the SDBS molecule. Figure 4.11 C and D show the PL map of MPC dispersed carbon nanotubes and MPC on its own. What these show is that the dispersion with carbon nanotubes is a clean dispersion with strong peak heights corresponding to the 6, 5 dominant chirality of the CoMoCat nanotubes in question with 8, 4 chirality also showing a bright response. What this also shows is that MPC in itself does not illicit a reaction in the PL

which means the PL map in Figure 4.11 C is the dispersed carbon nanotubes alone and not the surfactant used.

What this data shows is that carbon nanotubes can be dispersed using MPC as a biologically safe surfactant and that these can be comparable to SDS dispersed carbon nanotubes.

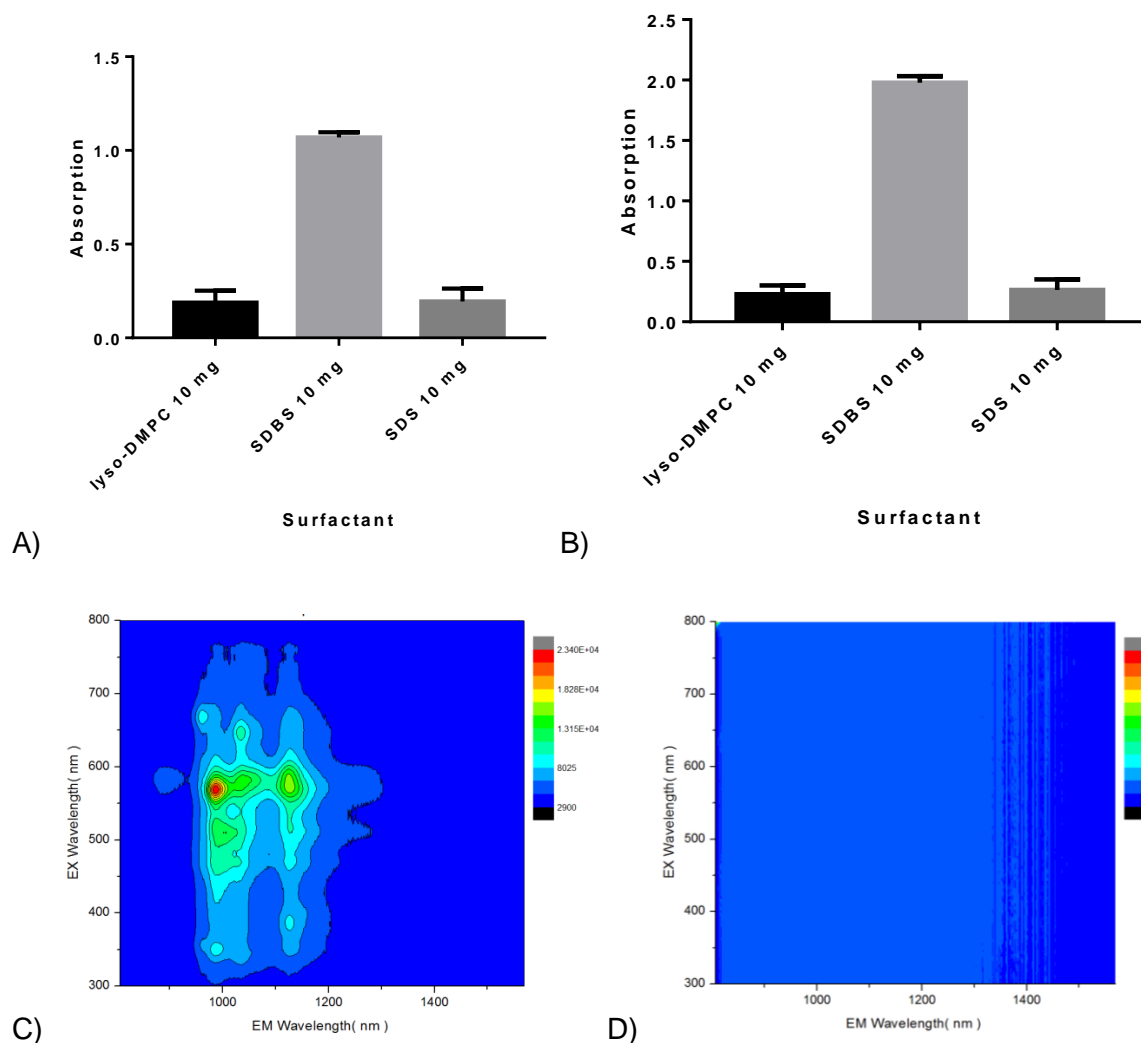


Figure 4.11: All runs were with Bioruptor® Plus, 0.01 % carbon nanotube concentration, 0.1 % surfactant concentration, 13°C water bath temperature, 2 mL sample size, Nalgene™ Polycarbonate tubes, cycle set up of 60 cycles of 60 seconds on, 15 seconds off, L power level. Ultracentrifugation for 150 minutes at 40, 000 G at 17°C. A) Average peak heights at 566 nm for each of the three surfactants tested. B) Average peak heights at 976 nm for each of the three surfactants tested. C) PL dispersion of MPC dispersed carbon nanotubes. D) PL of MPC without carbon nanotubes present.

4.3.3.2 Dispersion of carbon nanotubes using the phospholipid DMPC as the surfactant

Many surfactants used for dispersion of carbon nanotubes, such as SDS and SDBS, are toxic and cannot be used for pharmaceutical formulations. By contrast, double-chained phospholipids are considered non – toxic and are used in multiple formulations currently on the market. However, phospholipids are considered to be curvophobic as their 3D structures are approximated as cylinders and their packing assumes bilayers. Therefore wrapping around a cylindrical object such as a carbon nanotube is not geometrically preferable (Wu et al., 2006). To test this, the lipid DMPC was used to try and disperse SW carbon nanotubes. This is different to the MPC previously used as it has two fatty acid chains and not one, which alters the shape of the surfactant.

The results in Figure 4.12 show the complete lack of carbon nanotube dispersion with virtually no peaks between 370 and 1200 nm. This is compared to dispersion using SDS and SDBS which show good peaks at approximately 570 nm and 980 nm which correspond to the 6,5 chirality of the carbon nanotubes used. This confirms the idea that by using a lipid that conforms to a cylinder structure, it is unable to wrap around the carbon nanotube and aid in the water dispersion.

Although this work has confirmed that double chained phospholipids cannot disperse carbons, other work however has shown that it is possible to use phospholipids by adding a small amount of 2C18-PEG. Furthermore, the amount of 2C18-PEG needed to disperse the same amount of SW carbon nanotubes is greatly reduced by the co-adsorption of common phospholipids such as 2C10-choline (Sato and Sano, 2014). Another possibility would be to

use the geometrically preferred lysophospholipids whereby the cone shape allows the lysophospholipids to wrap around the SW carbon nanotube in a semi-spherical curvature along SWNT axis and along the circumference of SWNT (Wu et al., 2006, Alberts et al., 2015).

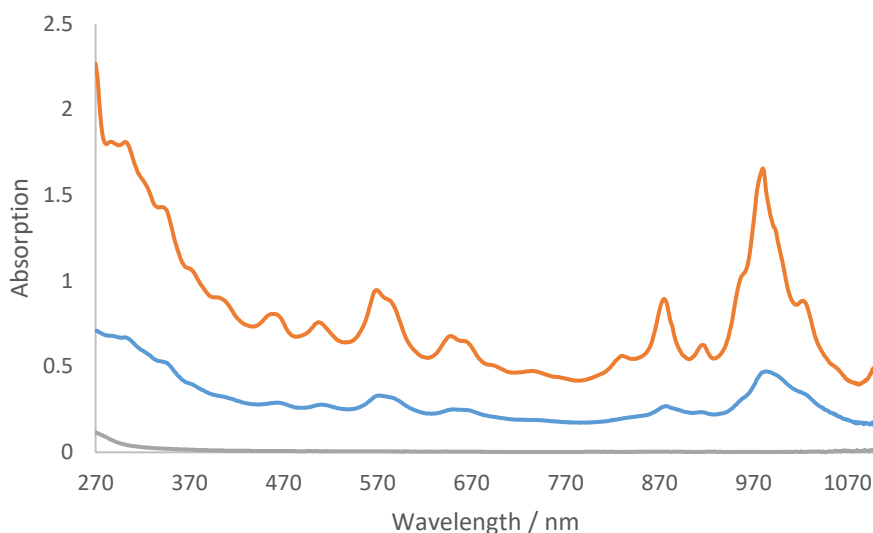


Figure 4.12: All runs were with Bioruptor® Plus, 0.01 % carbon nanotubes concentration, 0.1 % surfactant concentration, 2 mL sample size, Nalgene™ Polycarbonate tubes, cycle set up of 60 cycles of 60 seconds on, 15 seconds off, L power level. Ultracentrifugation for 150 minutes at 40, 000 G at 17°C. Results represent n = 3. DMPC (grey), SDBS (orange) and SDS (blue).

4.3.4 Combination of surfactants

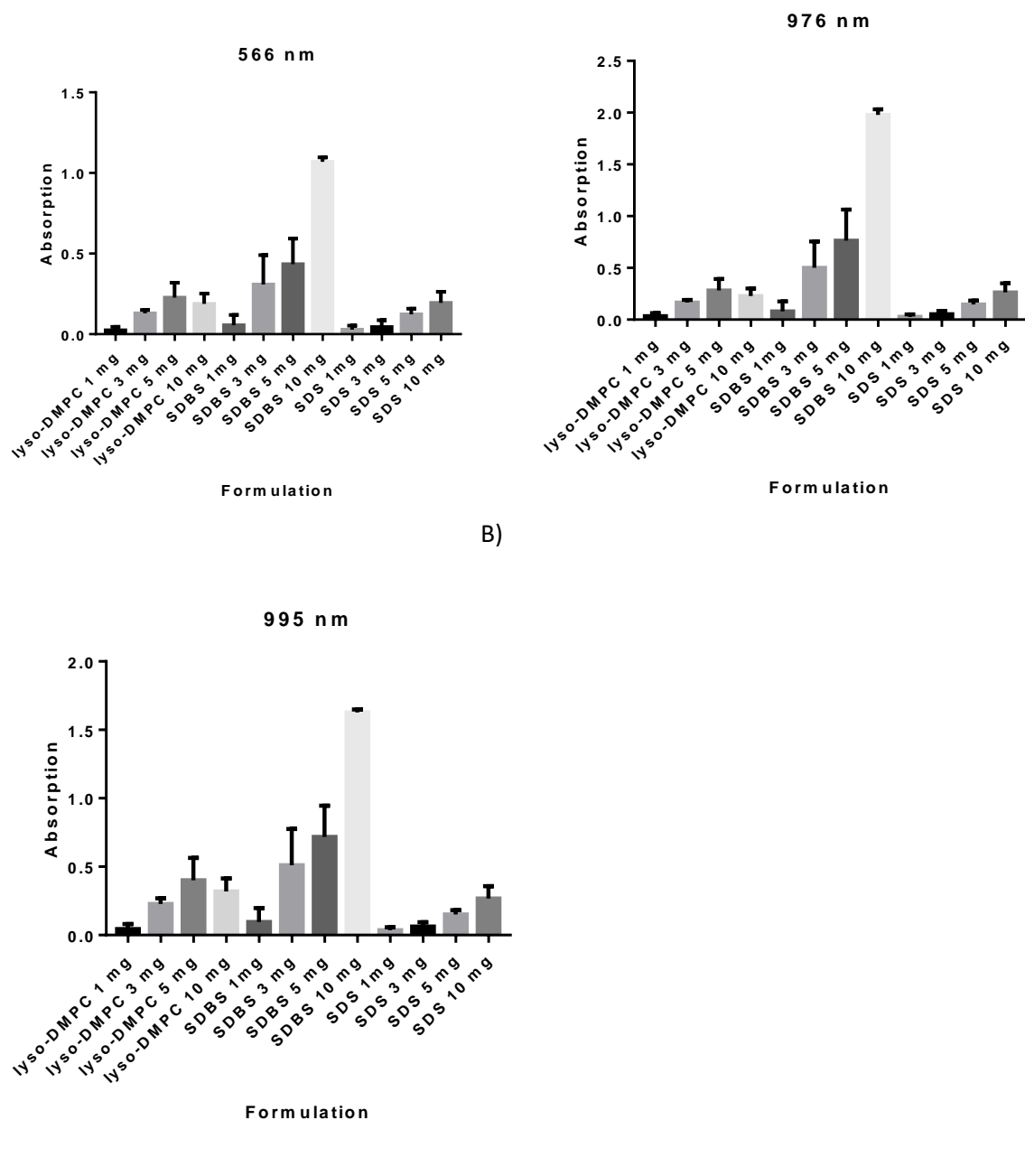
4.3.4.1 Carbon nanotube dispersion surfactant study comparing like for like surfactants

Surfactant choice is known to have a great effect on how efficacious the dispersion of carbon nanotubes is using the Bioruptor® bath sonication system. SDS and SDBS are both standards used within the carbon nanotubes field but both are toxic to the human body and are therefore unsuitable for dispersion of carbon nanotubes for biological purposes. Other surfactants that could be used include sodium cholate (SDOC) and lysophospholipids and in this study, it was the lysophospholipid MPC that was investigated to see whether it could be used to disperse carbon nanotubes, at what concentrations and how it compares to the other surfactants. Therefore each surfactant was sonicated at concentrations ranging from 0.1 to 1 mg / mL with a constant concentration of 0.1 mg / mL of carbon nanotubes.

The UV- Vis data clearly shows in Figures 4.13 A – C that the MPC and SDS are similarly matched in how efficacious they are at dispersing the carbon nanotubes. Interestingly, the MPC showed a shift in the 976 nm peak up to around 995 nm. This could be due to some kind of interaction occurring between the carbon nanotubes and the MPC such as dielectric screening. It was also shown that SDS continued to show an increase in the dispersion efficiency through the concentrations, but MPC maxed out at 0.5 mg mL and showed a small but not significant decrease in peak height when 1 mg / mL of MPC was used. SDBS was shown to be far and away the best at dispersing the carbon nanotubes under these conditions. This is due to the benzene ring being present and interacting with the carbon nanotube surface to create $\pi - \pi$ bond interactions. This greatly increases the ability of the SDBS to disperse the carbon nanotubes individually.

The PL data shows the different concentrations of SDBS, shown in Figures 4.14 A - C, at the concentrations 0.1 – 0.5 mg / mL diluted to concentrations of 1 in 10, 1 in 25 and 1 in 50. What they show is that clearly the concentrations of carbon nanotubes decreases as you decrease the surfactant concentration but also that as you decrease the concentration, more of the other chiralities such as 7, 5 and 8, 4 are shown and also some electron transfer between them, indicating more small bundles present as opposed to individual tubes being the majority seen with the 1 mg / mL samples. The SDS, shown in Figures 4.14 D - F, data for 1 and 0.5 mg / mL also showed a similar pattern, although at a lower dilution factor and in fact by the time 0.1 mg is tested, nothing can be seen at all. The MPC data, as shown in Figures 4.15 A - C, showed that MPC is far more likely to disperse the tubes individually and preferentially disperse 6, 5 tubes as the PL map is very similar to a 1 mg / mL sample and this pattern continues down to 0.1 mg / mL. What these figures show is that the different surfactants have different dispersal characteristics. This could be useful if a specific chirality is required as choosing a specific surfactant could give rise to an increase in the concentration of that particular chirality.

Also all the samples showed that as you decrease the concentration of surfactant, you get a decrease in carbon nanotube concentration and as this decreases, there is more electron transfer seen and more of the other chiralities within the sample seen as well.



C)

Figure 4.13: All runs were with Bioruptor® Plus, 0.01 % carbon nanotube concentration, 0.1 to 1 % surfactant concentration, 13°C water bath temperature, 2 mL sample size, Nalgene™ Polycarbonate tubes, cycle set up of 60 cycles of 60 seconds on, 15 seconds off, L power level. Ultracentrifugation for 150 minutes at 40, 000 G at 17°C. A) Absorption peak height at 566 nm for each sample at each surfactant concentration. B) Absorption peak height at 976 nm for each sample at each surfactant concentration. C) Absorption peak height at 995 nm for each sample at each surfactant concentration.

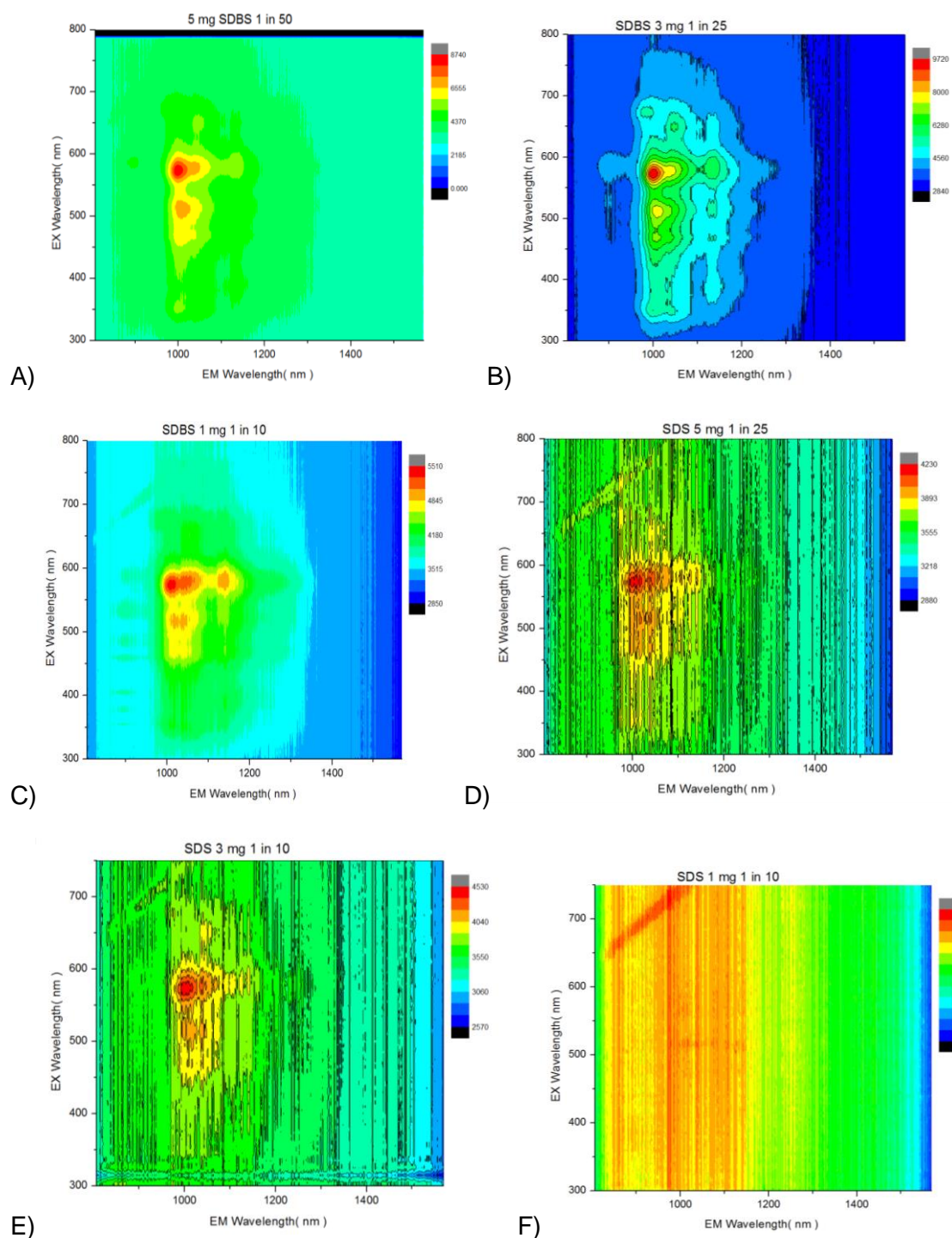


Figure 4.14 All runs were with Bioruptor® Plus, 0.01 % carbon nanotube concentration, 0.1 to 1 % surfactant concentration, 13°C water bath temperature, 2 mL sample size, Nalgene™ Polycarbonate tubes, cycle set up of 60 cycles of 60 seconds on, 15 seconds off, L power level. Ultracentrifugation for 150 minutes at 40, 000 G at 17°C. A) PL plot of SDBS 5 mg sample. B) PL plot of SDBS 3 mg sample. C) PL plot of SDBS 1 mg sample. D) PL plot of SDS 5 mg sample. E) PL plot of SDS 3 mg sample. F) PL plot of SDS 1 mg sample.

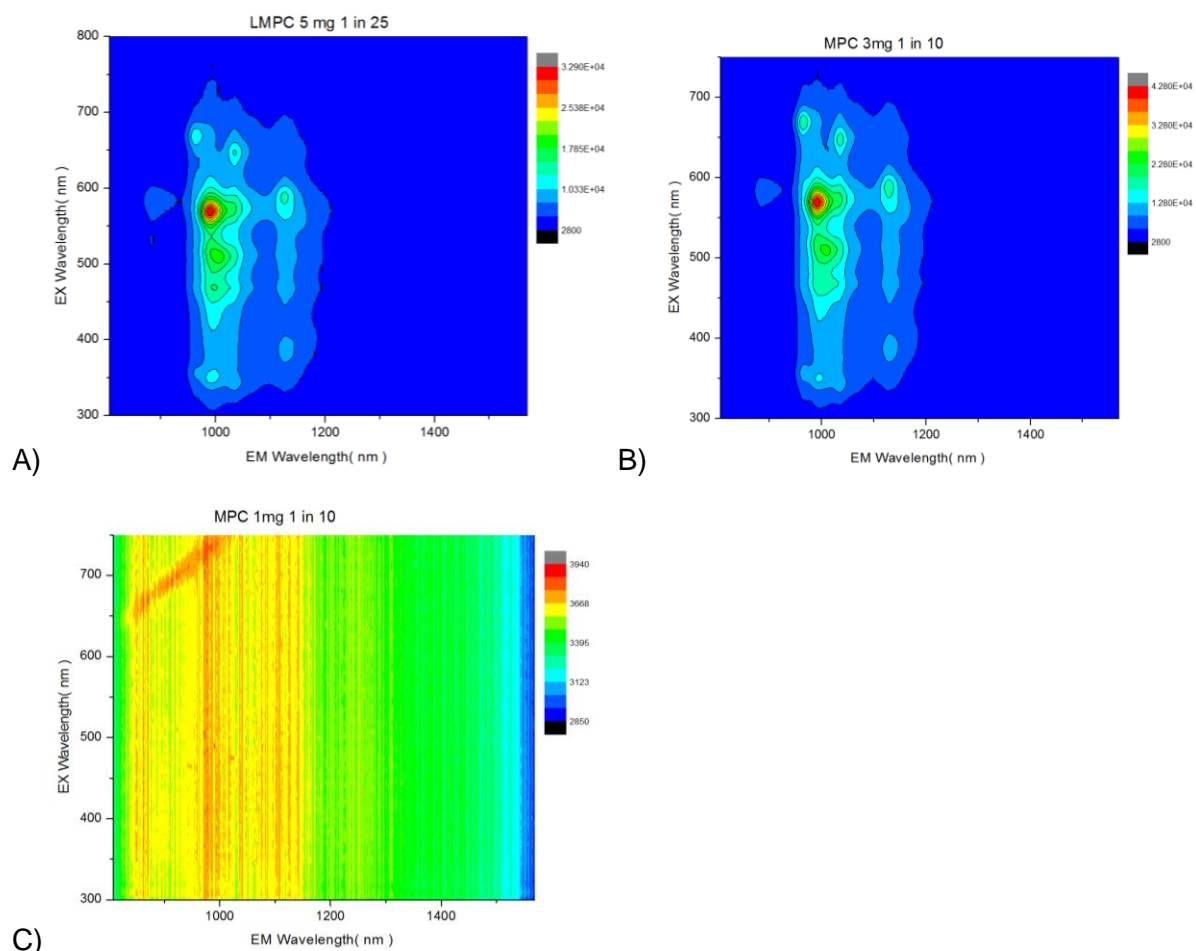


Figure 4.15: All runs were with Bioruptor® Plus, 0.01 % carbon nanotube concentration, 0.1 to 1 % surfactant concentration, 13°C water bath temperature, 2 mL sample size, Nalgene™ Polycarbonate tubes, cycle set up of 60 cycles of 60 seconds on, 15 seconds off, L power level. Ultracentrifugation for 150 minutes at 40, 000 G at 17°C. A) PL plot of MPC 5 mg sample. B) PL plot of MPC 3mg sample. C) PL plot of MPC 1 mg sample.

4.3.4.2 Stability study of water dispersed carbon nanotubes using SDS, SDBS and MPC

Stability studies are an important part to any particle formulation particularly any that could be used in a pharmaceutical context. This is because it is important from both a safety and a regulation stand point that it is known what exactly is in a formulation and that over time, this will not change in between the formulation being made and it being administered.

What the stability study data showed was that formulations made using either SDBS or MPC were both stable and kept at near 100 % concentration. This is shown in Figures 4.16 in the actual peak height absorption values and in Figures 4.17 as a percentage compared to the initial week 0 sample. This is important because if the carbon nanotubes were to lose the surfactant that surrounds them, they will become hydrophobic. This will cause them to form larger and larger bundles which will then come out of solution. This was only seen with the SDS dispersed carbon nanotubes and this could be down to a lack of a benzene ring which the SDBS molecule has which adds to the stability. These results showed that for a 6 month period, either SDBS or MPC could be used as a surfactant and not see a significant drop in the concentration and therefore stability of the carbon nanotubes it is surrounding.

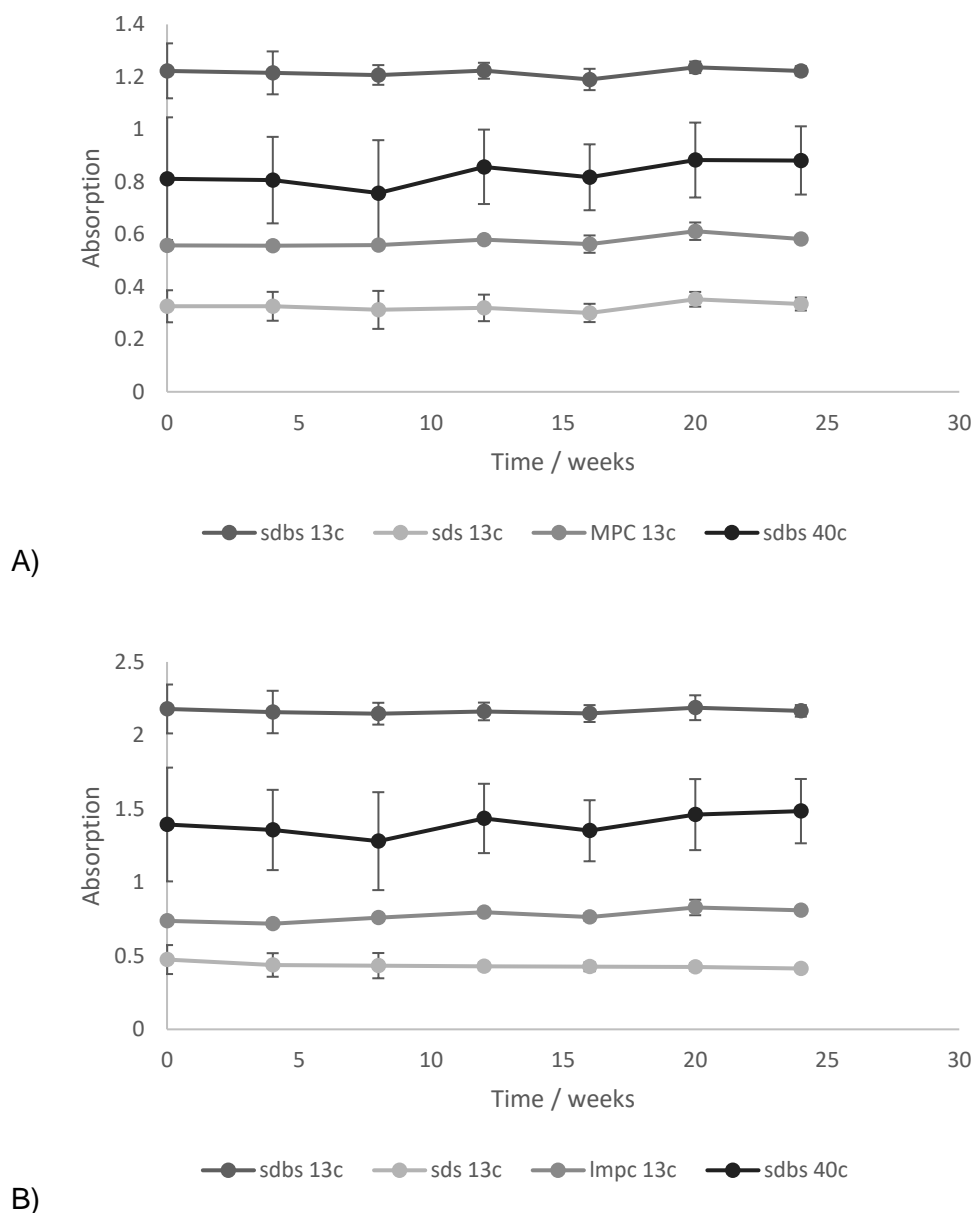


Figure 4.16 All runs were with Bioruptor® Plus, 0.01 % carbon nanotube concentration, 0.1% surfactant concentration, 13 or 40 °C water bath temperature, 2 mL sample size, Nalgene™ Polycarbonate tubes, cycle set up of 60 cycles of 60 seconds on, 15 seconds off, L power level. Ultracentrifugation for 150 minutes at 40, 000 G at 17°C. A) Absorption peak height value at 566 nm for each stability study sample. B) Absorption peak height value at 976 nm for each stability study sample.

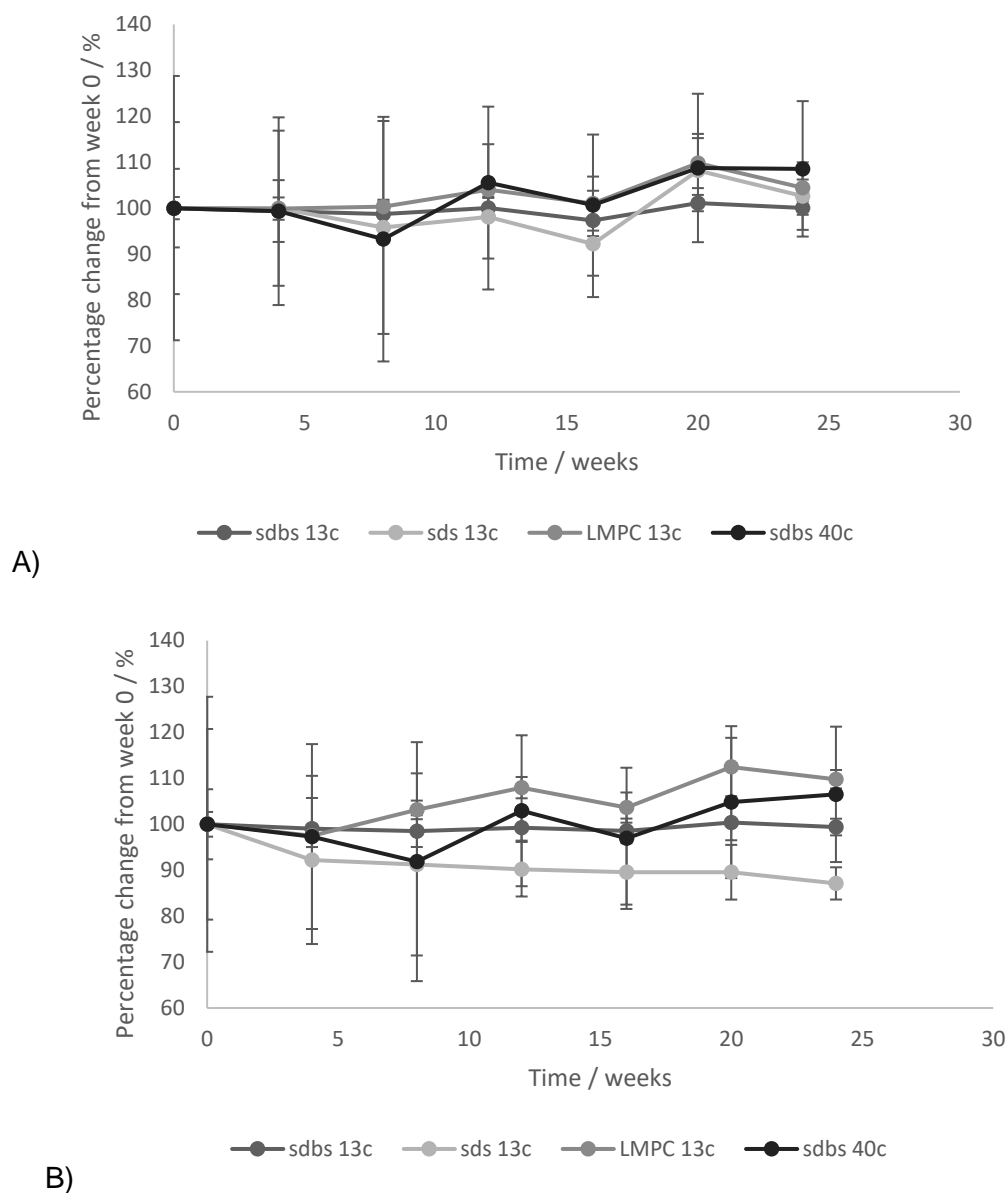


Figure 4.17: All runs were with Bioruptor® Plus, 0.01 % carbon nanotube concentration, 0.1% surfactant concentration, 13 or 40 °C water bath temperature, 2 mL sample size, Nalgene™ Polycarbonate tubes, cycle set up of 60 cycles of 60 seconds on, 15 seconds off, L power level. Ultracentrifugation for 150 minutes at 40, 000 G at 17°C. A) Percentage difference from week 0 for each stability study sample at 566 nm. B) Percentage difference from week 0 for each stability study sample at 976 nm.

4.4. Conclusion

In conclusion, a number of different factors were shown to have an influence on how a surfactant performed at dispersing carbon nanotubes. It was shown firstly that your choice of surfactant has a large effect on how well the carbon nanotubes were dispersed. It was shown that the simple addition of a benzene ring to a molecule was enough to significantly increase the carbon nanotubes dispersion, in the case of SDS compared to SDBS. However with these surfactants being toxic, alternatives were required. The comparison of MPC and DMPC to the other two surfactants also showed some key factors. The addition of a second fatty acid meant that DMPC could not conform to the correct shape and therefore dispersed almost no carbon nanotubes at all. However MPC, with its single chain, could disperse carbon nanotubes as well as SDS and kept them stable for up to 6 months. When compared to one another, it was shown that MPC had very similar dispersion properties and abilities to SDS which confirms that the benzene ring of SDBS is a significant factor in the efficacy of carbon nanotube dispersion using SDBS.

It was also shown that temperature is another important factor to take into consideration. Even though it was never shown that temperature could be used to control bundle size, it was shown that too high a temperature would see a comparative drop in the concentration of carbon nanotubes. The sonication time on and off however was shown not to affect carbon nanotube dispersion efficacy with 60 seconds on, 15 seconds off and 10 seconds on, 5 seconds off having similar dispersion results for the same total sonication time.

Probe sonication was finally also shown to be a viable alternative for carbon nanotube dispersion which is in line with previous work already done. With the use of an ice bath, carbon nanotubes were dispersed successfully using a similar amount of time. The ice bath was important as probe sonication introduces a lot of heat into the system and as shown with the

bath sonication work, an increase in temperature does relate to a decrease in carbon nanotube dispersion efficacy.

5. Carbon nanotube modification and addition to liposomal solution

5.1 Aim and objectives

Carbon nanotubes are hydrophobic in nature and so need modification if they are to be soluble in water and be useful for many different biological applications. This is done through either covalent or non-covalent functionalisation. Covalent functionalisation works by chemically modifying the actual carbon nanotube structure and introducing defects. These defects are then modified with various chemical groups which increase the hydrophilicity of the carbon nanotube. The aim of this work was to investigate carbon nanotube modification through the addition of oleum and nitric acid. The objectives were to formulate a protocol for this modification and investigate any post chemical treatment that might be required. This included cutting the carbon nanotubes; either through chemical treatment or through mechanical treatment using a bath or probe sonicator. The final objective was to add some of these modified tubes with liposomes and investigate the initial interaction between the two different systems.

5.2 Materials and methods

5.2.1 Carbon nanotube carboxylation

5.2.1.1 Chemical treatment procedure

General synthetic procedure.

40 mg of either HiPco or CoMoCat carbon nanotubes were mixed for 24 hours in 20 ml of oleum (20% wt. sulfur trioxide). A homogeneous black solution was formed. A mixture of oleum: nitric acid (70%), 10:10 ml was added slowly to the nanotubes solution under cooling.

The reaction mixture was kept for 2 hours on the sand bath at either 20 or 65°C. 120 ml of water was poured in afterwards slowly and left for coagulation for 12 hours. Black flake-like coagulate appeared. The precipitate was separated by filtration through a 5 µm Teflon membrane under vacuum. The precipitate on the filter is dispersed in 5 ml of methanol, coagulated by 20 ml of Diethyl Ether, filtered and washed by Diethyl Ether. Additionally washings were conducted with Diethyl Ether and the dry carbon nanotubes were dried in air on the filter paper.

5.2.1.2 Dispersion of carbon nanotubes post chemical treatment

0.1 mg / mL of the chemically treated carbon nanotubes were dispersed in water and allowed to stand for 5 minutes. If required, 1mg / mL of SDBS was added to the sample and a short period of sonication of 15 cycles of 60 seconds on, 15 seconds off, was applied to disperse the treated carbon nanotubes. SDBS was the only surfactant chosen because it is the most efficacious and in this experiment, it was simply used to investigate if any hydrophobic carbon nanotube structure still remained. These were then analysed using UV – Vis – NIR, DLS, TEM and PLE.

5.2.2 Carbon nanotube cutting with probe

Initially 1 mg of CoMoCat carbon nanotubes weighed out into glass vial. 10 mg of SDBS added along with 10 mL of water. Sample then sonicated for 1 hour using probe sonicator set to 40 % (100 W) with a pulse cycle set to 0.5. Sample then ultra-centrifuged at 45000 rpm for 2 hours at 17 °C. This power level was found to be insufficient as nearly all the nanotubes were still bundles and therefore were removed during ultra-centrifugation and so was increased to

100 %. Sonication time then increased to 2 hours. The probe sonicator was also used with samples at 3, 4 hours to increase the chances of cutting the tubes and therefore getting the short tubes required and all samples analysed using UV – Vis and PL (Gao et al., 2015).

5.2.3 Carbon nanotube cutting with bath

Initially 1 mg of CoMoCat carbon nanotubes weighed out into glass vial. 10 mg of SDBS added along with 10 mL of water. Sample then sonicated for 1 to 3 cycles using low power on the Bioruptor® Plus with 60 cycles of 60 seconds on, 15 seconds off at 20 °C. Samples were then ultra-centrifuged at 45000 rpm for 2 hours at 17 °C and subsequently analysed using UV – Vis – NIR and PL.

5.2.4 Carbon nanotube addition to liposomes

0.2 mg of chemically treated carbon nanotubes that were treated at 65 °C in the previous work in a 1 mg / mL solution were added to 1.8 mL of DMPC MLVs that were previously formed using the lipid film hydration method into a 50 mL polycarbonate tube with sonication aid. The samples were then sonicated for 15 cycles of 60 seconds on, 15 seconds off at 45 °C at high power. These were then analysed using DLS, UV – Vis – NIR and PL. This was performed in triplicate.

3 samples of 0.2 mL of chemically treated carbon nanotubes that were treated at 20 °C in the previous work in a 1mg / mL solution were sonicated for two sets of 60 cycles of 90 seconds on, 30 seconds off at 13 °C at high power. Then these samples were each added to 1.8 mL of DMPC MLVs formed using the lipid film hydration method into a 50 mL polycarbonate tube.

The samples were then sonicated for 15 cycles of 60 seconds on, 15 seconds off at 45 °C at high power. These were then analysed using DLS, UV – Vis – NIR and PL.

5.2.5 Analysis of carbon nanotubes

5.2.5.1 UV – Vis spectroscopy

Analysis was conducted using the Genesys 10s UV – Vis spectrometer (Thermo Fisher Scientific, Waltham, Massachusetts, United States) (Fernandes et al., 2015). The wavelength scanning range for the UV – Vis spectrometer was from 270 to 1100 nm using a plastic clear sided cuvette. The scan interval was set to 1 nm for the UV – Vis spectrometer. 3 mL of sample was placed into the cuvette and analysed after a blank of deionised water had been ran.

5.2.5.2 Photo luminescence mapping

PL analysis of carbon nanotubes has previously been described by Lutsyk et al and Tan et al (Lutsyk et al., 2016, Tan et al., 2007). Briefly, the fluorescence emission spectra at various excitation wavelengths were recorded using a Horiba NanoLog excitation–emission spectrofluorometer equipped with a nitrogen-cooled InGaAs array detector to generate PL excitation-emission maps (PLE maps), with the X-axis representing the wavelength of the PL emission, λ_{EM} , and the Y-axis representing the excitation wavelength, λ_{EX} . Entrance/exit slits of 14 nm in width were used for both the excitation and emission monochromators in the NIR PL measurements. Analysis was ran for the EM between 300 and 800 nm in increments of 5 nm and EM measured between 815 and 1450 nm using a 30 second integration time. The

time-resolved PL decays were measured using a LifeSpec II spectrofluorometer (Edinburgh Instruments Ltd., UK) to perform time-correlated single-photon counting (TCSPC) under excitation by a picosecond pulsed diode laser at 405 nm.

5.2.5.3 Size analysis using DLS

DLS analysis of carbon nanotubes was ran using a 100 μ L sample in 1.9 mL of distilled water and were characterised for their size and PDI using a Brookhaven Nanobrook 90 plus zeta (Scimed, Cheshire, UK).

5.2.5.4 TEM

The high resolution Transmission Electron Microscopy (TEM) images were obtained with the JEOL JEM2100F system equipped Field Emission Electron gun. The measurements were carried out at 100kV accelerating voltage. Additionally, the TEM's Energy Dispersive X-ray Spectrometer was used for element analysis of control CNT samples.

5.3 Results and Discussion

5.3.1 Chemical cutting and carboxylation of carbon nanotubes

5.3.1.1 Basic HiPco carbon nanotube data

There are two types of carbon nanotubes being investigated for carboxylated functionalisation; HiPco and CoMoCat. The HiPco tubes are a different product due to their increased dispersion in types of tubes, chiralities and sizes and also the much increased amount of catalyst and amorphous carbon found which can take 50 to 80 % of the overall weight. CoMoCat tubes are of much better quality with up to 95% of the weight being carbon nanotubes and at least 40% being of the single chirality of 6,5. To this end, the initial experiments with carboxylation were done with the HiPco tubes to ensure a method is created that can then be used with the CoMoCat tubes without wasting too many of the expensive CoMoCat tubes. To this end, HiPco tubes were investigated using SDBS to disperse them first of all to give a PL map and UV – Vis spectrum to compare to the carboxylated tubes, as shown in Figures 5.1 A - B. It was also important to check with the CoMoCat tubes whether any significant peaks were seen over and above the 1100 nm wavelength and this was done by using D₂O and shown in Figure 5.1 C – D. Figure 5.2 A – C shows the structure of these CoMoCat pristine carbon nanotubes. What these show are generally quite tight bundles of tubes and on closer inspection, the tube surface is not kinked and shows no sign of breakages with no short tubes shown and no sign of defects showing that non – covalent functionalisation has no effect on the actual carbon nanotube structure.

What these show is that HiPco carbon nanotubes are a lot more diverse in the CNT's chiralities. There are many CNT peaks within the 1400 nm zone, which need for analysis D₂O

to avoid water absorption in the samples. The CoMoCat samples do not show optical absorption beyond 1300nm and therefore can be ran using just normal distilled water.

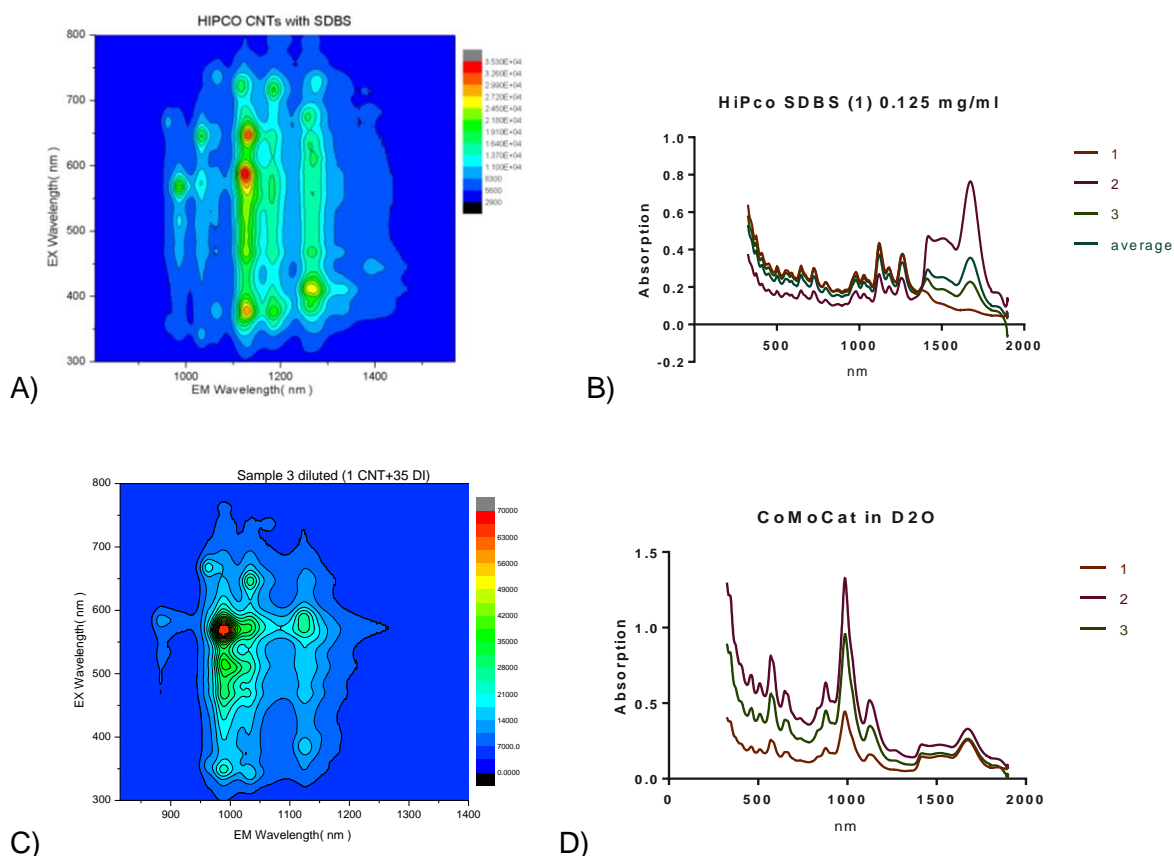


Figure 5.1: All runs were with Bioruptor® Plus, 0.01 % carbon nanotube concentration, 0.1% surfactant concentration, 13 or 40 °C water bath temperature, 2 mL sample size, Nalgene™ Polycarbonate tubes, cycle set up of 60 cycles of 60 seconds on, 15 seconds off, L power level. Ultracentrifugation for 150 minutes at 40, 000 G at 17°C. A) PL plot of a typical HiPco carbon nanotube sample dispersed with SDBS. B) UV – Vis – NIR plot of HiPco carbon nanotubes in D₂O. C) UV – Vis – NIR plot of CoMoCat carbon nanotubes in D₂O.

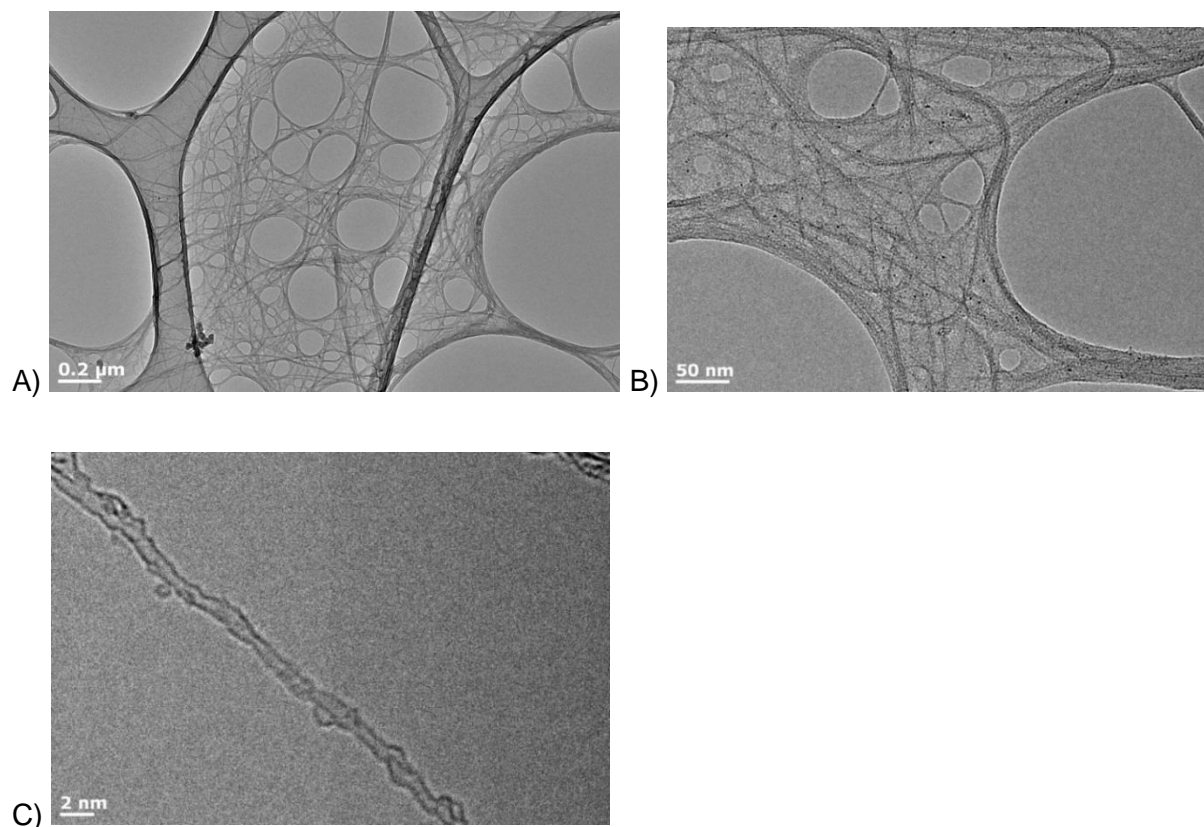


Figure 5.2: A - C: The CoMoCat sample initial - All runs were with Bioruptor® Plus, 0.01 % carbon nanotube concentration, 0.1% surfactant concentration, 13 or 40 °C water bath temperature, 2 mL sample size, Nalgene™ Polycarbonate tubes, cycle set up of 60 cycles of 60 seconds on, 15 seconds off, L power level. Ultracentrifugation for 150 minutes at 40, 000 G at 17°C. CoMoCat nanotubes, dispersed in NMP 0.01 mg / ml (standard US, hard plastic Eppendorf), centrifuged at 13400 rpm, 30 min, deposited on a standard TEM grid.

5.3.1.2 Carbon nanotubes carboxylated with oleum experiment

Carbon nanotube carboxylation using oleum and nitric acid was developed using the Chen et al paper as a starting point. As the results show, most of the samples show no peaks on the UV data or on the PL plots. The luminescence yield is however extremely sensitive to nanotube backbone integrities. In particular, the shortening of nanotube lengths creates a number of defect sites (including at the nanotube ends) such that carbon nanotube luminescence vanishes when the distance between defect sites becomes shorter than the exciton diffusion lengths. This implies that it is challenging to detect luminescent carbon nanotubes shorter than typically 100 nm at the single tube level (Gao et al., 2015).

The UV data in Figure 5.3 shows that none of samples have any peaks once they have been treated with acid, owing to the defects that are now present on the carbon nanotube surface. This compares to Figure 5.1 D which shows a number of peaks associated with the different chiralities found in the CoMoCat tubes. There are no peaks shown for the samples after centrifugation or after surfactant was added. This infers that the tubes have been heavily modified and defected.

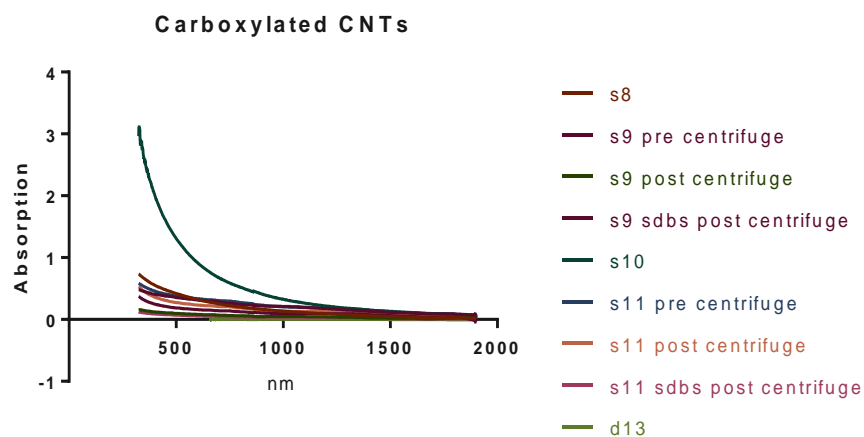


Figure 5.3: 40 mg initial carbon nanotube weight oleum: nitric acid carboxylation modification method, s8 at 65 °C sand bath temperature, s11 at 20 °C sand bath temperature, UV – Vis – NIR data for each of the samples.

The CoMoCat carbon nanotubes that were treated with the acid at 20 °C were shown to have no discernible chirality map using the PL as shown below in Figure 3.3. After centrifugation was completed, the PL data still showed no discernible peaks. After the surfactant SDBS was added however, there were discernible peaks correlating to the CoMoCat carbon nanotube shown before in Figure 5.4. What this shows is that the carbon nanotubes modified at 20 °C still retain some of their chirality and structure and therefore that the carbon nanotube structure is at least in some way still intact.

The TEM data in Figure 5.5 shows a reduced concentration compared to the initial tubes with a much looser spread of carbon nanotubes. This infers they are better dispersed compared to carbon nanotubes non-covalently dispersed with a surfactant such as SDBS. The close up shows the surface is more pockmarked than before which shows defects starting to appear.

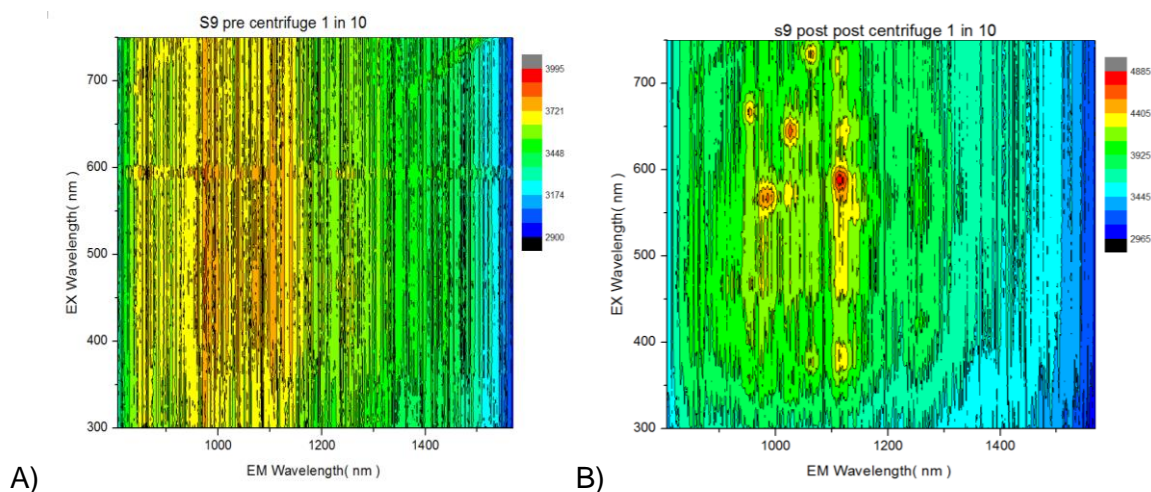


Figure 5.4: 40 mg initial CoMoCat carbon nanotube weight, oleum: nitric acid carboxylation modification method, s9 at 20 °C sand bath temperature. A) Pre centrifuge sample. B) Post centrifuge and surfactant addition sample.

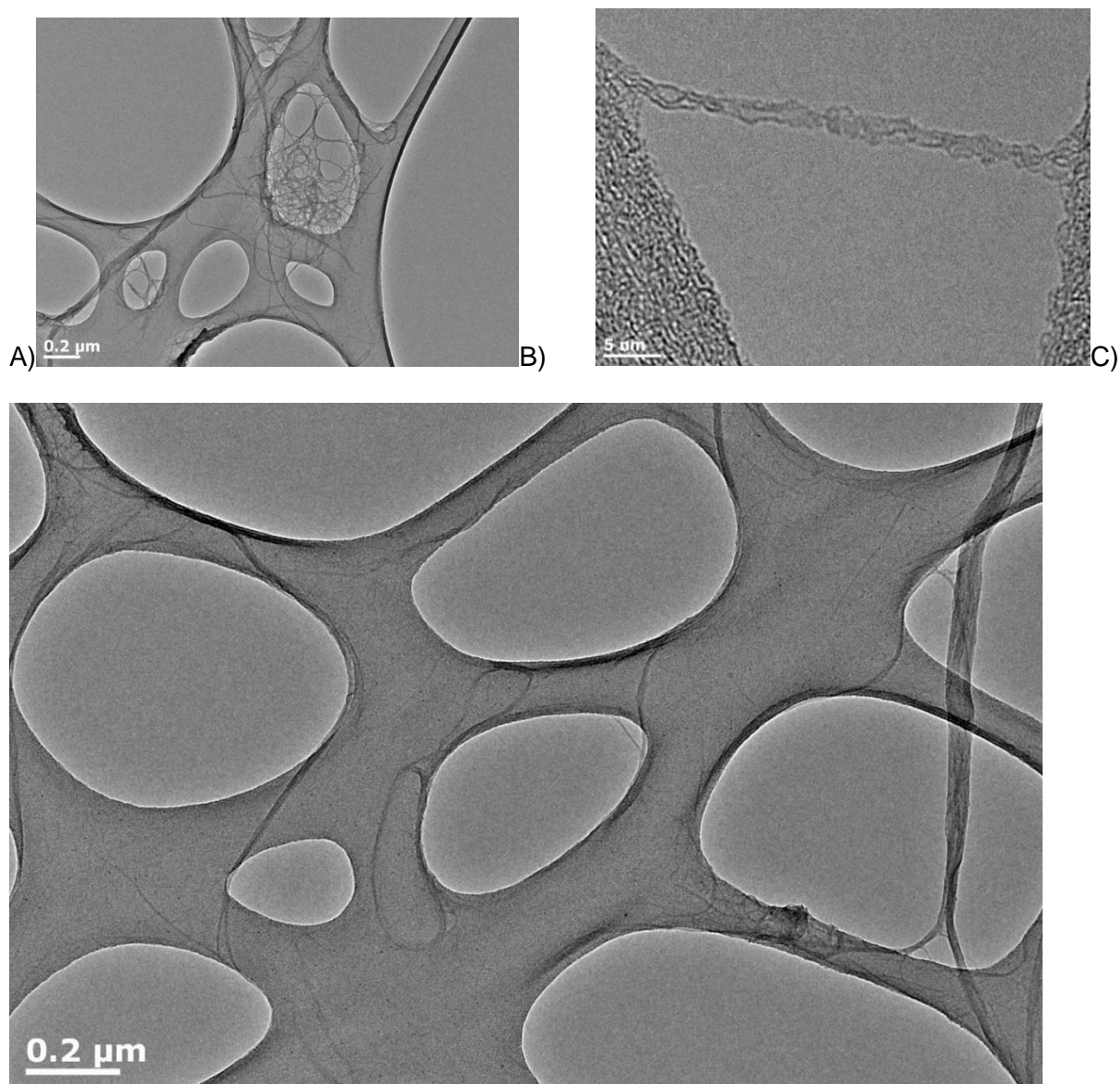


Figure 5.5: A - C: Sample D13_17 - CoMoCat nanotubes after oxidative treatment at 20 ° C. The dry sample was dispersed in NMP 0.01 mg / ml (standard US, Eppendorf's from hard plastic), centrifuged 13400 rpm, 30 min, deposited on a standard TEM grid. The tubes are tangled, but less dense than for initial CoMoCat, there are metal particles in them, but clearly there are less of them than in CoMoCat. Individual tubes are the same curves and dirty. Length of tubes: bundles of several microns, as in CoMoCat. It is possible to find individual bundles with 200 – 500 nanometres in length.

The CoMoCat carbon nanotubes shown below in Figure 5.6 show that at 65 °C sand bath temperature, there is again no PL peaks shown which again infers that the carbon nanotubes were defected. However what the TEM data shows is that the tubes were in fact more than defected but were almost completely destroyed at the higher temperature. Instead there are other amorphous carbon particles in solution.

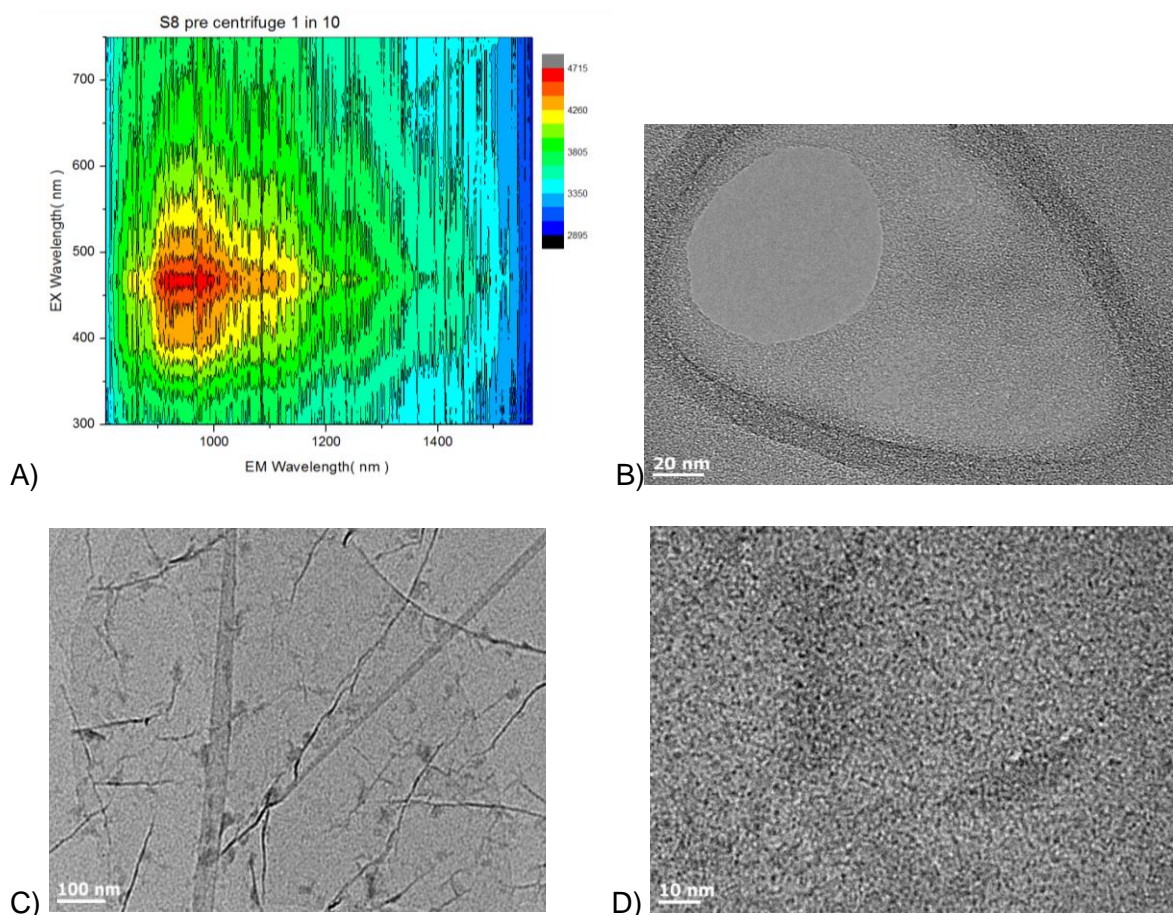


Figure 5.6 A - D: Sample s8_17. A) PL map of CoMoCat nanotubes after oxidative treatment at 65 ° C. B – D) TEM of CoMoCat nanotubes after oxidative treatment at 65 ° C. The dry sample (1 mg / ml) is dispersed (standard US, hard Eppendorf) in aqueous NaOH (10⁻³ mol / L), centrifuged 13400 rpm, 30 minutes (quite a lot of sediment - obviously aging of the sample, diluted 10-fold, again sound + centrifugation). The deposition is on the standard TEM grid (in Aston). We observe an amorphous matter that clogs the pores of the grating. Perhaps some dark particles, about 20 nm in size which are quickly deteriorating under the beam (so we could not make a good picture in high resolution).

HiPco carbon nanotubes were also dispersed at the 20 and 65 °C temperatures. Figure 5.7 A shows that at 65 °C the tubes again lost all the peaks which associate with the chirality of the HiPco tubes. Figure 5.7 B and C show that at 20 °C, tubes were again not seen after chemical treatment using the PL, but after centrifugation and addition of the surfactant SDBS, the tube map associated with the HiPco tubes was again seen which shows that again at 20 °C, the tubes are defected but do not lose all their chirality and therefore do not lose all of their structure.

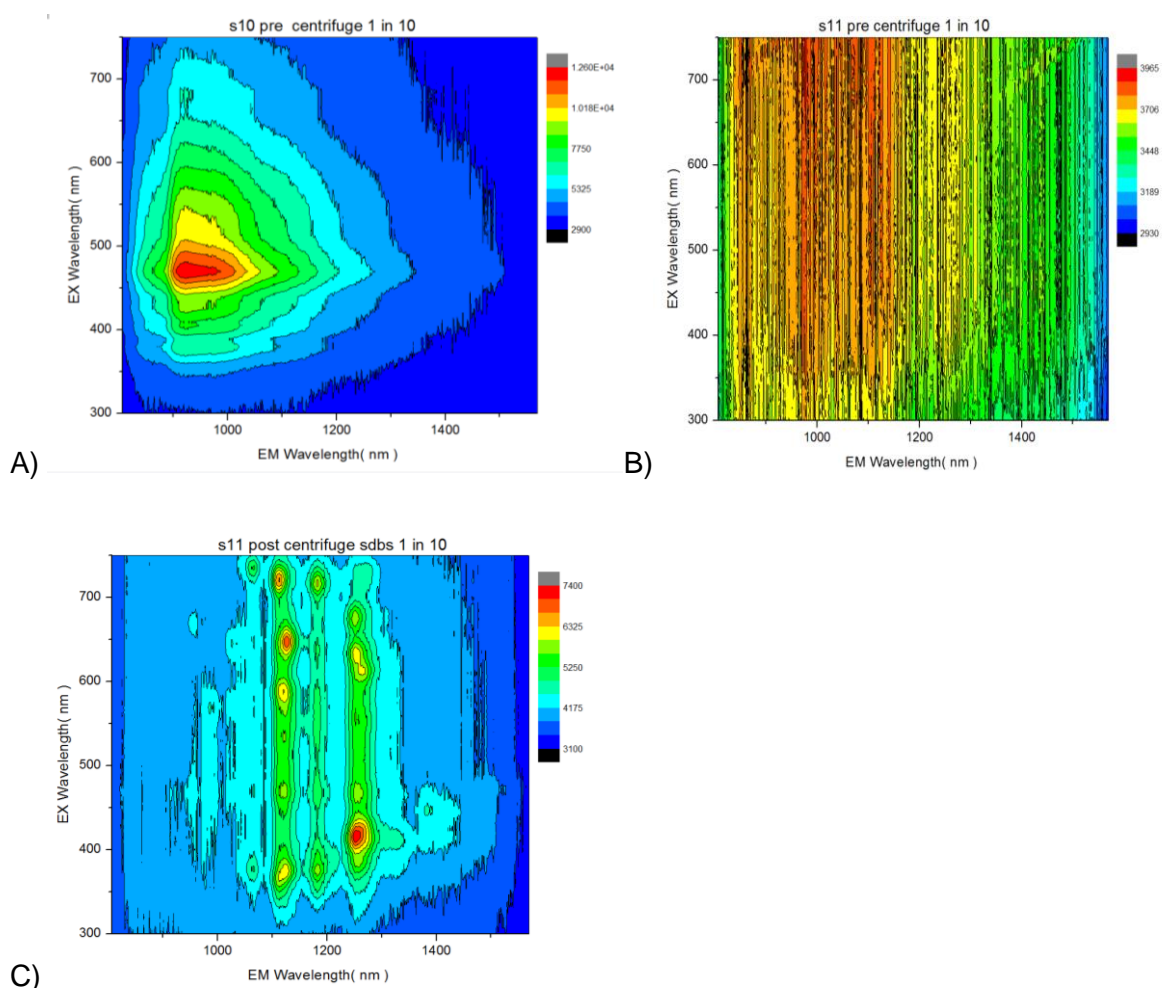
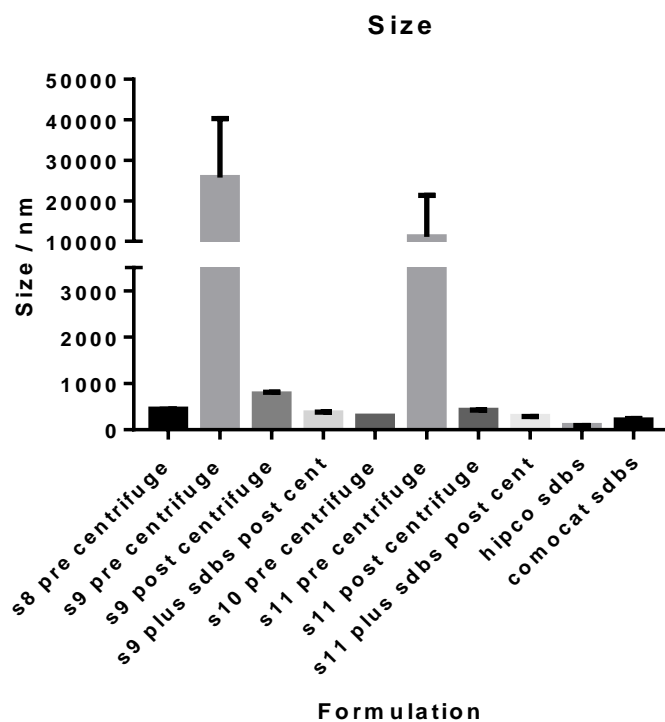
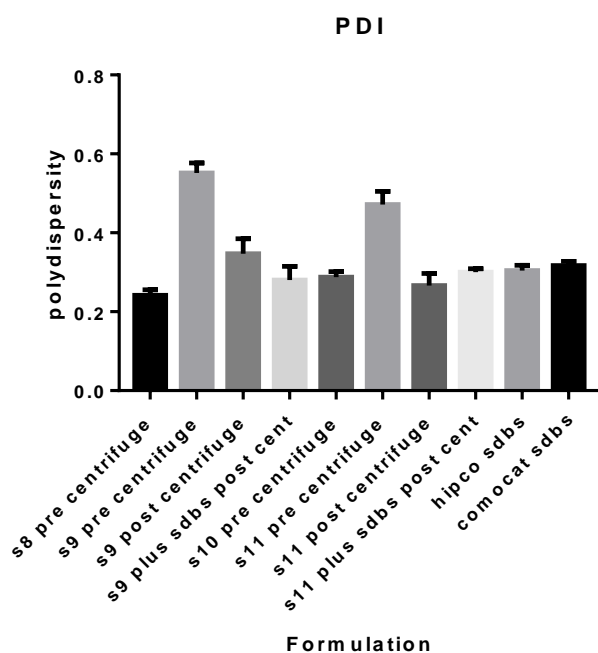


Figure 5.7: 40 mg initial HiPco carbon nanotube weight, oleum: nitric acid carboxylation modification method, s10 at 65 °C sand bath temperature, s11 at 20 °C sand bath temperature. A) Pre centrifuge sample. B) Post centrifuge sample. C) Post centrifuge with surfactant addition sample.

The size and PDI of the carbon nanotubes are shown below in Figure 5.8 to try to determine whether DLS can be used to show a reduction in carbon nanotube size. What was found was that carbon nanotubes dispersed at 20 °C showed a large size in the micron scale which would indicate a lower level of dispersion compared to those dispersed with surfactant. However once these were centrifuged, the size of the sample reduced down to the nano range indicating that large bundles of carbon nanotubes were removed through this process. However at 65 °C, the carbon nanotubes stayed in the nano range. This indicates that these were much more dispersed than those treated at 20 °C which follows the TEM data which showed that those treated at 65 °C were broken up but those at 20 °C were just defected and still retained most of their structure.



A)



B)

Figure 5.8: 40 mg initial carbon nanotube weight oleum: nitric acid carboxylation modification method, s8 and s10 at 65 °C sand bath temperature, s9 and s11 at 20 °C sand bath temperature. A) DLS data for all samples. B) PDI data for all samples.

5.3.2 Cutting of carbon nanotubes using the probe and bath sonicators

5.3.2.1 Carbon nanotubes cut using probe sonicator

Previous work has shown that by probe sonicating at high power for a long period of time, it is possible to cut carbon nanotubes down to sizes of below 100 nm. The aim of this work was to follow their methods and find out whether this is repeatable and whether we could use these in conjunction with the covalently functionalized carbon nanotubes and be able to get a direct comparison.

Figure 5.9 A and B shows that as you increase the power you get a much improved dispersion efficiency as well comparing 40 % to 100 %. This is also obvious as the dilution factors went from 1 in 10 to 1 in 50. What this data also showed was that as we increased the amount of time sonicated, an increase in the dispersion concentration was seen which is shown in the UV data in Figure 5.9 C. This goes above what was seen previously with the probe sonicator and above what was seen with any of the bath sonicator samples and therefore shows as you sonicate for longer and longer periods of time, more carbon nanotubes are dispersed. This was shown for up to 4 hours of sonication however no significant changes were seen in the samples or in the PL or UV – Vis – NIR data shown in Figure 5.10 which indicated that no changes to the structures of the carbon nanotubes were taking place. Without these changes or defects, the carbon nanotubes will remain in their long state and not be cut.

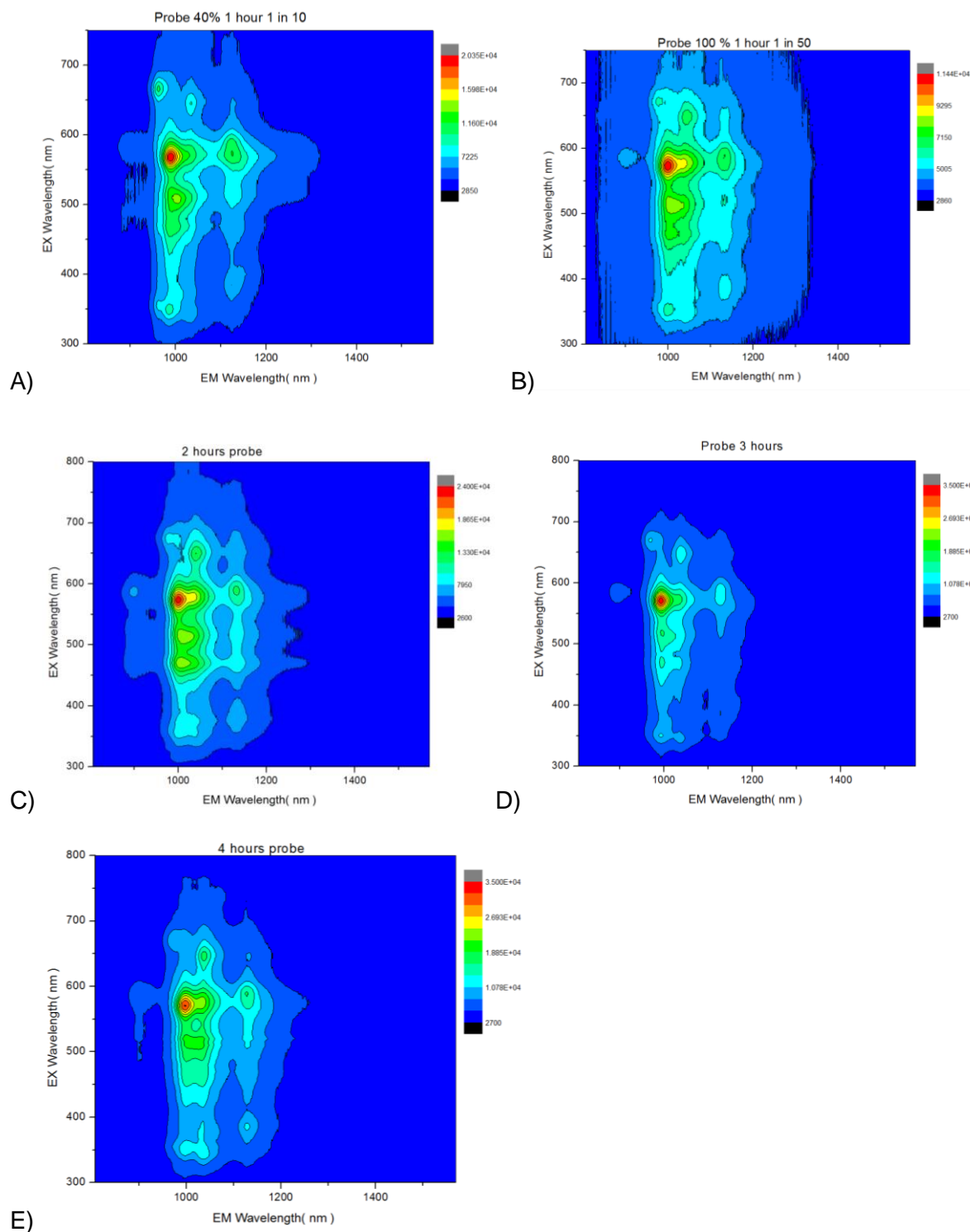
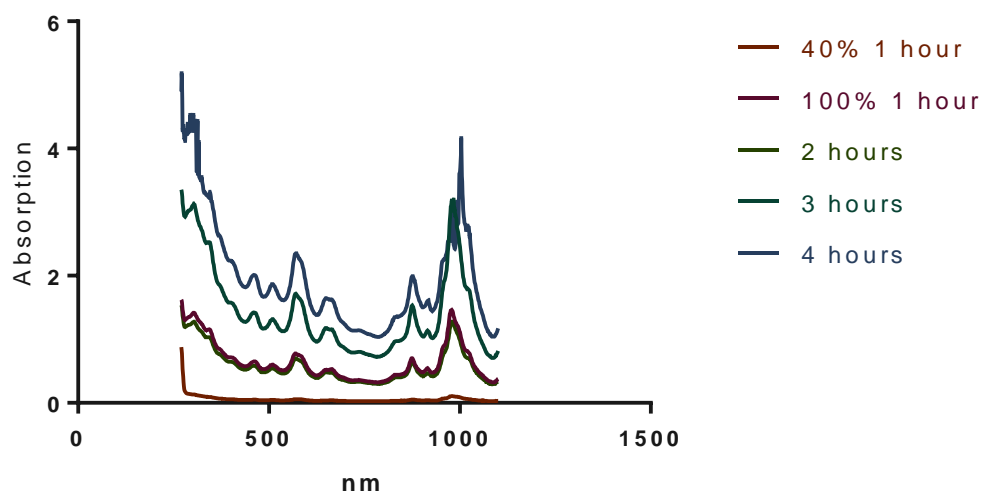


Figure 5.9: A) Probe sonicated carbon nanotubes after 1 hour at 40 %. B) Probe sonicated carbon nanotubes after 1 hour at 100 %. C) Probe sonicated carbon nanotubes after 2 hours. D) Probe sonicated carbon nanotubes after 3 hours. E) Probe sonicated carbon nanotubes after 4 hours.

probe sonication cutting carbon nanotubes



F)

Figure 5.10: F. DLS of probe sonicated carbon nanotubes from 1 to 4 hours.

5.3.2.2 Carbon nanotube cutting using the bath

Similar experiments were carried out using the bath sonicator, the Bioruptor® Plus. Previous discussions with Diagenode had limited the time the sonicator could be used in one sitting before allowed to rest and cool as approximately 3 hours. Therefore up to 3 sets of sonication were investigated with either 1, 2 or 3 sets of 60 cycles of 60 seconds on, 15 seconds off.

The results below show in Figure 5.11 no significant changes in any of the PLE maps. The UV data showed that there was an increase in carbon nanotube concentration after 2 sets but then it reduced again after 3 sets. This could be due to the increase in time allowing more carbon nanotubes to be dispersed, similar to the data shown with the probe sonicator. The reduction could then be attributed to the surfactant lapsing off the surface of the carbon nanotubes as the increase in time means the machine heats up and the solution within the plastic tube heats up also.

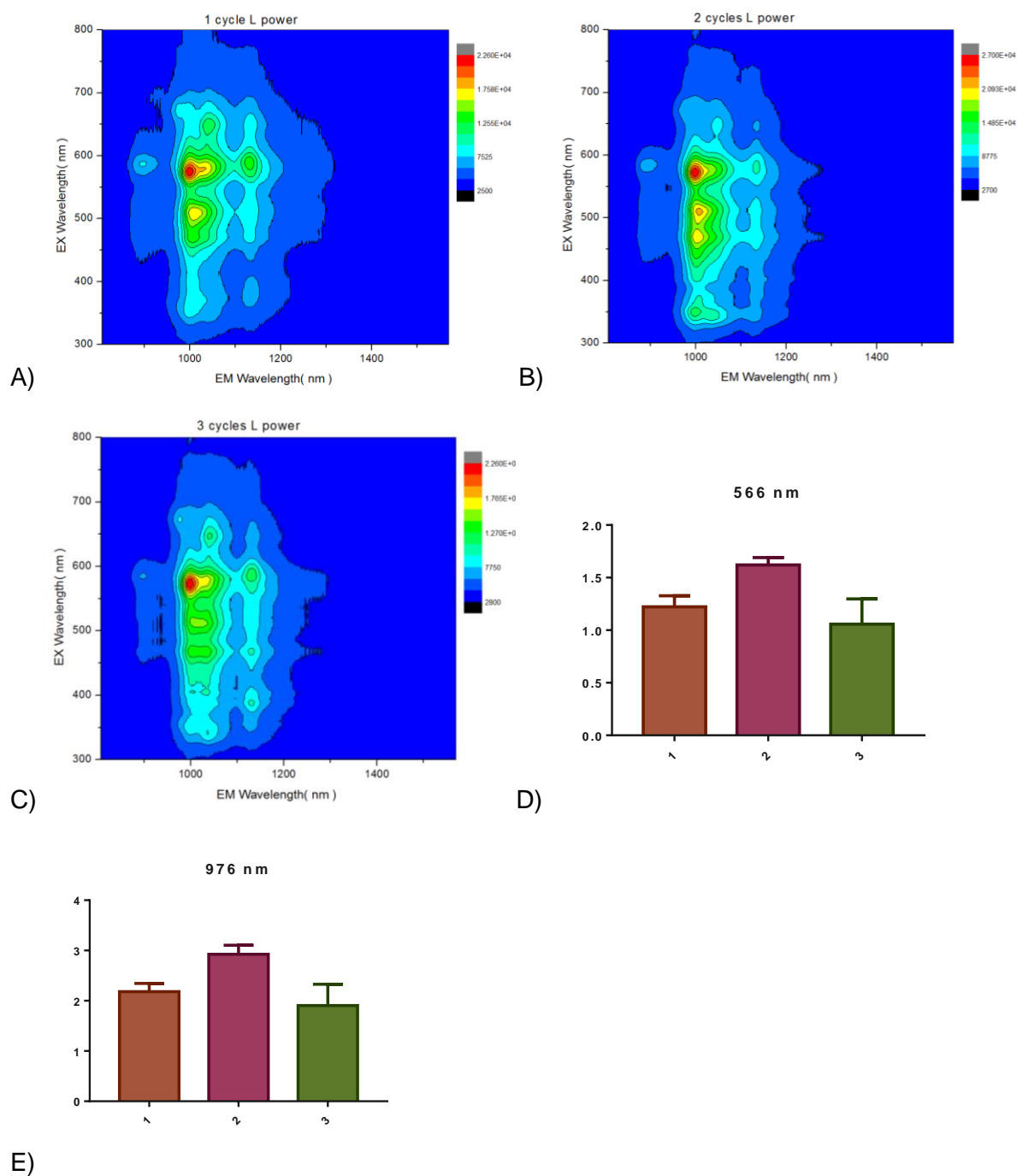


Figure 5.11: A) Bath sonicated carbon nanotubes after 1 cycle. B) Bath sonicated carbon nanotubes after 2 cycles. C) Bath sonicated carbon nanotubes after 3 cycles. D) UV – Vis peak heights at 566 nm. E) UV – Vis heights at 976 nm.

5.3.3 Addition of carbon nanotubes to liposomes

The final part of this work was to try and combine the chemically treated carbon nanotubes with liposomes to form a complex. The method employed involved forming MLVs using the lipid film hydration method and then sonicating these with the carbon nanotubes. The hope was that as these were sonicated and broken up and reduced in size to form SUVs, these would also interact with the carbon nanotubes allowing the complex to form with the tubes either inside the liposome, in the lipid bilayer or on the outside of the liposome.

The results below in Figure 5.12 showed that the size of the liposomes were reduced to between 100 and 200 nm in diameter. There was no significant size difference shown between the 65 °C treated tubes and the 20°C treated tubes once added to the liposomes and the solutions were clear. The UV data in Figure 5.12 C and PL data in Figure 5.13 both show that there are no carbon nanotubes present that are free of defects or at least they are unable to be detected using these methods.

What these initial results showed was that the addition of carbon nanotubes to a liposome formulation made using the Bioruptor bath sonication systems does not adversely affect the liposomes and does form a clear solution that can be analysed. What the results showed for the thesis is that carbon nanotubes and liposomes could be sonicated together. The next step would be to analyse these using TEM and other imaging software to investigate how these two entities have interacted, if at all, through this process. This would then inform whether the carbon nanotubes are located within the liposomes or not. If they were, then this would show that sonication could be used as a simple method of forming the complex that was desired for this thesis and if not, then other methods such as covalent functionalisation and attachment would be investigated as alternate methods for forming the liposome – carbon nanotube complex.

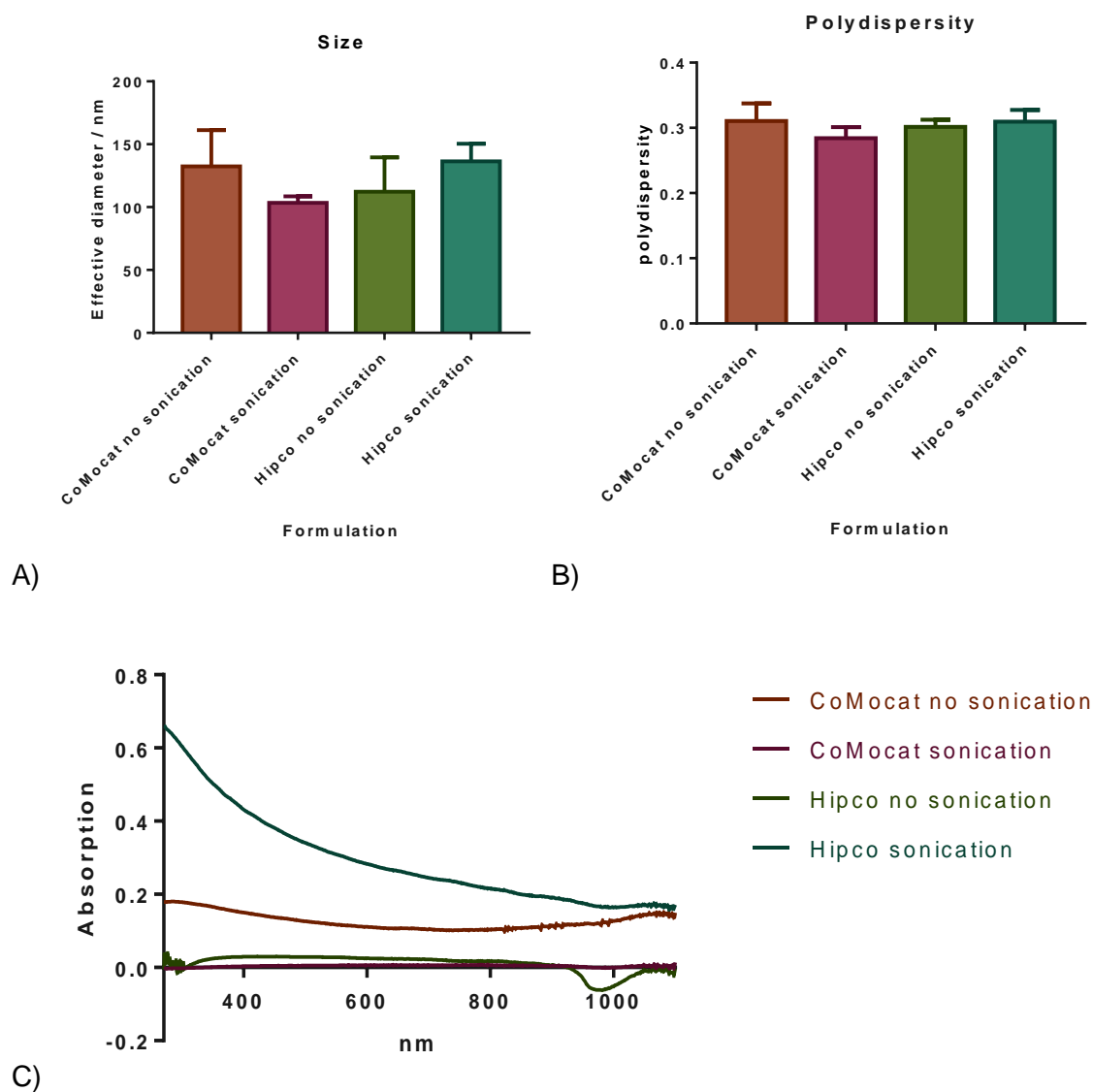


Figure 5.12: A) DLS size of liposomes in conjunction with carbon nanotubes either sonicated beforehand or not. B) PDI of liposomes in conjunction with carbon nanotubes either sonicated beforehand or not. C) UV – Vis data showing both types of carbon nanotubes before or after sonication.

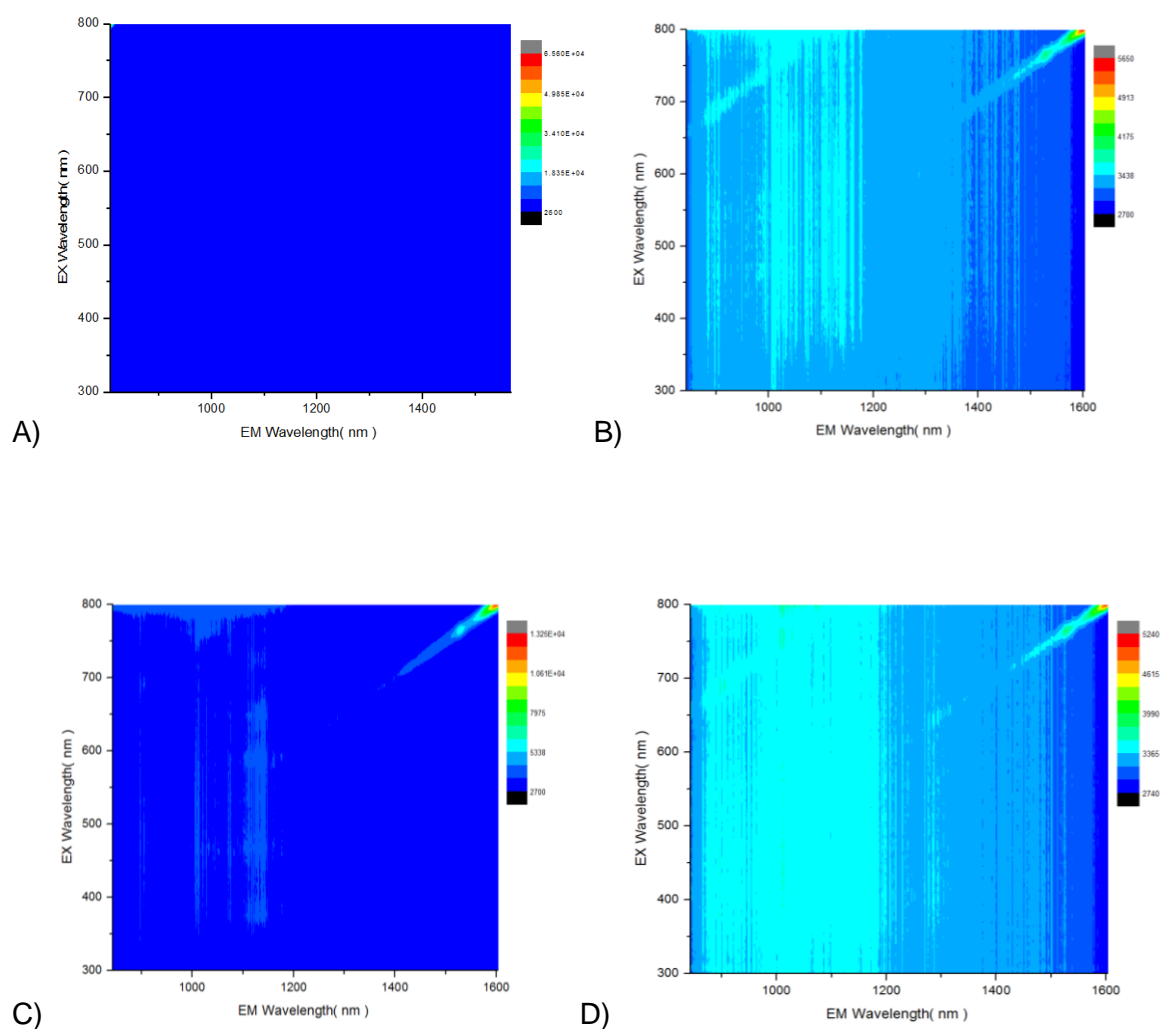


Figure 5.13: A) carbon nanotubes plus liposomes with no sonication – HiPco carbon nanotubes. B) Carbon nanotubes plus liposomes with no sonication – CoMoCat carbon nanotubes. C) Carbon nanotubes plus liposomes with sonication – HiPco carbon nanotubes. D) Carbon nanotubes plus liposomes with sonication – CoMoCat carbon nanotubes.

5.4 Conclusions

In conclusion, it was shown that carbon nanotubes could be chemically treated using oleum and nitric acid in combination with heat. These tubes were shown to become defected with treated at 20 °C but their structure was destroyed when treated at 65 °C. This is important to know as this implies that by altering the treatment temperature, different carbon structures and different rates of defect could be tuned with the carbon nanotubes. This would then allow a multitude of different applications to be investigated depending on the structure required.

It was also shown that the Bioruptor® Plus could not be used for carbon nanotube cutting as the power and time required to do so is beyond the limits of the machine. However this could be used if the carbon nanotubes are already defected, such as those chemically treated at 20 °C.

6. Final discussion and conclusion

6.1 Final conclusions

6.1.1 Liposome formation and size reduction

Liposome size reduction is an important method as it allows for liposomes to become more homogeneous in size and composition and for them to hide from the immune system. This lack of detection means the liposomes can reach the site of action and deliver their drug payload before they are ingested and removed by the immune system. For vaccine development the size of liposomes can elicit different immune responses which therefore means some size reduction from the MLV size range is still necessary. For example, Henriksen-Lacey et al were able to show that different vesicle sizes gave rise to differences in cell proliferation, IL – 10 production and the movement of liposomes to the lymph nodes (Henriksen-Lacey et al., 2011).

There are a number of methods for reducing the size of liposomes including extrusion, high shear mixing and sonication. Sonication is split into two methods; probe sonication and bath sonication. Probe sonication is more widely used due to the low cost of equipment, high power exerted by the probe and quick turnaround of samples. However problems occur with contamination from titanium particles from the probe, a lack of proper temperature control beyond the use of an ice bath and only being able to do one at a time. Bath sonication seems to overcome these problems by sonicating samples in plastic tubes within a temperature regulated bath. This removes the problems of throughput, temperature degradation and contamination. However previous bath sonicators have struggled to have the power required to break apart the liposomes allowing them to reform into the smaller spheres.

This work showed that liposomes could be reduced in size using Diagenodes Bioruptor® bath sonication systems. Once the liposomes were formed using the lipid film hydration method, MLV were successfully reduced in size using these systems. All systems were shown to

reduce the liposomes to sub-micron size and some conditions were shown to reduce liposome size to below 100 nm. This would mean these liposomes and therefore these systems could be used to reduce liposomes down to a size where they could be used for drug delivery. Many factors were shown to influence the rate at which liposomes were reduced in size. These included time, power level, concentration, volume, temperature, and plastic choice. These liposomes were also produced in a sealed environment inside plastic tubes ranging in size from 1.5 mL up to 50 mL with sample volumes ranging from 0.1 mL up to 5 mL with between 3 and 6 samples sonicated in one go. This range of sample volumes allows for initial testing to be done with very small volumes and therefore keeping costs reduced and then once a formulation is decided upon, the sample volume can then be increased using the same Bioruptor® system. The temperature control the water bath brings also allows for many different lipids to be used without the fear of lipid degradation occurring due to the sample being heated up. With the Bioruptor® systems, liposomes can be sonicated from just above freezing up to approximately 50 °C.

6.1.2 Bioruptor® protocols

The Bioruptor® Plus bath sonication system was used to test out drug loading using example lipophilic drugs. These were albendazole, carbamazepine and propofol. It was shown with varying degrees of success that this system could be used to load liposomes with a lipophilic drug embedded into the bilayer. The most successful of the three was carbamazepine using methods 2 and 3. These methods produced better results as the drug was added at a late stage. This meant that there was less chance of the drug being lost due to the number of steps in the process. Albendazole had difficulty being dispersed in the water based liposomal solution and was found to instead coat the inside of the plastic tube in which it was being sonicated. This then lead to a reduced loading concentration. Propofol was also found to

interact with the plastic tube and in fact begin to degrade the tube itself. Though the drug loading itself was not successful and could not be taken any further, it was shown that the Bioruptor® could be used for drug loading. It is important to note that unlike probe sonication where a glass bottle is used, drugs should be checked to make sure they do not interact with the plastic tubes being used. That being said, the introduction of a water bath and lack of a titanium probe does make this process viable for further work as these benefits would still be present if a more suitable drug is used.

During my time at Diagenode, I spent some time working on bath sonicator characterisation. This characterisation is important because by understanding what happens during the sonication process, changes can be made to the design or the method that can improve the sonication process and therefore the results achieved. This can be done through a number of methods and the one we looked at was by following the process of I_2 formation from the free radical of iodine obtained after sonication of a KI solution in the presence of a catalyst. The process of sonication produces H_2O_2 which interacts with the KI to form the iodine and therefore change the colour from clear to yellow.

What the results showed was that a smaller sample volume gave more complete sonication. The reduced sample volume means that there is more of the finite quanta of sonic energy to be given per mL to the sample. This in turn increases cavitation and allows for an increase in iodine production. There was no significant differences seen between the samples when sonicated in two different types of plastic and no significant difference either between the low and high powered samples. A decrease in temperature saw a decrease in sonication efficiency as is expected as the molecules within the sample move slower at a lower temperature. However at a much higher temperature not conducted during this study, there would also be a decrease in sonication efficiency as too high a temperature means that the cavitation effect actually starts to decrease. This feeds back into the liposome formulation work as too high a temperature would mean that liposomes would not be broken down and

reduced in size as effectively which means high transition temperature lipids would be difficult to break down efficiently using these systems.

Another important use for the Bioruptor® bath sonication systems is in the extraction of DNA. Therefore efficiency tests were carried out to see whether more components for the Diagenode DNA extraction kit could be sourced in house and to see whether further improvements in the process could be made. What the results showed was that the addition of a filter lead to reduced sample prep time but also a reduced DNA concentration at the end. The choice of buffer results showed an improved DNA extraction from the new buffers although these results were not significant. Finally the longer the samples were left to shake, the larger the DNA extraction concentration was found to be.

6.1.3 Non covalent functionalisation of carbon nanotubes

Water dispersion of carbon nanotubes was shown to be successful using a number of different Bioruptor® bath sonication systems. There were a number of different factors that were shown to influence carbon nanotube dispersion efficiency.

Temperature was also shown to affect carbon nanotube dispersion efficiency with either too high or too low a temperature reducing the efficacy. The too low temperature means there is not enough energy in the system to break apart the surfactant molecules and carbon nanotube molecules to allow them to disperse successfully. However too high a temperature means too much energy in the system. This high energy means that the surfactant has a tendency to lapse away from the carbon nanotube surface that reduces the carbon nanotube dispersion efficiency.

The choice of surfactant was shown to greatly affect the dispersion efficiency of the carbon nanotubes. This is due to the size and structure of the surfactant molecules, the presence or

absence of benzene rings that can associate with the carbon nanotube structure using π - π bonding in the case of SDBS compared to SDS. However these surfactants aren't suitable for biological uses and therefore alternatives were investigated. DMPC and MPC are both phospholipids with either one or two fatty acid chains. The presence of two chains in DMPC leads to a cylindrical molecular shape which is unsuitable for carbon nanotube dispersion as was shown with the results. However MPC has a more conical shape which allows for them to form around the carbon nanotube sphere and disperse the carbon nanotube successfully. It was also shown that the SDBS and MPC dispersed carbon nanotubes were more stable over a long period of time, in this case 6 months, compared to the SDS dispersed carbon nanotubes. MPC was directly compared to SDS and SDBS and was shown to have similar dispersion efficacy compared to SDS which infers that the benzene ring associated with SDBS is vital for increasing dispersion efficacy.

Finally probe sonication was also shown to be a viable way of dispersing carbon nanotubes with the aid of an ice bath. The use of an ice bath is required as probe sonication leads to a quick increase in sample temperature which previous work showed a decrease in carbon nanotube dispersion efficiency.

6.1.4 Covalent functionalisation of carbon nanotubes

Covalent functionalisation of carbon nanotubes was achieved through the use of nitric acid and oleum in combination with heat. The tubes were either defected at lower temperatures or completely destroyed through higher temperatures. This is important as defects are required to start the shortening process but too much heat means the tubes are not only shortened but are broken down into small carbon graphene pieces.

It was also shown that the Bioruptor® Plus could not be used for carbon nanotube cutting as the power and time required to do so is beyond the limits of the machine. However, this could be used if the carbon nanotubes are already defected, such as those chemically treated at 20 °C.

6.2 Further work

Previously published research has looked into creating complexes formed from carbon nanotubes and liposomes. These have included nanotrains with liposomes attached to the surface of a carbon nanotube and nanotube porins which have been carbon nanotubes inserted into the bilayer of a liposome. Previous work has also shown that carbon nanotubes could be seen as a valid adjuvant due to their ability to increase the immune system response (Gottardi and Douradinha, 2013). This is dependent on the carbon nanotubes size, chirality, number of layers and surface modifications. Liposomes meanwhile have been shown to allow a controlled slow release of an antigen and improve antigen stability and presentation of the antigen to the immune system.

My PhD is a BBSRC case project sponsored by Diagenode and focussed on formulating new protocols for the formation of liposomes using their in house Bioruptor® bath sonicator systems. This was successful and was shown to be comparable to probe sonication whilst also allowing for more samples to be sonicated per run and for larger volumes to be sonicated as well. The same bath sonicators were then also shown to be able to disperse carbon nanotubes using surfactants including SDBS and MPC which would allow for biologically safe surfactant dispersed carbon nanotubes to be used in conjunction with liposomes formed using the same bath sonicator.

Further work would look into formulating several different liposome carbon nanotube complexes and to investigate their ability to deliver vaccines with the carbon nanotube acting

as the adjuvant. Several complexes could be formulated initially with carbon nanotubes inside the liposome or attached to the outside and with individual complexes and also nanotrains. These carbon nanotubes would be either covalently or non-covalently functionalised and some would be shortened through a combination of chemical and/or mechanical means. Graphene oxide and reduced graphene oxide would also be complexed with the liposomes to see whether this carbon based chemical could be used in place of the carbon nanotubes. This is because graphene oxide can be directly dispersed with water, shows less toxicity compared to carbon nanotubes and has been shown previously to be a valid adjuvant for a vaccine delivery system (Xu et al., 2016). The formulations that are successfully made during this time will then be used for the in vitro work.

The complexes would then be loaded with an example antigen and tested against the component parts with and without the antigen to determine whether the complexes give an increased cell response compared to the liposomes or carbon nanotubes on their own. This would be done to show that the complex as a whole would give a larger immune response than just its component parts. This would be done through in vitro work with the ability of the complexes to attract the immune system components, how well the antigen is ingested, and the toxicology profile of the complexes being investigated.

Finally, in vivo work would comprise of comparing the complexes against both their components and other possible market vaccine delivery systems to see whether there is an improvement on the efficacy compared to current systems as well as migration and ingestion of the antigen and toxicology of the complex.

7. References

- AHMED, K., GRIBBON, P. N. & JONES, M. N. 2002. The application of confocal microscopy to the study of liposome adsorption onto bacterial biofilms. *J Liposome Res*, 12, 285-300.
- AKBARZADEH, A., REZAEI-SADABADY, R., DAVARAN, S., JOO, S. W., ZARGHAMI, N., HANIFEHPOUR, Y., SAMIEI, M., KOUHI, M. & NEJATI-KOSHKI, K. 2013. Liposome: classification, preparation, and applications. *Nanoscale Res Lett*, 8, 102.
- AL FARAJ, A., SHAIK, A. S., RATEMI, E. & HALWANI, R. 2016. Combination of drug-conjugated SWCNT nanocarriers for efficient therapy of cancer stem cells in a breast cancer animal model. *Journal of Controlled Release*, 225, 240-251.
- ALBERTS, B., JOHNSON, A., LEWIS, J., MORGAN, D., RAFF, M., ROBERTS, K. & WALTER, P. 2015. *Molecular Biology of the Cell*, Garland Science.
- ALI, F., REINERT, L., LEVEQUE, J. M., DUCLAUX, L., MULLER, F., SAEED, S. & SHAH, S. S. 2014. Effect of sonication conditions: solvent, time, temperature and reactor type on the preparation of micron sized vermiculite particles. *Ultrason Sonochem*, 21, 1002-9.
- ALI, M. H., MOGHADDAM, B., KIRBY, D. J., MOHAMMED, A. R. & PERRIE, Y. 2013. The role of lipid geometry in designing liposomes for the solubilisation of poorly water soluble drugs. *Int J Pharm*, 453, 225-32.
- ALONSO, M. J. & GARCIA-FUENTES, M. 2014. *Nano-Oncologicals: New Targeting and Delivery Approaches*, Springer International Publishing.
- ANDREASAN, L., WOOD, G. AND CHRISTENSEN, D. . 2013. *Methods for producing liposomes*. WO 2013004234 A2.
- ANSARI, R., DALIRI, M. & HOSSEINZADEH, M. 2013. On the van der Waals interaction of carbon nanotubes as electromechanical nanothermometers. *Acta Mechanica Sinica*, 29, 622-632.
- ASGARI, M. & LOHRASBI, E. 2013. Comparison of Single-Walled and Multiwalled Carbon Nanotubes Durability as Pt Support in Gas Diffusion Electrodes. *ISRN Electrochemistry*, 2013, 7.
- ASHCROFT, J. M., HARTMAN, K. B., MACKEYEV, Y., HOFMANN, C., PHEASANT, S., ALEMANY, L. B. & WILSON, L. J. 2006. Functionalization of individual ultra-short single-walled carbon nanotubes. *Nanotechnology*, 17, 5033-5037.
- ATTAL, S., THIRUVENGADATHAN, R. & REGEV, O. 2006. Determination of the Concentration of Single-Walled Carbon Nanotubes in Aqueous Dispersions Using UV-Visible Absorption Spectroscopy. *Analytical Chemistry*, 78, 8098-8104.
- AVANTI. 2015. *Preparation of Liposomes* [Online]. Available: http://www.avantilipids.com/index.php?option=com_content&view=article&id=1384&Itemid=372 [Accessed 11/02/15 2015].
- AVANTI. 2018. *Phase transition temperatures* [Online]. Available: <https://avantilipids.com/tech-support/physical-properties/phase-transition-temps/> [Accessed 31/01/18].
- AZIZ, M. A., PARK, S., JON, S. & YANG, H. 2007. Amperometric immunosensing using an indium tin oxide electrode modified with multi-walled carbon nanotube and poly(ethylene glycol)-silane copolymer. *Chemical Communications*, 2610-2612.
- BAJORIA, R. & CONTRACTOR, S. F. 1997. Effect of Surface Charge of Small Unilamellar Liposomes on Uptake and Transfer of Carboxyfluorescein across the Perfused Human Term Placenta. *Pediatr Res*, 42, 520-527.
- BAK, S. T., STAUNSTRUP, N. H., STARNAWSKA, A., DAUGAARD, T. F., NYENGAARD, J. R., NYENGAARD, M., BORGLUM, A., MORS, O., DORPH-PETERSEN, K. A. & NIELSEN, A. L. 2016. Evaluating the Feasibility of DNA Methylation Analyses Using Long-Term Archived Brain Formalin-Fixed Paraffin-Embedded Samples. *Mol Neurobiol*.
- BALASUBRAMANIAN, K. & BURGHARD, M. 2005. Chemically Functionalized Carbon Nanotubes. *Small*, 1, 180-192.
- BANGHAM, A. D., STANDISH, M. M. & WATKINS, J. C. 1965. Diffusion of univalent ions across the lamellae of swollen phospholipids. *Journal of Molecular Biology*, 13, 238-IN27.

- BARBEAU, J., CAMMAS-MARION, S., AUVRAY, P. & BENVEGNI, T. 2011. Preparation and Characterization of Stealth Archaeosomes Based on a Synthetic PEGylated Archaeal Tetraether Lipid. *Journal of Drug Delivery*, 2011, 11.
- BELLUCCI, S. 2005. Carbon nanotubes: physics and applications. *physica status solidi (c)*, 2, 34-47.
- BERGER, N., SACHSE, A., BENDER, J., SCHUBERT, R. & BRANDL, M. 2001. Filter extrusion of liposomes using different devices: comparison of liposome size, encapsulation efficiency, and process characteristics. *International Journal of Pharmaceutics*, 223, 55-68.
- BHARDWAJ, U. & BURGESS, D. J. 2010. Physicochemical properties of extruded and non-extruded liposomes containing the hydrophobic drug dexamethasone. *International Journal of Pharmaceutics*, 388, 181-189.
- BREVENOV, M., MUNDT, J., BENFIELD, J., TREAT-CLEMONS, L., KALUSCHE, G., MEREDITH, J., PORTER, G., FURTADO, M. R. & SHEWALE, J. G. 2009. Automated Extraction of DNA from Forensic Sample Types Using the PrepFiler Automated Forensic DNA Extraction Kit. *JALA: Journal of the Association for Laboratory Automation*, 14, 294-302.
- BRISCHETTO, S., TORNABENE, F., FANTUZZI, N. & BACCIOCCHI, M. 2015. Refined 2D and Exact 3D Shell Models for the Free Vibration Analysis of Single- and Double-Walled Carbon Nanotubes. *Technologies*, 3, 259.
- CAGDAS, F. M., ERTUGRAL, N., BUCAK, S. & ATAY, N. Z. 2011. Effect of preparation method and cholesterol on drug encapsulation studies by phospholipid liposomes. *Pharm Dev Technol*, 16, 408-14.
- CHAPMAN, C. J., ERDAHL, W. E., TAYLOR, R. W. & PFEIFFER, D. R. 1991. Effects of solute concentration on the entrapment of solutes in phospholipid vesicles prepared by freeze-thaw extrusion. *Chemistry and Physics of Lipids*, 60, 201-208.
- CHE, G., LAKSHMI, B. B., FISHER, E. R. & MARTIN, C. R. 1998. Carbon nanotubule membranes for electrochemical energy storage and production. *Nature*, 393, 346-349.
- CHEN, G., SEKI, Y., KIMURA, H., SAKURAI, S., YUMURA, M., HATA, K. & FUTABA, D. N. 2014. Diameter control of single-walled carbon nanotube forests from 1.3–3.0 nm by arc plasma deposition. *Scientific Reports*, 4, 3804.
- CHEN, R. F. & KNUTSON, J. R. 1988. Mechanism of fluorescence concentration quenching of carboxyfluorescein in liposomes: energy transfer to nonfluorescent dimers. *Anal Biochem*, 172, 61-77.
- CHEN, Z., KOBASHI, K., RAUWALD, U., BOOKER, R., FAN, H., HWANG, W. F. & TOUR, J. M. 2006. Soluble ultra-short single-walled carbon nanotubes. *J Am Chem Soc*, 128, 10568-71.
- COATES, C. J., KELLY, S. M. & NAIRN, J. 2011. Possible role of phosphatidylserine-hemocyanin interaction in the innate immune response of *Limulus polyphemus*. *Developmental and Comparative Immunology*, 35, 155-163.
- COLEMAN, J. N., KHAN, U., BLAU, W. J. & GUN'KO, Y. K. 2006. Small but strong: A review of the mechanical properties of carbon nanotube–polymer composites. *Carbon*, 44, 1624-1652.
- DAS, D. 1978. *Biochemistry*, Academic Publishers.
- DE VOLDER, M. F. L., TAWFICK, S. H., BAUGHMAN, R. H. & HART, A. J. 2013. Carbon Nanotubes: Present and Future Commercial Applications. *Science*, 339, 535-539.
- DEBRA A. DEDERICH, G. O., TONI GARNER, AMANDA DENN, ANGELICA SUTTON, MICHAEL ESCOTTO, ASHLEY MARTINDALE, OLIVER DELGADO, DONNA M. MUZNY, RICHARD A. GIBBS, MICHAEL L. METZKER; , VOLUME 30, ISSUE 7, 1 APRIL 2002, PAGES E32, 2002. Glass bead purification of plasmid template DNA for high throughput sequencing of mammalian genomes. *Nucleic Acids Research*, 30.
- DEMENTO, S. L., SIEFERT, A. L., BANDYOPADHYAY, A., SHARP, F. A. & FAHMY, T. M. Pathogen-associated molecular patterns on biomaterials: a paradigm for engineering new vaccines. *Trends in Biotechnology*, 29, 294-306.

- DIAGENODE. *FFPE extraction kit for Bioruptor Pico* [Online]. Available: <https://www.diagenode.com/en/p/ffpe-dna-extraction-kit-bioruptor-pico-50-rxns> [Accessed].
- DIAGENODE. 2015. *Bioruptor systems* [Online]. Available: <http://www.diagenode.com/en/catalog/shearing-technologies-54/bioruptor--55/> [Accessed 09/03/15 2015].
- DIETRICH, J., ANDREASEN, L. V., ANDERSEN, P. & AGGER, E. M. 2014. Inducing Dose Sparing with Inactivated Polio Virus Formulated in Adjuvant CAF01. *PLoS ONE*, 9, e100879.
- DILLON, A. C., JONES, K. M., BEKKEDAH, T. A., KIANG, C. H., BETHUNE, D. S. & HEBEN, M. J. 1997. Storage of hydrogen in single-walled carbon nanotubes. *Nature*, 386, 377-379.
- DOMINGUEZ, A., FERNANDEZ, A., GONZALEZ, N., IGLESIAS, E. & MONTENEGRO, L. 1997. Determination of Critical Micelle Concentration of Some Surfactants by Three Techniques. *Journal of Chemical Education*, 74, 1227.
- DONG WOOK CHANG, I.-Y. J., JONG-BEOM BAEK AND LIMING DAI 2010. Efficient dispersion of singlewalled carbon nanotubes by novel amphiphilic dendrimers in water and substitution of the pre-adsorbed dendrimers with conventional surfactants and lipids. *Chem Comm*, 46, 7924–7926.
- DONKOR, D. A. & TANG, X. S. 2014. Tube length and cell type-dependent cellular responses to ultra-short single-walled carbon nanotube. *Biomaterials*, 35, 3121-3131.
- DRESSELHAUS, M. S., DRESSELHAUS, G., SAITO, R. & JORIO, A. 2005. Raman spectroscopy of carbon nanotubes. *Physics Reports*, 409, 47-99.
- DUA, J. S., RANA, A. C., BHANDARI, A. K. 2012. LIPOSOME: METHODS OF PREPARATION AND APPLICATIONS *International Journal of Pharmaceutical Studies and Research* 3, 14 - 20.
- DUCAT, E., EVRARD, B., PEULEN, O. & PIEL, G. 2011. Cellular uptake of liposomes monitored by confocal microscopy and flow cytometry. *Journal of Drug Delivery Science and Technology*, 21, 469-477.
- DUMÉE, L., SEARS, K., SCHÜTZ, J., FINN, N., DUKE, M. & GRAY, S. 2013. Influence of the Sonication Temperature on the Debundling Kinetics of Carbon Nanotubes in Propan-2-ol. *Nanomaterials*, 3, 70.
- DUMORTIER, H. 2013. When carbon nanotubes encounter the immune system: Desirable and undesirable effects. *Advanced Drug Delivery Reviews*, 65, 2120-2126.
- DUZGUNES, N. 2003. *Liposomes*, Elsevier Science.
- DUZGUNES, N. 2005. *Liposomes, Part E*, Elsevier Science.
- DYKE, C. A. & TOUR, J. M. 2004. Overcoming the Insolubility of Carbon Nanotubes Through High Degrees of Sidewall Functionalization. *Chemistry – A European Journal*, 10, 812-817.
- EATEMADI, A., DARAEE, H., KARIMKHANLOO, H., KOUHI, M., ZARGHAMI, N., AKBARZADEH, A., ABASI, M., HANIFEHPOUR, Y. & JOO, S. W. 2014. Carbon nanotubes: properties, synthesis, purification, and medical applications. *Nanoscale Research Letters*, 9, 393-393.
- EMINOVIC, I., KARAMEHIC, J., GAVRANKAPETANOVIC, F. & HELJIC, B. 2005. A simple method of DNA extraction in solving difficult criminal cases. *Med Arh*, 59, 57-8.
- ESPLANDIU, M. J., PACIOS, M., CYGANEK, L., BARTROLI, J. & VALLE, M. D. 2009. Enhancing the electrochemical response of myoglobin with carbon nanotube electrodes. *Nanotechnology*, 20, 355502.
- EUROPEAN MEDICINES AGENCY 2013. Revised priority list for studies on off-patent paediatric medicinal products
- FADEL, T. R. & FAHMY, T. M. 2014. Immunotherapy applications of carbon nanotubes: from design to safe applications. *Trends Biotechnol*, 32, 198-209.
- FAGAN, J. A., BECKER, M. L., CHUN, J. & HOBBIIE, E. K. 2008. Length Fractionation of Carbon Nanotubes Using Centrifugation. *Advanced Materials*, 20, 1609-1613.

- FAÏD, F., CONTAMINE, F., WILHELM, A. M. & DELMAS, H. 1998. Comparison of ultrasound effects in different reactors at 20kHz. *Ultrasonics Sonochemistry*, 5, 119-124.
- FAN, Y. & ZHANG, Q. 2013. Development of liposomal formulations: From concept to clinical investigations. *Asian Journal of Pharmaceutical Sciences*, 8, 81-87.
- FERNANDES, R. M. F., ABREU, B., CLARO, B., BUZAGLO, M., REGEV, O., FURÓ, I. & MARQUES, E. F. 2015. Dispersing Carbon Nanotubes with Ionic Surfactants under Controlled Conditions: Comparisons and Insight. *Langmuir*, 31, 10955-10965.
- FOGED, C., RADES, T., PERRIE, Y. & HOOK, S. 2014. *Subunit Vaccine Delivery*, Springer New York.
- FORSSEN, E. A., MALEBRUNE, R., ADLERMOORE, J. P., LEE, M. J. A., SCHMIDT, P. G., KRASIEVA, T. B., SHIMIZU, S. & TROMBERG, B. J. 1996. Fluorescence imaging studies for the disposition of daunorubicin liposomes (DaunoXome) within tumor tissue. *Cancer Research*, 56, 2066-2075.
- GANESH, E. N. 2013. Single Walled and Multi Walled Carbon Nanotube Structure, Synthesis and Applications. *International Journal of Innovative Technology and Exploring Engineering*, 2, 311 -320.
- GAO, Z., OUDJEDI, L., FAES, R., MOROTE, F., JAILLET, C., POULIN, P., LOUNIS, B. & COGNET, L. 2015. Optical detection of individual ultra-short carbon nanotubes enables their length characterization down to 10 nm. *Scientific Reports*, 5.
- GARCIA-FANDINO, R. & SANSOM, M. S. P. 2012. Designing biomimetic pores based on carbon nanotubes. *Proceedings of the National Academy of Sciences of the United States of America*, 109, 6939-6944.
- GOTTARDI, R. & DOURADINHA, B. 2013. Carbon nanotubes as a novel tool for vaccination against infectious diseases and cancer. *Journal of Nanobiotechnology*, 11, 30-30.
- GRAEVE, M. & JANSSEN, D. 2009. Improved separation and quantification of neutral and polar lipid classes by HPLC–ELSD using a monolithic silica phase: Application to exceptional marine lipids. *Journal of Chromatography B*, 877, 1815-1819.
- GREGORIADIS, G. & PERRIE, Y. 2010. Liposomes. *Encyclopedia of Life Sciences (ELS)*. John Wiley & Sons, Ltd: Chichester., 1-8.
- GULDI, D. M. & MARTÍN, N. 2010. *Carbon Nanotubes and Related Structures: Synthesis, Characterization, Functionalization, and Applications*, Wiley.
- HADIAN, Z., SAHARI, M. A., MOGHIMI, H. R. & BARZEGAR, M. 2014. Formulation, characterization and optimization of liposomes containing eicosapentaenoic and docosahexaenoic acids; a methodology approach. *Iran J Pharm Res*, 13, 393-404.
- HAMILTON, R. F., XIANG, C., LI, M., KA, I., YANG, F., MA, D., PORTER, D. W., WU, N. & HOLIAN, A. 2013. Purification and sidewall functionalization of multiwalled carbon nanotubes and resulting bioactivity in two macrophage models. *Inhal Toxicol*, 25.
- HARDCASTLE, J. L., BALL, J. C., HONG, Q., MARKEN, F., COMPTON, R. G., BULL, S. D. & DAVIES, S. G. 2000. Sonoelectrochemical and sonochemical effects of cavitation: correlation with interfacial cavitation induced by 20 kHz ultrasound. *Ultrasonics Sonochemistry*, 7, 7-14.
- HASAN, T., SUN, Z., TAN, P., POPA, D., FLAHAUT, E., KELLEHER, E. J., BONACCORSO, F., WANG, F., JIANG, Z., TORRISI, F., PRIVITERA, G., NICOLOSI, V. & FERRARI, A. C. 2014. Double-wall carbon nanotubes for wide-band, ultrafast pulse generation. *ACS Nano*, 8, 4836-47.
- HASEGAWA, T. & YOSIOKA, K. 1969. Acoustic-Radiation Force on a Solid Elastic Sphere. *The Journal of the Acoustical Society of America*, 46, 1139-1143.
- HE, H., PHAM-HUY, L. A., DRAMOU, P., XIAO, D., ZUO, P. & PHAM-HUY, C. 2013a. Carbon Nanotubes: Applications in Pharmacy and Medicine. *BioMed Research International*, 2013, 12.
- HE, M., JIANG, H., LIU, B., FEDOTOV, P. V., CHERNOV, A. I., OBRAZTSOVA, E. D., CAVALCA, F., WAGNER, J. B., HANSEN, T. W., ANOSHKIN, I. V., OBRAZTSOVA, E. A., BELKIN, A. V., SAIRANEN, E., NASIBULIN, A. G., LEHTONEN, J. & KAUPPINEN, E. I. 2013b. Chiral-Selective Growth of Single-Walled Carbon Nanotubes on Lattice-Mismatched Epitaxial Cobalt Nanoparticles. *Scientific Reports*, 3, 1460.

- HEISTER, E., NEVES, V., LAMPRECHT, C., SILVA, S. R. P., COLEY, H. M. & MCFADDEN, J. 2012. Drug loading, dispersion stability, and therapeutic efficacy in targeted drug delivery with carbon nanotubes. *Carbon*, 50, 622-632.
- HENRIKSEN-LACEY, M., BRAMWELL, V. W., CHRISTENSEN, D., AGGER, E. M., ANDERSEN, P. & PERRIE, Y. 2010. Liposomes based on dimethyldioctadecylammonium promote a depot effect and enhance immunogenicity of soluble antigen. *J Control Release*, 142, 180-6.
- HENRIKSEN-LACEY, M., DEVITT, A. & PERRIE, Y. 2011. The vesicle size of DDA:TDB liposomal adjuvants plays a role in the cell-mediated immune response but has no significant effect on antibody production. *J Control Release*, 154, 131-7.
- HIELSCHER. 2015. *Probe-Type Sonication vs. Ultrasonic Bath: An Efficiency Comparison* [Online]. Available: <http://www.hielscher.com/probe-type-sonication-vs-ultrasonic-bath-an-efficiency-comparison.htm> [Accessed 2/3/15].
- HOFF-OLSEN, P., MEVAG, B., STAALSTROM, E., HOVDE, B., EGELAND, T. & OLAISEN, B. 1999. Extraction of DNA from decomposed human tissue. An evaluation of five extraction methods for short tandem repeat typing. *Forensic Sci Int*, 105, 171-83.
- HUANG, J., BUBOLTZ, J. T. & FEIGENSON, G. W. 1999. Maximum solubility of cholesterol in phosphatidylcholine and phosphatidylethanolamine bilayers. *Biochimica et Biophysica Acta - Biomembranes*, 1417, 89-100.
- IJIMA, S. 1991. Helical microtubules of graphitic carbon. *Nature*, 354, 56-58.
- ISRAELACHVILI, J. N. 2011. *Intermolecular and Surface Forces: Revised Third Edition*, Elsevier Science.
- JAHN, A., VREELAND, W. N., DEVOE, D. L., LOCASCIO, L. E. & GAITAN, M. 2007. Microfluidic Directed Formation of Liposomes of Controlled Size. *Langmuir*, 23, 6289-6293.
- JAIN, K. K. 2008. *Drug Delivery Systems*, Humana Press.
- JHA, N. & RAMAPRABHU, S. 2010. Development of Au nanoparticles dispersed carbon nanotube-based biosensor for the detection of paraoxon. *Nanoscale*, 2, 806-810.
- JORIO, A., DRESSELHAUS, G. & DRESSELHAUS, M. S. 2007. *Carbon Nanotubes: Advanced Topics in the Synthesis, Structure, Properties and Applications*, Springer Berlin Heidelberg.
- JOSHI, S., SINGH-MOON, R. P., WANG, M., CHAUDHURI, D. B., HOLCOMB, M., STRAUBINGER, N. L., BRUCE, J. N., BIGIO, I. J. & STRAUBINGER, R. M. 2014. Transient cerebral hypoperfusion assisted intraarterial cationic liposome delivery to brain tissue. *Journal of neuro-oncology*, 118, 73-82.
- KAMPERDIJK, E. W. A., NIEUWENHUIS, P. & HOEFESMIT, E. C. M. 2012. *Dendritic Cells in Fundamental and Clinical Immunology*, Springer US.
- KARCHEMSKI, F., ZUCKER, D., BARENHOLZ, Y. & REGEV, O. 2012. Carbon nanotubes-liposomes conjugate as a platform for drug delivery into cells. *J Control Release*, 160, 339-45.
- KASTNER, E., KAUR, R., LOWRY, D., MOGHADDAM, B., WILKINSON, A. & PERRIE, Y. 2014. High-throughput manufacturing of size-tuned liposomes by a new microfluidics method using enhanced statistical tools for characterization. *International Journal of Pharmaceutics*, 477, 361-368.
- KASTNER, E., VERMA, V., LOWRY, D. & PERRIE, Y. 2015. Microfluidic-controlled manufacture of liposomes for the solubilisation of a poorly water soluble drug. *Int J Pharm*, 485, 122-30.
- KAUR, R., HENRIKSEN-LACEY, M., WILKHU, J., DEVITT, A., CHRISTENSEN, D. & PERRIE, Y. 2014. Effect of incorporating cholesterol into DDA:TDB liposomal adjuvants on bilayer properties, biodistribution, and immune responses. *Mol Pharm*, 11, 197-207.
- KHADKA, P., RO, J., KIM, H., KIM, I., KIM, J. T., KIM, H., CHO, J. M., YUN, G. & LEE, J. 2014. Pharmaceutical particle technologies: An approach to improve drug solubility, dissolution and bioavailability. *Asian Journal of Pharmaceutical Sciences*, 9, 304-316.
- KIM, J. C. 2015. Hydroxyethyl acrylate-based copolymer-immobilized liposomes as UV and thermo dual-triggerable carriers. *European Journal of Lipid Science and Technology*, 117, 45-54.

- KIM, K., GENG, J., TUNUGUNTALA, R., COMOLLI, L. R., GRIGOROPOULOS, C. P., AJO-FRANKLIN, C. M. & NOY, A. 2014. Osmotically-Driven Transport in Carbon Nanotube Porins. *Nano Letters*, 14, 7051-7056.
- KIM, P. & LIEBER, C. M. 1999. Nanotube nanotweezers. *Science*, 286, 2148-50.
- KIM, T. H., DO, C., KANG, S. H., LEE, M. J., LIM, S. H. & CHOI, S. M. 2012. Highly ordered superstructures of single wall carbon nanotube-liposome complexes. *Soft Matter*, 8, 9073-9078.
- KIMURA, T., SAKAMOTO, T., LEVEQUE, J.-M., SOHMIYA, H., FUJITA, M., IKEDA, S. & ANDO, T. 1996. Standardization of ultrasonic power for sonochemical reaction. *Ultrasonics Sonochemistry*, 3, S157-S161.
- KIMURA, Y., KIOKA, N., KATO, H., MATSUO, M. & UEDA, K. 2007. Modulation of drug-stimulated ATPase activity of human MDR1/P-glycoprotein by cholesterol. *Biochem J*, 401, 597-605.
- KONDURU, N. V., TYURINA, Y. Y., FENG, W., BASOVA, L. V., BELIKOVA, N. A., BAYIR, H., CLARK, K., RUBIN, M., STOLZ, D., VALLHOV, H., SCHEYNIUS, A., WITASP, E., FADEEL, B., KICHAMBARE, P. D., STAR, A., KISIN, E. R., MURRAY, A. R., SHVEDOVA, A. A. & KAGAN, V. E. 2009. Phosphatidylserine targets single-walled carbon nanotubes to professional phagocytes in vitro and in vivo. *PLoS One*, 4.
- KONG, J., FRANKLIN, N. R., ZHOU, C., CHAPLINE, M. G., PENG, S., CHO, K. & DAI, H. 2000. Nanotube molecular wires as chemical sensors. *Science*, 287, 622-5.
- KORADIA, D. K. & PARIKH, H. R. 2012. Dissolution enhancement of albendazole through nanocrystal formulation. *Journal of Pharmacy & Bioallied Sciences*, 4, S62-S63.
- KOVACEVIC, I., PAROJCIC, J., HOMSEK, I., TUBIC-GROZDANIS, M. & LANGGUTH, P. 2009. Justification of biowaiver for carbamazepine, a low soluble high permeable compound, in solid dosage forms based on IVIVC and gastrointestinal simulation. *Mol Pharm*, 6, 40-7.
- KREUTER, J. 1994. *Colloidal Drug Delivery Systems*, Taylor & Francis.
- LANKIN, V. Z., TIKHAZE, A. K. & OSIS, Y. G. 2002. Modeling the cascade of enzymatic reactions in liposomes including successive free radical peroxidation, reduction, and hydrolysis of phospholipid polyenoic acyls for studying the effect of these processes on the structural-dynamic parameters of the membranes. *Biochemistry (Mosc)*, 67, 566-74.
- LAPINSKI, M. M., CASTRO-FORERO, A., GREINER, A. J., OFOLI, R. Y. & BLANCHARD, G. J. 2007. Comparison of liposomes formed by sonication and extrusion: rotational and translational diffusion of an embedded chromophore. *Langmuir*, 23, 11677-83.
- LASIC, D. D. & BARENHOLZ, Y. 1996. *Handbook of Nonmedical Applications of Liposomes, Vol IV From Gene Delivery and Diagnosis to Ecology*, Taylor & Francis.
- LASIC, Y. B. A. D. D. 1996. *Handbook of nonmedical applications of liposomes*, USA, CRC press.
- LI, J. & ZHANG, Y. 2006. Cutting of multi walled carbon nanotubes. *Applied Surface Science*, 252, 2944-2948.
- LIU, A. L. 2011. *Advances in Planar Lipid Bilayers and Liposomes*, Elsevier Science.
- LIU, C. & CHENG, H.-M. 2016. Controlled Growth of Semiconducting and Metallic Single-Wall Carbon Nanotubes. *Journal of the American Chemical Society*, 138, 6690-6698.
- LIU, G., WANG, Y., HU, Y., YU, X., ZHU, B. & WANG, G. 2016. Functionalized Multi-Wall Carbon Nanotubes Enhance Transfection and Expression Efficiency of Plasmid DNA in Fish Cells. *Int J Mol Sci*, 17, 335.
- LIU, K., DESLIPPE, J., XIAO, F., CAPAZ, R. B., HONG, X., ALONI, S., ZETTL, A., WANG, W., BAI, X., LOUIE, S. G., WANG, E. & WANG, F. 2012. An atlas of carbon nanotube optical transitions. *Nat Nano*, 7, 325-329.
- LIU, L., YANG, C., ZHAO, K., LI, J. & WU, H.-C. 2013. Ultrashort single-walled carbon nanotubes in a lipid bilayer as a new nanopore sensor. *Nature Communications*, 4, 2989.
- LIU, R. 2008. *Water-Insoluble Drug Formulation, Second Edition*, CRC Press.
- LUCCI, M., SESSA, V., ORLANDUCCI, S., TAMBURRI, E., TOSCHI, F., TERRANOVA, M. L., REALE, A., FIORELLO, A. & FALESSI, C. A carbon nanotube-based quartz crystal nanobalance for

- NH³⁺ detection : Toward the assembling of a sensing platform. *Advances in Sensors and Interface*, 2007. IWASI 2007. 2nd International Workshop on, 26-27 June 2007 2007. 1-4.
- LUTSYK, P., ARIF, R., HRUBY, J., BUKIVSKYI, A., VINIJCHUK, O., SHANDURA, M., YAKUBOVSKYI, V., KOVTUN, Y., RANCE, G. A., FAY, M., PIRYATINSKI, Y., KACHKOVSKY, O., VERBITSKY, A. & ROZHIN, A. 2016. A sensing mechanism for the detection of carbon nanotubes using selective photoluminescent probes based on ionic complexes with organic dyes. *Light Sci Appl*, 5, e16028.
- MA, Q., JEBB, M., TWEEDLE, M. F. & WILSON, L. J. 2013. X-ray absorption spectroscopy study of Gd³⁺-loaded ultra-short carbon nanotubes. In: WU, Z. Y. (ed.) *15th International Conference on X-Ray Absorption Fine Structure*.
- MAJUMDAR, S., KUMAR, P. S. & PANDIT, A. B. 1998. Effect of liquid-phase properties on ultrasound intensity and cavitation activity. *Ultrasonics Sonochemistry*, 5, 113-118.
- MALHOTRA, R., PATEL, V., VAQUÉ, J. P., GUTKIND, J. S. & RUSLING, J. F. 2010. Ultrasensitive Electrochemical Immunosensor for Oral Cancer Biomarker IL-6 Using Carbon Nanotube Forest Electrodes and Multilabel Amplification. *Analytical Chemistry*, 82, 3118-3123.
- MASON, T. J. 1991. *Practical sonochemistry: User's guide to applications in chemistry and chemical engineering*, New York, E. Horwood.
- MASON, T. J. 1996. Sonochemistry: Uses of Ultrasound in Chemistry and Related Disciplines. In: SIEGEL, R. J. (ed.) *Ultrasound Angioplasty*. Boston, MA: Springer US.
- MAULUCCI, G., DE SPIRITO, M., ARCOVITO, G., BOFFI, F., CASTELLANO, A. C. & BRIGANTI, G. 2005. Particle size distribution in DMPC vesicles solutions undergoing different sonication times. *Biophys J*, 88, 3545-50.
- MENGER, F. M. 1979. The structure of micelles. *Accounts of Chemical Research*, 12, 111-117.
- MEYYAPPAN, M. 2004. *Carbon Nanotubes: Science and Applications*, CRC Press.
- MISHRA, G. P., BAGUI, M., TAMBOLI, V. & MITRA, A. K. 2011. Recent Applications of Liposomes in Ophthalmic Drug Delivery. *Journal of Drug Delivery*, 2011, 14.
- MIYAKO, E., KONO, K., YUBA, E., HOSOKAWA, C., NAGAI, H. & HAGIHARA, Y. 2012. Carbon nanotube–liposome supramolecular nanotrains for intelligent molecular-transport systems. *Nat Commun*, 3, 1226.
- MOHAMMADI, M., GHANBARZADEH, B. & HAMISHEHKAR, H. 2014. Formulation of Nanoliposomal Vitamin D3 for Potential Application in Beverage Fortification. *Advanced Pharmaceutical Bulletin*, 4, 569-575.
- MORÉ, M. I., HERRICK, J. B., SILVA, M. C., GHIOSE, W. C. & MADSEN, E. L. 1994. Quantitative cell lysis of indigenous microorganisms and rapid extraction of microbial DNA from sediment. *Applied and Environmental Microbiology*, 60, 1572-1580.
- MUNGE, B. S., FISHER, J., MILLORD, L. N., KRAUSE, C. E., DOWD, R. S. & RUSLING, J. F. 2010. Sensitive electrochemical immunosensor for matrix metalloproteinase-3 based on single-wall carbon nanotubes. *Analyst*, 135, 1345-1350.
- N. A. ABDUL NASIR, R. N. A., R. AGARWAL, N. NUKOLOVA, V. CHEKNONIN, N. MOHD ISMAIL 2013 "Ocular Tissue Distribution of Topically Applied PEGylated and Non-PEGylated Liposomes". *Advanced Materials Research*, 832, 1-8.
- NASCENTES, C. C., KORN, M., SOUSA, C. S. & ARRUDA, M. A. Z. 2001. Use of ultrasonic baths for analytical applications: a new approach for optimisation conditions. *Journal of the Brazilian Chemical Society*, 12, 57-63.
- NAYAR, R., HOPE, M. J. & CULLIS, P. R. 1989. Generation of large unilamellar vesicles from long-chain saturated phosphatidylcholines by extrusion technique. *BBA - Biomembranes*, 986, 200-206.
- NIEMCZEWSKI, B. 2007. Observations of water cavitation intensity under practical ultrasonic cleaning conditions. *Ultrasonics Sonochemistry*, 14, 13-18.
- NISH, A., HWANG, J.-Y., DOIG, J. & NICHOLAS, R. J. 2007. Highly selective dispersion of single-walled carbon nanotubes using aromatic polymers. *Nat Nano*, 2, 640-646.

- NJUGUNA, J., VANLI, O. A. & LIANG, R. 2015. A Review of Spectral Methods for Dispersion Characterization of Carbon Nanotubes in Aqueous Suspensions. *Journal of Spectroscopy*, 2015, 11.
- OLSON, F., HUNT, C. A., SZOKA, F. C., VAIL, W. J. & PAPAHAADJOPOULOS, D. 1979. Preparation of liposomes of defined size distribution by extrusion through polycarbonate membranes. *Biochimica et Biophysica Acta (BBA) - Biomembranes*, 557, 9-23.
- ORECCHIONI, M., BEDOGNETTI, D., SGARRELLA, F., MARINCOLA, F. M., BIANCO, A. & DELOGU, L. G. 2014. Impact of carbon nanotubes and graphene on immune cells. *Journal of Translational Medicine*, 12, 1-11.
- PAN, C., XU, S., ZOU, H., GUO, Z., ZHANG, Y. & GUO, B. 2005. Carbon nanotubes as adsorbent of solid-phase extraction and matrix for laser desorption/ionization mass spectrometry. *Journal of the American Society for Mass Spectrometry*, 16, 263-270.
- PAN, H., LI, J. & FENG, Y. 2010. Carbon Nanotubes for Supercapacitor. *Nanoscale Research Letters*, 5, 654-668.
- PARKER, R. J., SIEBER, S. M. & WEINSTEIN, J. N. 1981. Effect of liposome encapsulation of a fluorescent dye on its uptake by the lymphatics of the rat. *Pharmacology*, 23, 128-36.
- PENG, L.-M., ZHANG, Z. & WANG, S. 2014. Carbon nanotube electronics: recent advances. *Materials Today*, 17, 433-442.
- PHILIPPOT, J. R. & SCHUBER, F. 1994. *Liposomes as Tools in Basic Research and Industry*, Taylor & Francis.
- PIAO, Y., MEANY, B., POWELL, L. R., VALLEY, N., KWON, H., SCHATZ, G. C. & WANG, Y. 2013. Brightening of carbon nanotube photoluminescence through the incorporation of sp³ defects. *Nat Chem*, 5, 840-845.
- PLANEIX, J. M., COUSTEL, N., COQ, B., BROTONS, V., KUMBHAR, P. S., DUTARTRE, R., GENESTE, P., BERNIER, P. & AJAYAN, P. M. 1994. Application of Carbon Nanotubes as Supports in Heterogeneous Catalysis. *Journal of the American Chemical Society*, 116, 7935-7936.
- PONDMAN, K. M., SOBIK, M., NAYAK, A., TSOLAKI, A. G., JÄKEL, A., FLAHAUT, E., HAMPEL, S., TEN HAKEN, B., SIM, R. B. & KISHORE, U. 2014. Complement activation by carbon nanotubes and its influence on the phagocytosis and cytokine response by macrophages. *Nanomedicine: Nanotechnology, Biology and Medicine*, 10, 1287-1299.
- PUGIN, B. 1987. Qualitative characterization of ultrasound reactors for heterogeneous sonochemistry. *Ultrasonics*, 25, 49-55.
- RALSTON, E., HJELMELAND, L. M., KLAUSNER, R. D., WEINSTEIN, J. N. & BLUMENTHAL, R. 1981. Carboxyfluorescein as a probe for liposome-cell interactions effect of impurities, and purification of the dye. *Biochimica et Biophysica Acta (BBA) - Biomembranes*, 649, 133-137.
- RANCE, G. A., MARSH, D. H., NICHOLAS, R. J. & KHLOBYSTOV, A. N. 2010. UV-vis absorption spectroscopy of carbon nanotubes: Relationship between the π -electron plasmon and nanotube diameter. *Chemical Physics Letters*, 493, 19-23.
- RATHOD, S. & DESHPANDE, S. G. 2010. Design and Evaluation of Liposomal Formulation of Pilocarpine Nitrate. *Indian Journal of Pharmaceutical Sciences*, 72, 155-160.
- ROCHA, J. M., KALO, P. J., OLLILAINEN, V. & MALCATA, F. X. 2010. Separation and identification of neutral cereal lipids by normal phase high-performance liquid chromatography, using evaporative light-scattering and electrospray mass spectrometry for detection. *Journal of Chromatography A*, 1217, 3013-3025.
- RODRÍGUEZ-ALCALÁ, L. M. & FONTECHA, J. 2010. Major lipid classes separation of buttermilk, and cows, goats and ewes milk by high performance liquid chromatography with an evaporative light scattering detector focused on the phospholipid fraction. *Journal of Chromatography A*, 1217, 3063-3066.
- RUSS, M., RAHATEKAR, S. S., KOZIOL, K., FARMER, B. & PENG, H.-X. 2013. Length-dependent electrical and thermal properties of carbon nanotube-loaded epoxy nanocomposites. *Composites Science and Technology*, 81, 42-47.

- RYBAK-SMITH, M. J. & SIM, R. B. 2011. Complement activation by carbon nanotubes. *Advanced Drug Delivery Reviews*, 63, 1031-1041.
- SAFAROVA, K., DVORAK, A., KUBINEK, R., VUJTEK, M., REK A. 2007. Usage of AFM, SEM and TEM for the research of carbon nanotubes *Modern Research and Educational Topics in Microscopy*, 513 - 519.
- SÁNCHEZ, S., ROLDÁN, M., PÉREZ, S. & FÀBREGAS, E. 2008. Toward a Fast, Easy, and Versatile Immobilization of Biomolecules into Carbon Nanotube/Polysulfone-Based Biosensors for the Detection of hCG Hormone. *Analytical Chemistry*, 80, 6508-6514.
- SATISHKUMAR, B. C., BROWN, L. O., GAO, Y., WANG, C. C., WANG, H. L. & DOORN, S. K. 2007. Reversible fluorescence quenching in carbon nanotubes for biomolecular sensing. *Nat Nanotechnol*, 2, 560-4.
- SATO, Y. & SANO, M. 2014. Dispersing single-walled carbon nanotubes using common phospholipids with a small amount of polyethylene glycol-phospholipid additives. *Colloids and Surfaces a-Physicochemical and Engineering Aspects*, 441, 427-432.
- SCARDACI, V., ROZHIN, A. G., HENNRICH, F., MILNE, W. I. & FERRARI, A. C. 2007. Carbon nanotube-polymer composites for photonic devices. *Physica E: Low-dimensional Systems and Nanostructures*, 37, 115-118.
- SCHWENDENER, R. A. 2014. Liposomes as vaccine delivery systems: a review of the recent advances. *Therapeutic Advances in Vaccines*, 2, 159-182.
- SEFERS, S. E., RICKMYRE, J., BLACKMAN, A., LI, H., EDWARDS, K. & TANG, Y. W. 2006. QIAamp MinElute virus kit effectively extracts viral nucleic acids from cerebrospinal fluids and nasopharyngeal swabs. *J Clin Virol*, 35, 141-6.
- SHAMSIPUR, M., NAJAFI, M. & HOSSEINI, M.-R. M. 2010. Highly improved electrooxidation of glucose at a nickel(II) oxide/multi-walled carbon nanotube modified glassy carbon electrode. *Bioelectrochemistry*, 77, 120-124.
- SHARMA, A., SINGH, V., BOUGHER, T. L. & COLA, B. A. 2015. A carbon nanotube optical rectenna. *Nat Nano*, 10, 1027-1032.
- SHI, X., SITHARAMAN, B., PHAM, Q. P., LIANG, F., WU, K., BILLUPS, W. E., WILSON, L. J. & MIKOS, A. G. 2007. Fabrication of porous ultra-short single-walled carbon nanotube nanocomposite scaffolds for bone tissue engineering. *Biomaterials*, 28, 4078-4090.
- SHI, Y., REN, L., LI, D., GAO, H., AND YANG, B. 2013. Optimization Conditions for Single-Walled Carbon Nanotubes Dispersion. *Journal of Surface Engineered Materials and Advanced Technology*, 3, 6 - 12.
- SINNOTT, S. B. & ANDREWS, R. 2001. Carbon Nanotubes: Synthesis, Properties, and Applications. *Critical Reviews in Solid State and Materials Sciences*, 26, 145-249.
- SOCACIU, C., JESSEL, R. & DIEHL, H. A. 2000. Competitive carotenoid and cholesterol incorporation into liposomes: Effects on membrane phase transition, fluidity, polarity and anisotropy. *Chemistry and Physics of Lipids*, 106, 79-88.
- STEENBLOCK, E. R., WRZESINSKI, S. H., FLAVELL, R. A. & FAHMY, T. M. 2009. Antigen presentation on artificial acellular substrates: modular systems for flexible, adaptable immunotherapy. *Expert Opinion on Biological Therapy*, 9, 451-464.
- STEVENSON, M., BAILLIE, A. J. & RICHARDS, R. M. E. 1984. Quantification of uptake of liposomal carboxyfluorescein by professional phagocytes in-vitro. A flow microfluorimetric study on the J774 murine macrophage cell line. *Journal of Pharmacy and Pharmacology*, 36, 824-830.
- SULKOWSKI, W. W., PENTAK, D., NOWAK, K. & SULKOWSKA, A. 2005. The influence of temperature, cholesterol content and pH on liposome stability. *Journal of Molecular Structure*, 744, 737-747.
- SUN, X., ZARIC, S., DARANCIANG, D., WELSHER, K., LU, Y., LI, X. & DAI, H. 2008. Optical Properties of Ultrashort Semiconducting Single-Walled Carbon Nanotube Capsules Down to Sub-10 nm. *Journal of the American Chemical Society*, 130, 6551-6555.

- SUPPRIAN, T., SENITZ, D. & BECKMANN, H. 1993. Presentation of human neocortical neurons stained with the carbocyanine dye dil compared to the Golgi silver impregnation technique. *J Hirnforsch*, 34, 403-6.
- SZOKA, F., JR. & PAPAHAJOPOULOS, D. 1978. Procedure for preparation of liposomes with large internal aqueous space and high capture by reverse-phase evaporation. *Proc Natl Acad Sci U S A*, 75, 4194-8.
- TAN, P. H., ROZHIN, A. G., HASAN, T., HU, P., SCARDACI, V., MILNE, W. I. & FERRARI, A. C. 2007. Photoluminescence Spectroscopy of Carbon Nanotube Bundles: Evidence for Exciton Energy Transfer. *Physical Review Letters*, 99, 137402.
- TANAKA, T., URABE, Y., HIRAKAWA, T. & KATAURA, H. 2015. Simultaneous Chirality and Enantiomer Separation of Metallic Single-Wall Carbon Nanotubes by Gel Column Chromatography. *Analytical Chemistry*, 87, 9467-9472.
- TANDRUP SCHMIDT, S., FOGED, C., SMITH KORSHOLM, K., RADES, T. & CHRISTENSEN, D. 2016. Liposome-Based Adjuvants for Subunit Vaccines: Formulation Strategies for Subunit Antigens and Immunostimulators. *Pharmaceutics*, 8, 7.
- TANS, S. J., VERSCHUEREN, A. R. M. & DEKKER, C. 1998. Room-temperature transistor based on a single carbon nanotube. *Nature*, 393, 49-52.
- THOSTENSON, E. T., REN, Z. & CHOU, T.-W. 2001. Advances in the science and technology of carbon nanotubes and their composites: a review. *Composites Science and Technology*, 61, 1899-1912.
- TORCHILIN, V. & WEISSIG, V. 2003. *Liposomes: A Practical Approach*, OUP Oxford.
- TRAN, I. C., TUNUGUNTALA, R. H., KIM, K., LEE, J. R. I., WILLEY, T. M., WEISS, T. M., NOY, A. & VAN BUUREN, T. 2016. Structure of Carbon Nanotube Porins in Lipid Bilayers: An in Situ Small-Angle X-ray Scattering (SAXS) Study. *Nano Letters*, 16, 4019-4024.
- TROTTA, M., DEBERNARDI, F. & CAPUTO, O. 2003. Preparation of solid lipid nanoparticles by a solvent emulsification–diffusion technique. *International Journal of Pharmaceutics*, 257, 153-160.
- TSAI, H.-C., LIN, J.-Y., MARYANI, F., HUANG, C.-C. & IMAE, T. 2013. Drug-loading capacity and nuclear targeting of multiwalled carbon nanotubes grafted with anionic amphiphilic copolymers. *International Journal of Nanomedicine*, 8, 4427-4440.
- TSANG, S. C., HARRIS, P. J. F. & GREEN, M. L. H. 1993. Thinning and opening of carbon nanotubes by oxidation using carbon dioxide. *Nature*, 362, 520-522.
- TUNUGUNTALA, R. H., ALLEN, F. I., KIM, K., BELLIVEAU, A. & NOY, A. 2016. Ultrafast proton transport in sub-1-nm diameter carbon nanotube porins. *Nature Nanotechnology*, 11, 639-+.
- TUNUGUNTALA, R. H., CHEN, X., BELLIVEAU, A., ALLEN, F. I. & NOY, A. 2017. High-Yield Synthesis and Optical Properties of Carbon Nanotube Porins. *The Journal of Physical Chemistry C*, 121, 3117-3125.
- TURANEK, J. 1994. Fast-protein liquid chromatography system as a tool for liposome preparation by the extrusion procedure. *Analytical Biochemistry*, 218, 352-357.
- VAISMAN, L., WAGNER, H. D. & MAROM, G. 2006. The role of surfactants in dispersion of carbon nanotubes. *Advances in Colloid and Interface Science*, 128–130, 37-46.
- VAN SWAAY, D. & DEMELLO, A. 2013. Microfluidic methods for forming liposomes. *Lab on a Chip*, 13, 752-767.
- VEETIL, J. V. & YE, K. 2009. Tailored carbon nanotubes for tissue engineering applications. *Biotechnol Prog*, 25, 709-21.
- VEMURI, S., YU, C.-D., DEGROOT, J. S. & ROOSDORP, N. 1990. In Vitro Interaction of Sized and Unsized Liposome Vesicles with High Density Lipo Proteins. *Drug Development and Industrial Pharmacy*, 16, 1579-1584.
- VENKATESWARLU I, J. R. V., RAMESH Y, VISWANATHA REDDY M, PRAVALLIKA CH, SUNEETHA KC 2011. A Review on Liposomes. *Research Journal of Pharmaceutical, Biological and Chemical Sciences*, 2, 739-751.

- VERMA, D. D., VERMA, S., BLUME, G. & FAHR, A. 2003. Liposomes increase skin penetration of entrapped and non-entrapped hydrophilic substances into human skin: a skin penetration and confocal laser scanning microscopy study. *Eur J Pharm Biopharm*, 55, 271-7.
- VISWANATHAN, S., RANI, C., VIJAY ANAND, A. & HO, J.-A. A. 2009. Disposable electrochemical immunosensor for carcinoembryonic antigen using ferrocene liposomes and MWCNT screen-printed electrode. *Biosensors and Bioelectronics*, 24, 1984-1989.
- VITIELLO, G., LUCHINI, A., D'ERRICO, G., SANTAMARIA, R., CAPUOZZO, A., IRACE, C., MONTESARCHIO, D. & PADUANO, L. 2015. Cationic liposomes as efficient nanocarriers for the drug delivery of an anticancer cholesterol-based ruthenium complex. *Journal of Materials Chemistry B*, 3, 3011-3023.
- VO-DINH, T. 2003. *Biomedical Photonics Handbook*, Taylor & Francis.
- VUICHARD, S., BORER, U., BOTTINELLI, M., COSSU, C., MALIK, N., MEIER, V., GEHRIG, C., SULZER, A., MOREROD, M.-L. & CASTELLA, V. 2011. Differential DNA extraction of challenging simulated sexual-assault samples: a Swiss collaborative study. *Investigative Genetics*, 2, 11.
- WAGNER, A. & VORAUER-UHL, K. 2011. Liposome Technology for Industrial Purposes. *Journal of Drug Delivery*, 2011.
- WALSH, P. S., METZGER, D. A. & HIGUCHI, R. 1991. Chelex 100 as a medium for simple extraction of DNA for PCR-based typing from forensic material. *Biotechniques*, 10, 506-13.
- WANG, H., ZHOU, W., HO, D. L., WINEY, K. I., FISCHER, J. E., GLINKA, C. J. & HOBBI, E. K. 2004. Dispersing Single-Walled Carbon Nanotubes with Surfactants: A Small Angle Neutron Scattering Study. *Nano Letters*, 4, 1789-1793.
- WANG, X., JIANG, Q., XU, W., CAI, W., INOUE, Y. & ZHU, Y. 2013. Effect of carbon nanotube length on thermal, electrical and mechanical properties of CNT/bismaleimide composites. *Carbon*, 53, 145-152.
- WEIR, C., MOREL-KOPP, M. C., GILL, A., TINWORTH, K., LADD, L., HUNYOR, S. N. & WARD, C. 2008. Mesenchymal stem cells: isolation, characterisation and in vivo fluorescent dye tracking. *Heart Lung Circ*, 17, 395-403.
- WEPASNICK, K. A., SMITH, B. A., BITTER, J. L. & HOWARD FAIRBROTHER, D. 2010. Chemical and structural characterization of carbon nanotube surfaces. *Analytical and Bioanalytical Chemistry*, 396, 1003-1014.
- WONG, C. P., MOON, K. S. & LI, Y. 2009. *Nano-Bio- Electronic, Photonic and MEMS Packaging*, Springer US.
- WOODBURY, D. J., RICHARDSON, E. S., GRIGG, A. W., WELLING, R. D. & KNUDSON, B. H. 2006. Reducing liposome size with ultrasound: bimodal size distributions. *J Liposome Res*, 16, 57-80.
- WOZNIAK, K. M., VORNOV, J. J., MISTRY, B. M., WU, Y., RAIS, R. & SLUSHER, B. S. 2015. Gastrointestinal delivery of propofol from fospropofol: its bioavailability and activity in rodents and human volunteers. *Journal of Translational Medicine*, 13, 170.
- WU, Y., HUDSON, J. S., LU, Q., MOORE, J. M., MOUNT, A. S., RAO, A. M., ALEXOV, E. & KE, P. C. 2006. Coating Single-Walled Carbon Nanotubes with Phospholipids. *The Journal of Physical Chemistry B*, 110, 2475-2478.
- XING, J., LIU, Z., HUANG, Y., QIN, T., BO, R., ZHENG, S., LUO, L., HUANG, Y., NIU, Y. & WANG, D. 2016. Lentinan-Modified Carbon Nanotubes as an Antigen Delivery System Modulate Immune Response in Vitro and in Vivo. *ACS Applied Materials & Interfaces*, 8, 19276-19283.
- XU, H., ZENG, L., XING, S., SHI, G., XIAN, Y. & JIN, L. 2008. Microwave-radiated synthesis of gold nanoparticles/carbon nanotubes composites and its application to voltammetric detection of trace mercury(II). *Electrochemistry Communications*, 10, 1839-1843.
- XU, L., XIANG, J., LIU, Y., XU, J., LUO, Y., FENG, L., LIU, Z. & PENG, R. 2016. Functionalized graphene oxide serves as a novel vaccine nano-adjuvant for robust stimulation of cellular immunity. *Nanoscale*, 8, 3785-3795.

- YANG, J., XU, Y., ZHANG, R., WANG, Y., HE, P. & FANG, Y. 2009. Direct Electrochemistry and Electrocatalysis of the Hemoglobin Immobilized on Diazonium-Functionalized Aligned Carbon Nanotubes Electrode. *Electroanalysis*, 21, 1672-1677.
- YANG, K., YI, Z., JING, Q., YUE, R., JIANG, W. & LIN, D. 2013. Sonication-assisted dispersion of carbon nanotubes in aqueous solutions of the anionic surfactant SDBS: The role of sonication energy. *Chinese Science Bulletin*, 58, 2082-2090.
- YANG, N., CHEN, X., REN, T., ZHANG, P. & YANG, D. 2015. Carbon nanotube based biosensors. *Sensors and Actuators B: Chemical*, 207, Part A, 690-715.
- YANG, Y., XIE, L., CHEN, Z., LIU, M., ZHU, T. & LIU, Z. 2005. Purification and length separation of single-walled carbon nanotubes using chromatographic method. *Synthetic Metals*, 155, 455-460.
- YU, B., LEE, R. J. & LEE, L. J. 2009. Microfluidic methods for production of liposomes. *Methods Enzymol*, 465, 129-41.
- ZAKERI-MILANI, P., ISLAMBULCHILAR, Z., MAJIDPOUR, F., JANNATABADI, E., LOTFIPOUR, F. & VALIZADEH, H. 2014. A study on enhanced intestinal permeability of clarithromycin nanoparticles. *Brazilian Journal of Pharmaceutical Sciences*, 50, 121-129.
- ZHANG, Q., HUANG, J.-Q., QIAN, W.-Z., ZHANG, Y.-Y. & WEI, F. 2013. The Road for Nanomaterials Industry: A Review of Carbon Nanotube Production, Post-Treatment, and Bulk Applications for Composites and Energy Storage. *Small*, 9, 1237-1265.
- ZHANG, W., ZHANG, Z. & ZHANG, Y. 2011. The application of carbon nanotubes in target drug delivery systems for cancer therapies. *Nanoscale Research Letters*, 6, 555-555.
- ZHBANOV, A. I., POGORELOV, E. G. & CHANG, Y.-C. 2010. Van der Waals Interaction between Two Crossed Carbon Nanotubes. *ACS Nano*, 4, 5937-5945.
- ZHBANOV, A. I., SINITSYN, N. I. & TORGASHOV, G. V. Nanoelectronic Devices Based on Carbon Nanotubes. *Radiophysics and Quantum Electronics*, 47, 435-452.
- ZHOU, J., LU, Q., TONG, Y., WEI, W. & LIU, S. 2012. Detection of DNA damage by using hairpin molecular beacon probes and graphene oxide. *Talanta*, 99, 625-30.
- ZIEGLER, K. J., GU, Z., PENG, H., FLOR, E. L., HAUGE, R. H. & SMALLEY, R. E. 2005a. Controlled Oxidative Cutting of Single-Walled Carbon Nanotubes. *Journal of the American Chemical Society*, 127, 1541-1547.
- ZIEGLER, K. J., GU, Z., SHAVER, J., CHEN, Z., FLOR, E. L., SCHMIDT, D. J., CHAN, C., HAUGE, R. H. & SMALLEY, R. E. 2005b. Cutting single-walled carbon nanotubes. *Nanotechnology*, 16, S539-44.
- ZIENIUK, J. & CHIVERS, R. C. 1976. Measurement of ultrasonic exposure with radiation force and thermal methods. *Ultrasonics*, 14, 161-172.